DOE/NV/10805--T1

Dosimetry using Environmental and Biological Materials.

Final Report September, 1996

DOE Contract DE-FC08-89NV10805

with additonal support under subcontract

LLNL-6288-08 DOE-95-ES-1768

E. Haskell, G. Kenner, R. Hayes

Center for Applied Dosimetry
University of Utah
825N 300W #107
Salt Lake City UT 84103

DISCLAIMER

Dosimetry using Environmental and Biological Materials.

Final Report September, 1996

DOE Contract DE-FC08-89NV10805

with additonal support under subcontract

LLNL-6288-08 DOE-95-ES-1768

E. Haskell, G. Kenner, R. Hayes

Center for Applied Dosimetry
University of Utah
825N 300W #107
Salt Lake City UT 84103

Dosimetry using Environmental and Biological Materials. Radiobiology Division, University of Utah

E. Haskell, G. Kenner, R. Hayes

Introduction

The Center for Applied Dosimety (formerly the TL/EPR Laboratory) of the University of Utah was established in 1981 to address social and political demand for retrospective measurement of doses delivered to communities downwind of the Nevada Test Site during the 1950's and 60's. Since that time incidents of even greater social impact have occurred or come to light: the nuclear accident at Chernobyl in 1986, the massive exposures at the Mayak processing plant in the Urals, the populations exposed to fallout from Soviet testing in Semipalitinsk, the vast inventories of nuclear waste awaiting disposal, the decades of leaks, spills and releases by DOE facilities and the growing realization that the aging of the world's nuclear power plants makes future accidents not just likely, but inevitable.

Although theoretical models have been the traditional tool for assessment of doses delivered by nuclear accidents, their use is now accompanied by increasing political and scientific demand for physical measurements which 1) provide site specific dose information related directly to the original events, 2) can be used to verify and augment the theoretical models and 3) can be performed and replicated by independent laboratories.

Background

During the past several years meetings held on four continents have resulted in a unanimous call for the synthesis of a common methodology and for the further development of methods of retrospective dosimetry which can provide quantitative estimates of dose to exposed individuals in populated areas. A working paper drafted under joint sponsorship of the European Union (EU), the IAEA, GSF and GAST in Germany outlined scientific recommendations for the reconstruction of radiation doses in accident situations. Luminescence techniques were recommended to "1) provide benchmark dose evaluations for modeling calculations and comparisons with other techniques used in dose reconstruction for populated areas and 2) integrated dose evaluations for areas continuously populated since the accident but which lack monitoring data". The paper recommends continued development and optimization of the techniques, specifically for "standardization, optimization of sample selection for comparisons with modeling calculations, uncertainty analysis,

intercomparison and validation". EPR techniques were recommended for dosimetry of individuals who received the highest doses and additional development and validation were considered essential.

This report details a four year effort to improve the sensitivity and reliability of retrospective methods, to collaborate with laboratories engaged in related research and to share the technology with startup laboratories seeking similar capabilities. Because of our experience in the development and application of dosimetry techniques for accident situations, we have been in a unique position to contribute to the development, coordination and implementation of quality assurance programs in laboratories currently, or soon to be, engaged in the measurement and dissemination of dosimetry information.

Accomplishments

Our research program has focused on validation of EPR as a dosimetry tool and on optimization of the technique by reducing the lower limits of detection, simplifying the process of sample preparation and analysis and speeding analysis to allow greater throughput in routine measurement situations. This research has resulted in a total of 20 manuscripts which have been published, are in press, or have been submitted for publication.

Synthetic Hydroxyapatite

We have investigated the basic dosimetric properties of enamel by studying synthetically grown hydroxyapatite doped with varying concentrations of CO_3^{2-} (Appendix 1). We found that the radiation sensitive signal used for dosimetry in enamel at g= 2.0018 does not appear in pure hydroxyapatite but is present in CO_3^{2-} doped material and increases in sensitivity with increasing CO_3^{2-} concentration. The native signal of enamel is not present with any of the synthetic preparations.

Light Effects

Factors influencing the accuracy of dosimetry with enamel have also been investigated. We observed the growth of a large signal in enamel near g = 2.0018, upon exposure to UV irradiation as well as sunlight (Appendix 2). We later, more systematically investigated the phenomenon (Appendix 3). and discovered that 1) UV increases the radiation sensitive component of enamel, 2) UV increases the native signal of enamel and 3) UV induces additional signals that might prove useful in assessing and making

corrections for the total UV dose received. A dose depth profile indicated that the penetration depth of the effect is approximately 100 μm.

Grain size effects

On a visit to our laboratory, Dr. V. Polyakov of Tallinn, Estonia observed a phenomenon which indicated that the size of the enamel grain being used for analysis was a factor in the sensitivity of the EPR signal to radiation (Appendix 4). We subsequently investigated the effect further and discovered that the effect was not only grain size dependent, but also was a function of whether the sample was irradiated before or after the tooth had been reduced to a powder for analysis. Samples which had been irradiated after crushing showed a different sensitivity to radiation than those irradiated prior to crushing. The grain size range of 250 to 600 μm was shown to minimize the effect (Appendix 5). We again addressed this effect during the visit by Dr. Sholom. In this case we treated all grains thoroughly in concentrated NaOH. The effect was still observed, however the magnitude of the sensitivity change was drastically reduced. The maximum change was seen to occur for grains less than 75μm and the effect was approximately 10%.

Transient radiation induced signals

Transient radiation induced signals reported in archaeological specimens of teeth prompted us to investigate these effects in modern enamel (Appendix 6). We discovered that the effect was significant on the g = 2.0018 signal normally used for dosimetry, that the signal reduced to near background levels after approximately 1 month, and that the transient signals could be removed by heating to 90°C for 2 hours.

Dosimetry using dentine

Our observation that removal of the organic component of bone could be achieved with the use of Soxhlett treatment in diethyltriamine, with reduction of the normally obscuring native signal by several orders of magnitude (Appendix 7) led us to propose the use of dentine in conjunction with enamel for dosimetry of internal emitters (Appendix 8). We have also proposed (Appendix 9) a more extensive investigation of the utility of dentine as a dosimeter of internal emitters and have suggested that comparison of enamel and dentine of teeth exposed to injected or inhaled radionuclides as part of completed, long range beagle studies could be used for correlation with known organ doses for both lifetime and serial

sacrifice data. We have collected several hundred teeth from beagles from the Utah studies for use in such a project.

Goniometry

The variation in EPR signal intensity and position resulting from anisotropies in enamel have been virtually eliminated with our use of a constant rotation goniometer during sample measurement (Appendix 10). This procedure has resulted in our being able to use large portions of enamel and even whole deciduous teeth (Appendix 11). The dose response characteristics indicate that doses of less than 100 mGy can now be measured. The ability to use whole deciduous teeth opens the possibility for the use of EPR as a screening technique of milk teeth in the event of a future nuclear accident on the scale of that at Chernobyl (Appendix 12).

Optimization of measurement protocol

Because of the time consuming nature of the additive dose method of EPR analysis, where a sample is repeatedly measured, dosed and remeasured, we have developed a mathematical optimization method which specifies the size of the doses to be applied and the number required to achieve a desired level of precision. (Appendix 13). This procedure should greatly reduce the time required for routine EPR analysis. The widespread utility of the method for systems showing a linear response prompted us to prepare a condensed version for general application for a mathematics journal (Appendix 14).

Other EPR dosimeters

In an effort to expand the utility of EPR dosimetry we investigated the dosimetric properties of a number of common materials. The most promising of those is common sheetrock which can be used for dosimetry over the course of approximately 6 months following irradiation (Appendix 15). A short letter was published in Health Physics to quickly get this information to the radiation protection community (Appendix 16).

Curve fitting.

We have developed computerized routines which allow us to simulate the native signal of enamel as well as the radiation induced signal. This approach is promising for future dosimetry but has not been a recent priority due to our characterization of numerous additional EPR signals which would require complex modeling.

Blind EPR Intercomparisons.

We have participated in two blind EPR intercomparisons. The first was organized by ECP-10, the dosimetry research program of the European Union. This intercomparison involved 9 laboratories which were given a homogeneous mixture of enamel from over 40 teeth. The grains were irradiated after crushing and the test did not address some of the effects we have described above. The results were as follows:

1000 mGy samples: ± 25% for 6 labs
500 mGy samples: ± 25% for 5 labs
250 mGy samples: ±100 mGy for 5 labs
100 mGy samples: ±100 mGy for 4 labs
0 mGy samples: ±100 mGy for 4 labs

No laboratory achieved ±10% for analysis of the 100 mGy samples. The report of the Utah groups findings in the process of participating in this effort are summarized in Appendix 17.

The second was a bilateral intercomparison between our laboratory and that of V. Chumak and S. Sholom in the Ukraine. This intercomparison involved measurement of teeth which were irradiated prior to crushing. The results (Appendix 18) showed that at dose levels of approximately 250 mGy, doses could be measured with an accuracy of approximately 25%. Methods were used by both laboratories to quantify the dose from dental x-rays that the teeth may have received.

An additional intercomparison is planned which will examine effects associated exclusively with different methods of sample preparation and analysis (Appendix 19).

Dental x-rays

Our analysis of teeth removed at a local dental clinic indicates that x-ray doses may not be has high as we had previously feared (Appendix 18). The use of a lead sheet behind the x-ray film as well as the localized exposures makes it unlikely that doses in excess of 10 mGy will be delivered to a given tooth during a routine series of x-rays. Since adult teeth are currently used for analyses, x-rays given prior to ingrowth of secondary teeth will not be a consideration. This coupled with the fact that dental

visits tend to decline significantly in adulthood means that lifetime doses to adult teeth should rarely reach 50 mGy.

Problems identified with EPR analyses

The transient radiation induced signals, light induced signals, and the grain size effect are all potential sources of error in EPR analysis. Fortunately, with a knowledge of these effects, errors may be avoided by appropriate preanneal in the case of the transient signals, using only molars or wisdom teeth in the case of the light induced signals, and treating the sample with NaOH prior to analysis, or using whole teeth or large portions of teeth in the case of the grain size effect.

Distribution of Information

The results of our studies and the current status of retrospective dosimetry using EPR and/or TL have been reported to the radiation measurement community through invited talks at IRPA96 (Appendix 20), the 2nd Hiroshima Semipalatinsk Workshop (Appendix 12), the International Workshop on Radiation Exposures by Nuclear Facilities (Appendix 21), (Appendix 22) and the Space Radiation Damage and Biodosimetry Workshop (Appendix 23). A collaborative paper summarizing chromosomal as well as solid state methods has been submitted to Radiation Research (Appendix 24).

Luminescence Research

Alpha Dose Measurements in Ceramic Toilet Tanks

In an effort to address the need for retrospective dosimetry of alpha and beta emitters in previously contaminated water supplies we have investigated methods for measuring doses deposited on the inner surface of toilet tanks using luminescence techniques. Because the range of alphas and low energy betas may be only micrometers, traditional thin section methods for obtaining dose versus depth profiles are not feasible. We instead developed a method which involves removal of the outer portion of thin sections by surface polishing. Measurements can then be made on a number of sections from which successively deeper layers have been removed. We have thus been able to generate a dose versus depth profile from artificially irradiated porcelain tanks which corresponds to the

absorption profile calculated from measurement of thin sections removed from the exposed surface. Development of the technique was the subject of a Master's thesis, a draft of which is included in Appendix 25.

Automation of TL Imaging and Analysis Software

Many luminescence laboratories throughout Europe involved in joint dosimetry efforts with the Former Soviet Union use Riso TL readers manufactured in Denmark. Our laboratory uses custom manufactured TL readers made through the joint effort of Daybreak Nuclear and Medical Systems and the University of Utah. Over the past 10 years we have developed an extensive suite of software tools to control our data collection equipment and to perform a variety of types of analysis for retrospective measurements. As a part of this study we have modifed our software allowing control of laser input and control of our TL and OSL imaging systems. Unfortunately the software for the Riso reader is less well suited for retrospective dosimetry and much more difficult to use. At the suggestion of researchers in laboratories which use the Riso equipment we have adapted the software for compatibility with the Riso system. This will greatly simplify the training procedures for those laboratories in the FSU which will obtain Riso luminescence system. The software capabilities are described in Appendix 26.

Scientific training and exchange

Our experience in the development and application of dosimetry techniques for accident situations has put us in a unique position to contribute to the development, coordination and implementation of quality assurance programs in laboratories currently, or soon to be, engaged in the measurement and dissemination of dosimetry information. During the course of the contract we have hosted visiting scientists from three regions of the former Soviet Union. Dr. Alexi Kondrashov from Obninsk visited the laboratory for a period of 2 weeks for preliminary training in TL techniques. Drs. S. Sholom and V. Chumak visited for two weeks to complete a blind bilateral intercomparison and Dr. Sholom visited again for a period of two months in the spring of 1996 for an extensive period of basic EPR research. We are currently hosting Mr. Nickolai Bougrov from the Urals for training in TL techniques for a period of 2 months.

Our luminescence software allows remote data collection and analysis over the internet. We are pilot testing this software by providing Nick Bougrouv remote software which he will use on his return to Russia. Samples left in our laboratory will be run remotely and his training in TL

techniques can continue. Since many of the startup laboratories which hope to be engaged in TL measurements are not yet functional, this method may provide not only inexpensive training under our supervision, but also the analysis and characterization of field samples long before they would otherwise have been examined.

Collaboration with Dosimetry Efforts of the European Community.

In addition to ongoing collaborative efforts with individual laboratories in Europe and the former Soviet Union, we have accepted an invitation to participate in a collaborative dosimetry project under Framework IV (FIV) of the European Union (EU). The project involves laboratories throughout Western Europe and includes laboratories in the Former Soviet Union (FSU) under a complementary program known as Copernicus. The purpose of these programs is to assess the feasibility of solid state and biological methods for retrospective dosimetry as well as modeling efforts which may be applied to accident sites in the FSU. The projects are built on two previous programs with which we have been involved, most recently the EU program ECP-10, and an IAEA Cooperative Research Program originally established through our initiative.

Our involvement with the FIV program provides the opportunity of full participation and significant input into the design and implementation of the research program. Funding is severely limited for all participants of the program, however funds to all workshops and contractors' meetings are being provided for our participation.

The collaboration of our laboratory with others throughout Europe and the FSU involved in retrospective dosimetry provides an opportunity to leverage limited research funds and to pool the scientific expertise and analytical capabilities of established laboratories with those which are just entering the field. The inclusion of startup laboratories into the collaborative effort insures that the quality of research and routine dosimetric measurements which they will ultimately produce will conform to protocols and guidelines to be established through the FIV and Copernicus efforts. This quality assurance is also in the interests of ongoing bilateral epidemiological studies between the U.S. and FSU.

Our participation with the European Community dosimetry effort has involved close collaboration on both TL and EPR projects. We participated in a field trip from Moscow to Kiev in 1995 involving sample collection and training of FSU scientists in methods of sample collection

and documentation. We are involved in ongoing intercomparisons with laboratories at Obninsk as well as laboratories in Kiev and the Urals.

The scope of the Framework IV program for TL and EPR is extensive and will require additional support if we are to participate effectively. Appendix 19 is an outline of the current protocol for determination of preparation effects associated with EPR analysis of tooth enamel which was developed with our input at the first contractors meeting in May. This study alone will require approximately 1 year for completion and is only one of many envisioned for the project.

Collaboration with Ukrainian Scientific Center for Radiation Medicine (USCRM).

We have worked very closely with Drs. Chumak and Sholom of the USCRM over the past several years. Both investigators visited our laboratory for research purposes, Drs. Chumak and Sholom in September of 1995 for a two week period, and Dr. Sholom again in April of this year for a period of two months. In December of 1995, Robert Hayes of our laboratory visited the USCRM for training in the sample preparation and analysis techniques in use at their facility. The collaboration has resulted in a number of publications involving potential problems and solutions to environmental and preparation effects associated with EPR dosimetry of enamel. It has also included a bilateral, blind intercomparison of artificially dosed teeth, as well as joint analyses of matching teeth from Chernobyl liquidators. The research has identified areas requiring further research to assess the potential impact on EPR dosimetry and we propose to continue the collaboration in the directions which have been identified. These areas include further investigation into the effect of solar radiation on tooth enamel, the effect of sample rotation on reducing lower limits of detection, the influence of transient irradiation effects on dose estimates, and the influence of annealing procedures on organic portions of enamel.

The USCRM is also initiating TL measurements on ceramics and porcelain insulators taken from the contaminated areas as well as the power plant itself. The USCRM has little previous experience with TL analysis and we feel that it is important to provide training and oversight for these measurements. We propose bilateral training visits between our two laboratories and replicate measurements on actual field samples as well as intercomparisons on blind irradiated samples in a manner similar to that performed on irradiated enamel.

Collaboration with the Urals Research Center for Radiation Medicine (URCRM)

Nickolai Bougrov of the URCRM is presently visiting our laboratory for a period of two months for training in the techniques of TL preparation and analysis. His laboratory in the Urals is not yet established, however once equipped it will be involved in routine measurement of ceramic and porcelain samples removed from the contaminated regions of the Urals. We anticipate close cooperation during the training phase and during the establishment of the analytical capabilities of his laboratory.

Collaboration with the Urals Institute of Metal Physics.

Dr. Alex Romanyuhka has spent considerable time in the EPR laboratory of Dr. Albrecht Wieser at GSF in Germany and is developing considerable expertise in EPR analysis of enamel. We have collaborated with Dr. Romanyuhka and Dr. Wieser on development oı methodology for EPR analysis of internal emitters using differential measurements of dentine in addition to enamel, and we anticipate continued collaboration on methodology and analysis of enamel samples collected from individuals in the exposed regions of the Urals.

Collaboration with the Medical Radiological Research Center (MRRC), Obninsk, Russia

Dr. Alexi Kondrashov from the MRRC visited or laboratory for training in TL techniques and for analysis of samples of electrical insulator brought from regions of Russia contaminated by Chernobyl fallout. In August of 1995 EH visited the MRRC and participated in the EU program of field work in Russia, Belarus and the Ukraine involving training in sample collection, background dosimetry and documentation of ceramic samples from contaminated regions.

Recommendations

General Recommendations

EPR dosimetry of enamel is in a very rapid stage of development. At this point nothing has been observed to cast fundamental doubt on the validity of the technique for retrospective accident dosimetry. It appears that measurement of doses of less than 100 mGy will be feasible on a routine

basis in the near future, and that doses of less than 50 mGy will be possible with additional effort. As sensitivities reach these and lower dose levels the contribution from dental x-rays will become increasingly important. Dental x-ray doses to the general population have been examined in Japan and it would be useful to have a similar data set for x-rays in the U.S. as well as exposed regions of Russia and the Ukraine. The U.S. military personnel who were exposed to above ground testing are now reaching the age where periodontal disease will necessitate removal of teeth in many individuals. These teeth would make excellent lifetime dosimeters which would retain a record of exposure to radiation from nuclear exercises.

Specific Recommendations

Collaboration with Dosimetry Efforts of the European Community.

1) Participation in EPR group of the FIV project, if continued, will involve selection, preparation and analysis of 10 teeth as specified in Appendix 19. The purpose of this study is to determine the uncertainties associated with different methods of preparation and analysis of enamel samples.

2) Participation in the TL group of the FIV project will involve intercalibration and intercomparison of approximately 10 brick, tile and porcelain insulator samples taken from contaminated regions in the FSU. A set of bricks from Zaborie, a contaminated settlement in Russia has been collected and should be analyzed for comparative purposes. Samples should also be analyzed from the Ukraine as well as the Urals region of Russia. We recommend participation in two contractors meeting in Germany. Travel funds will be provided by the European Union project, Framework IV.

Collaboration with Ukrainian Scientific Center for Radiation Medicine

1) Work with the USCRM should involve close collaboration on problems identified in recent collaborative efforts. We propose to verify the depth of penetration of UV light into enamel and devise protocols for removal of light exposed regions of teeth. The USCRM has developed the capability of measurement using a constant rotation goniometer similar to the one developed by us. Measurement of large, intact portions of enamel should be undertaken to assess the extent of

reductions in sample preparation time which may be achieved. Our current results indicate that virtually all sample preparation can be eliminated with the use of goniometry. A second intercomparison should be undertaken between the two groups, USCRM using their standard methods of sample purification, and our laboratory using goniometry on portions of sample from the same teeth. We should also expand our intercomparison on liquidators' teeth using the methods deemed most suitable for analysis based on the results of the previously mentioned study.

2) We recommend a TL training visit to our laboratory by Dr. Sholom. The visit would involve training in methods for sample preparation and analysis. Dose depth profiles would be obtained for brick, tile and porcelain insulators. Dr. Sholom should also be trained on our remote control and analysis capabilities accessible from the Ukraine via the internet to our laboratory equipment. We suggest a working visit to the USCRM for purposes of training in sample collection as well as TL analysis on existing equipment in their facility. Their equipment is best suited for personnel dosimetry with commercial TLDs, however the group has had some success in analysis of quartz from brick and tile.

Collaboration with the Urals Research Center for Radiation Medicine

1) Nickolai Bougrov is present in our laboratory as a visiting scientist. He is being trained in techniques for sample preparation and TL analysis on our equipment and has brought with him five samples from the Chelyabinsk region. The initial analyses performed on these samples will be useful in characterizing the TL from samples from the region and will provide preliminary measurements on dose from selected structures. Other samples from the same structures have been analyzed by Dr. Y. Goksu at GSF and a joint paper will result from comparison of our analyses performed with the quartz inclusion method with her analyses performed with the fine grain technique. Additional samples will be sent to our laboratory as they are collected for analysis by us and, as with the USCRM, by remote analysis. A trip to the URCRM is recommended for additional sample collection, background dosimetry and analysis on the URCRM once it is obtained and in operation.

Collaboration with the Urals Institute of Metal Physics.

1) Many teeth have been collected in the Urals region under the initiative of Dr. Romanyuhka. Some of these have been analyzed at GSF in collaboration with Dr. Wieser. We propose replicate analysis on a set

of teeth for which more than one tooth has been removed from an individual during the course of routine dental extraction. These analysis would be performed in our laboratory by Dr. Romanyuhka during an extended visit. Some of the teeth collected have also been analyzed for internal emitters (Sr-90, Pu-239) using a Soxhletting technique. We propose to analyze a subset of the teeth using soxhletting extraction of the organic material from the dentine. Once the laboratory of Dr. Romanyuhka is operational we propose to visit the facility and assist with replicate measurements on his equipment. A blind intercomparison and intercalibration should be performed once the laboratory is operational.

Collaboration with the Medical Radiological Research Center

In addition to the TL work being initiated at the MRRC, a massive effort in EPR dosimetry of teeth has been undertaken. Over 2,000 teeth have been analyzed from contaminated regions of Russia, and the expertise in EPR dosimetry which has resulted is enormous. We feel that the participation of such highly experienced laboratories as the MRRC would be of great benefit to the overall program of enamel EPR dosimetry involving the Chernobyl accident as well as exposure from the Mayak facility. Since replication and verification of results is a goal of the dosimetry program, the participation of independent laboratories may have significant scientific benefits.

APPENDICES

Number	Title
1.	EPR Properties and Dose Response of Hydroxyapatite and Carbonated Apatites. (Submitted to *Calcif. Tissue Int.*)
2.	Light Sensitivity of EPR Signals in Enamel. (Not submitted in deference to other independent discoveries of the same effect, May 1995)
3.	Properties of Light Induced EPR Signals in Enamel and Their Possible Interference with Gamma-Induced Signals. (in preparation)
4.	Effect of Mechanically Induced Background Signal on EPR Dosimetry of Tooth Enamel. (*Radiat. Meas.* **24**(3): 245-254, 1995)
5.	Preparation-induced Errors in EPR Dosimetry of Enamel: Pre- and Post-crushing Sensitivity. (*Radiat. Meas.* in press)
6.	Influence of Crushing and Additive Irradiation Procedures on EPR Dosimetry of Tooth Enamel. (In preparation)
7.	EPR Dosimetry of Bone Gains Accuracy by Isolation of Calcified Tissue. (*Appl. Radiat. Isot.* **45**(4):525-526, 1994)
8.	Dentine as an EPR Dosimeter for Determination of ^{239}Pu and ^{90}Sr Doses to Internal Organs: A Feasibility Study. (Proposal)
9.	Electron Paramagnetic Resonance Dosimetry of Dentine Following Removal of Organic Material. (*Health Phys.* **68**(4):579-584, 1995)
10.	Improved Accuracy of EPR Dosimetry Using a Constant Rotation Goniometer. (*Radiat. Meas.* in press)

11. EPR Dosimetry of Whole Deciduous Tooth using a Constant Rotation Goniometer and Background Subtraction with a Dentine Standard. (In preparation)

12. EPR Dosimetry of Teeth in Past and Future Accidents: A Prospective Look at a Retrospective Method. (Presented at the Third Workshop for the Evaluation of Atomic Bomb Radiation Doses in Hiroshima and Nagasaki. Japan. July 26-27.)

13. A Mathematical Approach to Optimal Selection of Dose Values in the Additive Dose Method of EPR Dosimetry. (*Radiat. Meas.* in press)

14. Optimal Design for Error Minimization in Single Variable Linear Regression Extrapolation. (Submitted to *SIAM Journal on Applied Mathematics*)

15. Plasterboard as a Potential EPR Emergency Dosimeter. (In preparation).

16. Plasterboard as an Emergency EPR Dosimeter. (*Health Phys.* **71**(1):95, 1996)

17. Interlaboratory Comparison of EPR Techniques for Measuring Radiation Exposure of Enamel (ECP-10 Project): Report by the TL/EPR Laboratory of the University of Utah. (Internal report)

18. An EPR Intercomparison Using Teeth Irradiated Prior to Crushing. (*Radiat. Meas.* in press)

19. FIV, Dose Reconstruction, EPR with teeth - Investigations on sample preparation techniques. (Intercomparison protocol)

20. Retrospective Dosimetry using EPR and TL Techniques: A Status Report. (Presented at the International Congress on Radiation Protection. Vienna, Austria April 15-19, 1996)

21. Luminescence Techniques for Dose Reconstruction in Accident Situations: Technical Aspects and Results of Application. (Presented at the International Workshop on Radiation Exposures by Nuclear Facilities-Evidence of the Impact on Health. Portsmouth, England July 9-12, 1996)

22. Luminescence Techniques for Dose Reconstruction in Accident Situations Possibilities, Limitations and Uncertainties. (Presented at the International Workshop on Radiation Exposures by Nuclear Facilities-Evidence of the Impact on Health. Portsmouth, England July 9-12, 1996)

23. EPR Techniques for Space Biodosimetry. (Presented at the Space Radiation Damage and Biodosimetry Workshop, Houston, Texas Sept. 9, 1996)

24. Challenges in Dose Reconstruction: Examples from Chernobyl, Hiroshima, Biomarkers and Environmental Materials. (Submitted to *Radiat. Res.)*

25. Thermoluminescence Measurement of Externally Applied Alpha Doses. Masters Thesis (Maureen Lynn Gilbert, Draft, Aug, 1996)

26. The Development of a Computer Control System for Retrospective Luminescence Dosimetry. (Instruction manual written at the Center for Applied Dosimetry, University of Utah, 1996)

APPENDIX 1.

EPR Properties and Dose Response of Hydroxyapatite and Carbonated Apatites. (Submitted to *Calcif. Tissue Int.*) Reprint removed at

APPENDIX 2.

Light Sensitivity of EPR Signals in Enamel. (Not submitted in deference to other independent discoveries of the same effect, May 1995)

LIGHT SENSITIVITY OF EPR SIGNALS IN ENAMEL

E.H. Haskell, R.B. Hayes and G.H. Kenner*
Division of Radiobiology, College of Medicine, University of Utah,
Salt Lake City, UT 84112

ABSTRACT

We have investigated the Electron Paramagnetic Resonance (EPR) signal which appears at Lande value, g = 2.0038 when enamel is crushed. This signal is sensitized by exposure to light while the perpendicular component of the hydroxyapatite signal at g = 2.0018 is apparently unaffected. Further, we determined that the light exposed, mechanically induced signal attenuates with time and have verified that its intensity decreases with increasing power.

Key words: enamel, EPR, radiation, teeth, hydroxyapatite, light

INTRODUCTION

The nuclear accident at Chernobyl, recent incidents in Estonia, Taiwan and the former Soviet Union and concerns about the aging of nuclear plants world-wide, have stimulated renewed interest in retrospective dosimetry of environmental and biological materials. Of particular concern are questions about sensitivity and reproducibility of the methods used. Problem areas identified

include the effects of mechanical trauma during sample preparation, temperature, machine operating parameters and exposure to light (Nakajima 1982; Nishiwaki and Shimano 1990; Rhodes and Grun 1991).

Electron Paramagnetic Resonance (EPR) of hard tissues has been shown to be a powerful tool for estimating radiation exposures (Brady et al. 1968; Caracelli et al. 1986; Desrosier 1991; Desrosier et al. 1991; Haskell et al. 1995; Ishii and Ikeya 1990; Pass and Aldrich 1985; Pass et al. 1990; Regulla and Deffner 1989; Sagstuen et al. 1983; Swartz 1965; Wieser et al. 1994) as well as for dating geological events (Grun et al. 1990; Hennig et al. 1981; Ikeya and Miki 1980; Rink and Schwarcz in press; Stringer et al. 1989). Unfortunately, it is subject to artifacts resulting from sample preparation.

A mechanically induced, radiation sensitive signal with a Lande factor of g = 2.0038 is formed when enamel is crushed during sample preparation (Desrosier et al. 1989; Polyakov et al. in press; Tatsumi-Miyajima and Okajima 1985). This signal overlaps the perpendicular component of the hydroxyapatite signal resulting in incorrect estimates of the equivalent dose (ED) (Polyakov et al., in press). The purpose of this study was to determine the possible light sensitivity of the mechanically induced and hydroxyapatite signals.

MATERIALS AND METHODS

Enamel grains, 150-250μ in diameter, were scanned, irradiated with 1.5 Gy using a ^{60}Co source† and rescanned, followed by

illumination for 17 hours with a 30W quartz halogen microscope lamp[‡] rated at 10,000 foot candles at 3 feet, and a third scanning.

The specimen was remeasured one week later. An additional scan was made with the power set at 127 mW. The other parameters remained the same. The 127 mW signal was not normalized for the power increase.

The EPR analysis was done using a conventional X band spectrometer[§] . Parameters used were power, 8 mW, field modulation, 100 kHz, modulation amplitude, 0.5 mT, room temperature, receiver gain of 1 x 10^5, microwave resonance frequency of 9.74 gHz. Scan width was 5.0 mT. Weak pitch was used as the reference standard.

A spectrum consisted of 10 scans over a 4.3 min time period. Ten spectra were made for each data point in the first experiment while three spectra were made for each data point in the second part. The sample was shaken and rotated between taking each spectrum. Approximately 100 mg of powder was placed in a 1/4 inch x 7 inch (0.635 cm x 17.8 cm) quartz EPR sampling tube[‖] . The samples were stored at room temperature and low (ambient) humidity.

RESULTS

Figure 1 shows EPR spectra of the specimen measured before irradiation, after ^{60}Co irradiation with 1.5 Gy, followed by illumination for 36 hours with a quartz halogen microscope lamp. The Lande centers of the perpendicular (g = 2.0018) and parallel (g =

1.9960) components of the hydroxyapatite signal and the mechanically induced signal (g = 2.0036) are shown.

The magnitude of the mechanical signal is increased by irradiation and exposure to light (peak A and inverse peak C). The perpendicular component of the hydroxyapatite signal is apparently not affected by light (concurrency of peak B). Exposure to light causes a slight increase in the size of the parallel component of the hydroxyapatite signal which may be due to noise.

Figure 2 shows the results of remeasuring the specimen, 30 days later. The size of the light exposed mechanical signal was decreased (peak A and inverse peak C). Increasing the power to 127 mW resulted in a disappearance of the mechanically induced signal.

DISCUSSION

A survey of the EPR literature of bone and teeth show that a number of signals have been reported which must be distinquished from each other. Minor problems arise in doing this because of variations in the values reported for the perpendicular component of the hydroxyapatite signal which range from 1.996 to about 2.004. Our method of getting around this problem is to arbitrarily assign the value of g = 2.0018 to this signal and adjust the other signals accordingly. A Lande value of g = 2.0018 was selected because there appears to be a consensus among workers that this is the correct value.

If this is done then major, documented signals have been reported at 2.0048, 2.0038, 2.002, 2.0018 and 1.9960. The signal at

$g = 2.0048$ is generally believed to be of organic origin. It is not present in enamel or deorganified dentine. The signal at $g = 2.002$ (Desrosiers et al, 1989) is caused by severe mechanical trauma such as using a dental drill to create enamel granules. This is probably the signal reported by Marino and Becker 1968, when bone grains are prepared using a ball mill. The signals at $g = 2.0018$ and $g = 1.9960$ are the perpendicular and parallel components of the hydroxyapatite signal.

The signal reported at $g = 2.0038$ in enamel is caused by the mechanical trauma associated with gentle crushing. Whether it is organic or inorganic in origin is unknown. Evidence suggesting organic origin is saturation behavior similar to that of the $g = 2.0048$ signal when microwave power is increased. Also, the signal is absent in deorganified dentine (Haskell et al., 1995). Polyakov et al. (in press) showed that it is radiation sensitive.

Exposure to light has been shown to bleach signals used to measure radiation exposure using thermoluminescence (TL) and optically stimulated luminescence (OSL) techniques. Exposure can occur while the specimens are "in situ" in the field, or during sample preparation in the laboratory.

Nakajima (1982) has shown that exposure to light increases the strength of the signal seen in lucite following irradiation. He concluded that the differences could probably be ignored.

Although the magnitude of the perpendicular component of the hydroxyapatite signal is probably not affected by light, serious errors occur because of the extensive overlap which occurs between it and

the mechanically induced signal. This error can result in serious dose overestimates if corrections are not made.

The two principle areas where light might be a problem are exposure of the teeth when the mouth is open subsequent to radiation exposure, and during storage and processing of teeth once they have been extracted.

The near absence of any effect by light on the perpendicular and parallel components of the hydroxyapatite signal would indicate that there is no need for concern until processing of the extracted teeth has begun. Following extraction, storage in the dark is possibly good technique though probably not necessary.

Potential problems should not occur until the dentine is separated from the enamel. In our laboratory, this is done by separating the root and the crown with a cut-off saw. The dentine is removed from the crown by grinding it out using a dental drill under illumination from a circular-shaped fluorescent lamp. At this point, there would be minimal trauma to the enamel because the majority of the damage is done to the dentine. Further evidence of minimal trauma is the absence of the $g = 2.002$ signal reported by Desroisiers in the final processed specimens.

The mechanical trauma to the enamel is done by crushing the caps in a hydraulic press. From this point onwards, care should be taken to avoid exposing the specimens to light.

The signal can be eliminated by increasing the EPR power, a procedure recommended by Pass et al. (1990), Desrosiers et al. (1993) and Copeland et al. (1993). While it is tempting to minimize the effect of the mechanically induced signal in this manner while

increasing the magnitude of the inorganic signal, there are some theoretical problems involved. Foremost among these is decreased ability to separate overlapping signals. It is also important to remember that following microwave power saturation, EPR signals become smaller and possibly increase in width (Wertz and Bolton, 1986).

Possibly the best method for determining optimum EPR power, is to do a study in which the errors are determined at various power levels and use the data to select an optimum.

CONCLUSION

The mechanically induced signal generated at g = 2.0038 is sensitive to light. The effect can be minimized by controlling lighting during sample preparation.

Light has minimal or no direct effect on the hydroxyapatite signals located at g = 2.0018 amd g = 1.9960, hence it should not be a problem until the specimen has been crushed.

Acknowledgements

This work was supported by U.S. Department of Energy Contract DE-FC08-89NV10805.

REFERENCES

Brady, J.H.; Aarestad, N.O.; Swartz, H.M.; In vivo dosimetry by electron spin resonance spectroscopy. Health Physics 15: 43-47; 1968.

Caracelli, I.; Terille, M.C.; Mascarenhas, S.; Electron Spin Resonance Dosimetric Properties of Bone. Health Physics 50: 259-263; 1986.

Copeland, J.F.; Kase, K.R.; Chabot, G.E.; Greenaway, F.T.; Inglis, G.B.; Spectral energy effects in ESR bone dosimetry: photons and electrons. Appl. Radiat Isot. 44: 101-06; 1993.

Desrosiers, M.F.; Simic, M.G.; Eichmiller, F.C.; Johnston, A.D.; Bowen, R.L.; Mechanically-induced Generation of Radicals in Tooth Enamel. Int. J. Radiat. Appl. Instrum. Part A 40: 1195-1197; 1989.

Desrosiers, M.F.; In vivo assessment of radiation exposure. Health Physics 61: 859-861; 1991.

Desrosiers, M.F.; Coursey, B.M.; Avila, M.J.; Parks, N.J.; Radiation doses. Nature 349: 287-289; 1991.

Desrosiers, M.F.; Avila, M.J.; Schauer, D.A.; Coursey, B.M.; Parks, N.J.; Experimental validation of radiopharmaceutical absorbed dose to mineralized bone tissue. Appl. Radiat. Isot. 44: 459-463; 1993.

Grun, R.; Beaumont, P.B.; Stringer, C.B.; ESR dating evidence for early modern humans at Border Cave in South Africa. Nature 344: 537-539; 1990.

Haskell, E.H.; Kenner, G.H.; Hayes, R.B.; EPR dosimetry of dentine following removal of organic material. Health Physics 68: 579-584; 1995.

Hennig, G.J.; Herr, W.; Weber, E.; Xiroti, N.I.; ESR dating of the fossil hominid cranium from Petralona Cave, Greece. Nature 292: 533-536; 1981.

Ikeya, M.; Miki, T.; Electron spin resonance dating of animal and human bones. Science 207: 977-978; 1980.

Ishii, H.; Ikeya, M.; An Electron Spin Resonance System for In-vivo Human Teeth Dosimetry. Jap. Jnl. of Appl. Phys. 29: 871-875; 1990.

Marino, A.A.; Becker, R.O. Mechanically induced free radicals in bone. Nature, 218:466-467; 1968.

Nakajima, T.; The use of organic substances as emergency dosimeters. Int. J. Appl. Radiat. Isot. 33: 1077-1084; 1982.

Nakajima, T.; Sugar as an emergency populace dosimeter for radiation accidents. Health Physics 55: 951-955; 1988.

Nishiwaki, Y.; Shimano, T.; Uncertainties in Dose Estimatation Under Emergency Conditions and ESR Dosimetry with Human Teeth. Radiation Protection Dosimetry 34: 295-297; 1990.

Pass, B.; Aldrich, J.E.; Dental enamel as an in vivo radiation dosimeter. Med. Phys. 12: 305-307; 1985.

Pass, B.; Aldrich, J.E.; Scallion, P.L.; An Analysis of Paramagnetic Centers in Irradiated Dentin Using Electron Spin Resonance. Calcif. Tissue Int 46: 166-168; 1990.

Polyakov, V.; Haskell, E.; Kenner, G.; Huett, G.; Hayes, R.; Effect of mechanically induced background signal on EPR dosimetry of tooth enamel. Radiation Measurements Accepted 1994.

Regulla, D.F.; Deffner, U.; Dose Estimation by ESR Spectroscopy at a Fatal Radiation Accident. Appl. Radiat. Isot. 40: 1039-1043; 1989.

Rhodes, E.J.; Grün, R.; ESR behaviour of the paramagnetic centre at g=2.0018 in tooth enamel. Ancient TL 9: 14-18; 1991.

Rink, W.J.; Schwarcz, H.P.; Dose Response of ESR Signals in Tooth Enamel. Int. J. Radiat. Appl. Instrum., Part D: Radiation Measurements 00: 000-000; 1994.

Sagstuen, E.; Theisen, H.; Henriksen, T.; Dosimetry by ESR spectroscopy following a radiation accident. Health Physics (UK) 45: 961-968; 1983.

Stringer, C.B.; Grun, R.; Schwarcz, H.P.; Goldberg, P.; ESR dates for the hominid burial site of Es Skhul in Israel. Nature 338: 756-758; 1989.

Swartz, H.M.; Long-lived electron spin resonances in rats irradiated at room temperature. Radiation Research 24: 579-586; 1965.

Tatsumi-Miyajima, J.; Okajima, S.; ESR dosimetry using human tooth enamel. ESR Dating and Dosimetry: 397-405; 1985.

Wertz, J.E.; Bolton, J.R.; Electron Spin Resonance: 456; 1986.

Wieser, A.; Haskell, E.; Kenner, G.; Bruenger, F.; EPR Dosimetry of Bone Gains Accuracy by Isolation of Calcified Tissue. Appl. Radiat. Isot. 45: 525-526; 1994.

FIGURE CAPTIONS

Fig. 1 - Results of irradiating an enamel sample. Peak A is the upper component of the g = 2.0036 signal. Peak B is the upper component of the g = 2.0018 signal. Inverse peak C is the lower component of the g =2.0018 signal. a) circles: preirradiation. b) squares: 1 Gy ^{60}Co irradiation. c) diamonds: 1 Gy ^{60}Co irradiation followed by 17 hour exposure to light from a quartz halogen microscope lamp.

Fig. 2 - Effect of time and EPR power on the magnitude of the mechanically induced and hydroxyapatite signals. Peak A is the upper component of the g = 2.0036 signal. Peak B is the upper component of the g = 2.0018 signal. Inverse peak C is the lower component of the g =2.0018 signal. a) circles: 1 Gy 60Co irradiation. b) squares: 1 Gy 60Co irradiation followed by 17 hour exposure to light. c) diamond: same as (b) but remeasured seven days later at 8 mW. d) crosses: same as (c) except remeasured at 127 mW.

FOOTNOTES

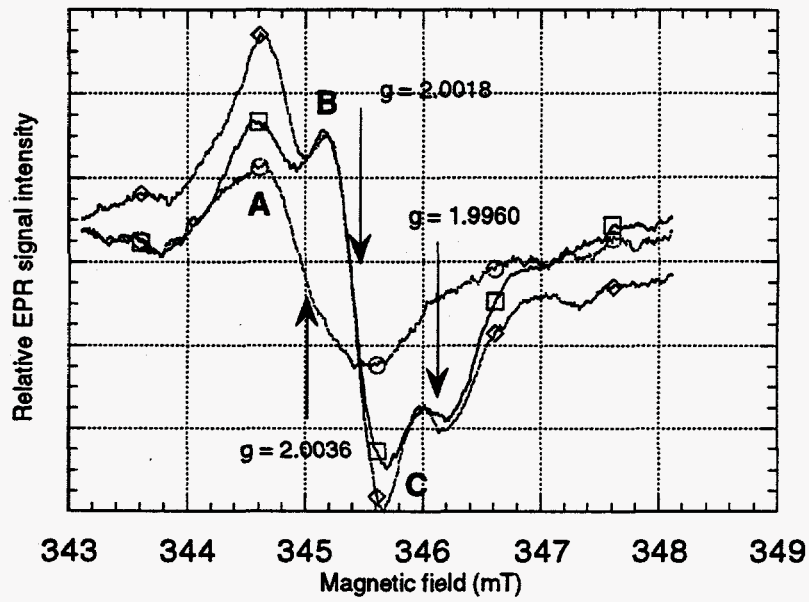
Relative EPR signal intensity
B
A
g = 2.0018
g = 1.9960
g = 2.0036
C
343
344
345
346
347
348
349
Magnetic field (mT)

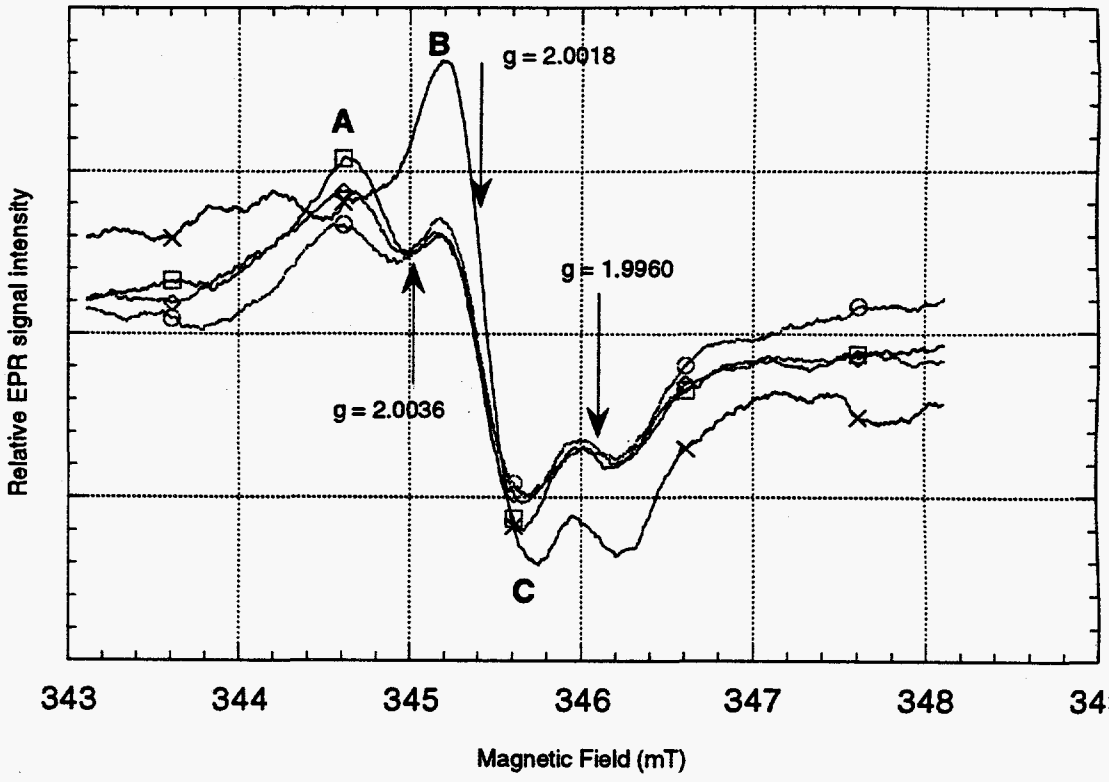
B
g = 2.0018
A
g = 1.9960
g = 2.0036
C
Relative EPR signal intensity
343
344
345
346
347
348
Magnetic Field (mT)

* Radiobiology Laboratory, Building 586, University of Utah, Salt Lake City, UT 84112
† U.S. Nuclear, 801 North Lake Street, Burbank, CA.
‡ Fiber-Lite, model 190, Dolan Jenner Industries, Woburn, MA.
§ Bruker ESP300E, Bruker Instruments, Manning Park, Billerica, MA.
‖ Wilmad Glass, Route 40 and Oak Road, Bena, NJ 08310.

APPENDIX 3.

Properties of Light Induced EPR Signals in Enamel and Their Possible Interference with Gamma-Induced Signals. (in preparation)

PROPERTIES OF LIGHT INDUCED EPR SIGNALS IN ENAMEL AND THEIR POSSIBLE INTERFERENCE WITH GAMMA-INDUCED SIGNALS

S.V. Sholom*, E.H. Haskell†, R.B. Hayes†, V.V. Chumak* and G.H. Kennert†

*Scientific Center of Radiation Medicine, Kiev, Ukraine and †Center for Applied Dosimetry, University of Utah, Salt Lake City, UT 84112

Abstract - Exposure of enamel to U.V. light (sunlight and artificial) results in EPR signals with g-factors of of 2.0018 (perpendicular), 1.9975 (parallel), 2.0045, 2.0052 and 2.0083. The first two signals correspond to the components of the radiation induced signal and the third signal corresponds to the native signal reported in dosimetry and dating studies. The remaining two signals were found to be stable and sensitive to both gamma and sunlight exposure. Their sensitivity response to light and radiation was considerably different which gives rise to the possibility that the g = 2.0052 and g = 2.0083 signals might be used as indicators of the dose resulting from light exposure.

1. INTRODUCTION

The problem of accounting for the influence of sunlight exposure on the radiation induced EPR signal in enamel has not been resolved. It is known, that sunlight affects both the signal at g = 2.0045 (Oduwole and Sales, 1991) and the anisotropic signal with $g_{\perp}$ = 2.0018, $g_{\parallel}$ = 1.9975 (Ivannikov *et al.*, in press), of which the latter is usually used for retrospective dose determination (Aldrich and Pass, 1988; Ikeya, 1994; Serezhenkov *et al.*, 1992) and archeological dating (Grun et al., 1987; Grun, 1991). This phenomena may be a real threat to EPR dosimetry, since at the present time it is not possible to distinquish

between radiation and sunlight induced fractions of the signal at $g_{\perp} = 2.0018$, $g_{\parallel} = 1.9975$. One possible solution is to exclude incisors from dosimetry studies as these are the teeth most affected by sunlight. However, such an approach seems to be oversimplified. In certain cases not only incisors, but canines and even molars may be subjected to sunlight exposure. In addition, it should be taken into account that in some cases in the states of the former Soviet Union, exposure to ultraviolet light is used as a medical procedure. In these cases dose reconstruction is even more difficult. Therefore, it would be desirable to have some indicators of possible exposure of enamel to sunlight or ultraviolet light. The present work is dedicated to establishing such criteria.

2. MATERIALS AND METHODS

Enamel grains in the size range 250-600 μm were obtained by mechanical removal of dentine from tooth caps by means of a dental drill with subsequent crushing in an agate mortar. Four samples designated S2, S5, S6 and T2 were prepared. In addition, an enamel plate with a thickness of 1.10 ± 0.01 mm was prepared by polishing bulk enamel on a diamond disk. This plate was called F2 and was used for determining the light dose profile.

The enamel samples were exposed in the following manner. The sample S5 was exposed in a plastic cuvette covered with a UV light transparent quartz plate. This plate was used to protect the sample from weathering. Exposure of this sample was only done on sunny days. The sample was exposed for a total of 10 days. The EPR spectra were collected at the end of each exposure day. Measurements were also made during the time between sunny days. The sample S6 was exposed under a wide spectrum UV lamp (Oriel, model 66187) at a distance of ca. 15 cm from lens. The EPR spectra of this sample was registered for different intervals of exposure time in the range from 1 second up to several hours. The samples S2 and F2 were exposed under a monochromatic UV lamp with a

wavelength of 254 nm (Eprom Eraser, model DE-4) at a distance 4 cm from lamp axis. The total exposure time was 8 hours, the plate F2 was exposed from two sides during 4 hours each. Sample T2 was irradiated using a Co-60 gamma-source (Isotope Product Laboratory, Burbank, CA 91504) with a dose of 80 Gy.

The spectra registration was done with a x-band EPR spectrometer, model ESP 300E, Bruker Insruments. Microwave power and modulation amplitude were varied over a wide range. Other parameters of spectra registration were as follows: modulation frequency 100 kHz, sweep width 10 mT, time constant 20 ms, conversion time 20 ms, number of accumulations 60-120. The 3rd and 4th lines of Mn2+ : MgO were used as an "in situ" standard, placed within the resonator cavity. Intensity of the EPR signals were measured as peak-to-peak values following manipulation of the original spectra. All manipulation were done after g-factor normalization of the original spectra.

The spectra of samples recorded at a microwave powers of more than 2 mW were corrected by subtracting the spectra of an empty tube which were registered under same conditions and during the same day as the spectra of the studied sample. This resulted in considerable reductions of influence of spectrometer drifts on the accuracy of low intensity signal measurements.

The spectrum of a standard native signal was subtracted when the intensity of the signal with $g_{\perp} = 2.0018$, $g_{\parallel} = 1.9975$ was measured (only the g-perpendicular component was used). This standard signal was obtained from a mixture of enamel from 30-40 non-irradiated teeth of people under 25-year age. The intensity of the standard native signal was adjusted to equal the intensity of the native signal of the analyzed spectrum.

Finally the spectrum of a standard radiation induced signal was subtracted when parameters of EPR signals with $g = 2.0052$ and $g = 2.0083$ were determined. This spectra corresponded to sample T2 and was registered more than one month after irradiation so that all transient signals had decayed. Parameters of registration were the same as for spectra of investigated sample.

Sample F2 was etched in a low concentration (0.1 %) solution of HCl to determine EPR signal intensity profiles. The spectrum of the sample was recorded after every 1.5 min. of stepwise etching.

3. RESULTS

Fig. 1 shows the results of evaluating sample S5. The parameters were chosen to comply with values actually used in EPR dosimetry. The microwave power was 10 mW and the modulation amplitude 0.5 mT. Spectrum a corresponds to the original non-irradiated sample, spectrum b to the sample after exposure on the roof for 10 sunny days. Spectra c and d were obtained as a result of subtraction according to following relationship

$$c,d = a - k \times b, \qquad (1)$$

where the coefficient k was equal to 1.0 and 2.0 for spectra c and d respectively.

The positions of the four different signals are indicated with numbers 1-4 and are defined in the caption for Fig. 1. In the next figure (Fig. 2.) the spectra of sample S6 are shown. They were recorded with the same parameters of registration as the previous ones. The spectra in Fig. 2 are as follows: spectrum a corresponds to spectrum of the sample before irradiation, spectrum b, after exposure for 15 hours under a wide-spectrum UV lamp, spectra c and d were obtained in the same way as spectra c and d in Fig. 1. For clarity, spectrum d is shown at 2X magnification.

It can be seen in Figs. 1 and 2 that ultraviolet light produces the same set of EPR signals as sunlight exposure, but with a slightly different intensity.

The spectra of samples T2 and S2 which were taken with a microwave power of 0.4 mW and modulation amplitude of 0.2 mT are shown in the Fig. 3. Spectrum a shows the T2 sample which received a gamma dose of 80 Gy, spectrum b is sample S2 after

exposure to 8 hours of monochromatic UV with a wavelength of 254 nm, spectrum c is the result of subtracting b and a according to formula (1) with some coefficient k and spectrum d is the result of subtraction of spectrum c and the scaled spectrum of sample S2 before exposure. After these manipulations we can clearly see the peak corresponding to g = 2.0052.

Fig. 4. shows the increase in signal size as a function of exposure time. Curve a corresponds to the signal at $g_{\perp} = 2.0018$, $g_{\parallel} = 1.9975$ in sample S5. This increase was expressed in terms of dose using Co-60 calibration. Curve b shows the change for the g = 2.0045 signal in sample S6. This curve was normalized to the initial value seen before exposure.

The time axis for the curve a is time of exposure to sunlight, while for curve b this is exposure time under the broad spectrum UV lamp. Curve a shows a linear growth of signal intensity with a slightly changing day-to-day increment, while the curve b saturates as a factor of 6 is approached.

Fig. 5 shows the intensity profile of signals generated by UV exposure as a function of depth from the surface of exposed sample. Curve 1 is the intensity profile of the signal at $g_{\perp} = 2.0018$, $g_{\parallel} = 1.9975$, curve 2 is the signal at g = 2.0052. Extrapolation of the experimental points was done assuming exponential decrease, the coefficients used were -0.016 mm^{-1} and -0.0092 mm^{-1} for curves 1 and 2 respectively.

4. DISCUSSION

As can be seen in Figs. 1 and 2, sunlight and UV light exposure generate the same parametric centers in enamel. This made it practical in some cases to use U.V. light generated signals as a substitute for those generated by sunlight which is relatively ineffective. In particular, g-factors and widths determined in this study were done using samples exposed under ultraviolet lamps.

An example of such a determination is shown in the Fig. 3 for the signal at g = 2.0052. It was previously found that this signal was seen better at low microwave power levels. Consequently, a microwave power 0.4 mW and modulation amplitude 0.2 mT were chosen for registration of the spectra shown in Fig. 3. The spectra of sample S2, which was exposed during 8 hours under ultraviolet lamp with wavelength 254 nm, and T2, which was irradiated with dose 80 Gy with the Co-60 source, were recorded with these parameters. A comparison of initial spectra of samples S2 and T2 (a and b in the Fig. 3) showed that gamma and UV exposure generate the same set of lines in EPR spectra, but the intensity ratio of different EPR lines was significantly different for these two types of exposure. This difference is clearly seen in the Fig. 3 for the line with g = 2.0052, where the ratio of its intensity to intensity of line at g = 2.0018 is several times higher in the case of UV exposure than for gamma-ray exposure. Properties of the signal at g = 2.0088 are quite similar, although this signal is more pronounced at the higher microwave power. In addition, this signal is normally overlapped with strong neighboring signals (as may be seen in Fig. 3, a and b).

Different intensity ratios of EPR signals in enamel after gamma and UV exposure, together with different behavior of intensity of these signals as a function of microwave power, gives rise to the possibility of separating EPR signals at g = 2.0052 and g = 2.0088 in enamel by subtraction. The final result of such subtraction is shown in the Fig. 3d, for the signal at g = 2.0052. As a criteria of correctness of the applied procedure we have used the fact that EPR spectra of enamel after sunlight and ultraviolet light exposure could be rather well described using only three different EPR signals at low microwave power and four signals at moderate levels of microwave power; two of three (four) signals are well-known EPR signals in enamel at g = 2.0045 and $g_{\perp}$ = 2.0018, $g_{\parallel}$ = 1.9975. Comparative analysis of spectra after gamma and UV exposure revealed, that gamma radiation may also produce stable EPR centers at g = 2.0052 and g = 2.0088. In particular, the enamel peak close to g = 2.0056 which is usually observed after irradiation of samples with a gamma-

dose of less than 50 Gy at low and moderate levels of microwave power, is actually a result of overlapping of two signals: one with g = 2.0052, the oother at $g_{\perp}$ = 2.0018, $g_{\parallel}$ = 1.9975, Therefore, this peak is not related to the native signal at g = 2.0045.

The signals at g = 2.0052 and g = 2.0088 are quite stable. There were no changes when the samples were heated to 95 C for 72 hours. The difference in yield of the described signals for various types of exposure suggests using it as a criterion to determine how much sunlight an investigated sample received. The intensity ratio of g = 2.0088 and g = 2.0018 signals after removal of the g = 2.0045 signal by subtraction, is one possible example. As may be seen in Fig. 1d, this ratio is equal to ca. 0.33 for the sample which was exposed to sunlight only. At the other extreme is exposure to gamma radiation only. In this case the ratio is close to zero. It is natural to expect that the ratio will be between 0 and 0.33 for samples exposed to both radiation and sunlight. This information could be used to correct the value of the g = 2.0018 signal.

Presently, there are many questions which need to be answered before this technique can be used. In particular, as may be seen from Fig. 5, the intensity of light-induced signals attenuate considerably with depth of enamel, and it is not yet clear whether the ratio remains unchanged or if it depends on the thickness of the enamel layer in the tooth. Solving this and other problems is necessary if we want to determine precisely contributions of sunlight exposure to intensity of EPR signal with g = 2.0018 in enamel.

The increase of intensity of the signal with $g_{\perp}$ = 2.0018, $g_{\parallel}$ = 1.9975 is illustrated in Fig. 4a. The signal induced by one sunny day corresponds to a dose of 209 mGy of gamma irradiation. Fig. 4 shows that this intensity increase varied for different days. This is probably related to varying cloud conditions, solar activity, etc., which were not taken into account.

The complex behavior of the g = 2.0045 signal also causes problems with estimating the magnitude of the g = 2.0018 signal. Concerning this problem, the intensity of the g = 2.0045 signal of sample S5 increased ca. 2.36 times on the first day and then

dropped to 1.42 times for the second exposure day. After the second exposure day the intensity change increased up to 3.09, then dropped down again to 1.68, 42 hours later. These fluctuations continued for the duration of the experiment. As can be seen in Fig. 4b, the intensity of the native signal may increase ca. 6 times due to UV exposure and then decreases to a higher than initial level after UV exposure ceases. Precise estimation of the native signal is also hampered because intensity of other EPR signals in enamel increase significantly with exposure time and these signals hinder the measurement of the signal with g = 2.0045. Anyway, it is clear that such complex behavior of the g = 2.0045 signal leads to difficulties in determination of intensity of the $g_{\perp}$ = 2.0018, $g_{\parallel}$ = 1.9975 signal if a subtraction technique is used. The following criteria of subtraction was used for getting curve a in Fig. 4. The coefficient of subtraction was selected in such a way that the resulting spectrum looked similar to curve d in the Fig. 1. Clearly, the accuracy of such a method is better when the intensity of the signal at $g_{\perp}$ = 2.0018, $g_{\parallel}$ = 1.9975 is higher, i.e. the total exposure time of the sample to sunlight was high.

Finally, a short comment the data in Fig. 5. The depth at which the signals attenuated by a factor of g = 2.718 was determined. This value was equal to 63 μm for the EPR signal with $g_{\perp}$ = 2.0018, $g_{\parallel}$ = 1.9975 and 109 μm for the signal with g = 2.0052. Taking into account that the sample used in the dose profile study was exposed to monochromatic light (with wavelength of 254 nm), the difference in intensity profiles of different EPR signals may be explained by an indirect mechanism of generating EPR centers with ultraviolet light. First, the energy is probably transferred from photons to some intermediate carriers (e.g. electrons, scattered photons, etc.) which, in their turn, interact with corresponding centers in enamel and bring them to the paramagnetic state. If this is so, then the energy of the intermediate carriers may range from minimum values up to a maximum which depends on the different free path distances. If different paramagnetic centers in enamel are generated by carriers with different energies (and mean free path distances), then we will have intensity profiles of the type seen in Fig. 5.

Using data of Fig. 5, it is possible to estimate how much enamel needs to be removed from a tooth to reduce the contribution of UV component to the total dose.

We can use the following empirical relationship to determine how much enamel to remove from incisors. The total surface area of enamel is ca. 50 mm^2. The weight of pure enamel in an incisor is ca. 150 mg. Assuming that we need to remove the surface layer to a depth of 63 μm and taking into account that the density of enamel is 2.75 g/cm^3, then ca. 86 mg of enamel should be removed. Thus, ca. 64 mg of enamel remains, which may be enough if the gamma dose is on the order of 200 mGy or more. The real loss of enamel due to etching may be significantly reduced if etching could be applied to external (front) part of incisor only. This may be achieved by cutting the tooth in two (inner and outer) parts and etching the front half only which has a dentine layer on the back. Combining the method of etching with the method of estimating the ratio of the signals at g = 2.0088 and g = 2.0018 will allow an increase the accuracy of dose determination in enamel exposed to sunlight and gamma irradiation.

5. CONCLUSION

It has been shown that exposure to sunlight will produce at least four different paramagnetic centers in enamel. Two of these centers are well-known with g = 2.0045 and $g_\perp$ = 2.0018, $g_\parallel$ = 1.9975, the other two with g-factors of 2.0052 and 2.0088 were identified in the present work by means of varying microwave power and selective subtraction of spectra. It was found that the spectra of samples exposed to sunlight and gamma irradiation have the same sets of EPR signals, but with different relative line intensities. This property combined with using intensity profiles of some the light induced EPR signals may be used to correct the g = 2.0018, g =1.9975 signal for light exposure.

Acknowledgements -- Supported by the U.S. Department of Energy, Contract DE-FC08-89NV10805 and U.S. Department of Energy by Lawrence Livermore National Laboratory under contract no. W-7405-ENG-48.

REFERENCES

Aldrich J.E. and Pass B. (1988) Determinating Radiation Exposure from Nuclear Accidents and Atomic Tests using Dental Enamel. Healht Phys. **54**, 469-471.

Chumak, V., Bailiff, I., Baran, N., Bougai, A., Dubovsky, S., Feedosov, I., Finin, V., Haskell, E., Hayes, R., Ivannikov, A., Kenner, G., Kirillov, V., Khlamidova, L., Kolesnik, S., Liidja, G., Likhtarev, I., Lippmaa, E., Maksimenko, V., Meijer, A., Minenko, V., Pasalskaya, L., Past, J., Puskar, J., Radchuk, V., Sholom, S., Skvortzov, V., Stepanenko, V., Vaher, U., Wieser, A. (in press) The first international intercomparison of EPR dosimetry with teeth: first results. *Appl. Radiat. Isot.*.

Grun R. (1991) Potential and problems of ESR dating. *Nucl. Tracks and Radiat. Meas.* **18**, 143-153.

Grun R., Schwarcz H.P., Zymela S. (1987) Electron spin resonance dating of tooth enamel. *Can. J. Earth Sci.* **24**, 1022-1037.

Ikeya M. (1994) ESR and ESR microscopy in geosciences and radiation dosimetry. *Appl. Magn. Reson.* **7**, 237-255.

Ivannikov, A.I., Skvortzov, V.G., Tikunov, D.D., et.al. (in press) Development of tooth enamel EPR-spectroscopy method for individual dosimetry: arising of stable paramagnetic centers in enamel exposed to ultraviolet and solar light illumination. *Appl. Radiat. Isot.*.

Oduwole, A.D. and Sales, K.D. (1991) ESR signals in bones: interference from Fe3+ ions and a new method of dating. *Nucl. Tracks Radiat. Meas.* **18**, 213-221.

Serezhenkov V.A., Domracheva E.V., Klevezal G.A. (1992) Radiation dosimetry for residents of the Chernobyl region: a comparison of cytogenetic and electron spin resonance methods. *Rad. Prot. Dos.* **42**, 33-36.

FIGURE CAPTIONS

Fig. 1. EPR Spectra of sample S5 recorded at 10 mW microwave power and 0.5 mT modulation amplitude. Spectrum a was collected before exposure, spectrum b - after 10 days exposure to sunlight, c - result of subtracting spectra a from spectra b using k = 1.0 (see text), d - subtraction of the same spectra, but with k = 2.0. The positions of four EPR signals, which are usually generated by sunlight or ultraviolet light, are numbered 1 through 4. The g-factors of these lines are: line 1, 2.0045, line 2, 2.0052, line 3, 2.0018 and line 4, 2.0088. The first three values correspond to the center points of the signals while the value given for line 4 is the low field maximum.

Fig. 2. EPR Spectra of the sample S2 recorded at 10 mW microwave power and 0.4 mT modulation. Spectrum a was collected before exposure, spectrum b - after 15 hours exposure to UV light, c - result of subtracting spectrum a from spectrum b using k = 1.0, d - the result of subtracting spectrum a from spectrum b with k = 2.0. See Fig. 1 for other details.

Fig. 3. Effects of gamma irradiation and UV exposure. Spectrum a - sample T2 after 80 Gy gamma ray irradiation, spectrum b - sample S2 after 8 hours of exposure with 254 nm UV lamp, spectrum c - obtained by subtracting spectrum a from spectrum b

using an arbitrary k, spectra d - result of subtracting the spectrum of sample S2 taken before irradiation (not shown in this figure) from spectrum c. The signal shown in figure is primarily line 2 (g = 2.0052).

Fig. 4. Intensity of signals with $g_{\perp}$ = 2.0018, $g_{\parallel}$ = 1.9975 (curve a) and with g = 2.0045 (curve b) as function of exposure time for the sunlight and ultraviolet light respectively. The fit to curve b is a pair of saturating exponentials fit which is indicative of multiple signals being present, a single saturating exponential gave a visually bad.

Fig. 5. Attenuation of intensity of the light induced signals in tooth enamel as function of depth from the surface of tooth. Line 1 is the signal with $g_{\perp}$ = 2.0018, $g_{\parallel}$ = 1.9975, line 2 - the signal with g = 2.0052.

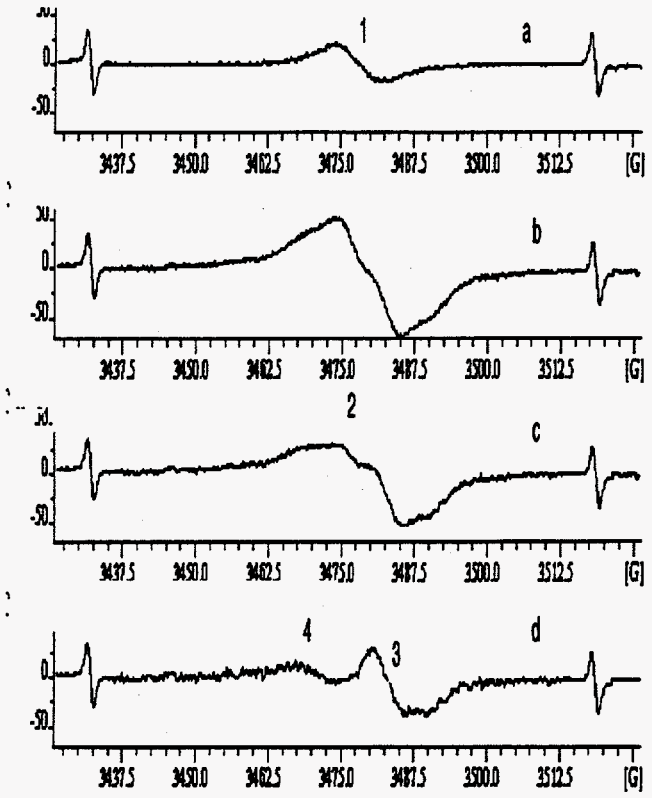
1
a
0
-50
3437.5
3450.0
3462.5
3475.0
3487.5
3500.0
3512.5
[G]
b
2
c
4
3
d

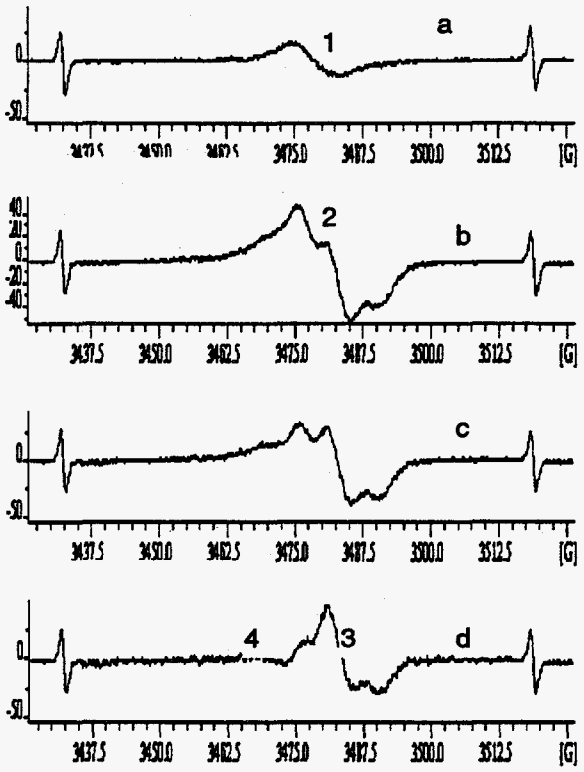
1
a
2
b
c
4
3
d
[G]

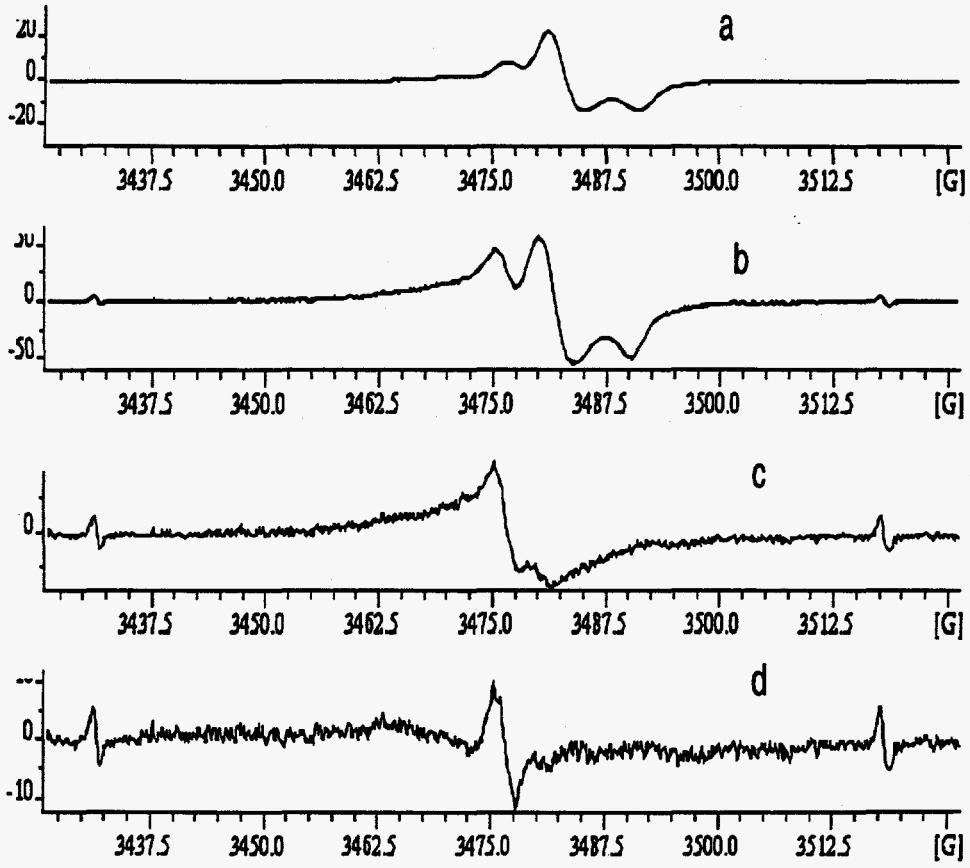
a
20
0
-20
3437.5
3450.0
3462.5
3475.0
3487.5
3500.0
3512.5
[G]
b
50
0
-50
3437.5
3450.0
3462.5
3475.0
3487.5
3500.0
3512.5
[G]
c
0
3437.5
3450.0
3462.5
3475.0
3487.5
3500.0
3512.5
[G]
d
0
-10
3437.5
3450.0
3462.5
3475.0
3487.5
3500.0
3512.5
[G]

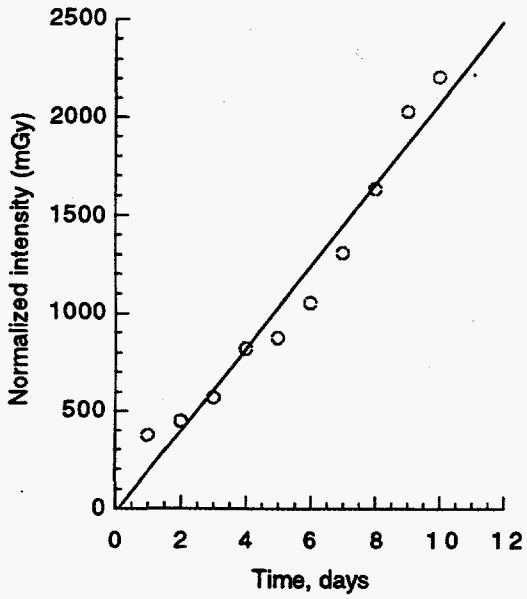
Normalized intensity (mGy)
2500
2000
1500
1000
500
0
0 2 4 6 8 10 12
Time, days

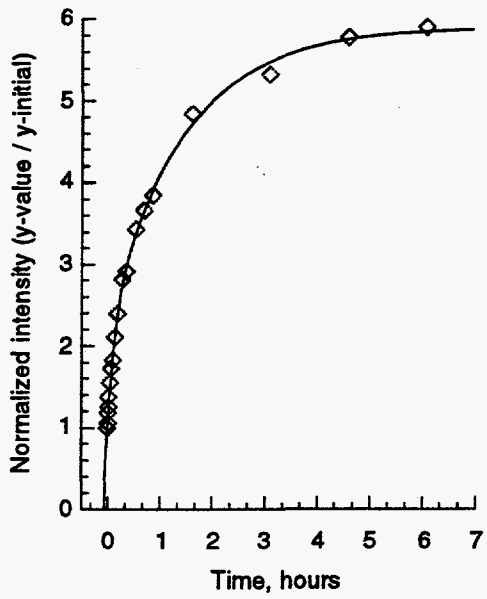
Normalized intensity (y-value / y-initial)
6
5
4
3
2
1
0
0 1 2 3 4 5 6 7
Time, hours

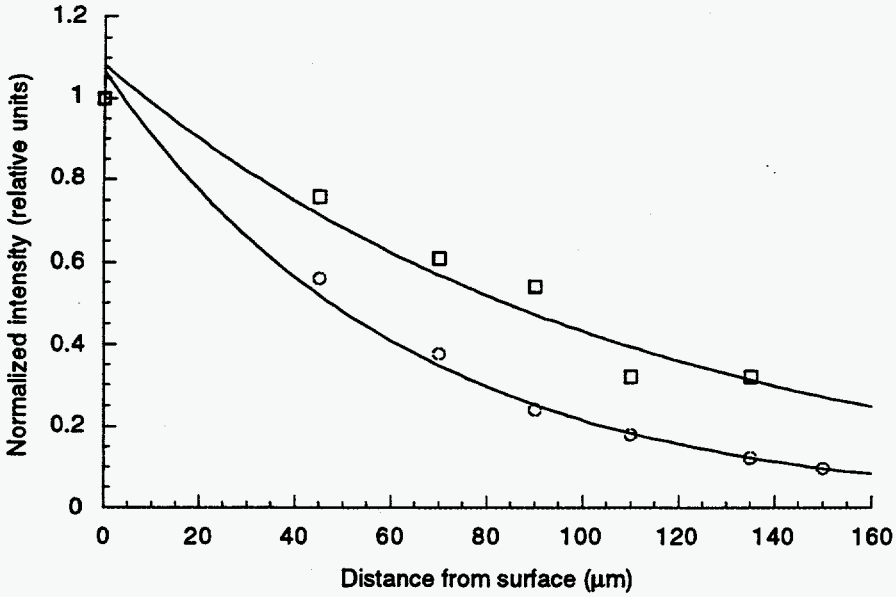
1.2
1
0.8
0.6
0.4
0.2
0
Normalized intensity (relative units)
0
20
40
60
80
100
120
140
160
Distance from surface (µm)

APPENDIX 4.

Effect of Mechanically Induced Background Signal on EPR Dosimetry of Tooth Enamel. (*Radiat. Meas.* **24**(3): 245-254, 1995)

Reprint removed for separate cycling

APPENDIX 5.

Preparation-induced Errors in EPR Dosimetry of Enamel: Pre- and Post-crushing Sensitivity. (*Radiat. Meas.* in press) preprint removed

APPENDIX 6.

Influence of Crushing and Additive Irradiation Procedures on EPR Dosimetry of Tooth Enamel. (In preparation)

INFLUENCE OF CRUSHING AND ADDITIVE IRRADIATION PROCEDURES ON EPR DOSIMETRY OF TOOTH ENAMEL

S.V. Sholom*, E.H. Haskell†, R.B. Hayes†, V.V. Chumak* and G.H. Kennert

*Scientific Center of Radiation Medicine, Kiev, Ukraine; and †Center for Applied Dosimetry, University of Utah, Salt Lake City, UT 84112

Abstract - The effect of the crushing and additive dose procedures used in EPR dosimetry of enamel was studied on the signals with g-factors of 2.0045 and $g_{\perp}$ = 2.0018, $g_{\parallel}$ = 1.9975. Eight fractions, ranging in size from <75 micrometers to 2 mm, were prepared from one tooth. Two cases were investigated: crushing of a non-irradiated sample and of a sample previously irradiated (6 Gy from ^{60}Co gamma ray source). In the non-irradiated study, the intensity of the native signal at 2.0045 increased by circa 1.75 times as the grain size decreased from maximum to minimum. A small decrease in radiation sensitivity (< 8%) was also observed with decreasing grain size. In the irradiated samples, crushing resulted in slight variations of reconstructed doses from expected values, but the worst possible case (grain sizes < 75 μm) showed that additional errors were less than 10%.

The radiation sensitivity of enamel measured immediately after exposure is underestimated. It increases by about 15% in the first month. Based on the decomposition of the observed spectra, a new interpretation of transient signals is proposed which explains the above phenomena. Recommendations about how to use this interpretaion in retrospective EPR dosimetry are given.

1. INTRODUCTION

The First international intercomparison of EPR technique using tooth enamel (Chumak *et al.*, 1996A) showed that the results obtained by different techniques may differ strongly especially at low doses, even with homogeneous enamel samples. One possible reason for this could be artifacts arising during sample preparation and irradiation procedures. The following steps are usually followed in evaluating radiation exposure.

* separation of enamel.
* preprocessing of enamel (crushing, chemical treatment, etc.).

* irradiation.

* recording of EPR spectra.

* determination of intensity of radiation induced signal.

* determination of value of the accident dose absorbed in enamel by taking into account the components due to sample preparation, irradiation, environmental exposure and diagnostic x-ray exposure.

Any of the above procedures may influence the results of dose reconstruction. It is known from the literature (Desrosiers *et al.*, 1989, Iwasaki *et al.*, 1993, Marino and Becker, 1968, Polyakov *et al.*, 1995, Tatsumi-Miyajima and Okajima, 1985), that both the native EPR signal at g = 2.0045 and the radiation-induced, anisotropic signal at $g_{\perp}$ = 2.0018, $g_{\parallel}$ = 1.9975 may change during crushing of enamel. It is also known (Oduwole and Sales, 1994), that additive laboratory irradiation generates short-lived EPR signals, which may influence the intensity of the radiation-induced signal.

The aim of this work was to investigate the influence of the enamel crushing and laboratory irradiation procedures, which are usually used in routine EPR-dosimetry. The parameters studied were intensity and radiation sensitivity of two of the main paramagnetic centers at g = 2.0045 and $g_{\perp}$ = 2.0018, $g_{\parallel}$ = 1.9975. In relation to crushing effects, this work continues the previous investigation done by Polyakov *et al.* (1995) and Haskell *et al.* (1996). Here we have extended the range of grain size fractions, and applied the subtraction method used by the SCRM (Scientific Center of Radiation Medicine AMS Ukraine), for analysis of spectra (Chumak *et al.*,1996B). In addition, we evaluated both unirradiated and irradiated samples.

Relative to laboratory irradiation, we changed the doses used by Odowole and Sales (1994), to those actually used in EPR dosimetry. Also, we investigated the details of the transient EPR signals by varying the microwave power. This results in a new interpretation of the observed EPR signals in enamel close to g = 2.0. Empirical coeffiecients were also established for correction of intensity of the signal at g = 2.0018, when measured soon after irradiation.

2. MATERIALS AND METHODS

Enamel for the experiments was obtained from routinely extracted teeth of patients less than 25 years-old at one of the student clinics in Kiev, Ukraine. The first step was the selection of samples for the crushing experiments. We decided to use enamel from only one tooth to avoid any influences of non-homogeneity of composition and properties. A very large tooth was chosen. The weight of pure enamel from this tooth was 675 mg. This tooth was designated as S1. The comparison of its EPR spectra with the spectra of other molars showed that it approximated the average intensity and shape of the native signal for grain sizes of 250-600 μm. In addition, it demonstrated average radiation sensitivity. The tooth was crushed into 4-6 big pieces using stomatological surgeon's pliars. The enamel was separated from the dentine by etching the pieces in KOH solution at 60 °C in an ultrasonic bath (Branson 1210, Shelton, Conn). The KOH solution was periodically changed. The reaction was stopped after a few days of such treatment (the precise time depended on individual properties of teeth) and only pure enamel was left in the tube. By using this type of separation we obtained enamel which was not affected by crushing.

During chemical separation some of the big pieces broke up into smaller pieces. The separated enamel was divided into two parts: one part destined for crushing before irradiation with a weight of 339 mg, and a second part, consisting of 19 large pieces with a combined weight 336 mg and average size of 2-3 mm, destined for irradiation after crushing. Thus, we considered this part as free from mechanically-stimulated signals.

The part destined for crushing before irradiation was crushed using a mortar and pestle into the following fractions, 600-850, 425-600, 250-425, 150-250, 106-150, 75-106 and <75 μm (the corresponding aliquots were designated as S1-1 to S1-7). The second part was crushed into the same fractions following irradiation (S1-8 to S1-14). Table 1 shows the characteristics of the aliquots.

The samples for investigating transient signals were obtained from a mixture of enamel from several teeth. The 250-600 μm fraction was used following crushing with a mortar and pestle. The total weight of the enamel was 1350 mg, it was divided into 17 aliquots of 76-78 mg each. The aliquots were labeled as Tr1-Tr17 and divided into pairs Tr1-Tr2, Tr3-Tr4, and irradiated withdifferent doses. The sample Tr17 was used as a native signal standard.

The specimens were irradiated with using a Co-60 source with a dose rate of 0.80 Gy/min (Isotope Product Laboratory, Burbank, CA 91504). The dose of 6 Gy was administered to the second part of sample S1 as an analog of some "unknown" accident dose.

Seven additional exposures of 2 Gy each were done to determine the radiation sensitivity of individual aliquots (Chumak *et al.*, 1995). This exposure and corresponding EPR scanning was done on all aliquots of sample S1 on the same day. This reduced possible errors due to daily variations in EPR spectrometer performance. The Tr1-Tr16 aliquots were irradiated with 0.5 Gy - 100 Gy. One of each pair was annealed at 95 C for 2 hours, while the other was used to observe daily changes in the intensity of the EPR signals at ambient temperature.

Recording of EPR spectra was done using an x-band EPR spectrometer (Bruker, model ESP300E). If not stated otherwise, the following parameters were used, microwave power 10 mW, modulation frequency 100 kHz, modulation amplitude 0.4 mT, sweep width 10 mT, time constant 20 ms, conversion time 20ms, 30 to 60 sweeps. Calibration of g-factor values was done using the third and fourth lines of a Mn2+:MgO standard continuously placed in the resonator.

The intensity of the $g_{\perp}$ EPR signals were measured peak-to-peak after corrections were made on the original spectra which included subtraction of an empty tube spectra, recorded during the same day and with the same parameters as the sample (exceptions were made for high doses and low power where the influence of resonator baseline instability was negligible). An addtional subtraction of the native signal was done during measurement of the radiation induced signal. In this case, the maxima of the native signal of the standard spectra is adjusted until it is the same as the maxima of the native signal of the the radiation induced spectrum.

3. RESULTS AND DISCUSSION

3.1 *Crushing experiment.*

Crushing of non-irradiated samples mainly results in a dependence of native signal intensity on grain size (Fig. 1). We can see that intensity of the native signal has a tendency to monotonically increase within the investigated size range from 1, that corresponds to signal in big grains, up to 1.75, that

corresponds to signal in the grains with size less than 75 μm. The slight increase in intensity of grains of size 600-850 is probably without significance since later rechecking of the spectra showed increased spectrometer noise during the recording of these spectra. The dependency shown in Fig. 1 is probably due to generation of additional centers on the surface of sample during the crushing procedure. It is clear also from this dependency, that the quantity of additional centers generated during crushing is not linearly proportional to the increase of total surface area of the sample during this procedure, but has slight dependence on the characteristic size. We tried to estimate this empirically. The best extrapolation corresponds to a dependency between intensity of signal and mean of characteristic size in the following manner:

$$\text{Intensity1} / \text{Intensity2} = (\text{Size2}/\text{Size1})^{1/2}$$

in the size range ~100 to 300 μm. Above 300 μm the native signal intensity does not depend on size, while for values less, than 100 μm we do not have enough experimental data. This behavior of the native signal intensity probably relates to the composite multilevel volume arrangement of enamel, which results in only those surface centers which have orientation along the prism axis becoming paramagnetic.

No other major effects of crushing on non-irradiated samples were observed. The spectra of samples with smaller grain sizes frequently have additional low-intensity EPR signals, but these signals usually possess random properties, and they may be removed by additional purification of the sample, including heavy liquid separation and base-treatment in an ultrasonic bath.

Table 2 shows the effects of crushing on the sensitivity of irradiated specimens. In evaluating this data, allowance must be made for the small size of the possible effects and the influence of the finite, but reproducible measurement errors. In our estimation, based on the reproducibility of results with unirradiated spectra, these errors lie within ~2%. There is a small reduction in radiation sensitivity with decreasing sample size (~8%) of non-irradiated enamel (column 1). Also seen is a small increase in radiation sensitivity of pre-irradiated compared to non-pre-irradiated specimens (column 1 vs. column 2).

It is possible to explain this qualitatively by assuming, that only the center at $g_{\perp} = 2.0018$, $g_{\parallel} = 1.9975$, which is located in the volume of the sample (Callens *et al.*, 1995; Kenner *et al.*, submitted) may become paramagnetic due to gamma irradiation. By decreasing the size of grains, we increase the total surface of sample and therefore the numbers of pre-centers, which are placed within the thin surface layer. Using this model we can estimate the thickness of the surface layer, whose pre-centers do not become paramagnetic with gamma irradiation. For this we use the fact that radiation sensitivity (which is proportional to the number of paramagnetic centers) was reduced by ~8% while the characteristic size was reduced by ~18 times (from 675 to 37.5 μm). If we suppose for simplicity that N is the total number of pre-centers which may become paramagnetic and designate S as the total surface of sample with a mean size 675 μm, ρ as the density of pre-centers and h as the thickness of the surface layer, within which the pre-centers are in the diamagnetic state, then for the EPR intensity of the radiation-induced centers for samples of 675 and 37.5 μm respectively, we can write:

$$I_{675} = A(N - Sh\rho) \qquad (1)$$

$$I_{37.5} = A(N - 18Sh\rho) \qquad (2)$$

where A is a proportionality coefficient based on the quantity of paramagnetic centers and intensity of EPR signal. Equation 2 takes into account that the total surface of the sample is increasing versus its characteristic size if the mass is constant. Taking the ratios of equation 1 to equation 2, and using the experimental value of ~1.08 for the ratio $I_{675}/_{137.5}$, we obtain:

$$h = 0.0043\ N/\rho S \qquad (3)$$

Assuming that enamel grains are preferentially round spheres with radius r=337.5 μm and taking into account that $S = S_{ik}$, $N = V_i\rho k$, were S_i and V_i are the corresponding surface and volume of one grain and k is the total number of grains in the sample, we can obtain the following value for h:

$h = 0.0043 \times \rho/3 \approx 0.5$ (μm)

We can also explain the tendency for small increases in radiation sensitivity of samples exposed before crushing using the above model. It appears that pre-centers, once they become paramagnetic, remain in that state, even when they reach the surface h-layer. We decided to estimate the influence of this sensitivity change in samples irradiated before crushing on the accuracy of estimated doses. For this purpose, we reconstructed the "unknown" dose of 6 Gy using different grain size fractions. The results are shown in column 4 of Table 2 with the relative deviation of measured values shown in column 5. An estimate of the accuracy of these measurements can be made by recognizing that all dose response curves of non-exposed, uncrushed specimens S1-1-. . .-S1-7, excluding the one with a grain size of less than 75 μm, intersected the dose-axes near the zero-point with deviations from zero of less than ±50 mGy (the S1-7 aliquot showed an initial dose of 340 mGy). We can see from Table 2 that in the worst case, when the fraction with a size of less than 75 μm was used, the additional errors in dose determination due to influence of crushing on radiation sensitivity is ~10 %, and is much smaller in the case of fractions in the range 100-850 μm.

3.2. *Experiment with transient signals.*

The results of the dose response study of samples with transient signals is shown in Fig. 2. The different lines correspond to the collection of EPR spectra at increasing time intervals. Curve 1 was measured one hour after exposure, curve 2, six days and curve 3, one month after exposure. The changes in sensitivity were: 6% after 6 days and 15% after one month. The last curve corresponds to saturation, as all transient signals relax by that time according to our data and that of Oduwole and Sales (1994).

We have also obtained the dose response curves for matched samples which were annealed at 95 C for 2 hours immediately after exposure. The resulting curve was practically the same as curve 3 in Fig. 2. Thus, there are two ways of removing transient signals in retrospective EPR-dosimetry. The first is to anneal the samples for 2 hours at a temperature of 90-95 °C following exposure. The second is based on

using empirical corrective coefficients. This is done as follows. The radiation induced signal intensity before subtraction is subtracted from the after exposure intensity. The resulting value is multiplied by a corrective coefficient based on time since exposure. If the spectra were measured on the same day, then this coefficient is equal c. 1.15. During the first week following exposure it decreases, by ~0.1 per day. During the next two weeks by ~0.1 every two days. By three weeks after exposure the coefficient becomes equal to 1.

Next we investigated the effect of microwave power on the transient signals. For this purpose the spectra of samples Tr15 and Tr16 were recorded using a wide range of microwave powers from a maximum of 200 mW, attenuation 0 dB, down to a few tens ofμW in steps of 3 dB. The original spectra of sample Tr15, corresponding to a measurement time of 3-4 hours after exposure, are shown in Fig. 3a. In the Fig. 3b the same spectra are shown, but after subtraction of the corresponding native signals from sample Tr16 which had been annealed for two hours at 95 °C. Spectra of the Tr15-Tr16 samples were recorded under the same conditions during 2 hours on the same day, minimizing additional errors. The modulation amplitude used for registration of Tr15-Tr16 samples spectra was chosen at 0.2 mT which corresponded to the width of the narrower transient signals. An additional adjustment was made for the magnitude of these spectra. Based on the data in Fig. 2, it was found that the differences in intensity of the $g_{\perp} = 2.0018$, $g_{\parallel} = 1.9975$ signals was such that the values of the Tr16 spectra were multiplied by 0.87 before subtraction even though the specimens had the same weight and received the same dose. The accuracy of this choice was shown by looking at the spectra taken at low microwave power (less than 0.1 mW), where spectra shown consisted of only one transient signal after subtraction (Fig. 4a, in which the resulting spectra corresponding to 0.0125 mW power is shown). The g-factor of this line and its width were 2.0034 and 0.24 mT respectively which is in good agreement with data of Oduwole and Sales, (1994). With increasing microwave power the spectra evolve and become like the one shown in Fig. 4b, which corresponds to power 1.6 mW. As before, we can see the signal with its center at g = 2.0034 in the middle of the spectra, but now it is slightly degraded by other signals. An explanation of the spectra seen in Fig. 4b could be that we have anadditional sextet at g = 2.0030 whose hyperfine splitting constant equals ~0.6 mT. Only the first and second lines of this center can be seen in the original spectrum. We can see the 5th and 6th lines after

subtraction of the $g_{\perp} = 2.0018$ and $g_{\parallel} = 1.9975$ signal, but the 3rd and 4th lines are still masked by the signal at $g = 2.0034$.

Using data from Fig. 3b, we plotted the power saturation curves for transient signal lines (Fig. 5). We can see that the signal from centers with $g = 2.0034$ is saturated at ~1 mW, while the intensity of the signal from line 1 of the assumed sextet, continues to increase up to maximum power. Taking into account that the signal from centers with $g = 2.0034$ strongly affects the stable radiation induced signal, preference should be given for a power on the order of 10 mW, at which the $g = 2.0034$ signal has saturated, but the intensity of the sextet is still small.

The question about the nature of transient signals is still open. Possibly, an experiment with using ENDOR may clear up whether we are dealing with 6 lines from one center or if the observed spectrum is a complicated superposition of lines from different centers. Anyway it is possible to say that observed transient signals shown in Fig. 3 are different from the native signal at $g = 2.0045$, which usually dominates in the unexposed enamel sample. The latter signal differs in many parameters including g-factor, width of line and power saturation curve from the corresponding parameters of transient signals.

4. SUMMARY

The experimental results provide possible explanations of the observed influence of the crushing procedures used in EPR dosimetry of tooth enamel on the paramagnetic centers at $g = 2.0045$ and $g_{\perp} = 2.0018$, $g_{\parallel} = 1.9975$. It was also shown that in the worst possible case, when we are using the fraction with grain size less than 75 μm for dose reconstruction the effect of crushing results in a maximum additional error of 10%. Detailed investigation of the properties of transient signals after gamma-ray exposure has suggested a new interpretation of their nature. The empirical corrective coefficients were determined which can be used to correct for the presence of transient signals.

Acknowledgements -- Supported by the U.S. Department of Energy, Contract DE-FC08-89NV10805 and U.S. Department of Energy by Lawrence Livermore National Laboratory under contract no. W-7405-ENG-48.

REFERENCES

Callens F, Moens P, Verbeeck R (1995) An EPR study of intact and powdered human tooth enamel dried at 400 °C. *Calcif. Tissue Int.* **56,** 543-548.

Chumak V., Bailiff I., Baran N., Bougai A., Dubovsky S., Feedosov I., Finin V., Haskell E., Hayes R., Ivannikov A., Kenner G., Kirillov V., Khlamidova L., Kolesnik S., Liidja G., Likhtarev I., Lippmaa E., Maksimenko V., Meijer A., Minenko V., Pasalskaya L., Past J., Puskar J., Radchuk V., Sholom S., Skvortzov V., Stepanenko V., Vaher U., Wieser A. (1996A) The first international intercomparison of EPR dosimetry with teeth: first results. *Appl. Radiat. Isot.* **47**(12).

Chumak V., Pavlenko Ju. and Sholom S. (1996B) An approach to the assesment of overall uncertainty of determination of dose using ESR technique. *Appl. Radiat. Isot.* **47**(12).

Desrosiers M.F., Simic M.G. Eichmiller F.C., Johnston A.D. and Bowen R.L. (1989) Mechanically-induced generation of radicals in tooth enamel. *Appl. Radiat. Isot.* **40,** 1195-1197.

Haskell E.H., Hayes R.B. and Kenner G.H. Preparation induced errors in EPR dosimetry of enamel: pre and post crushing sensitivity. *Appl. Radiat. Isot.* **47**(12).

Iwasaki M., Miyazawa C., Uesawa T. and Niwa K. (1993) Effect of sample grain size on the CO33-signal intensity in ESR dosimetry of human tooth enamel. *Radioisotopes* **42,** 470-473.

Kenner G.H., Haskell E.H., Hayes R.B., Baig A. and Higuchi W.I. (submitted) ESR properties and dose response of hydroxyapatite and carbonated apatites. *Calcif. Tissue Int.*

Marino A.A. and Becker R.O. (1968) Mechanically induced free radicals in bone. *Nature* **218,** 466-467.

Oduwole A.D. and Sales K.D. (1994) Transient ESR signals induced by g-irradiation in tooth enamel and in bone. *Quaternary Geochronology* **13,** 647-650.

Polyakov V., Haskell E., Kenner G., Huett G. and Hayes R. (1995) Effect of mechanically induced background signal on EPR dosimetry of tooth enamel. *Radiation Measurements* **24,** 249-254.

Tatsumi-Miyajima J. and Okajima S. (1985) ESR dosimetry using human tooth enamel. ESR Dating and Dosimetry (edited by M. Ikeya and T. Miki), IONICS, Tokyo), pp. 397-405.

Table 1. The original data characterizing aliquots of the sample S1. S1-1 to S1-7 were crushed before irradiation. S1-8 to S1-14 were irradiated post-crushing.

Number of aliquot	Size of grains, μm	Original weight of aliquot, mg
S1-1	600-850	47
S1-2	425-600	49
S1-3	250-425	50
S1-4	150-250	50
S1-5	106-150	35
S1-6	75-106	39.5
S1-7	less than 75	39
S1-8	600-850	46
S1-9	425-600	47
S1-10	250-425	47
S1-11	150-250	48.5
S1-12	106-150	34
S1-13	75-106	38.5
S1-14	less than 75	40

Table 2. Sensitivity of different grain size enamel samples corresponding to: 1) non-irradiated part of tooth (column 2), 2) part of tooth previously irradiated with dose of 6 Gy. (column 3). Also shown are the results of the dose determination for each sample (column 4) and the relative deviation of the values in column 4 from the administered dose (column 5).

Range of grain size, μm	Sensitivity of enamel of non-irradiated part of tooth	Sensitivity of enamel previously irradiated with dose of 6 Gy	Result of determination of dose 6 Gy using different grain size aliquots, Gy	Relative deviation of previous column data from given dose, %
600-850	34.3	34.4	5.75	-4.2
425-600	34.1	32.8	6.00	0
250-425	33.6	34.7	5.75	-4.2
150-250	33.9	34.8	5.5	-8.4
106-150	32.8	34.4	5.8	-3.3
75-106	32.3	33.2	6.25	+4.2
less 75	31.5	33.5	6.6	+10

FIGURE CAPTIONS

Fig. 1. Intensity of signal with g = 2.0045 in enamel as function of grain size.

Fig. 2. Measurements of dose response curves of enamel: 1 hour after irradiation (curve 1), 6 days after irradiation (curve 2) and 1 month after irradiation (curve 3).

Fig. 3. Spectra of sample with dose of 100 Gy, recorded at different microwave powers. The upper spectra in parts a and b correspond to the maximum microwave power 200 mW (attenuation 0 dB). The attenuation between each neighboring spectra is 3 dB, so that the bottom spectra correspond to circa 0.0638 mW power (45 dB attenuation). Set a are the original spectra. Set b are the results of subtracting appropriate signals of sample Tr16 from the spectra of set a and consists of "pure" transient signals.

Fig. 4. Comparison of the responses of the paramagnetic centers at $g_{\perp}$ = 2.0018, $g_{\parallel}$ = 1.9975 and g = 2.0045 to sunlight and ultraviolet light respectively as a function of time. Curve a is a plot of the intensity of the perpendicular component of th $g_{\perp}$ = 2.0018, $g_{\parallel}$ = 1.9975 signal in response to sunlight. The y-axis is expressed in terms of the amount of irradiation (mGy) required to obtain an equivalent response. Curve b is the response of the signal at g = 2.0045 to ultraviolet light and is normalized to the starting value.

Fig. 5. The power saturation curves of transient signals in the sample exposed to a dose of 100 Gy. Line 1 is the saturation curve for signals with centers at g = 2.0034. Line 2 is the saturation curve of the first component of the assumed sextet at g = 2.0030 (low field maximum at g = 2.0124). The inset is a magnified view of line 1 at lower powers.

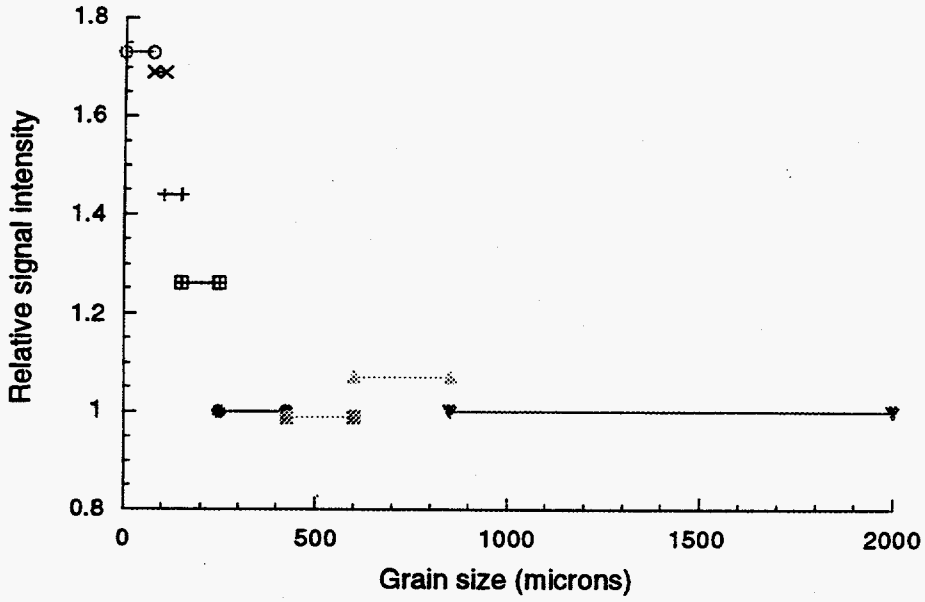
1.8
1.6
1.4
1.2
1
0.8
Relative signal intensity
0
500
1000
1500
2000
Grain size (microns)

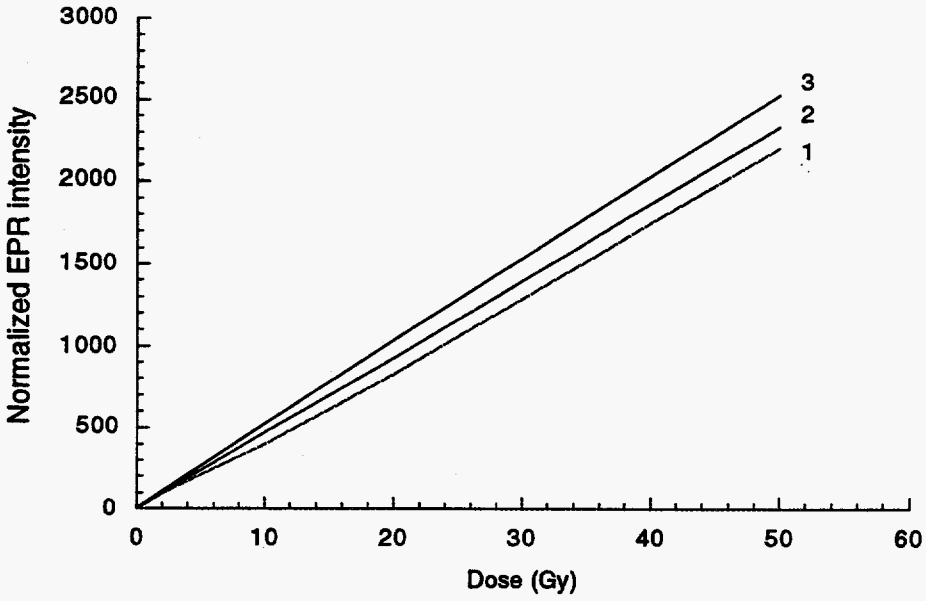
3000
2500
2000
1500
1000
500
0
Normalized EPR Intensity
0
10
20
30
40
50
60
Dose (Gy)
3
2
1

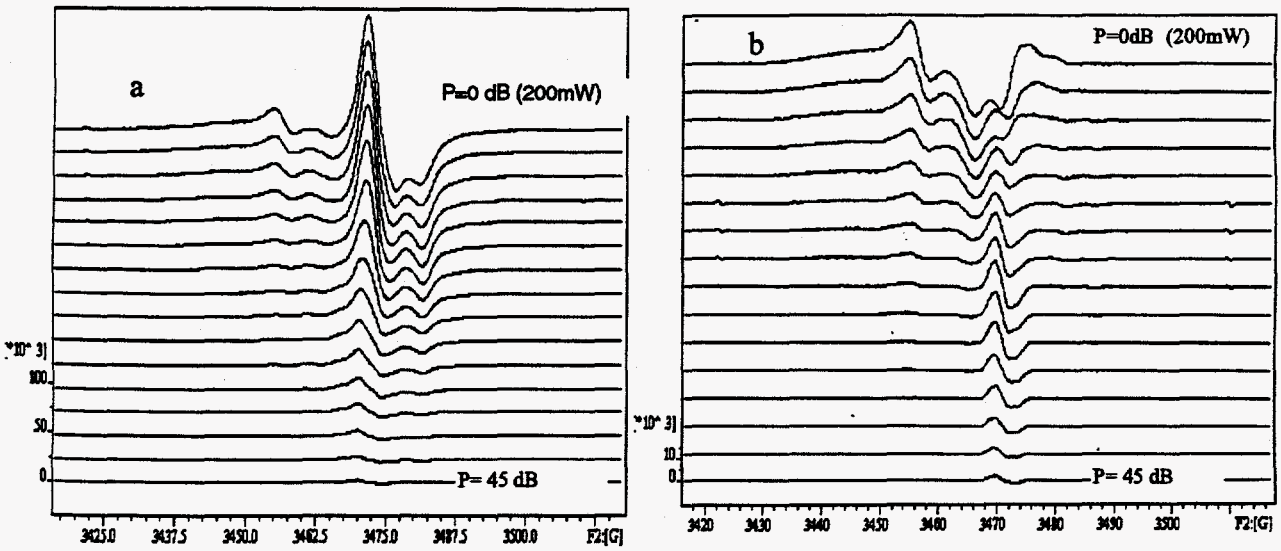
a
P=0 dB (200mW)
P= 45 dB
100
50
0
3425.0
3437.5
3450.0
3462.5
3475.0
3487.5
3500.0
F2:[G]
b
P=0dB (200mW)
P= 45 dB
10
0
3420
3430
3440
3450
3460
3470
3480
3490
3500
F2:[G]

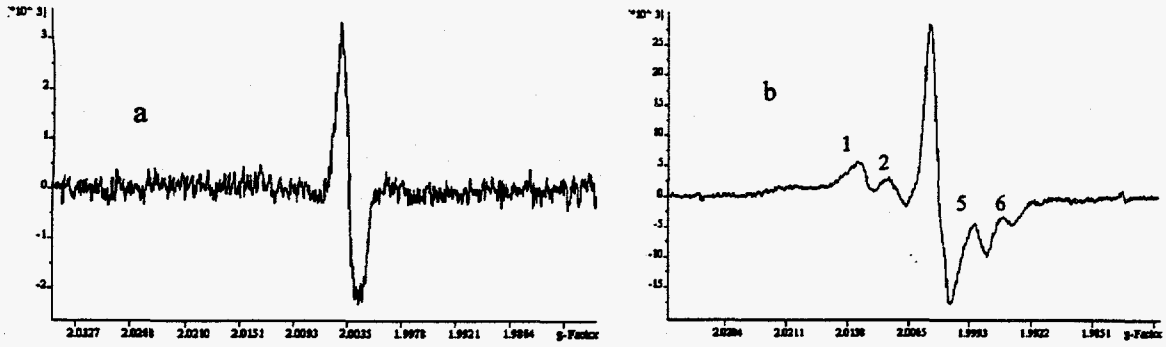
a
b
1
2
5
6

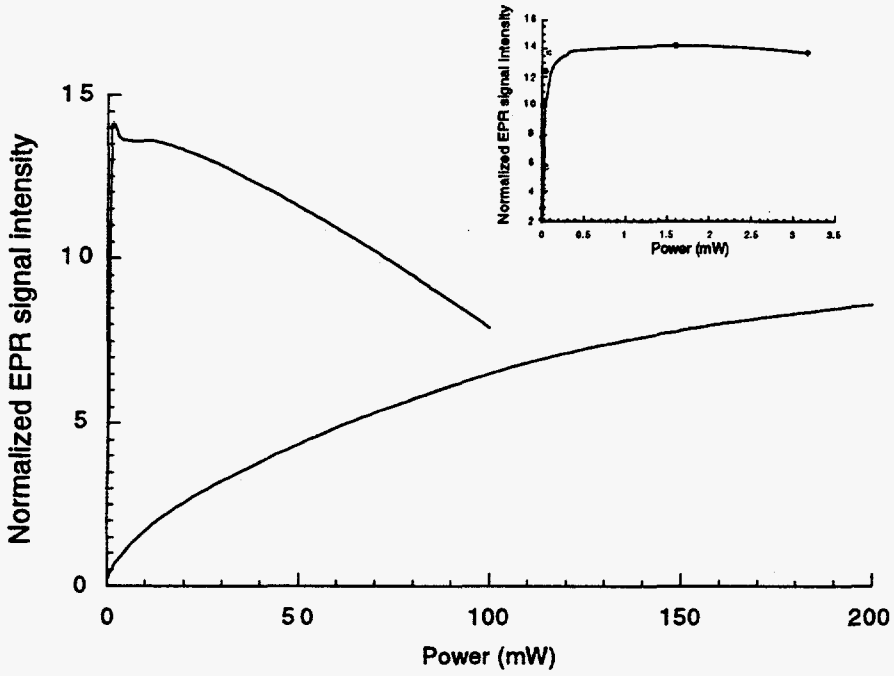
Normalized EPR signal intensity
15
10
5
0
0
50
100
150
200
Power (mW)
Normalized EPR signal intensity
Power (mW)

APPENDIX 7.

EPR Dosimetry of Bone Gains Accuracy by Isolation of Calcified Tissue. (*Appl. Radiat. Isot.* **45**(4):525-526, 1994) Reprint removed

APPENDIX 9.

Dentine as an EPR Dosimeter for Determination of ^{239}Pu and ^{90}Sr Doses to Internal Organs: A Feasibility Study. (Proposal)

Dentine as an EPR Dosimeter for Determination of ^{239}Pu and ^{90}Sr Doses to Internal Organs: A Feasibility Study

E. Haskell, G. Kenner, S. Miller and F. Bruenger
Division of Radiobiology, University of Utah

Summary
The success of the program outlined below in the Appendix depends upon 1) the sensitivity and stability of the dosimetric properties of dentine to alpha and beta irradiation, 2) the degree of uptake, and retention of radionuclides in dentine, 3) the degree of variation within and between animals exposed to similar concentrations of radionuclides and 4) the consistency with which organ doses may be inferred from measurements of dose or radionuclide concentration in dentine. To determine the feasibility of dentine as both an alpha and beta dosimeter as well as an indicator of cumulative dose to other body organs we propose to examine those factors most critical to these goals. Since certain results may rule out the utility of dentine as such a tool, while others may modify the approach to be taken in its development and implementation, we have arranged the order of investigation to allow termination or modification as indicated.

Factors most critical to success include:

1. sufficient sensitivity of dentine to alpha and beta irradiation to measure doses received by individuals in contaminated regions of the Urals,
2. good temporal stability of the alpha/beta radiation-induced signals in artificially irradiated dentine,
3. sufficient uptake by dentine of circulating radionuclides to allow accurate assessment of nuclide concentrations,
4. minimal variation in radionuclide uptake in the dentine of teeth in an individual,
5. minimal variation in radionuclide uptake in dentine of teeth from similarly exposed animals of the same age,
6. adequate *in vivo* stability of nuclide retention over the lifetime of an animal.
7. ability to correlate radionuclide concentration and/or EPR measured dose in dentine to dose in other body organs

Approach:

We propose an approach for determining feasibility which will addresses in order, those properties which are most critical to the utility of dentine as an indicator of cumulative organ doses from internal alpha and beta emitters. Stopping points are proposed based on results of the study and branching points where project modifications might be required are indicated.

Phase I.

The first phase of the study will examine (**A**) the dosimetric properties of dentine under conditions of alpha and beta irradiation. Poor dosimetric properties discovered at this stage will rule out the use of EPR dosimetry of dentine but will not rule out other methods of determining radionuclide concentration in dentine such as neutron induced autoradiography (NIAR) which could be substituted for EPR measurements. The first phase will therefore, simultaneously examine (**B**) the retention and deposition patterns of plutonium in dentine as measured by NIAR.
If both part A and B of phase I are successful then phase II will be undertaken using both EPR and NIAR. If part A is unsuccessful but part B is successful then phase II will be undertaken using only NIAR. If neither part A nor part B is successful then the feasibility study will be terminated following phase I.

Part A.
This part of Phase I will examine:

1) the sensitivity of the EPR signal due to alpha and beta irradiation at g=2.0018, the position of the well known gamma-ray sensitive signal, and of
2) the previously unreported alpha induced signals which we have observed at g values of 2.0568 and 2.0340. These measurements will involve alpha and beta irradiation of powdered dentine and determination of sensitivities relative to those of gamma rays.
3) Irradiated samples will be subjected to fading tests to determine stability of the signals over time. This phase of the study will require accurate determination of alpha dose applied to powdered dentine from a calibrated Pu source.
4) The effects of Soxhletting treatment at elevated temperatures for removal of organic constituents of dentine will also be examined by measuring dose to alpha irradiated dentine both before and after Soxhletting and by
5) measuring signal stability in Soxhletted and unSoxhletted dentine following isochronal treatment at elevated temperatures.

Part B.
Pu and Sr dose and radionuclide accumulation in dentine and enamel will be examined.

1) The degree of Pu uptake in dentine is expected to parallel the growth patterns of dentine. Using NIAR we will examine growth patterns in archived dentine specimens from animals of the Pu serial sacrifice study and compare those patterns to patterns reported in the human literature. If patterns are similar and deposition continues in the adult human on a scale similar to that seen in the beagle then the correlation of Pu levels in human to those in animals will be straightforward and teeth from humans of any age at time of exposure may be used for dose assessment. If large differences become apparent then it will be necessary to assess the effect of those differences on animal to human extrapolation and it may be necessary to limit application of the technique to humans of developmental age at the time of exposure.
2) Measurements by EPR of dose to dentine will be compared to NIAR determined concentrations of radionuclides in dentine. EPR measurements will be made of teeth having varying concentrations of Pu and Sr deposition and doses will be correlated with the actual radionuclide concentrations in the dentine. Variations in concentration and distribution of radionuclides in different teeth from the same animal will be examined.

Phase II.
If Phase I of the project proves successful Phase II will examine animal to animal variations and variations over time using selected tissues from life span and serial sacrifice studies at the University of Utah. These tissues are currently in storage. Phase II will also examine variations in the correlation of measured dose and radionuclide concentration in dentine to organ doses in animals from the same experimental group having similar life spans. If these correlations prove consistent between animals then Phase III (not detailed here) will be initiated to establish dentine/organ ratios for bone, liver, lung, spleen and lymph nodes in both life-span study animals and in the serial sacrifice animals.

1) **Variations from animal to animal.** Teeth from several animals from the same experimental group and of similar ages at time of death will be compared for radionuclide concentration and for measured dose to enamel and dentine to determine variations in nuclide concentration and dose deposition from animal to animal.

2) **Comparison of Pu-239 exposed animals with Pu-238 exposed animals from ITRI.**
Retention patterns in Pu-238 exposed animal differ significantly from those in Pu-239 expsed animals probably due to the increased activity of Pu-238 and the recoil effect of decay in dislodging Pu-238 accumulations. We will examine the retention patterns in teeth of animals from both groups using NIAR to determine if patterns in the two exposure groups are similar.

3) **Separation of dose due to internal emitters from dose due to external x-rays.** Enamel and dentine will be measured using EPR techniques and differences in dose will be compared to tabulated x-ray doses received by the same animals. This study will be conducted on animals which received substantial doses from x-ray examination (life-span study) and animals which received little or no dose from x-rays (serial sacrifice study).

Appendix
Dentine as an EPR Dosimeter for Determination of ^{239}Pu and ^{90}Sr Doses to Internal Organs

A Preliminary Proposal by

The Division of Radiobiology
University of Utah
Salt Lake City, Utah
and
The EPR Spectroscopy Center
The Institute of Metal Physics
Ekaterinburg, Russia

Abstract

A method is proposed which will allow assessment of cumulative dose from internal ^{239}Pu and ^{90}Sr in specific target organs of individuals of the Mayak and Techa River populations of Russia. The method exploits the unique differences in uptake and retention of circulating radionuclides in enamel versus dentine. With the use of databases generated from completed, long term animal studies (Utah beagle project), correlations will be made of concentrations of ^{239}Pu and ^{90}Sr in target organs of the animals versus new electron paramagnetic resonance (EPR) measurements of alpha and beta dose to preserved specimens of enamel and dentine from the same animals. Data from life-span versus serial sacrifice studies will allow incorporation of time resolved changes due to uptake, retention and remodeling of the various tissues of interest. Validation of the model in humans will be accomplished with the aid of tissues from the US Transuranium Tissue Registry as well as from tissues collected at autopsy from heavily exposed Mayak workers. Because no additional live animal experimentation will be required, the cost of the program will be minimal.

Background

The civilian and industrial populations at Mayak and the Techa River region of the Urals have primarily been exposed to three types of radiation contamination. To varying degrees these groups have received contributions of internal dose from ^{239}Pu (Mayak industrial workers), ^{90}Sr (civilians near the Techa River) and external gamma ray exposures from a variety of radionuclides including ^{137}Cs (both groups). Under the auspices of the JCCRER, the coordinating committee for the cooperative US-Russian agreement on radiation effects, epidemiological studies are being planned to allow assessment of the health effects from each of these radionuclides as a function of dose. Of key importance to the success of these efforts is accurate assessment of dose to target organs in individuals of the populations of interest.

EPR of enamel is increasingly recognized as a powerful dosimetric tool for the assessment of dose received from external gamma rays, and its value in assessing gamma ray doses to the Mayak/Techa River populations is anticipated. What is not widely known is that EPR also functions as a dosimeter of internal beta and alpha emitters in bone and dentine. Human dentine differs from bone, however, in that it does not undergo the continual remodeling process which is typical of mammalian bone. This has the effect that radionuclides deposited in dentine will deliver a dose of radiation which is retained throughout the lifetime of an individual. Similar doses delivered to bone are transient as are concentrations of radionuclides in bone and virtually every organ of the body. Although

the EPR measurement properties of dentine and enamel are quite similar, the ability of dentine to absorb a dose contribution from internal alpha and beta emitters distinguishes it from enamel. Internal dose to dentine can be resolved by subtraction of the external gamma ray dose measured in enamel.

This differentiation of dose from internal versus external emitters can be exploited in the case of the Mayak and Techa River populations due to the high doses received. The data from the teeth can be compared with similar data from the teeth of dogs to relate dose to dentine to concentration of radionuclides in internal organs. From this, it will be possible to estimate cumulative doses to specific target organs strictly on the basis of EPR measured dose.

Approach

Key to this goal will be the measurement of dentine and enamel in individuals of the Pu-exposed and the Sr-exposed populations and the direct estimation of dose from ^{239}Pu and/or ^{90}Sr through validation and use of an animal-to-human model. This model will yield cumulative dose information to specific target organs based on EPR analysis of enamel and dentine and will be independent of the level of radionuclide retention at the time of analysis. Effects of incorporation, decorporation and remodeling will be accounted for by the use of a time resolved animal model of Pu transport within the body developed from data collected from the long-term Utah beagle study. All necessary elements of the animal model have been recorded, archived and most are available in a computerized database. Also available are tissue samples of enamel and dentine to allow correlation of EPR measured dose to teeth with concentrations of radionuclide in target organs. The database includes measured and recorded concentrations of ^{239}Pu from the life-span study as well as tissue concentrations from the serial sacrificed, time resolved study population. ^{90}Sr data is also available, but has been worked up to a lesser extent

Implementation

Because the Mayak population is aging rapidly, the highest priority of the project must be establishment of a system for collection and retention of biological samples. Concurrent with this effort will be experimental verification of the accuracy, and establishment of the lower limits of detection of internal dose from both ^{239}Pu and ^{90}Sr. Following determination of the accuracy of EPR for the measurement of internal emitters in dentine at the dose levels expected in the study population (1 to many Gy) a study will be launched consisting of analysis of enamel and dentine in archived beagle specimens and correlation of measured dose to previously determined concentrations of ^{239}Pu in bone, liver, lung, spleen and lymph nodes. These correlations will be established using the extensive database of the Utah beagle study. The database consists of well characterized, recorded concentrations of radionuclides in virtually all body organs of over 400 animals. Experimental groups include ^{239}Pu and ^{90}Sr exposed and control populations. The ^{239}Pu and control groups have had all organs analyzed for total ^{239}Pu concentration in both the life-span and the serial sacrifice studies. The combination of these two will allow determination of uptake, excretion and remodeling associated with ^{239}Pu. By correlating ratios of dose to dentine with concentrations of ^{239}Pu in the target organs we will have a tool with potential application to individuals and human populations. Once ratios have been established in animals, a remaining task is validation of the model in humans and incorporation of species specific differences. This will be accomplished by a similar study of enamel/dentine doses and comparison with internal concentrations of ^{239}Pu in tissues taken from the US Transuranium Tissue Registry as well as from autopsy tissues collected from Mayak workers who have been exposed to high levels of ^{239}Pu contamination. These workers, through agreement with the Mayak research facility (FIB #1, branch 1 of the Moscow Institute for Biophysics under the direction of Prof. Lyubchanski), have agreed to

autopsy and organ donation. A mechanism will be required to insure the proper collection and preservation of tissue samples. Once the animal to human relationship has been determined, the model may be applied to other members of the population from whom teeth have been and will be collected.

A related and corresponding study involves determination of ^{90}Sr doses to target organs based on an approach similar to that described for ^{239}Pu. The difference in the two is that the animal database of ^{90}Sr concentration in specific organs is not as extensive as that for the Pu animals. Only whole body and skeletal burdens have been analyzed to date. Tissues are archived and available, however, and samples from selected animals can easily be ashed and counted. Comparison to humans will require close cooperation with the Urals Center for Radiation Medicine under the direction of Drs. Akleev and Degteva. A mechanism for collection of samples through autopsy will be required, as will a reliable, routine method of tooth collection through the local dental system.

Benefits

The results of this study will have benefits not only for the epidemiological studies planned for the exposed Urals population, but for future contaminations which may occur. The technique to be developed and applied will represent a fundamental contribution to our ability to perform organ-specific internal dosimetry at the level of the individual for two of the key contaminants of nuclear accidents. In addition, the health effects data previously generated from the massive Utah beagle study will gain a direct tie-in to health effects in humans without relying on the intermediate correlation to radium effects which has, until now, been required.

APPENDIX 10.

Improved Accuracy of EPR Dosimetry Using a Constant Rotation Goniometer. (*Radiat. Meas.* in press) removed

APPENDIX 11.

EPR Dosimetry of Whole Deciduous Tooth using a Constant Rotation Goniometer and Background Subtraction with a Dentine Standard. (In preparation)

EPR dosimetry of whole deciduous tooth using a constant rotation goniometer and background subtraction with a dentine standard.

E.H. Haskell, R.B. Hayes and G.H. Kenner

Center for Applied Dosimetry, University of Utah, Salt Lake City, UT 84112

We report here a rapid method of electron paramagnetic resonance (EPR) dosimetry of dental enamel which will allow screening of whole deciduous teeth of children following a nuclear accident. The technique requires virtually no sample preparation and is capable of measuring doses of less than 100 mGy. Teeth may be scanned for threshold dose levels without the need for added calibration doses and those of particular interest may be more accurately examined using the additive dose method. The success of the technique lies in the elimination of anisotropic effects by rotation of the sample during measurement together with subtraction of spectra from the empty cavity and a standard "background" tooth. normalization using in-cavity mn++ standards is also employed.

EPR spectroscopy is being used to measure radiation doses to the enamel and dentine of teeth of individuals exposed during the Chernobyl nuclear reactor accident. Teeth have been collected by dentists from exposed individuals during routine extractions, and used to document eligibility for government compensation as well as for epidemiological studies into the health effects of ionizing radiation. Although EPR measurements on teeth from mature individuals provide information on doses received they can only be obtained at random from the population. This limitation, together with the time consuming process of sample preparation and analysis, has made EPR dosimetry of teeth an unlikely candidate for screening of a population shortly following a nuclear accident.

There is, however, an abundant, readily available source of teeth from a subpopulation which is one of the groups at greatest risk, children 12 years old and younger. Between the ages of 6 and 13 years, children shed deciduous teeth at the rate of one every 3 to 6 months. With knowledge of the dosimetric value of the teeth, they could be saved and documented by parents for measurement of

radiation dose. That deciduous teeth were not used as dosimeters following the Chernobyl accident was likely due to immaturity of the technology plus the fact that deciduous teeth contain relatively small amounts of enamel both absolutely and relative to the dentine, making the process of separation both time consuming and difficult (1,2).

Considerable progress has been made recently on reducing the lower limits at which gamma ray exposure in tooth enamel can be detected. A recent intercomparision put the lowest detectable EPR dose to enamel at circa 100 mGy with a 45% accuracy (3). A follow-up intercomparison showed that the accuracy levels could be reduced to within 20% for doses of 175 to 250 mGy (4). The success of this effort was due to employing chemical purification of the samples and use of background subtraction techniques by the Scientific Center for Radiation Medicine (SCRM) of Ukraine (5) and the employment of the differential power method (6) by the University of Utah (Utah) group Subsequent to this, further accuracy has been obtained by the Utah group by employing a constant rotation goniometer and a technique for optimizing the distribution of sample points (7).

Untreated enamel has two major signals located at both g = 2.0045 and $g_{\perp}$ = 2.0018, $g_{\parallel}$ = 1.9975. These are commonly referred to as being the native and the radiation sensitive signals respectively. In addition to these there are a number of other signals attributed to such causes as mechanical trauma (8), heating, etc., as well as a number of transient signals (9) incurred by recent irradiation. In the case of enamel, further complications are caused by the addition of unknown doses due to dental x-rays and, in the case of front teeth, by sensitivity to UV light (10).

The importance of painstaking technique and proper removal of background signals cannot be overemphasized. Fig. 1 shows some of the problems which develop when this is not done. Here we have a dose response of the radiation sensitive signal from a single piece of enamel using a constant rotation goniometer. A residual analysis indicates that each point has a 21 mGy standard deviation. Note the uncertainty about the location of the y-intercept. The sample spectra contained a linear baseline offset with a positive slope which can be attributed to some kind of sample or cavity impurity. In this case the problem was failure to subtract out the native signal located at g = 2.0045, and background signals which are known to be dynamic.

Perhaps the best system for minimizing background signals is that employed by SCRM (5). The technique employed by SCRM uses an in cavity Mn^{++} standard combined with chemical purification of the sample and a system for subtracting out the dynamic background and the native signal. The in cavity Mn^{++} standard is used to correct for changes in frequency (g-factor) and intensity (Q-value). The SCRM technique includes a rigorous system of chemical purification which we did not employ in this study because we were studying whole specimens.

The background subtraction technique requires first obtaining sufficiently pure specimens. Once a pure specimen is obtained, it is annealed to remove transient signals, followed by scanning. The following background corrections are made. First of all, the spectrum of an empty EPR tube is subtracted to remove background noise caused by the tube itself. The EPR tube spectrum is superimposed over that of the sample spectrum by adjusting the positions of the third and fourth Mn^{++} lines. The values of the small regions containing the Mn^{++} lines are set to zero before subtraction so as not to remove them from the sample spectrum. Following this, the spectrum of a native signal standard is subtracted from the sample

spectrum. The native signal used for this subtraction must in a manner similar to that of the sample, have its empty cavity spectrum already subtracted out. The height of the native signal in the native signal standard is adjusted until it is the same as that of the native signal in the sample spectrum. Once again, adjustments are made to retain the third and fourth Mn^{++} lines.

Experimental. A healthy deciduous lower incisor was used which had never been irradiated. The entire cutting edge of the tooth had been worn down to the dentine. The sample was untreated except for an initial wiping down with methanol. Dried blood was visible on the root, surface yellowing was present on the exterior enamel surfaces and it had a split at the cutting edge extending 2/3 the length of the tooth. The tooth weighed 102.9 mg. The approximate dimensions of the tooth were 6.8 x 4.2 x 4.1 mm. The thickness of the cutting edge was 1.5 mm. The EPR tube used had a 4.9 mm inner diameter. When scanned, it was placed with the cutting edge down and centered in the cavity. This insured the highest possible enamel to dentine ratio during the scan.

The specimen used for obtaining the native signal standard was a carved dentine cylinder obtained by removing the enamel cap from

a wisdom tooth using a low speed diamond saw. It weighed 211.5 mg and had two cavities in one side which were part of the pulp cavity. It was approximately 3.9 x 10.7 mm and was scanned in an EPR tube with an inner diameter of 4 mm. Its bottom was rounded to fit snugly against the bottom of the EPR tube. Because of the low sensitivity of dentine compared to enamel and assuming that it had received a minimal exposure to dental x-rays, it was deemed to have a radiation sensitive signal sufficiently close to zero to be used as a native signal standard (Fig. 2).

A Bruker ESP300E x-band spectrometer was used (Bruker Instruments, Billerica, MA). Instrument parameters were 25 mW power, 10 mT scan width, 0.5 mT modulation amplitude, 10^5 receiver gain, 82 ms conversion time, 60 sweeps per spectra and a frequency of approximately 9.7 GHz. Irradiations were done with a U.S. Nuclear ^{60}Co source (Burbank, CA 91500). The rotation rate was 0.012/m.

The deciduous tooth and the native signal standard were annealed at 95°C, the deciduous tooth for 1 to 2 hours and the dentine for 30 min subsequent to each irradiation. The dentine and

the deciduous tooth were not scanned after annealing until their weights had risen to within 1% of their equilibrium values.

Once all the background signals have been eliminated, the following procedure was used to obtain the peak-to-peak values of the radiation sensitive signals. The resulting curves were first smoothed using the 25 point third order polynomial filter in the standard software package of the Bruker ESP300E. The value of 25 points was found empirically to be the maximum value that would not distort the radiation sensitive signal of enamel at 100 Gy exposure. Measurements were then made at g = 2.0034 (peak maxima) and 2.0007 (peak minima) of the perpendicular component of the radiation sensitive signal.

Results. The dose response for the deciduous tooth is shown in Fig. 3. Note that the 100 mGy dose can be readily distinguished from the 0 mGy dose. The maximum dose expected from background should be no more than a few tens of mGys. The large value obtained here of 98 ± 15 mGy can probably be attributed to U.V. light due to the sample being a front tooth.

Discussion. Retrospective EPR dosimetry can now be done on whole or partial pieces of bone and teeth with a large reduction in

sample preparation time. It is theoretically possible to extend such studies to shells, calcites, etc. The accuracy with which this can be achieved is now so high that measurements of bone and dentine can be made at levels previously attainable only by enamel, while the accuracy for enamel has been improved by an order of magnitude.

One important result of this study is that it is now possible to routinely screen deciduous teeth from children. Deciduous teeth are so small and have such a thin layer of enamel, that it is difficult to separate them into enamel and dentine fractions.

From standpoint of epidemiology of the population of young people following a nuclear mishap, the availability of deciduous teeth represents an important source of dosimetry data since they are continuously being shed on a routine basis. Further, many of the affected children will be shedding multiple teeth and in some instances will be generating new teeth. These new teeth will date from after the nuclear mishaps and can then also eventually be examined as built in controls following shedding.

REFERENCES AND NOTES

1. M. Ikeya, *New Applications of Electron Spin Resonance*, World Scientific:New York, (1993); M. ikeya and H. Ishii, *Appl. Radiat. Isot.* **40**, 1021-1027 (1989); H. Ishii and M. Ikeya, *Japanese Journal of Applied Physics* **29**, 871-875 (1990).

2. R. Grun, J.S. Brink, N.A. Spooner, L. Taylor, C.B. Stringer, R.G. Franciscus and A.S. Murray, *Nature* **382**, 500-501 (1996); R. Grun, *Ancient TL* **13**, 3-7 (1995). Grun has developed a technique for reproducibly positioning archeological specimens in the EPR chamber between irradiations. It may be possible to use this technique for low level dosimetry but there are a number of technical problems which would have to be resolved first, the most important of which would be subtraction of the native signal.

3. I. Bailiff, Ian, ed. *Final Report: Experimental Collaboration Programme Project ECP10, Retrospective Dosimetry and Dose Reconstruction.* CUC/CIS Chernobyl Collaborative Programme. 112p. Section 6.2.1.1 (1995).

4. E.H. Haskell, R.B. Hayes and G.H. Kenner, *Radiation Measurements,* (in press). The papers listed in references 4

and 7 were presented at the 8th International Conference on Luminescence and Electron Spin Resonance Dating, April 22-26, 1996, Canberra, Australia, and will be published as part of the proceedings.

5. V. Chumak, S. Sholom and I. Likhtarev. Presented at the 4th International Symposium on ESR Dosimetry and Application, Munich, Germany, May 15-19, 1995.

6. A.A. Romanyukha, E.A. Ignatiev, A.A. and A. Wieser. Presented at the 4th International Symposium on ESR Dosimetry and Application, Munich, Germany, May 15-19, 1995; V.A. Serezhenkov, I.A. Moroz, G.A. Klevezal and A.F. Vanin. Presented at the 4th International Symposium on ESR Dosimetry and Application, Munich, Germany, May 15-19, 1995.

7. E.H. Haskell, R.B. Hayes and G.H. Kenner, *Radiation Measurements* (in press); R.B. Hayes, E.H. Haskell and G.H. Kenner, *Radiation Measurements* (in press).

8. M.F. Desrosiers, M.G. Simic, F.C. Eichmiller, A.D. Johnston and R.L. Bowen *Appl. Radiat. Isot.* **40**,1195-1197 (1989); M.J. Tatsumi and S. Okajima, *ESR Dating and Dosimetry,* M. Ikeya

and T. Miki (Eds), pps. 397- 405. IONICS, Tokyo (1985); V. Polyakov, E. Haskell, G. Kenner, G. Huett and R. Hayes, *Radiation Measurements* **24**,249-254 (1995).

9. A.D. Oduwole and K.D. Sales, *Quat. Sci. Rev.* **13**,647-650 (1994).

10. A.I. Ivannikov, V.G. Skvortzov and D.D. Tikunov. Presented at the 4th International Symposium on ESR Dosimetry and Application, Munich, Germany, May 15-19, 1995.

11. The authors wish to thank David Smoot of the Salt Lake City FHP (Family Health Plan) Hospital who furnished some of the teeth used in this study. Supported by the U.S. Department of Energy, Contract DE-FC08-89NV10805 and U.S. Department of Energy by Lawrence Livermore National Laboratory under contract no. W-7405-ENG-48.

Figure Captions

Fig. 1. Dose response curve of a single enamel piece. It weighed 147 mg and was cut from an enamel cap whose dentine had been removed by grinding with a dental drill. The instrument parameters were the same as for the deciduous tooth except 3.5 mT scan width, 2.56 ms conversion time and ~1,000 sweeps per spectra.

Fig. 2. Dose response curve of the radiation sensitive signal for the dentine cylinder used as a native signal standard. A lower sensitivity is demonstrated relative to the whole tooth because of the zero enamel content. Note the close approximation to zero of the y-intercept. Residual analysis placed individual errors at 0.2 Gy, while the residual errors for pure enamel had previously been found to be 0.1-0.2 Gy for enamel (4). Slope = 27.3e3 ± 2e3. y-intercept = 2.3e3 ± 4.1e3.

Fig. 3. Dose response for deciduous tooth taken using a constant rotation goniometer and analyzed with the modified SCRM method. There are two superimposed points where the line crosses the y-axis. The lowest point at zero appears to be an

outlier. Slope = 167.7e3±8.2e3, y-intercept = 16.4e3±2.4e3. The dose estimate (x-intercept) is 98±15mGy. Residual analysis showed the standard deviation of each measurement was 35 mGy.

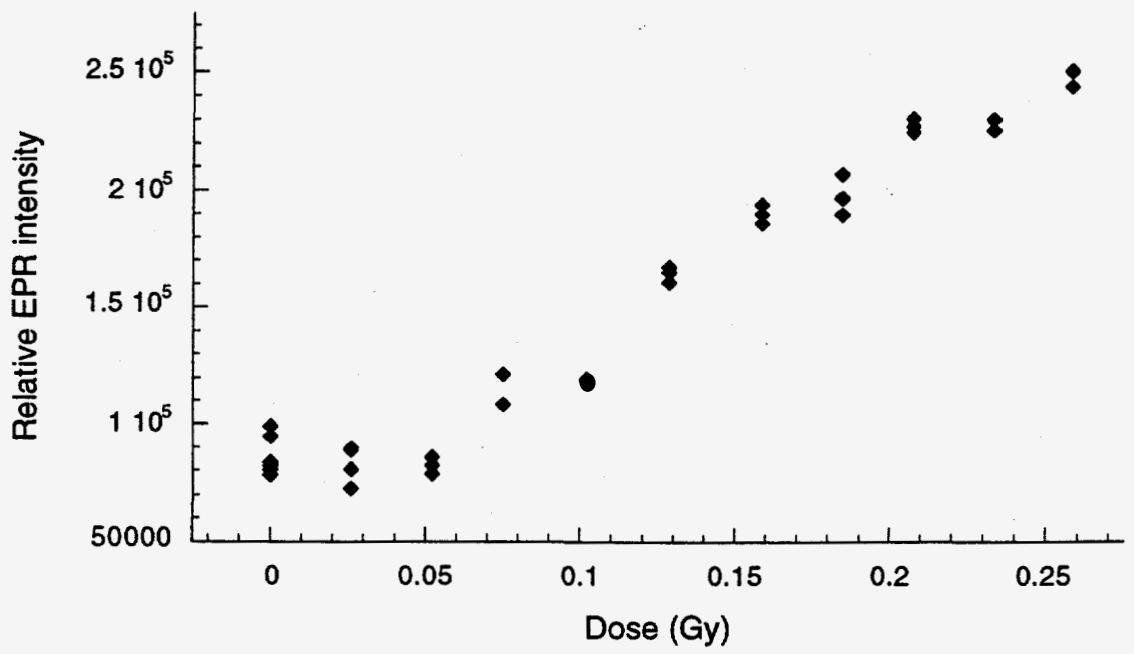

Figure 1 - Haskell et al. Deciduous tooth paper.

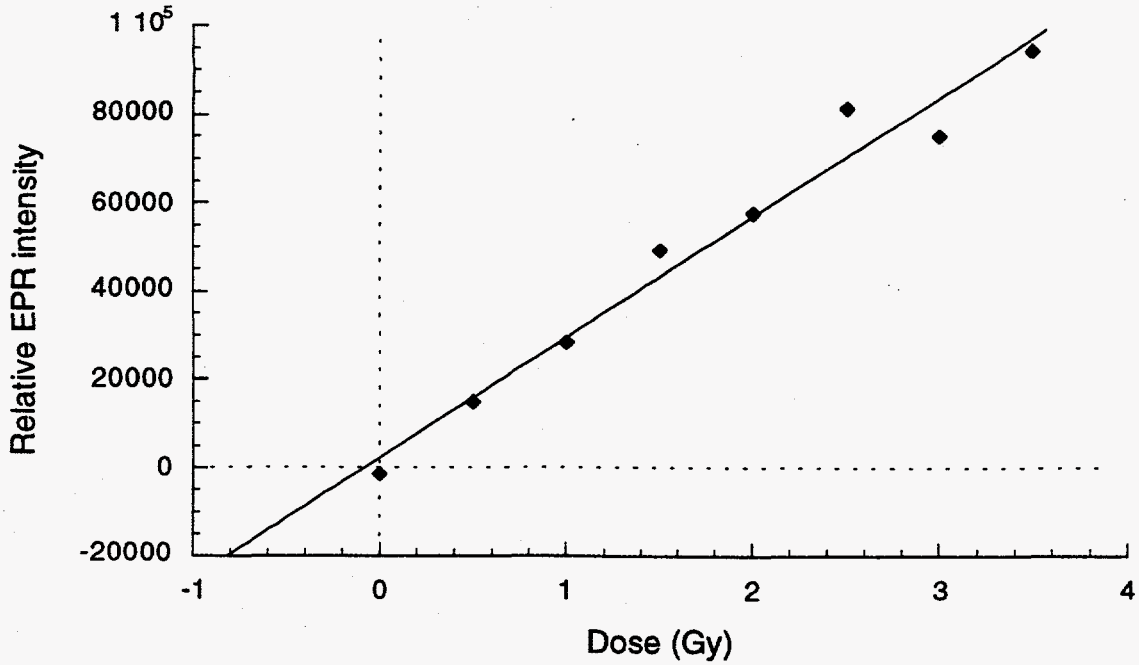

Figure 2 - Haskell et al. Deciduous tooth paper.

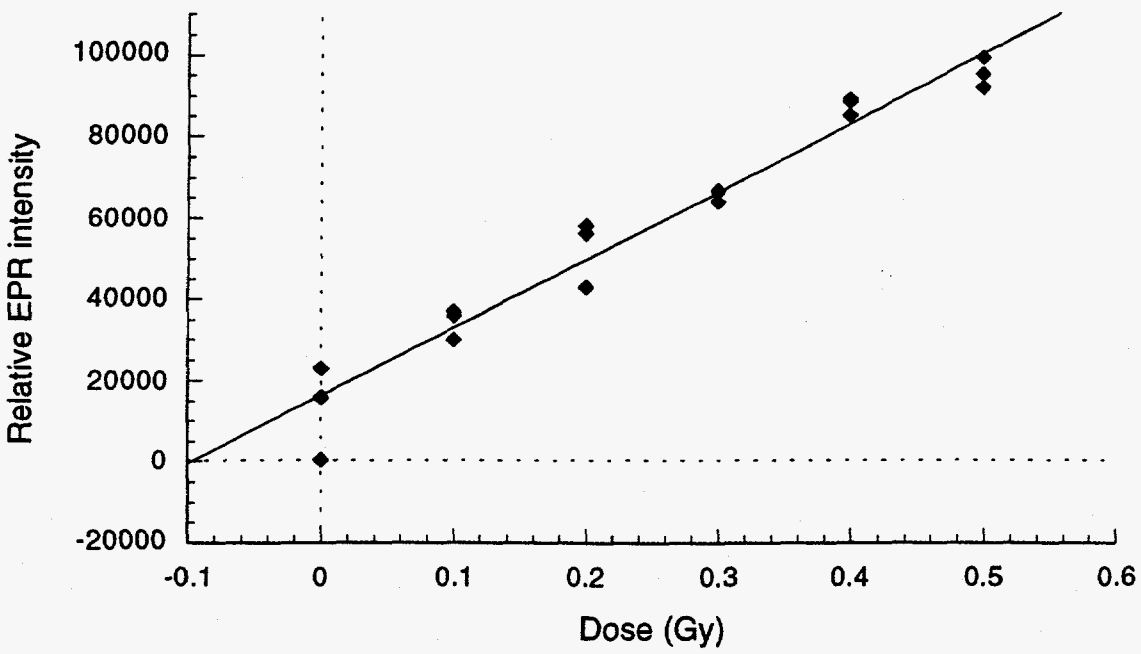

Figure 3 - Haskell et al. Deciduous tooth paper.

APPENDIX 12.

EPR Dosimetry of Teeth in Past and Future Accidents: A Prospective Look at a Retrospective Method. (Presented at the Third Workshop for the Evaluation of Atomic Bomb Radiation Doses in Hiroshima and Nagasaki. Japan. July 26-27.) Removed for separate cycling

APPENDIX 13.

A Mathematical Approach to Optimal Selection of Dose Values in the Additive Dose Method of EPR Dosimetry. (*Radiat. Meas.* in press) Removed

APPENDIX 14.

Optimal Design for Error Minimization in Single Variable Linear Regression Extrapolation. (Submitted to *SIAM Journal on Applied Mathematics*) Removed

APPENDIX 15.

Plasterboard as a Potential EPR Emergency Dosimeters. (In preparation).

Plasterboard as a Potential EPR Emergency Dosimeter

Proposed abbreviated title

EPR Emergency Dosimeter

E.H. HASKELL*, R.B. HAYES and G.H. KENNER

Division of Radiobiology, College of Medicine, University of Utah

Salt Lake City, UT 84112 USA

Direct all correspondence to

E.H. Haskell, Director
Center for Applied Dosimetry
825 North 300 West, Suite 107
Salt Lake City, UT 84103
Phone: 801-359-5962
FAX: 801-359-5862
email: e.haskell@m.cc.utah.edu

*Author for correspondence.

ABSTRACT

Plasterboard was found to have three radiation sensitive signals with spectroscopic splitting factors (g-factors) of 2.0148, 2.0094 and 2.0076 and half-lives of approximately 12, 6 and 3 months respectively. An incremental dose response using a ^{60}Co source determined that a dose of less than 1 Gy could be resolved.

SUMMARY

The feasibility of using plasterboard as EPR accident dosimeter was investigated. Plasterboard was found to have three radiation sensitive signals with spectroscopic splitting factors (g-factors) of 2.0148, 2.0094 and 2.0076 and half-lives of approximately 12, 6 and 3 months respectively. An incremental dose response using a ^{60}Co source of gamma rays determined that a dose of less than 1 Gy could be resolved.

Introduction

Measurement techniques for retrospective dosimetry are typically applied to environmental materials collected years or even decades following a radiation accident. Because of the extended time period between exposure and measurement the results are rarely used for medical decision making but more often for their contribution to risk analysis, compensation, regulation, and general knowledge. A primary requirement of samples which are suitable for long term dosimetry is a sensitive, stable radiation-induced signal. In the case of acute radiation exposures, however, such as industrial accidents or exposure of individuals through theft of high level radiation sources, the same techniques, if applied quickly, may provide information which may alter the course of medical treatment. Because prompt measurement reduces the requirements of signal stability, the number and types of potential dosimeters is greatly expanded.

Examples of residential dosimeters which have been studied include foodstuffs, drugs, clothing, houseware items, ceramics, plastics, wood and paper, rubbers and miscellaneous ornaments and jewelry (Table 1).

We have extended this list by examining the dosimetric properties of plasterboard. Plasterboard (also called sheetrock, wallboard and gypsum board) is a laminate of rehydrated gypsum and paper and is ubiquitous in nearly all homes and office buildings built in the United States since 1950. Gypsum is a dihydrate of calcium sulfate. Additives such as vermiculite (hydrated silicates) or fiberglass (fine glass filaments) are usually present.

Materials and Methods

Recently produced samples of plasterboard were obtained from two local builders supply houses and an older sample was removed from the wall of our laboratory. The samples were visually similar with fiberglass strands throughout. Eight samples were prepared and used as shown in Table 2.

Cylinders (3.5 mm x ~0.6-1.2 cm) were cut from the purchased sheet rock and manually shaped with a razor blade. A single cored specimen was removed from the laboratory wall with a 3.2 mm (1/8") cork borer. Samples used for isothermal annealing were crushed manually with a mortar and pestle.

The EPR analysis of the all samples was done using a Bruker ESP300E, X band spectrometer. Parameters for the plasterboard measurements were power 8 mW, field modulation 100 kHz, modulation amplitude 0.5 mT, room temperature, receiver gain 1 x 10^4, microwave resonance frequency 9.71 GHz. Scan widths were 60 (first SR1 test), 15 and 5 mT (SR8). Weak pitch was used as the reference standard. Further calibration of the signal position was done using the manganese impurity which was present in the plasterboard. Ten scans were recorded over a 4.3 minute time period for sheetrock samples SR1-7. The receiver time constant was 0.164 seconds. The specimens were placed in 3/16 inch (OD) x 7 inch (0.476 cm x 17.8 cm) long quartz EPR sampling tubes (Wilmad Glass, Bena, NJ 08310). Samples were stored at room temperature and low (ambient) humidity.

A constant rotation goniometer was used to ensure uniform scanning of specimen SR8. It was scanned 100 times for a total of 11.9 minutes at a rotation rate of 0.5 revolutions per minute for each spectrum. The receiver time constant was 40.96 x 10^{-3} secs. The other EPR parameters were as above.

A Systron Donner 6520 microwave counter (Concord, CA 94518) was used for the frequency determination. All gamma ray irradiations except SR4 were done with a U.S. Nuclear ^{60}Co source (Burbank, CA 91500) with a dose rate to water of 0.18 Gy min^{-1}. The source was calibrated with alanine EPR dosimeters(Albrecht Wieser, MessTechnik, Muenchen, Germany). SR4 was irradiated with gamma rays from a JL Shepherd & Associates, Mark I, Model 30, Series 6000, ^{137}Cs source (San Fernando, CA 91340-1823) with a dose rate to water of 32 Gy min^{-1}.

The following schedule was used for isochronal annealing.

15 minutes at 100° C.

15 minutes at 200° C.

20 minutes at 300° C.

20 minutes at 400° C.

Signal half-lives were determined by isothermal annealing at room temperature for 105 days.

Where possible, peaks were decomposed into their constituent parts using the Marquardt modification of the Levenberg Method (Press *et al.*, 1992) which was applied to the equation given in Atherton and Horwood, (1973) for resolving EPR line shapes. Peak to peak values for the resulting curves were then obtained.

Standard linear regression and saturating exponential analyses were applied to the dose response curves. (Spiegel, 1961; Berger *et al.*, 1987).

Results

Fig. 1 shows spectra obtained from 0 Gy and 782 Gy irradiation of SR1 scanned over 60 mT. Note the presence of six Mn^{2+} lines from impurities in the plasterboard. Many small differences are seen but there is a distinct radiation sensitive signal at g = 2.012.

Three maxima and an associated minimum are clearly seen in Fig. 2, which shows the 0 Gy and 782 Gy spectra over a 15 mT scan width. The maxima are designated as belonging to signals 1, 2 and 3 with g-factors of 2.0148, 2.0094 and 2.0076 respectively as determined using Marquardt-Levenberg fitting methods.

Fig. 3 shows the results of decomposing the radiation sensitive signal into its component parts using the Marquardt-Levenberg method following background subtraction. Three signals with g-factors of 2.0148, 2.0094 and 2.0076 and widths of 0.754, 0.938 and 0.370 mT are found immediately following irradiation when measurements are taken at 8 mW power. Evidence for the existence of a fourth radiation signal is seen when measurements are taken at 0.1 mT modulation amplitude.

Table 3 shows the half-lifes for the three signals with measurements taken from the maximum value of each peak to the common minimum. Signal 1 exhibited the greatest stability while signal 3 decayed the most rapidly.

Peak-to-peak differences between the signal 3 component of the composite signal (the most sensitive signal, Fig.2) and the associated minimum were used for the dose response measurements. The low level dose response studies using SR1, SR5 and SR6 showed non-significant increases in the EPR signal with increasing dose. The problem was attributed to the anisotrophy of the carved specimens. When the experiment was repeated using a constantly rotating goniometer, narrower scan width, and increased collection time (SR8), a dose estimate of 60 ± 54 mGy was obtained (Fig. 4). The response remained linear up to 25 Gy (Fig. 5).

Although the results of the isochronal study were flawed because we did not preheat the planchettes before adding the plasterboard sample, they clearly showed that signals 2 and 3 were annealed by heating to 200 °C while a residual signal 1 was still present. This corresponds with the results seen in Table 3 where signal 1 has the greatest lifetime while signal 3 has the lowest.

The plasterboard sample removed from the wall of the laboratory (SR7) showed responses similar to the recently manufactured samples. No attempt was made to generate a dose estimate for this older sample.

Discussion

Plaster or gypsum board has many properties which make it attractive as a potential radiation dosimeter. It is present in nearly all homes and buildings built in the United States after 1950. Further, it is an inexpensive material which can be readily repaired

when samples are removed for analysis. In addition, it has three radiation sensitive signals with different half-lives, all of which are of moderate length.

Annealing tests showed that radiation-induced signals 2 and 3 are virtually eliminated by heating at 200 °C for fifteen minutes, while the magnitude of signal 1 is drastically reduced. Since one of the steps in the manufacture of plasterboard is to calcine the gypsum at 250 °C, it appears likely that the EPR signals of freshly manufactured plasterboard have been zeroed.

Further indirect evidence that dehydration of gypsum followed by rehydration during manufacture is enough to zero radiation-sensitive signals, is the absence in our study of the long-lived signals reported by Yijian *et al.*, 1989, at g = 2.008, 2.004 and 2.002. This indicates rehydrated gypsum has a different set of defects when compared to native gypsum, particularly since their signal at g = 2.008 had different properties from ours.

A limitation of solid state radiation dosimeters is the accumulation of background signals with time. The primary sources of this radiation are cosmic rays and trace quantities of radioactive impurities in the dosimeter and the surrounding environment. In dosimeters of high stability, this necessitates a knowledge of the annealing date of the sample as well as the dose rate from natural sources of radiation. Plasterboard avoids this problem since its relatively short half-life precludes the buildup of a significant background signal. The drawback, of course, is the necessity of prompt sample collection and storage at reduced temperatures. Because plasterboard has three radiation sensitive signals of

differing half-life, the ratios of the signals could in principle provide independent information on the time since irradiation and the degree of fading from original signal levels. Fading corrections could then be applied to samples which had not been promptly collected, or had been stored at ambient temperatures. The variability of the composition of plasterboard must be investigated before such corrections are feasible on a routine basis since gypsum deposits used as starting materials most certainly vary in composition. Although all are based on a content of calcium sulfate, they differ in the amounts and types of other minerals which are present. This means that each sample must be analyzed individually unless the extent of variations are understood and characterized. This problem is offset to some extent since plasterboard in a given geographic location tends to originate from the same source.

This study shows that exposures of approximately 1 Gy or less can be reliably detected. Optimization of measurement parameters for the EPR signals associated with plasterboard should result in improvement of measurement sensitivity.

If the annealing properties of plasterboard demonstrated in this study are found to be common in other plasterboards, the EPR analysis of the material will have certain advantages over other EPR materials which show signal variation upon heating. Both bone and tooth enamel, for instance, require determination of a standard background signal which must be subtracted from the measured sample. Plasterboard on the other hand may provide its own background signal by a moderate temperature annealing procedure. This would allow background subtraction in 1) the additive dose

procedure, where separate aliquots of sample are given varying doses of radiation on top of the unknown dose and then measured, and potentially in 2) the multiple anneal process where samples are dosed, measured, annealed and then redosed and remeasured.

While plasterboard was found to be have good potential as an accident dosimeter, the other materials studied did not do as well. In keeping with the properties of most polymers studied to date, bisphenol A polycarbonate has a radiosensitive signal with a relatively short lifetime. It is possible of course, to minimize signal deterioration by lowering the temperature shortly following exposure.

Conclusions

Plasterboard can be used to detect radiation doses as low as 1 Gy and its half-life (approximately 3 to 12 months) is long enough for emergency measurements. It may be possible to use differential decay rates to estimate post-irradiation times.

Acknowledgements - Supported by the U.S. Department of Energy, Contract DE-FC08-89NV10805 and U.S. Department of Energy by Lawrence Livermore National Laboratory under contract no. W-7405-ENG-48. The ^{137}Ce source was provided by the Cancer Support Center/Huntsman Cancer Institute, grant #5P30CA42014, University of Utah.

References

Atherton N.M. and Horwood E. (1973) Electron Spin Resonance: Theory and Applications. New York: Halsted Press, pps. 43-44.

Azorin J., Guitierrez A., Munoz E. and Gleason R. (1989) Correlation of ESR with lyoluminescence dosimetry using some sugars. *Appl. Radiat. Isot.* **22,** 871.

Baccaro S., Buotempo U., Caccia B., Onori S. and Pantoloni M. (1994) ESR study of irradiated ethylene-propylene rubber. *Int. J. Appl. Radiat. Isot.* **44,** 1832.

Barthe J., Kamenopoulou V., Cattoire B. and Portal G. (1989) Dose evaluation from textile fibers: A post-determination of initial ESR signal. *Appl. Radiat. Isot.* **40,** 1029.

Berger G.W., Lockhart R.A. and Kuo J. (1987) Regression and error analysis applied to dose response curves in thermoluminescence dating. *Nucl. Tracks Radiat. Meas.* **13,** 177.

Brodski L. and Hutt G. (1993) Vitreous materials: prospects in retrospective dosimetry. In *The use of natural materials for solid-state dosimetry in accident zones and the environment* (Haskell E.H. Ed.), *Final report, IAEA.*

Dalgarno B.G. and McClymont J.D. (1989) Evaluation of ESR as a radiation dosimetry technique. *Appl. Radiat. Isot.* **40,** 1013.

Ginsbourg S.F., Babushkina T.A., Basova L.B. and Klimova T.P. (1995) ESR spectroscopy of building materials as a dosimetry technique. Proceedings of Fourth International ESR Conference, held at Munich, Germany, March 1995. Abstract MP-6.

Ikeya M., Baffa F.O. and Mascarenhas S. (1989) Quality assessment of coffee beans with ESR and gamma-ray irradiation. *Appl. Radiat. Isot.* **40,** 1219.

Ke W., Cunpu S. and Yuanming S. (1995) Dosimelogic properties of watch glass: A potential practical ESR dosimeter for nuclear accident. Proceedings of Fourth International ESR Conference, held at Munich, Germany, March 1995. Abstract MP-9.

Nakajima T. (1982) The use of organic substances as emergency dosimeters. *Int. J. Appl. Radiat. Isot.* **33,** 1077.

Nakajima T. (1988) Sugar as an emergency populace dosimeter for radiation accidents. *Health Physics* **55,** 951.

Nakajima T. (1989) Possibility of retrospective dosimetry for persons accidently exposed to ionizing radiation using electron spin resonance of sugar and mother-of-pearl. *Brit. J. Radiol.* **62,** 148.

Nakajima T., Fujimoto K. and Hashizume T. (1973) New gamma-ray exposure estimation method for radiation accident. *J. Nucl. Sci. Tech.* **10,** 202.

Nakajima T., Otsuki T. and Hara H. (1993) Radiation accident dosimetry using shells. *Appl. Radiat. Isot.* **44,** 91.

Press W.H., Teukolsky S.A., Vetterling W.T. and Flannery B.P. (1992) *Numerical Recipes in C.* Cambridge, U.K.: Cambridge University Press; pps. 681-688.

Regulla D.F. and Deffner U. (1989) Dose estimation by ESR spectroscopy at a fatal radiation accident. *Appl. Radiat. Isot.* **40,** 1039.

Spiegel M.R. (1961) Theory and Problems of Statistics. San Francisco, CA: McGraw-Hill Book Company.

Schauer D.A., Coursey B.M., Dick C.E., McLaughlin W.L., Puhl J.M., Desrosiers M.F. and Jacobsen A.D. (1993) A radiation accident at an industrial accelerator facility. *Health Physics*, **65,** 131.

Trivedi A. and Greenstock C.L. (1994) Use of sugars and hair for ESR emergency dosimeters. *Int. J. Appl. Radiat. Isot.*. **44,** 85.

Yijian C., Arakel A.V. and Jinfen L. (1989) Investigation of sensitive signals due to gamma-ray irradiation of chemical precipitates: A feasibility study for ESR dating of gypsum, phosphate and calcrete deposits. *Appl. Radiat. Isot.* **40,** 1163.

FIGURE CAPTIONS

Fig. 1. 600 mT wide scan of unirradiated (broken line) and 782 Gy irradiated plasterboard (solid line). Manganese line 4 from Mn impurities found in the plasterboard, is at g = 1.981. The combined composite for signals 1, 2 and 3 is at g = 2.012.

Fig. 2. 150 mT wide scan of spectra shown in Fig. 1. Signals 1, 2 and 3 can be distinquished from each other. Their respecitive g-factors are 2.0148, 2.0094 and 2.0076. There is possibly a weak signal at approximately 345.3 mT which we did not characterize. The signals at 339.8 and 348.6 mT were caused by Mn impurities as noted in Fig. 1. Broken line: unirradiated specimen. Solid line: 782 Gy irradiated specimen.

Fig. 3. Results of using the Marquardt-Levenberg method to decompose the normalized curve obtained by subtracting the background curve shown in Fig. 2 from the irradiated sample curve. Signals 1, 2 and 3 have g-factors of 2.0148, 2.0094 and 2.0076 and widths of 0.754, 0.938 and 0.370. Broken line: normalized signal. Solid lines: Component spectra of the normalized signal. 782 Gy irradiated specimen.

Fig. 4. Low dose response curve for normalized plasterboard. The specimens were constantly rotating while measurements were made. Dose given were 25, 50, 100, 200 and 400 mGy. The linear regression equation for the fitted line is $y = 0.299 + 18x$. $R = 0.997$.

Fig. 5. High dose response curve for normalized plasterboard. Doses given were 0, 1, 3, 6, 12 and 24 Gy. The equation for the line is $y = -29.006 + 128.02x$. $R = 0.98499$.

Table 1. Summary of potential residential EPR dosimeters

Material	Comments	References
Broad study	Environmental, pharmaceuticals & candies.	Dalgarno and McClymont, 1989.
Broad study	Common household and personnal items.	Nakajima, 1982.
Plexiglas, lucite	10% fading ~36 hours. Reduced at 0° C.	Nakajima, 1982.
Polyethylene	12% fading in ~2 days.	Nakajima, 1982.
Polypropylene	0.5 to 1.0 Gy detection limit.	Barthe *et al.*, 1989.
Plastic buttons	Fades faster than polyethylene.	Nakajima, 1982.
Wool	Rapid fading. Unsuitable.	Nakajima, 1982.
Cotton, cloth	12% fading in ~2 days.	Nakajima, 1982.
Cotton	0.5 to 1.0 Gy detection limit.	Barthe *et al.*, 1989.
Glass	20% fading in 24 hours. Detect 2 Gy.	Ke *et al.*, 1995.
	No fading in headlight glass.	Brodski and Hutt, 1993.
Plastic lens	Detect overexposure.	Schauer *et al.*, 1993.
Sugar, glutamate	200-500 mGy detection limit. Fades.	Trivedi and Greenstock, 1991
	Detect 40 mGy. Minimal fading	Nakajima, 1989.
	Lyoluminescence and EPR agree.	Azorin *et al.*, 1989.
Salt, pepper	Rejected in favor of sugar. Rapid decay.	Nakajima, 1988.
Coffee beans	Unsuitable due to aging decomposition.	Ikeya *et al.*, 1989.
Hair, nails	Rapid fading.	Nakajima, 1982.
	May be useable if proper workup done.	Trivedi and Greenstock, 1991.
	Dose distribution data needed.	Dalgarno and McClymont, 1989.
Ethylene-propylene rubber	Complicated by presence of anti-oxidants.	Baccaro *et al.*, 1991.
Pencils	Rapid decay.	Nakajima, 1989.
Wood	Rapid decay.	Nakajima, 1989.
Wood chops	Rapid decay.	Nakajima, 1989.
Newspaper	Rapid decay.	Nakajima, 1988.
Tissue paper	Rapid decay.	Nakajima, 1988.
Mother of Pearl	Minimal fading. Linear 1 to 12 Gy.	Nakajima, 1989.
Gypsum	Possibly use for dating.	Yijian *et al.*, 1989.
Pharceuticals	Piriton appears promising.	Dalgarno and McClymont, 1989.
	Glycerol failed.	
Heart tablets	Useable when calibrated properly.	Regulla and Deffner, 1989.
Shells	Potentially useable.	Nakajima *et al.*, 1993.
Building matl's	0.6 to 10 Gy minimal dose for bricks.	Ginsbourg *et al.*, 1995.

Table 2. Experimental protocol for sheetrock experiments.

ID	Form	Weight	Test	Pre-irrad.	Comment
SR1	Carved cylinder	95.3	Dose response	None	0, 21, 44, 95, 186, 365, 732, and 1450 mGy, Final dose of 782 Gy to check EPR properties
SR2	Carved cylinder	93	Dose response	None	0, 1, 3, 6, 12, 24 Gy.
SR3	Crushed	94	Isochronal annealing	None	Temp. stability of baseline. Multiple aliquots.
SR4	Crushed	76	Isochronal annealing	500 Gy	Multiple aliquots, cumulative heating.
SR5	Carved cylinder	56.4	Dose response	None	
SR6	Carved cylinder	47.8	Dose response	None	
SR7	1/8" diam core	67.4	Single dose	None	35 year old specimen from wall of laboratory
SR8	Carved cylinder	77.5	Dose response	None	Specimen was constantly rotating during measurements

Table 3. Summary of results for plasterboard, bisphenol A polycarbonate, neoprene rubber and pyrex glass.

Material	g-factor	Width (mT)	~Half-life
Plasterboard	2.0148	0.754	12 mos.
Plasterboard	2.0094	0.938	6 mos.
Plasterboard	2.0076	0.370	3 mos.

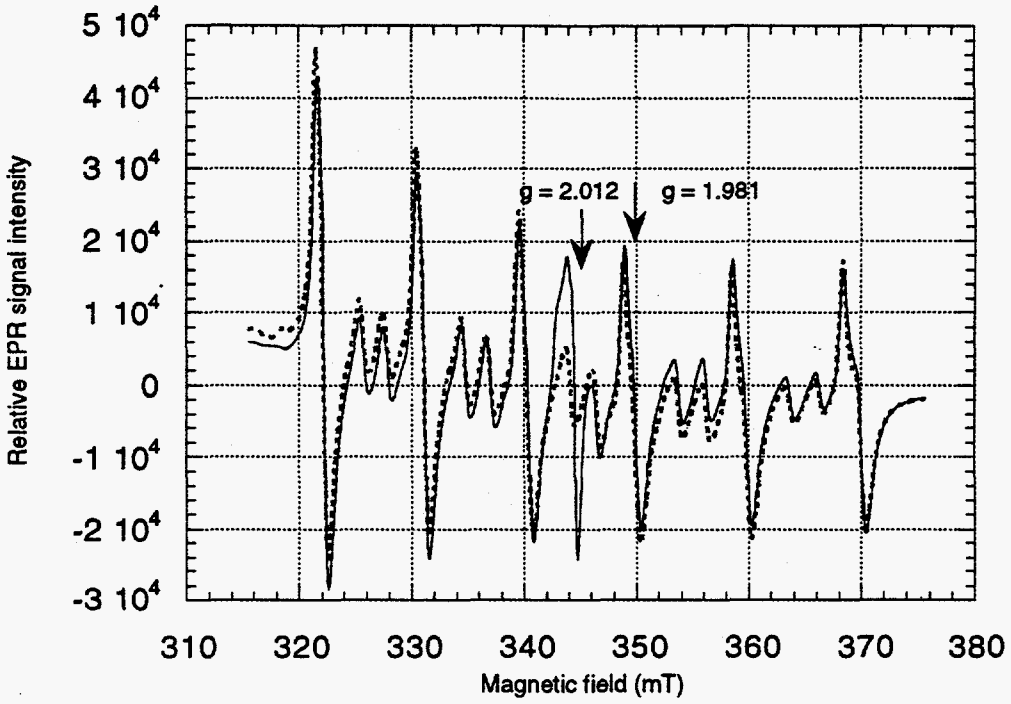
5 10^4
4 10^4
3 10^4
2 10^4
1 10^4
0
-1 10^4
-2 10^4
-3 10^4
Relative EPR signal intensity
g = 2.012
g = 1.981
310
320
330
340
350
360
370
380
Magnetic field (mT)

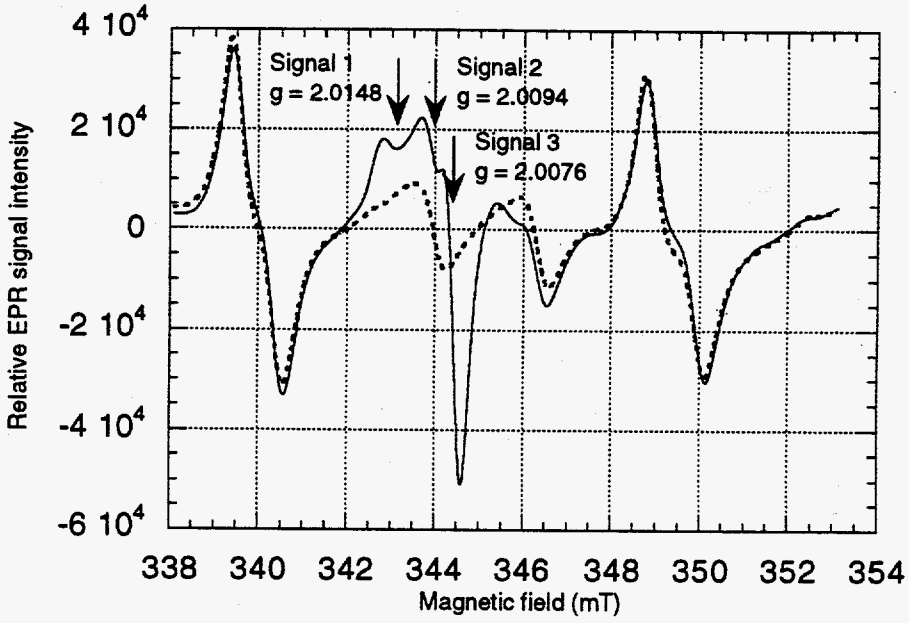
Signal 1
g = 2.0148
Signal 2
g = 2.0094
Signal 3
g = 2.0076
Relative EPR signal intensity
4 10^4
2 10^4
0
-2 10^4
-4 10^4
-6 10^4
338
340
342
344
346
348
350
352
354
Magnetic field (mT)

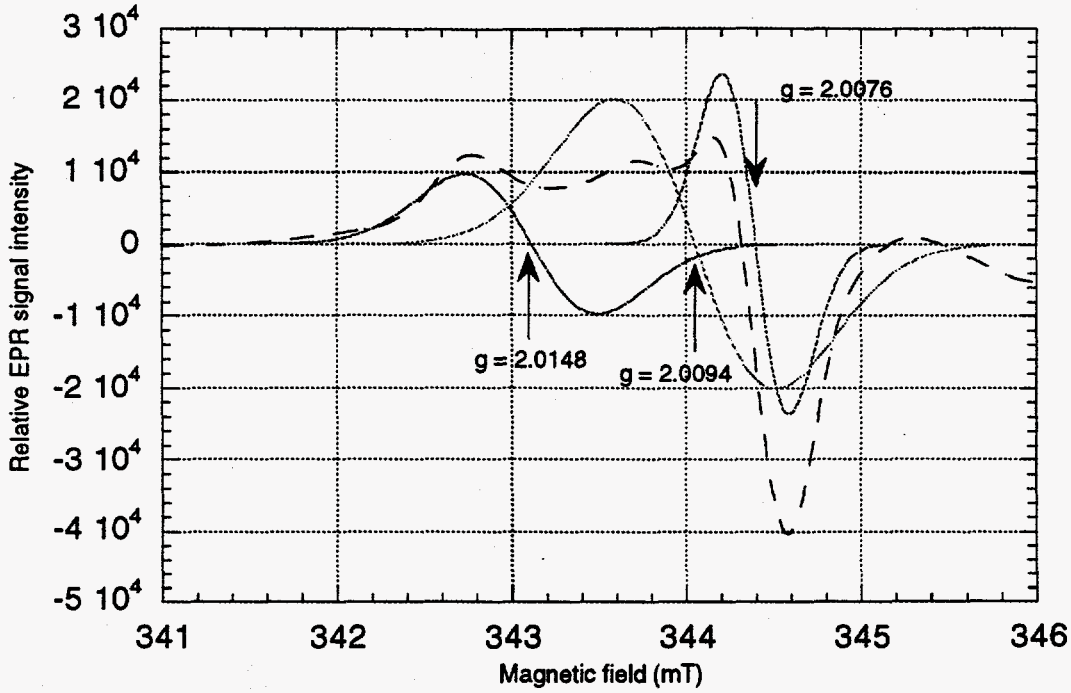
3 10^4
2 10^4
1 10^4
0
-1 10^4
-2 10^4
-3 10^4
-4 10^4
-5 10^4
Relative EPR signal intensity
341
342
343
344
345
346
Magnetic field (mT)
g = 2.0076
g = 2.0148
g = 2.0094

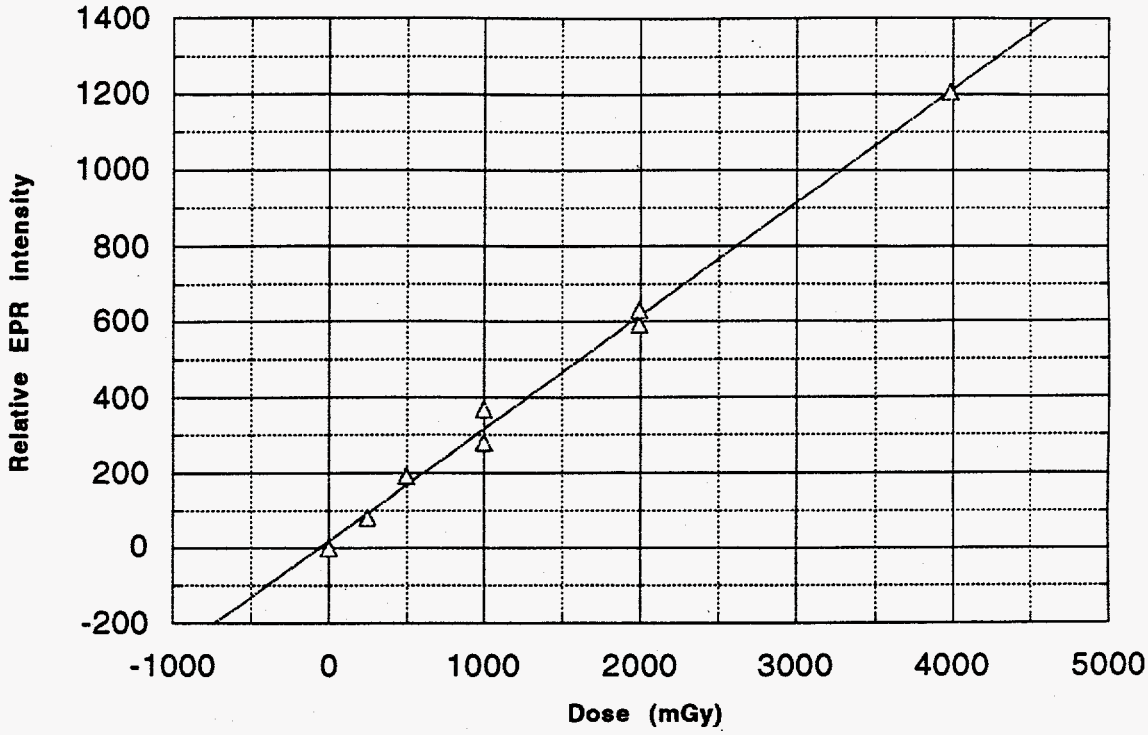
1400
1200
1000
800
600
400
200
0
-200
Relative EPR Intensity
-1000
0
1000
2000
3000
4000
5000
Dose (mGy)

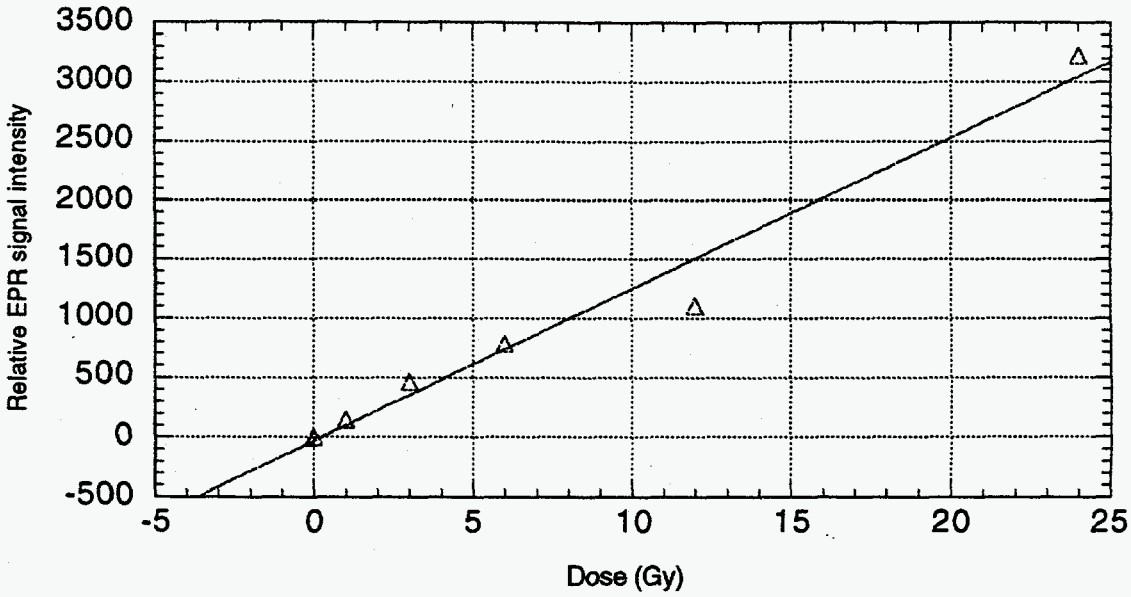
Relative EPR signal intensity
3500
3000
2500
2000
1500
1000
500
0
-500
-5
0
5
10
15
20
25
Dose (Gy)

APPENDIX 16.

Plasterboard as an Emergency EPR Dosimeter. (*Health Phys.* **71**(1):95, 1996)

Removed

APPENDIX 17.

Interlaboratory Comparison of EPR Techniques for Measuring Radiation Exposure of Enamel (ECP-10 Project): Report by the TL/EPR Laboratory of the University of Utah. (Internal report)

Interlaboratory Comparison of EPR Techniques for Measuring Radiation Exposure of Enamel (ECP-10 Project): Report by the TL/EPR Laboratory of the University of Utah

E.H. Haskell, R.B. Hayes and G.H. Kenner

Division of Radiobiology, University of Utah,
Salt Lake City, UT 84103

INTRODUCTION

Fourteen enamel samples, 150-250μ in diameter, were received which had been irradiated with 0, 100, 250, 500 and 1000 mGy. The doses received by the individual teeth were unknown. One specimen was found under the microscope to contain some filling material.

Since the doses given and the sizes of the groups were known, we first obtained EPR spectra on the as received specimens. By comparing spectra of the supposed unirradiated samples (the three lowest values), we were able to form groupings for those aliquots having the higher irradiations. We then did additive dose response measurements on the specimens whose errors were large enough that they overlapped groups. An imminent deadline prevented us from doing dose responses on all specimens.

The EPR analysis was done using a conventional X band spectrometer(Bruker ESP300E, Bruker Instruments, Manning Park, Billerica, MA). Parameters used were power 8 mW, field modulation 100 kHz, modulation amplitude 0.5 mT, room temperature, receiver gain of 1 x 10^5, microwave resonance frequency of 9.74 gHz. Scan width was 5.0 mT. Weak pitch was used as the reference standard. 10 scans were recorded over a 4.3 min time period for each sample. Approximately 100 mg of powder was placed in a 1/4 inch x 7 inch (0.635 cm x 17.8 cm) quartz EPR sampling tube(Wilmad Glass, Route 40 and Oak Road, Bena, NJ 08310). The samples were vacuum dried at room temperature. They were stored at room temperature and low (ambient) humidity.

This report is divided into three parts. The first part is a report on the intercomparison study proper. The second part deals with the potential light exposure problem. The third part deals with a signal drift problem which we successfully resolved.

INTERCOMPARISON STUDY

As mentioned in the introduction, we first ran EPR measurements on the as received specimens before any test doses were given. The three lowest doses were arbitrarily designated as being the unirradiated controls. The remaining specimens were then grouped according to their values. The standard errors about each specimen were examined and any specimens whose standard errors were such that they could have belonged to two adjacent groups were evaluated further using additive dose response methods.

Eight of the specimens were analyzed using the additive dose technique. These were N4, N6, N21, N58, N87, N88 and N90. A dose response was done on one of the 1 Gy aliquots (N100) due to its having a relatively significant departure from its partner sample. The results are shown in Figure 1.

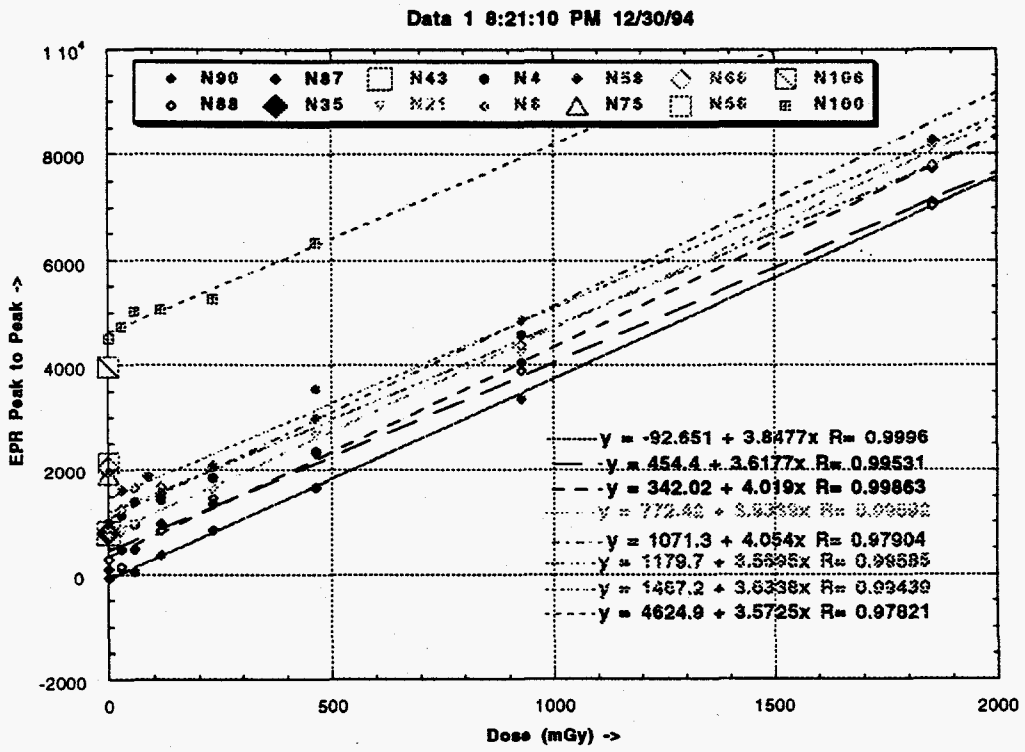

Figure 1 - Additive dose response curves for specimens whose radiation dose was questionable based on preliminary data.

The average slope of the dose response was 3.78* with a standard deviation of 0.21. A least squares fit of the dose grouping gave a slope of 3.87 with an expected error of 0.21.

Figure 2 shows the final results of the study. Six of the data points were from the preliminary study (N35, N43, N56, N66, N75, N106). Each of these six data points was from the averaged peak to peak values of three spectra. The three spectra were taken consecutively with the sample being shaken in the tube between each run. The standard errors of the means are shown on the graph.

For those samples which received a dose response, the dose estimate came from the y-intercept of that dose response. The standard errors shown for these samples in Figure 1, are the uncertainty in the intercept.

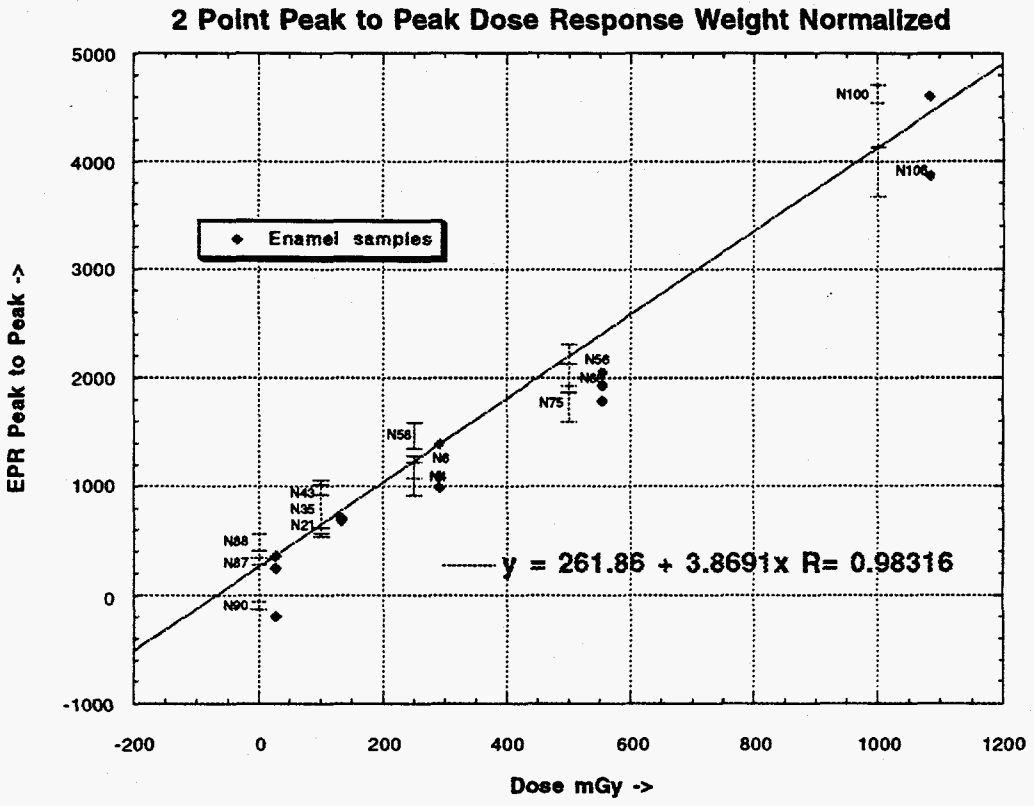

Figure 2 - Grouping of specimens based on as received EPR spectra.

* All slopes and their errors are in units of ESR Intensity/mGy

Based on the above results, we arranged the specimens into the groupings shown in Table 1. Note that the three 0 mGy specimens were tested using the additive dose response method.

0 mGy	100 mGy	250 mGy	500 mGy	1000 mGy
N90	N21	N4	N75	N106
N87	N35	N6	N66	N100
N88	N43	N58	N56	

Table 1

Using the linear fit to the grouping, we can find what our estimate would have been had we not the foreknowledge of the grouping categories. These dose estimates and their errors are given in Figure 3 and Table 2.

Note, these reported errors only reflect the error in the individual points as shown in the graph, and not any of the expected error in the linear fit.

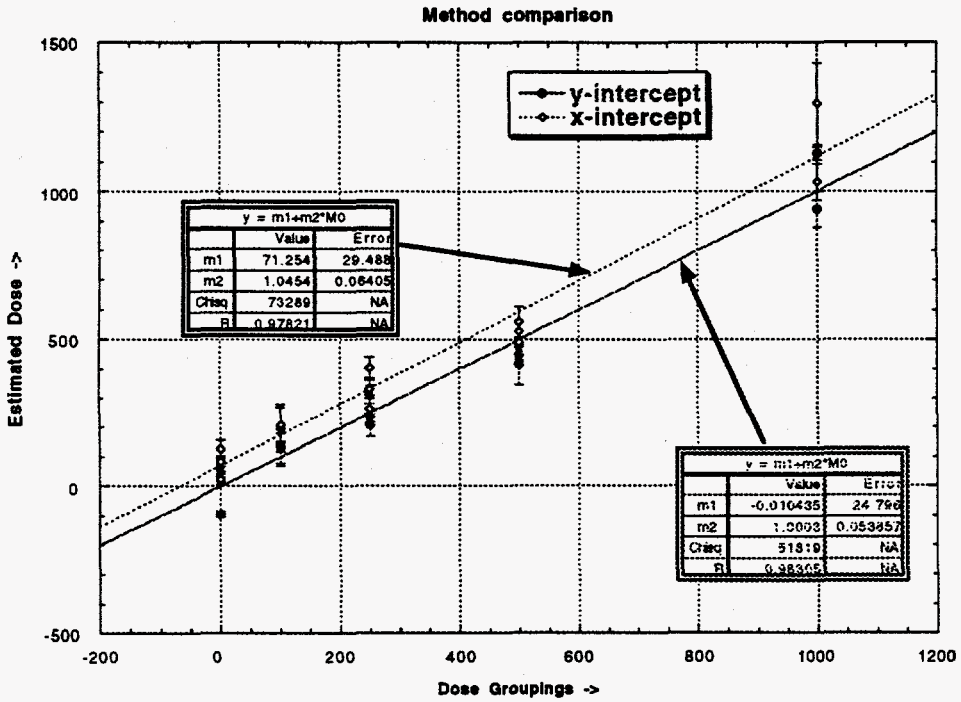

Figure 3 - Method comparison.

	N90	N87	N88	N21	N35	N43	N4
Dose Estimate (mGy)	-93	20.7	49.8	132	137	138	209
Expected Error (mGy)	9	17	28	15	58	68	39
	N6	N58	N75	N66	N56	N106	N100
Dose Estimate (mGy)	237	312	413	448	479	940	1128
Expected Error (mGy)	26	31	67	34	49	60	21

Table 2

SENSITIVITY TO LIGHT

As part of the work done for the intercomparison study, we have determined in enamel that the mechanically induced signal generated during sample preparation[6] is sensitized by exposure to light while the perpendicular component of the hydroxyapatite signal is unaffected. Further, we have determined that the mechanically induced signal attentuates with time and have verified that its intensity is power dependent.

Enamel grains, 150-250μ in diameter, were scanned, irradiated with 1.5 Gy using a ^{60}Co source and rescanned, followed by illumination for 17 hours with a quartz halogen microscope lamp and a third scanning (Figure 4). The magnitude of the mechanical signal is increased by irradiation and exposure to light (peak A). The perpendicular component of the hydroxyapatite signal is apparently not affected by light (concurrency of peak B). Exposure to light causes a slight increase in the size of the parallel component of the hydroxyapatite signal which may be due to noise.

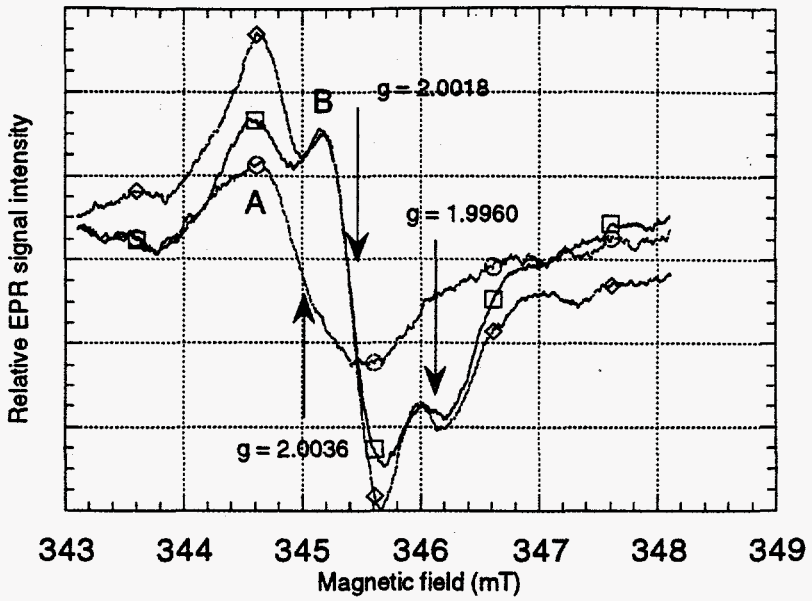

Figure 4 - Results of irradiating an enamel sample. Peak A is the upper component of the g = 2.0036 signal. Peak B is the upper component of the g = 2.0018 signal. a) circles: preirradiation. b) squares: 1 Gy ^{60}Co irradiation. c) diamonds: 1 Gy ^{60}Co irradiation followed by 17 hour exposure to light from a quartz halogen microscope lamp.

The specimen was remeasured one month later. An additional scan was made with the power set at 127 mW. The other parameters remained the same (Figure 5). The size of the light exposed mechanical signal decreased after 30 days. Increasing the power to 127 mW resulted in a disappearance of the mechanically induced signal. The 127 mW signal was not normalized for the power increase.

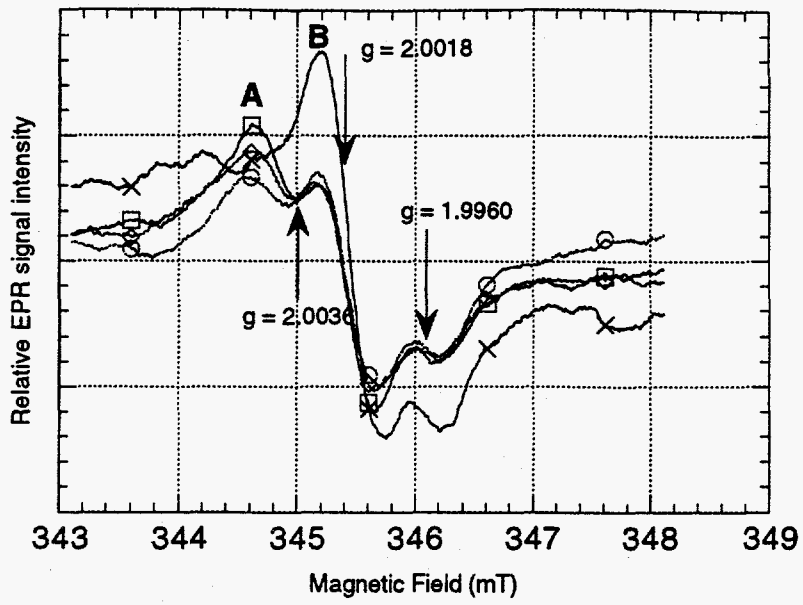

Figure 5 - Effect of time and EPR power on the magnitude of the mechanically induced and hydroxyapatite signals. Peak A is the upper component of the g = 2.0036 signal. Peak B is the upper component of the g = 2.0018 signal. a) circles: 1 Gy 60Co irradiation. b) squares: 1 Gy 60Co irradiation followed by 17 hour exposure to light. c) diamond: same as (b) but remeasured two days later at 8 mW. d) crosses: same as (c) except remeasured at 127 mW.

Assuming symmetrical distribution of signals about the center point, the following tentative conclusions can be drawn. 1.) The mechanically induced signal is both radiation and light sensitive (See peak A). 2.) The perpendicular component of the hydroxyapatite signal is radiation sensitive but not light sensitive. This is supported by the congruency of the upward peaks of the perpendicular component at position B. 3.) The parallel component of the hydroxyapatite signal is radiation sensitive but it is not possible to draw any conclusions about light sensitivity because of the small size of the signal and noise considerations.

Although the magnitude of the perpendicular component of the hydroxyapatite signal is probably not affected by light, serious errors occur because of the extensive overlap which occurs between it and

the mechanically induced signal. This error can result in serious dose overestimates if corrections are not made.

The signal can be eliminated by increasing the EPR power, a procedure recommended by Pass and Aldrich, Desroisiers, et al. and Copeland. While it is tempting to minimize the effect of the mechanically induced signal in this manner while increasing the magnitude of the inorganic signal, there are some theoretical problems involved. Foremost among these is decreased ability to separate overlapping signals. It is also important to remember that following saturation, EPR signals become smaller and possibly increase in width.

Possibly the best method for determining optimum EPR power, is to do a study in which the errors are determined at various power levels and use the data to select an optimum.

SIGNAL DRIFT

Also discovered in the course of doing the intercomparison experiment was an unaccounted drift of the signal following startup of the machine. It was found that six hours was necessary for the signal to stabilize (Figure 6).

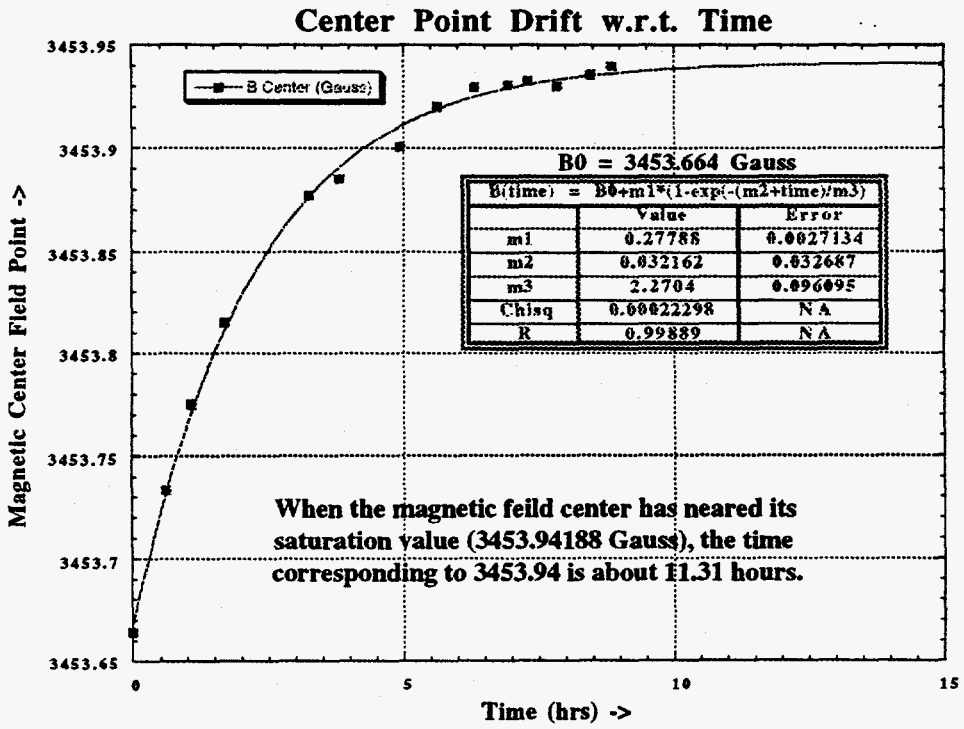

Figure 6 -

We did some rough calculations to determine the effect of this much signal drift on our measurements. The results are shown in Figure 7.

When we discovered we had this problem, we called Bruker Instruments Technical Support. They told us that they were having a similar problem when using a teflon pedestal in the resonating chamber and that we might have a similar problem with nylon. We then replaced the lower pedestal of the specimen chamber with a quartz tube and reran the experiment. The results are shown in Figure 7.

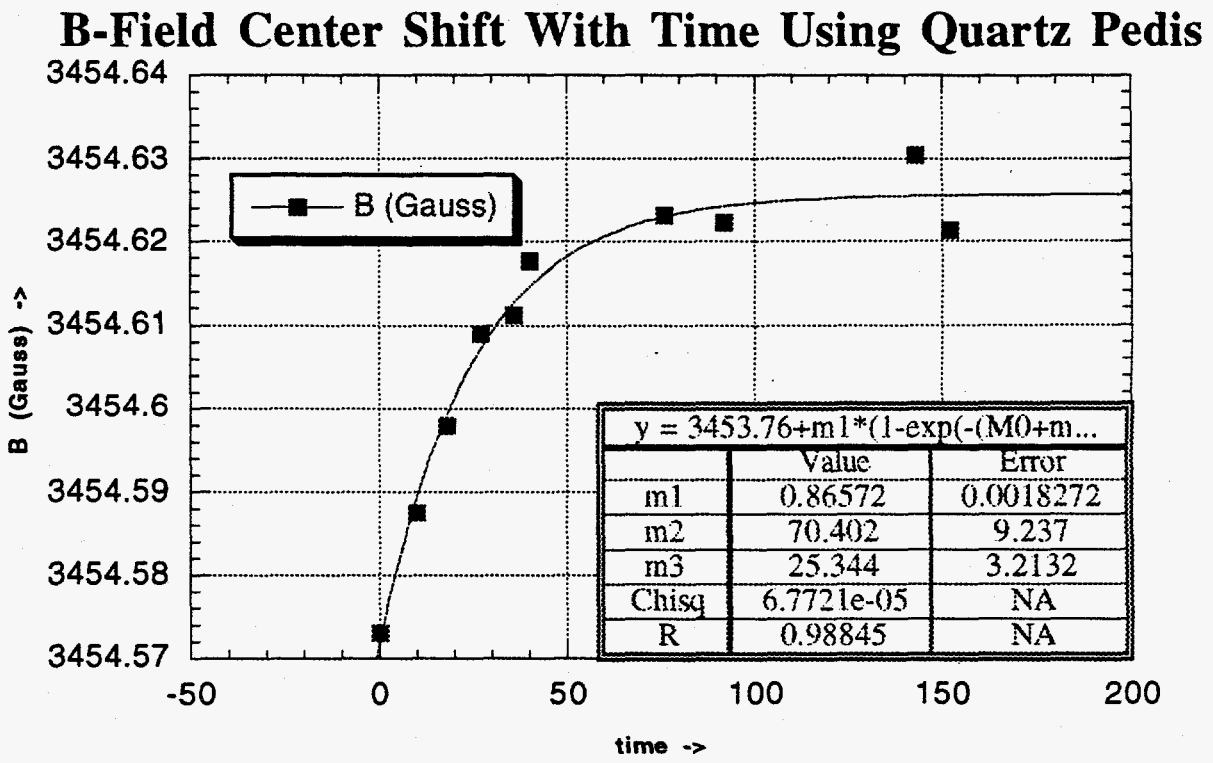

Figure 7 - Plot of quartz pedestal.

APPENDIX 18.

An EPR Intercomparison Using Teeth Irradiated Prior to Crushing. (*Radiat. Meas.* in press) Removed

APPENDIX 19.

FIV, Dose Reconstruction, EPR with teeth - Investigations on sample preparation techniques. (Intercomparison protocol)

FIV, Dose Reconstruction, EPR with teeth

Investigations on sample preparation techniques

FIV participants:	ISS, Rome
	GSF, Munich
Invited participants:	IMP, Ekaterinbourg
	MRRC, Obninsk
	URPI, Kiev
	UU, Utah

Objectives

Selection of the most suitable technique(s) for preparation of tooth enamel samples. It will be used to suggest a protocol for preparation of tooth enamel samples.

Each participant will chose one technique and suggest the most suitable set of EPR measurement parameters. Of special attention should be to determine an optimum level of microwave power. The quality criteria of a technique (including the set of measurement parameters) will be the reproducibility and the inter-sample variation of the quality parameters listed below. The best compromise needs to be found between reproducibility of background spectra and maximal intensity of the hydroxyapatite signal.

Milestones

November 96:	Comparison and discussion of results obtained by the participants for their own set of samples and technique. Pre-selection of techniques, exchange of samples and parameter sets.
February 97:	Comparison and discussion of results obtained by different participants for the same set of samples and measurement parameters. Final selection of techniques.

Quality parameters

The quality parameters are listed below and defined in the figures. They are chosen to allow for an objective comparison of EPR spectra measured by different spectrometers. The standard deviation of the parameters and the normalised signal amplitude will be a measure for the quality of the preparation technique. The quality parameters needs to be determined with the set of measurement parameters which are considered to be the best.

Background amplitude, Ab
Background position, H0b (g-value or field and frequency)
Background line width, dHb
Background symmetry factor, ratio dHb1/dHb2
Hydroxyapatite amplitude after 50 Gy irradiation, Ah50
Hydroxyapatite line width, dHh

Hydroxyapatite position, H0h (g-value or field and frequency)
Mean normalised background amplitude, ratio (mean Ab)/(mean Ah50)

For the chosen EPR measurement parameters the signal-to-noise ratio, (mean Ab)/N has to be determined. The noise amplitude, N, should be measured without sample.

For one representative unirradiated sample the background amplitude (Ab), the line width (dHb) and the symmetry factor (dH1/dH2) should be determined versus microwave power up to 200 mW.

For one representative 50 Gy irradiated sample the hydroxyapatite amplitude (Ah) should be determined versus microwave power up to 200 mW.

The 50 Gy irradiation has to be done with a 3 mm Plexiglas as build-up material by a ^{60}Co- or ^{137}Cs-source.

Samples

10 molars or wisdom teeth. Three of them has to be irradiated with 50 Gy for determination of the hydroxyapatite parameters. The remaining seven samples are used to determine the background parameters.

The conditions and time of storage of the samples after preparation should be given.

Measurements

Each sample has to be measured three times following refilling of the sample tube to determine the reproducibility. The orientation of the sample tube in the cavity has to be identical for all measurements.

Remarks

A quality assurance procedure including suitable reference samples to allow for comparison of accuracy of spectrometer parameter settings and signal intensities will be discussed at the meeting in November.

Figures for definition of quality parameters

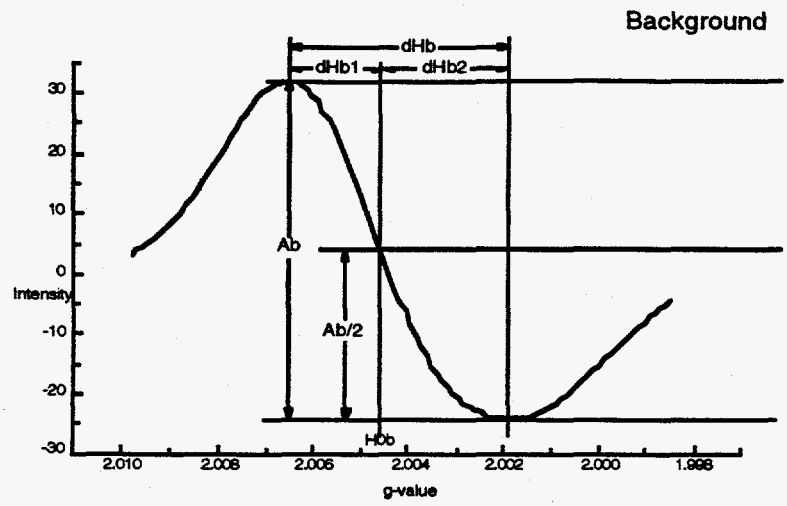

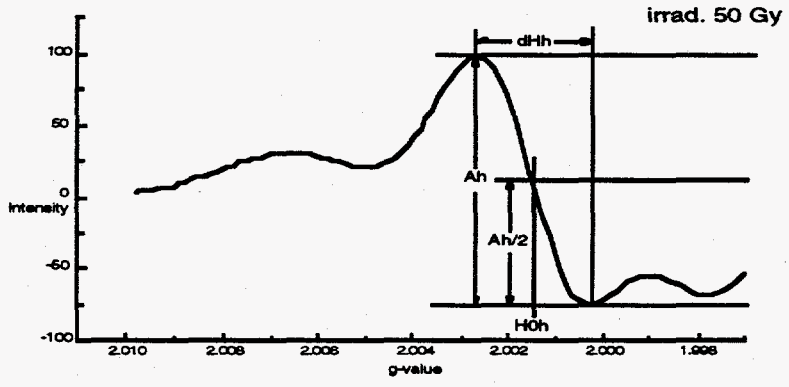

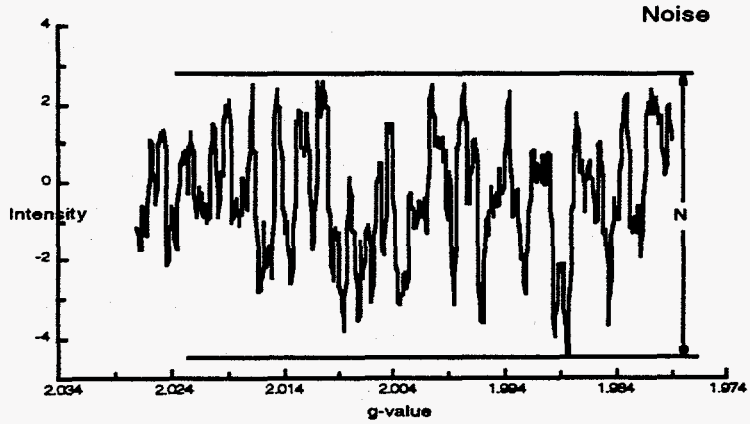

APPENDIX 20.

Retrospective Dosimetry using EPR and TL Techniques: A Status Report. (Presented at the International Congress on Radiation Protection. Vienna, Austria April 15-19, 1996) Removed for separate cycling

APPENDIX 21.

Luminescence Techniques for Dose Reconstruction in Accident Situations: Technical Aspects and Results of Application. (Presented at the International Workshop on Radiation Exposures by Nuclear Facilities-Evidence of the Impact on Health. Portsmouth, England July 9-12, 1996)

Removed for separate cycling

APPENDIX 22.

Luminescence Techniques for Dose Reconstruction in Accident Situations Possibilities, Limitations and Uncertainties. (Presented at the International Workshop on Radiation Exposures by Nuclear Facilities-Evidence of the Impact on Health. Portsmouth, England July 9-12, 1996)

Removed for separate cycling

APPENDIX 23.

EPR Techniques for Space Biodosimetry. (Presented at the Space Radiation Damage and Biodosimetry Workshop, Houston, Texas Sept. 9, 1996) Removed for separate cycling

APPENDIX 24.

Challenges in Dose Reconstruction: Examples from Chernobyl, Hiroshima, Biomarkers and Environmental Materials. (Submitted to *Radiat. Res.*) removed

APPENDIX 25.

Thermoluminescence Measurement of Externally Applied Alpha Doses. Masters Thesis (Maureen Lynn Gilbert, Draft, Aug, 1996)

THERMOLUMINESCENCE MEASUREMENT OF EXTERNALLY APPLIED ALPHA DOSES TO PORCELAIN

DRAFT

by

Maureen Lynn Gilbert

A thesis submitted to the faculty of
The University of Utah
in partial fulfillment of the requirements for the degree of

Master of Science

Department of Physics

University of Utah

August 1996

ABSTRACT

The main purpose of this project is to test the feasibility of a method to measure alpha radiation doses attributable to contamination of water supplies from nuclear power plants. Plants developing nuclear weapons were started in the late 1940's. Most of these plants have had radiation leakages, the extent of which is a subject of various investigations. In many cases reconstruction of doses relies on historical records, and in most cases actual measurements of dose are impossible.

This project studies the thermoluminescence (TL) properties of porcelain samples from the inside of porcelain tanks. Toilet tanks were used because samples from the inner surface are in constant contact with the local water supply. Also, because of the alpha particle's short path length, any external alpha irradiation absorbed by these porcelain samples most likely came from the water. Whether or not this procedure is feasible depends on how sensitive porcelain is to alpha irradiation and the resolution of dose versus depth which it is possible to obtain.

The sensitivity of porcelain to alpha irradiation was evaluated by comparing it with the sensitivity to beta irradiation. This was done by determining Aitken's a-value for porcelain coarse grains, fine grains, and slices. Also, by calibrating the alpha source in Gy to porcelain per second from the alpha energy, range, and flux, the accuracy of the a-value for slices was determined.

As part of a method to distinguish the TL produced by alpha irradiation from that produced by other sources, a dose versus depth analysis was done on the porcelain slices. The TL from the

external alpha irradiation disappeared at approximately 30 μm which corresponds to the range of the alpha particle. The depth analysis was done by sanding off the outer surface of the porcelain slices in increments of 10 μm.

The lowest detectable alpha dose using porcelain was found to be approximately 130 mGy to porcelain, for slices. This value is low enough to make the procedure worthy of further testing. With modifications, the alpha sensitivity of porcelain may be improved.

In a real life setting complications arise. For example, water in the pores of porcelain may absorb part of the natural external radiation which would otherwise reach the porcelain grains. Also, if the porcelain samples are not pure, there may be discrepancies in the TL measurements.

TABLE OF CONTENTS

LIST OF TABLES

LIST OF FIGURES

ACKNOWLEDGMENTS

I thank Dr. Edwin H. Haskell for all of his help and support during this project.

I also thank all the workers at The Center for Applied Dosimetry (formerly TL Laboratories) for their guidance in the project itself, and for helping with the preparation for my defense and writeup.

I also thank James F. Ziegler for providing his computer program to determine the range of the alpha particles in porcelain.

INTRODUCTION

The main purpose of this project is to test the feasibility of a method of measuring alpha radiation doses attributable to contamination of water supplies from nuclear power plants. Plants developing nuclear weapons were started in the late 1940's. Some of these plants have had radiation leakages. The extent of these releases, such as discharge of radionuclides into the Columbia River from Hanford,[1] escape of radioiodine into the air from Oakridge National Laboratory,[2] fallout from atomic weapons testing in the Marshall Islands,[3] and many others is a subject of various investigations. Similar nuclear processing plants in the former Soviet Union, such as one in the Cheljabinsk Region, have also had leakages which are being studied.[4] There have been more recent accidental releases of radiation as well. For example, there was an accidental release of soluble $^{137}CsCl$ in Goiania, Brazil[5] in 1987. In many cases reconstruction of doses relies on historical records, and in most cases actual measurements of dose are impossible.

This project is designed to examine the feasibility of a method of measuring of the cumulative dose deposited by alphas and low energy betas in a water supply. The method involves the thermoluminescence (TL) properties of porcelain from the inside surface of toilet tanks. Toilet tanks were chosen because samples are available from contaminated areas and porcelain is known to be a thermoluminescent material. The TL properties of porcelain after beta and gamma irradiations have been tested in the past.[6] This project will look into the TL properties of porcelain after alpha irradiations from a Cm-244 source

The sensitivity of porcelain to alpha irradiation will be evaluated by comparing the dose deposited per second by alpha irradiation to the dose deposited per second by beta irradiation. This comparison is done by using Aitken's a-value, which represents the inverse ratio of the alpha dose deposited to the beta dose which produces the same amount of TL. The dose deposited per second by the alpha source was also calculated using the energy, flux and range of the alphas emitted, and the density of the porcelain slices. The beta dose was also calibrated in dose delivered per second to porcelain, to ensure accurate measurements.

Aitken's a-value will be found for porcelain coarse grains, fine grains, and slices. Because of the optical attenuation in the coarse grains and slices, and the different geometry of the three forms, the a-value may be slightly different for each one. These values will be found by plotting the TL per alpha and beta doses, measuring the alpha flux per second, determining the optical attenuation in coarse grains and slices, and determining the TL per tracklength. The alpha irradiations are applied in vacuum to reduce absorption by air. These values, along with Aitken's equations for the a-values, will determine the a-values for porcelain coarse grains, fine grains and slices.

In order to distinguish the external alpha irradiation from the other sources, a dose depth analysis will be done on porcelain slices. Since the alpha has a much shorter range than betas and gammas, the TL produced from alpha irradiation will stop at or before the range of the alpha. Since the samples in this project were annealed of any previously existing irradiation, the plateau

should go to zero once the background has been subtracted off. In a real life situation, a dose depth profile for the internal radiation sources would need to be found before the external alpha irradiation can be clearly distinguished from the internal irradiation.

The method being tested will ideally be able to give a maximum limit of the external alpha dose deposits. The alpha sensitivity of porcelain slices is determined. The alpha sensitivity gives the lowest alpha and low energy beta dose which can be detected by this method. If the sensitivity is strong enough, then the method may be practical.

CHAPTER 1

USING THERMOLUMINESCENCE TO MEASURE ABSORBED RADIATION

1.1 Introduction to thermoluminescence

The light given off when an insulator or semiconductor is heated, after being irradiated with ionizing radiation, is referred to as thermoluminescence (TL). For crystalline substances, the thermoluminescence is often directly proportional to the amount of radiation absorbed.

This project uses porcelain samples from toilet tanks. Toilet tanks were chosen because the inside surface is in almost constant contact with the water supply. If the water supply is contaminated with alpha emitters, the porcelain surface of the tank will be directly irradiated. The porcelain samples used in this project were calibrated by how much TL was produced for different alpha and beta doses.

When radiation is absorbed by an insulator or semiconductor, ionization occurs, separating holes and electrons which get caught in traps at the localized energy levels. Heating the material releases the electrons, which may recombine with the holes. Electrons in deeper traps require more energy, and therefore require heating to higher temperatures, to escape. In other words, the deeper the trap, the higher the temperature to which the sample must be heated for thermoluminescence to occur. The amount of thermoluminescence observed is proportional to the number of electrons which may recombine with holes in the

luminescence centers to produce luminescence. For irradiation at certain temperatures, some materials emit an intensity of thermoluminescence that is directly proportional to the amount of radiation that has been absorbed.

Thermoluminescence is produced by the recombination of trapped electrons and holes accompanied by the emission of photons. A simple model describing this process consists of the valence band and the conduction band, with electron and hole traps in between [see Figure 1.1]. The trap T located above the equilibrium Fermi level (E_f) is empty before the absorption of radiation. Thus, it is a potential electron trap. The traps L, located below the Fermi level are full of electrons and are potential hole traps. These traps are referred to as recombination centers because they are where electrons recombine with the trapped holes, annihilating them. There are many of these potential hole traps in typical crystallites.

The absorption of radiation energy greater than the band-gap energy (E_C - E_V) ionizes some of the valence electrons, resulting in free electrons in the conduction band and free holes in the valence band (transition 1). Since porcelain is an insulator, the free electrons will not stay in the conduction band but will either recombine with a hole or fall into an electron trap (T). The electrons and holes may either recombine directly or indirectly. Recombining directly across the band gap is less likely than indirect recombination, because of the large energy gap. Indirect recombination will take place when free electrons in the conduction band jump down to a recombination center, annihilating the holes (transition 5). If an electron recombines

with a hole in a luminescence (L) trap, a photon is emitted and luminescence is produced. Indirect recombination usually takes place after electrons have fallen into the electron traps (T) (transition 2). When electrons fall into the traps (T), they must acquire enough energy to jump back up to the conduction band. One way in which this energy may be obtained is by heating the sample. The luminescence produced during heating is thermoluminescence.

Experimental results show that more than one luminescence peak can occur while a sample is being heated. This suggests that there are actually more than one level of electron and hole traps in the band gap. The depths of the electron traps help determine the temperature at which the luminescence peaks will occur [the deeper the electron trap (larger E), the higher the temperature at which the peak occurs]. The depth of a luminescence center determines the frequency of the emitted photon [the deeper the luminescence center, the higher the frequency of the emitted photon]. The height of the luminescence peaks (the number of photons emitted at that temperature) is directly proportional to how many electron hole pairs are recombining. For a more complete description of thermoluminescence, see Thermoluminescence of Solids by McKeever.[7]

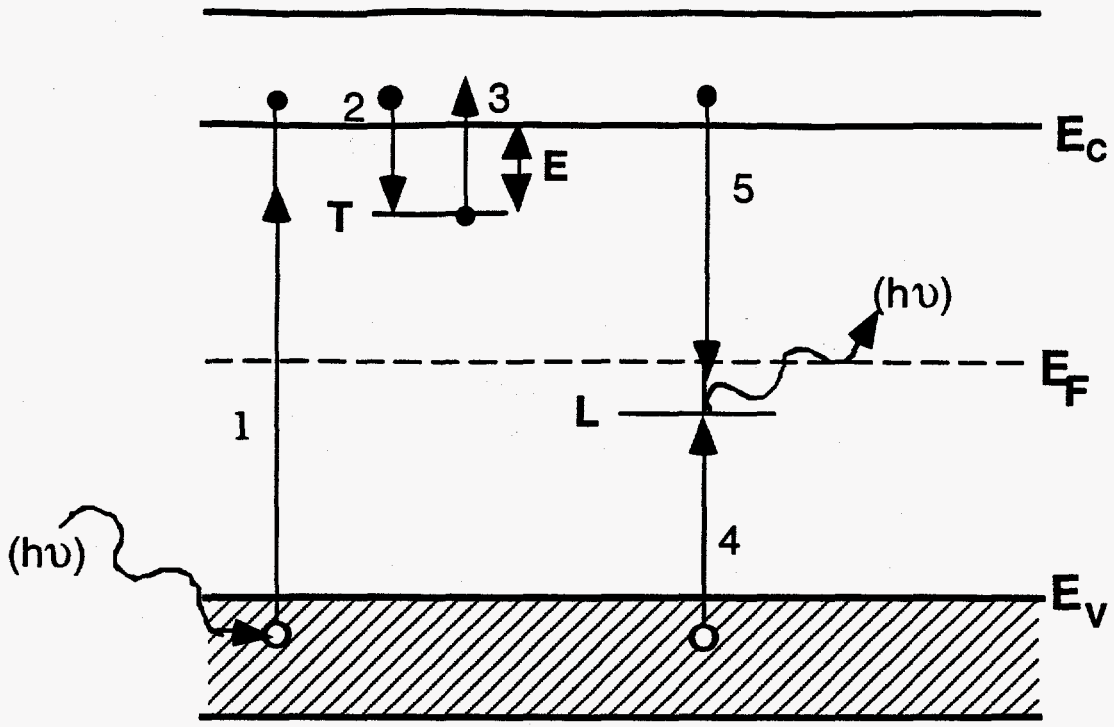

● Electrons

○ Holes

Figure 1.1: Simple Model of Thermoluminescence After absorbing radiation, some electrons are raised from the valence band (E_V) to the conduction band (E_C). Holes in the valence band may move to the hole trap (L). Electrons in the conduction band may either directly annihilate the holes in L or move to the electron trap (T), and then annihilate the holes in L after they gain enough energy to move back to the conduction band.

1.2 Measuring thermoluminescence

The basic process for producing and measuring thermoluminescence (TL) is as follows. After a sample has been irradiated, it is placed near the photocathode of a photomultiplier tube and heated at a controlled rate. As the sample is heated, the photons are detected by the photomultiplier tube which sends a pulse to an electronic counter. By monitoring the luminescence as a function of temperature, a glow curve (TL versus temperature) can be drawn [see Figure 1.2]. This curve represents the number of photons emitted at each temperature, and the area under this curve is often directly proportional to the amount of radiation absorbed, for some materials.

A more modern procedure of measuring thermoluminescence is by using a multisample automated TL reader. The TL reader used in this thesis contains a platter, protected from outside light, capable of holding 16 disks [see Figure 1.3], and was controlled by computer. The computer program rotates the platter until the specified disk location is aligned with the radiation source. Then, an elevator raises the specified disk to either a low or high position, defining how close to the radiation source the sample is (determined by user input to program), a shutter shielding the radiation source opens, and the disk is held there until it has received the desired radiation dose. Finally, the disk is lowered and the platter rotated until the same disk is aligned with a photomultiplier tube. The disk is then heated at a predetermined linear rate (5°C/second for this project) to a specified temperature; the photomultiplier tube detects the photons emitted during the heating process [see Figure 1.4]. Each time a photon is detected a

signal is sent to a circuit which counts the photons and sends the result to the computer. As the sample is being heated, the intensity of thermoluminescence is plotted as a function of temperature. Figure 1.2 shows a sample of one of these plots, referred to as a glow curve. This was for a 10 second [49 mGy to porcelain] beta dose to Al_2O_3:C (used for calibrating the beta source).

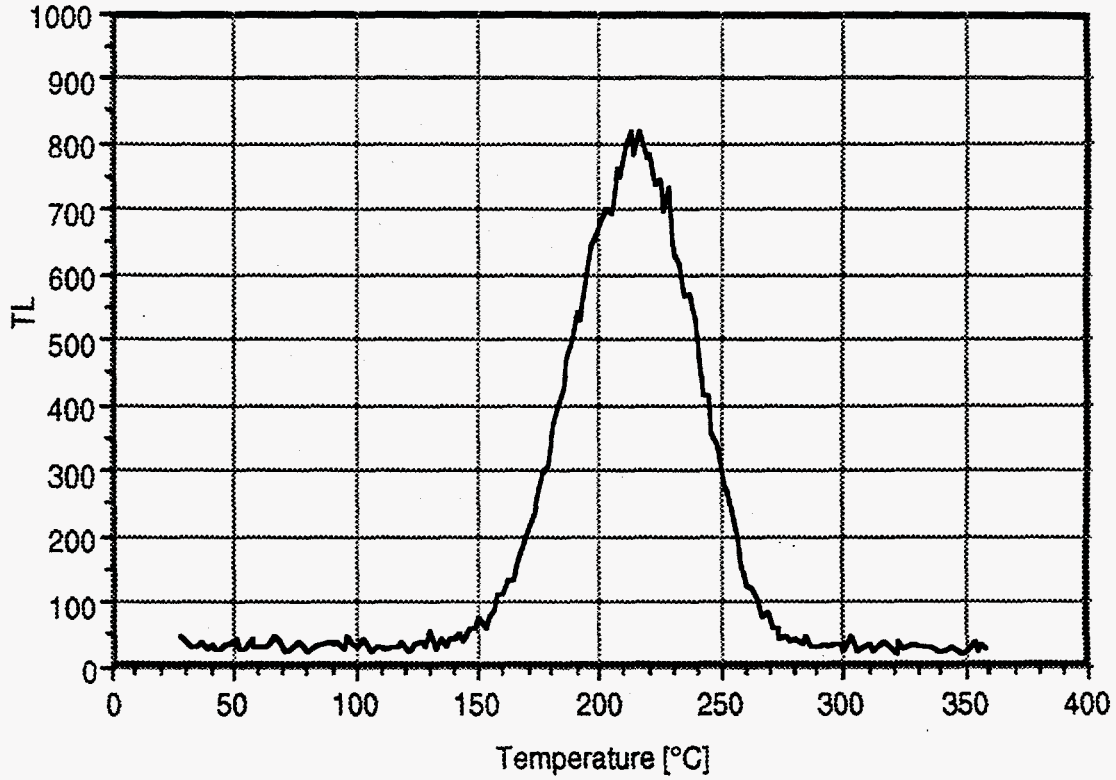

Figure 1.2: Glow Curve This is a plot of luminescence intensity (vertical axis) versus temperature (horizontal axis), in degrees Centigrade. The area under the peak is proportional to the amount of radiation absorbed by the material.

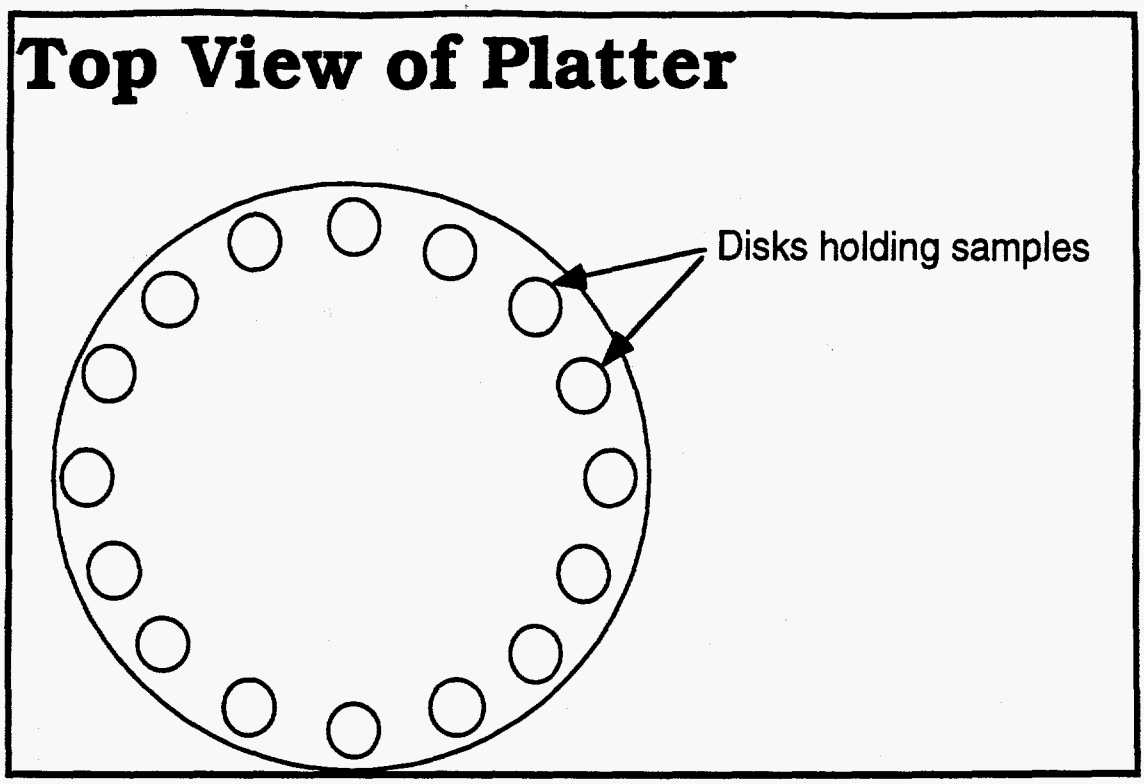

Figure 1.3: Platter used to hold disks with samples, in TL Reader

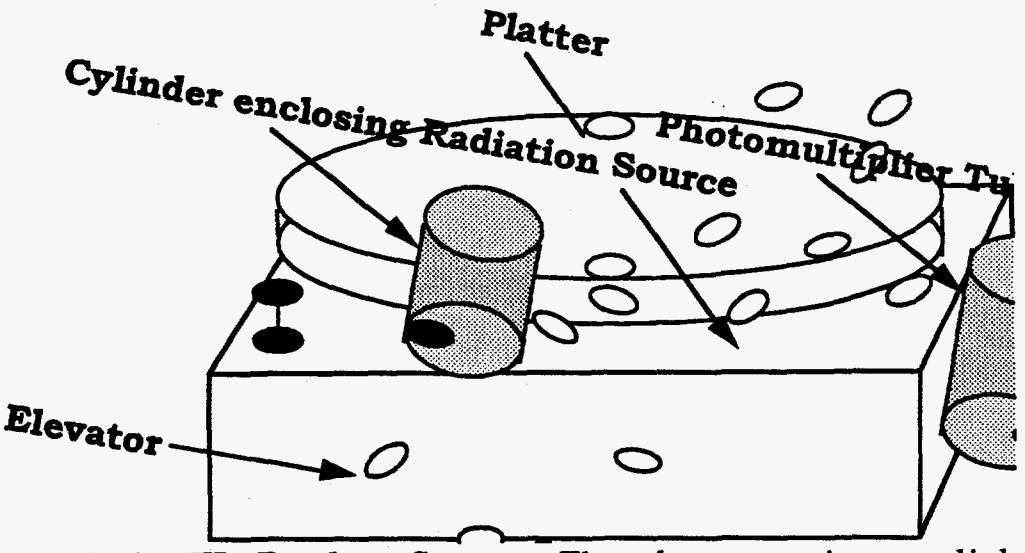

Figure 1.4: TL Reader Setup The elevator raises a disk holding a sample into the cylinder with the radiation source for a preset amount of time; then, the platter is rotated until the same disk is aligned with the photomultiplier tube, where the luminescence is measured while the sample is being heated. (The platter is covered by a protective cover.) The TL reader was developed in cooperation with Daybreak Nuclear and Medical Systems, Guilford, CT.

The computer summarizes the results by listing the disk number, the applied radiation dose, the rate at which the sample was heated, the glow curve, and the area underneath the glow curve (for integration limits set by the user). The peaks analyzed in this project, from porcelain samples, occur at approximately 210°C, at a linear heating rate of 5°C per second.

1.3 Predose technique

The predose technique is one method used to approximate how much beta and gamma radiation a sample has absorbed prior to any known test or calibration doses. This technique uses the change in sensitivity from irradiation and heating to determine the amount of beta and gamma radiation absorbed. The solid state properties of this procedure are best described using Zimmerman's model.[7] Zimmerman's technique was originally used to describe the method for quartz from pottery, but should apply just as well to any material displaying the predose effect, such as porcelain.[8] This procedure is illustrated in Figure 1.5 and Table 1.1.

As in the definition of thermoluminescence, there are electron traps (T and Z) and hole traps (L and R). The Z trap is used simply for charge balance and will not be illustrated in the processes. The T trap represents the trap from which the observed glow peak is coming. The peak examined in the predose technique occurs at approximately 110°C. The R hole trap is shallower than the L hole trap. Holes that are annihilated from the L hole trap produce luminescence. Hence, this trap is referred to as the luminescence center.

For the description with quartz, the firing of the pottery is assumed to be hot enough to anneal any previously existing defects due to irradiation. Next, some unknown amount of radiation, whether natural (e.g., uranium, thorium, K-40 and cosmic rays) or accidental (e.g., radioactive contamination), has been applied to the sample. Through the process of ionization, the irradiation deposits holes (e_u^+) in the reservoir (R) and electrons in electron traps T (e_t-). Over moderate times and at ambient temperatures, any electrons deposited in the electron trap (T) will

easily escape since the trap is shallow. In the laboratory, a small test dose is applied to the quartz. This deposits electrons in T (e_t^-) and holes in R (e_t^+). Next, the quartz is heated to just above 110°C. This thermal energy releases electrons in T. Those that recombine with holes in L produce a glow curve with a peak height of S_0. The quartz is heated to a higher temperature of 500°C in order for the majority of holes in R to be transferred to L. Another small beta test dose (e_t) is applied, and the quartz is again heated to 110°C. This time, a glow curve with a larger peak height of S_N is produced. The height of the glow curve is proportional to the sensitivity of the quartz. The increase in sensitivity from S_0 to S_N is caused by, and directly proportional to, the increase in the number of holes in the luminescence center (L), and the size of the unknown dose (e_u^+). If another test dose is applied, and the quartz is heated to just above 110°C a glow curve with the sample height (S_N) is produced, indicating that the heating to 500°C alone does not cause an increase in sensitivity.

Next, a calibrating beta dose (e_B) is applied. The larger dose deposits electrons in the T trap and holes in R traps. If another test dose is applied, and the quartz is heated to just above 110°C a glow curve with a smaller height (S_N') is produced. This decrease in sensitivity is referred to as radiation quenching. It is most likely caused by electrons from the irradiation reaching the luminescence traps directly or indirectly from very short lived traps, and annihilating some of the holes. The quartz is again heated to 500°C, transferring the holes in the reservoir to the luminescence centers, and draining any electrons in T. The application of the small test dose (e_t) and heating to just above

110°C are repeated. This glow curve has a larger peak height of S_{N+B}, showing another increase in the sensitivity, which is proportional to the applied larger beta dose.

The number of holes transferred to the L center from the reservoir (R) depends on the number of holes already in R. Thus, it is seen that the change in sensitivity between the first two glow curves ($S_N - S_0$) is directly proportional to the unknown radiation dose. Similarly, the change in sensitivity between the second two glow curves ($S_{N+B} - S_N'$) is directly proportional to the calibrating beta dose. Assuming that the constants of proportionality are the same, a relationship between the unknown dose (N) and the calibrating beta dose (B) is found:

$$N/B = (S_N - S_0)/(S_{N+B} - S_N') \qquad (1.1).$$

This relationship can be used to determine the approximate amount of beta and gamma radiation absorbed by the porcelain samples. In Table 1.1, α and σ are the proportionality constants representing the percentage of holes transferred from R to L during the heating to 500°C and the percentage of electrons from T which annihilate holes in L during the heating to just above 110°C.

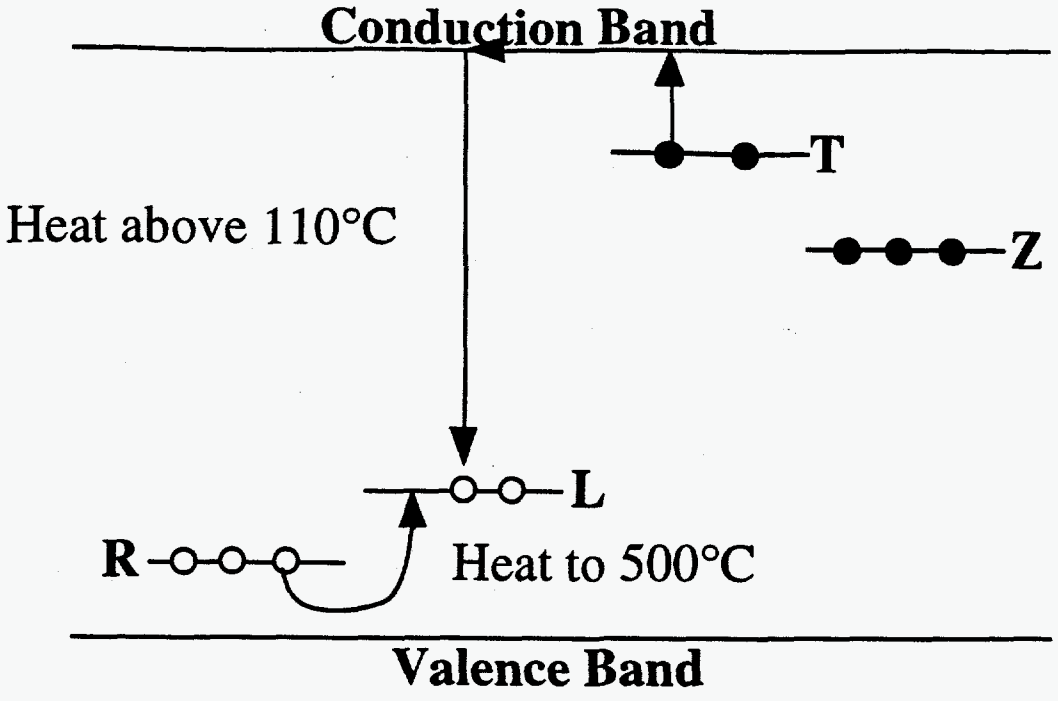

Figure 1.5: Zimmerman's Model for the Predose Effect in quartz

Table 1.1: Predose Technique

Electrons in T	Net Number of Holes Transferred to L	Holes in R	PROCEDURE
0	0	0	Firing of Pottery
0	0	e_u^+	Unknown radiation
e_t^-	0	$e_u^+ + e_t^+$	Small test dose
0	0	$e_u^+ + e_t^+$	Heat to just above 110°C [S_0]
0	$\alpha(e_u^+ + e_t^+)$	0	Heat to above 500°C
e_t^-	$\alpha(e_u^+ + e_t^+)$	e_t^+	Small test dose
0	$\alpha(e_u^+ + e_t^+) - \sigma(e_t^+)$	e_t^+	Heat to just above 110°C [S_N]
e_B^-	$\alpha(e_u^+ + e_t^+) - \sigma(e_t^+)$	$e_t^+ + e_B^+$	Calibration beta dose
0	$\alpha(e_u^+ + e_t^+) - \sigma(e_t^+ + e_B^+)$	$e_t^+ + e_B^+$	Heat to just above 110°C [S_N']
e_t^-	$\alpha(e_u^+ + e_t^+) - \sigma(e_t^+)$	$2e_t^+ + e_B^+$	Small test dose
0	$\alpha(e_u^+ + e_t^+) - \sigma(2e_t^+ + e_B^+)$	$2e_t^+ + e_B^+$	Heat to just above 110°C
0	$\alpha(e_u^+ + 3e_t^+ + e_B^+) - \sigma(2e_t^+ + e_B^+)$	0	Heat to above 500°C
e_t^-	$\alpha(e_u^+ + 3e_t^+ + e_B^+) - \sigma(2e_t^+ + e_B^+)$	e_t^+	Small test dose
0	$\alpha(e_u^+ + 3e_t^+ + e_B^+) - \sigma(3e_t^+ + e_B^+)$	e_t^+	Heat to just above 110°C [S_{N+B}]

CHAPTER 2

THE A-VALUE SYSTEM

2.1 Introduction

The a-value system is a method for determining the unknown amount of alpha radiation absorbed by a sample from a known beta dose which produces the same amount of thermoluminescence as the unknown alpha source. Since the TL for a given dose of alpha radiation is usually less than the TL for the same dose of beta radiation, and since a beta source is normally used for applying laboratory irradiation to samples it is necessary to know the relationship between the TL efficiency of alphas versus betas. The a-value was used in this project to calibrate the Gy to porcelain per second of irradiation, using a Cm-244 alpha source.

of the particle's energy. This system is simpler to use than the previously established k-value system[9], which uses parameters that are not independent of the particle's energy [k=(TL/Gy for alpha particles)/(TL/Gy for beta irradiation)]. Unlike the k-value, the a-value is unaffected by the obliquity of the particles and the thickness of the sample.

The a-value is the inverse of the ratio of the absorbed alpha dose per minute to the beta dose necessary to induce the same amount of thermoluminescence (TL). The reason for the use of the equivalent beta dose instead of the equivalent alpha dose is due to the fact that the betas will travel completely through the samples,

irradiating the entire sample. Thus, internal alpha sources, which irradiate throughout a sample, may be accounted for and used for dating. For purposes of this study an alpha dose was applied to the exterior of an annealed sample. Thus, the dose applied could be directly determined by calibrating the alpha source for the geometry and optical attenuation of the sample being examined. This provides a direct measurement of the alpha dose absorbed. This method is shown in Chapter 4.

2.2 The a-value for coarse grain porcelain

The equation[9] representing the a-value for coarse grain samples, in measurable quantities, is:

$$a = 2/3[(x'*D)/(13*\eta'*R*S)] \qquad (2.1)$$

where x' is the beta dose equivalent in terms of TL output to one minute of alpha irradiation, D is the diameter of a spherical grain, η' is the ratio of the average TL per unit length of track for the case of total absorption of an alpha particle (alpha thick) to that for an alpha thin sample $[(\varepsilon_S)'/(\varepsilon_S)]$, R is the range of the alpha particle in the sample, and S is the alpha flux in counts/μm^2/minute. Each of the parameters listed in Eq. (2.1) was determined experimentally. The procedures for finding them are shown in the following subsections of Section 2.2.

2.2.1 Finding the range of an alpha particle in porcelain

In order to determine the range of an alpha particle through the porcelain samples, the mass density of the porcelain and the energy of the alphas being absorbed must be determined. The

average mass density of the porcelain samples used was found to be 2.285 g/cm^3. The energies of the alphas are 5.806 MeV (77% yield) and 5.763 MeV (23% yield), for the Cm-244 alpha source used. The alpha source has a half-life of 18 years. The range of an alpha particle with this energy, through porcelain of the specified mass density, was found using a group of computer programs supplied by James F. Ziegler.[10]

Entering the values of the mass density of porcelain [$Al_2O_3SiO_2$] (2.285 g/cm^3) and the alpha energies, for the alpha source used, into Ziegler's programs, Stopping and Range of Ions in Matter [SRIM], the ranges are found to be 28.20 microns for the 5.806 MeV alphas (77% yield) and 27.88 microns for the 5.763 MeV (23% yield) alphas. Since the ranges of the two alpha energies emitted are so close, the average range will be used for all of the calculations in this project. These ranges are comparable to the values for alpha particles, of the same energy, traveling through silicon dioxide of the same mass density, 27.51 microns (for the 5.806 MeV alphas) and 27.20 microns (for the 5.763 MeV alphas).[11] The range of an alpha particle through porcelain is slightly larger than the range through silicon dioxide mainly because the range of a particle through a material is inversely proportional to the atomic density of the material, and the atomic density of porcelain [$8.49*10^{21}$ atoms/cm^3] is smaller than the atomic density of silicon dioxide [$2.29*10^{22}$ atoms/cm^3] (for the same mass densities). The atomic densities were found by dividing the mass density (2.285 g/cm^3) by the atomic mass (in grams per atom) of the corresponding compound.

SRIM uses quantum mechanics and statistics to determine how the alpha particles and porcelain atoms interact. The scientific theories used are described in detail in the book The Stopping and Range of Ions in Solids.[12] The programs use the Monte Carlo method to calculate how the alpha particles slow down and scatter while traveling through the porcelain.

2.2.2 Sample preparation

Some of the porcelain samples in this project were crushed into alpha thick coarse grains. The samples were crushed using a hydraulic press, with the maximum pressure set at 4000 psi. The alpha thick grains had a diameter much larger than the range of an alpha particle through porcelain. Sieves were used to isolate coarse grains of diameters between 150 and 250 microns; the range of the alpha particles from the alpha source used is approximately 28 microns [see Section 2.2.1].

All of these samples were first washed in distilled water, followed by a methanol wash, and three times in an ultrasonic bath in spectral grade acetone for 1 minute each. None of the samples were exposed to magnetic separation or acid etching. The samples were then annealed by heating them to 1100°C for 3 hours in air.

The alpha thick grains were distributed on the disks in aliquots averaging at 9.3 mg, making sure that the grains covered the entire face of the disk in a flat layer. Assuming that the alphas enter the porcelain grains in a parallel flux, they will travel only the length of their range. Thus, it does not matter if these alpha thick grains are stacked or not. The disks were then distributed onto the platter for the TL reader.

Coarse grains of Al_2O_3:C were used to calibrate the beta source. Approximately 200 mg of Al_2O_3:C coarse grains were annealed by heating them to 900°C for fifteen minutes in air. Next, approximately 50 mg of the annealed sample were irradiated with Cobalt-60 [a 7 Ci gamma source from U.S. Nuclear in Burbank, CA] for 91 seconds (equivalent to 0.2 Gy to porcelain). Part of the irradiated sample was then placed on four separate disks (approximately 3 mg per disk). Likewise, approximately 3 mg of the annealed sample were placed on each of the remaining 12 disks. The disks are nickel plated copper 9.70 mm in diameter and 0.32 mm thick.

2.2.3 Calibrating the beta source

The thermoluminescence for the gamma irradiated Al_2O_3:C samples was measured. Then, a background thermoluminescence reading was done with the same four samples. The background thermoluminescence is any thermoluminescence that was not induced by the calibration source. By subtracting this off, the thermoluminescence that was caused strictly by the calibration source can be more accurately determined. With the elevator in the high position for beta irradiation, the thermoluminescence for 30 seconds of beta irradiation was found, for new samples. The laboratory beta source (B3) used in this project was Sr-90/Y-90, 40 mCi, from Isotope Products in Burbank, CA. This thermoluminescence peak (at ~270°C, for a heating rate of 5°C/second) was compared to the peaks from the gamma irradiated samples, also occurring at approximately 270°C. The same heating rate was used for all the TL readings in this project.

The beta peak was approximately five times the size of the gamma peaks. Therefore, the beta dose was adjusted to 6 seconds, and, with the elevator in the high position for beta irradiation, the TL was found for the next sample. The 6 second dose was only 16.5% off from the gamma peak. The TL for the remaining samples was found for beta doses around 6 seconds, with the elevator in the high position for beta irradiation. A final TL measurement was done on all the samples for the same beta dose (10 seconds); these were used for normalization, described in the next paragraph.

After setting the integration limits (245°C to 295°C) to enclose the peaks, the computer found the area under each peak. The average area under the background peaks (background TL) was found and subtracted from all the other peaks. The average area under the normalization peaks (the peaks for which all the samples were given a beta irradiation dose of 10 seconds) was found. Next, the area under each normalization peak was divided by this average. These new values represent the normalization factor for each disk. The normalized values used for the beta calibration were found by dividing the area under each peak by the normalization factor for the corresponding disk.

The average normalized TL versus the beta dose [in seconds] is plotted in Figure 2.1. From this plot, the average normalized TL per unit dose [in seconds] is found to be 2020 ± 510 [a.u./sec] {a.u. are arbitrary units representing the relative TL intensity}. Similarly, the average normalized dose per TL a.u. for the gamma dose (in Gy to porcelain) is 9.01E-06 ± 0.32E-06 [Gy to porcelain/a.u.]. Multiplying these together, the dose delivered per

second from the beta source to the sample is 18.2 ± 4.7 (mGy to porcelain)/second, for the elevator in the high position.

The average TL per second, from the normalization data, was found to be 2230 ± 470 [a.u./sec]. The average TL per second, for the other data, taken before the normalization data, was found to be 2200 ± 380 [a.u./sec]. The samples were annealed by the heating process during each TL reading. Thus, the normalization data were taken after the samples had been annealed once by the TL reader (during the first data reading), and the other data were taken before the samples had been annealed by the TL reader. The values for TL per second agree well within their uncertainties. This means that the sensitivity was not significantly changed by the heating process.

The general procedure for measuring and normalizing the TL from beta irradiation was repeated with the elevator in the low position. This average normalized TL versus the beta dose [in seconds] is shown in Figure 2.2. From this plot, the average normalized TL per dose [in seconds] is found to be 42400 ± 2700 [a.u./sec]. The larger TL values are due to the removal a neutral density filter in the photomultiplier tube. Similarly, the average normalized dose per TL for the gamma dose (in Gy to porcelain) is 1.151E-07 ± 0.022E-07 [Gy to porcelain/a.u.]. Multiplying these together, the dose delivered per second from the laboratory beta source to the sample is 4.875 ± 0.095 (mGy to porcelain)/second, for the elevator in the low position.

The average TL per second from the normalization data, was found to be 47000 ± 9800 [a.u./sec]. The average TL per second,

for the data taken before the normalization data, was found to be 44700 ± 9600 [a.u./sec]. There was no change in sensitivity within ±5%.

Multiplying the TL per second by the Gy per TL, the dose per second [(Gy to porcelain) per second] for the beta source was determined for both elevator settings. The amount of radiation [in mGy to porcelain] delivered per second from the beta source was found to be 18.2 ± 1.1 for the elevator in the high setting, and 4.88 ± 0.10 for the elevator in the low setting.

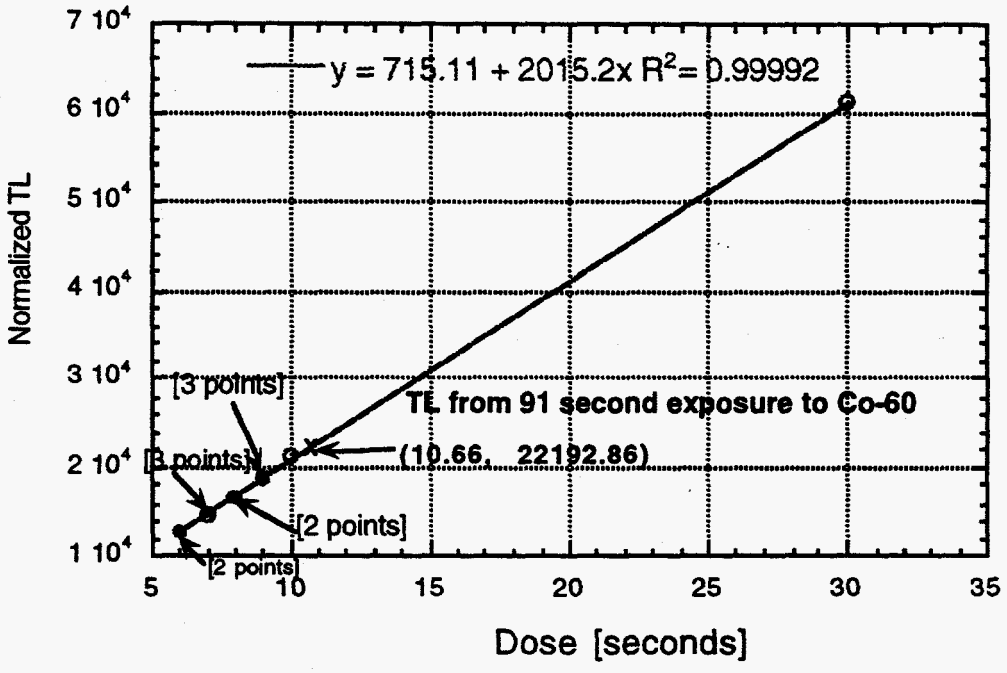

Figure 2.1: Normalized TL versus Beta Dose (Elevator High) Plot of the normalized TL versus dose (in seconds), with the elevator high, using the beta source [SR-90/Y-90]. This plot shows the linear relationship between the TL and the dose of irradiation. By doing a linear curve fit and finding where the amount of TL from the 91 second gamma irradiation occurs

[(TL from gamma)=(TL from beta)], the beta source was calibrated in Gy to porcelain for each second of irradiation.

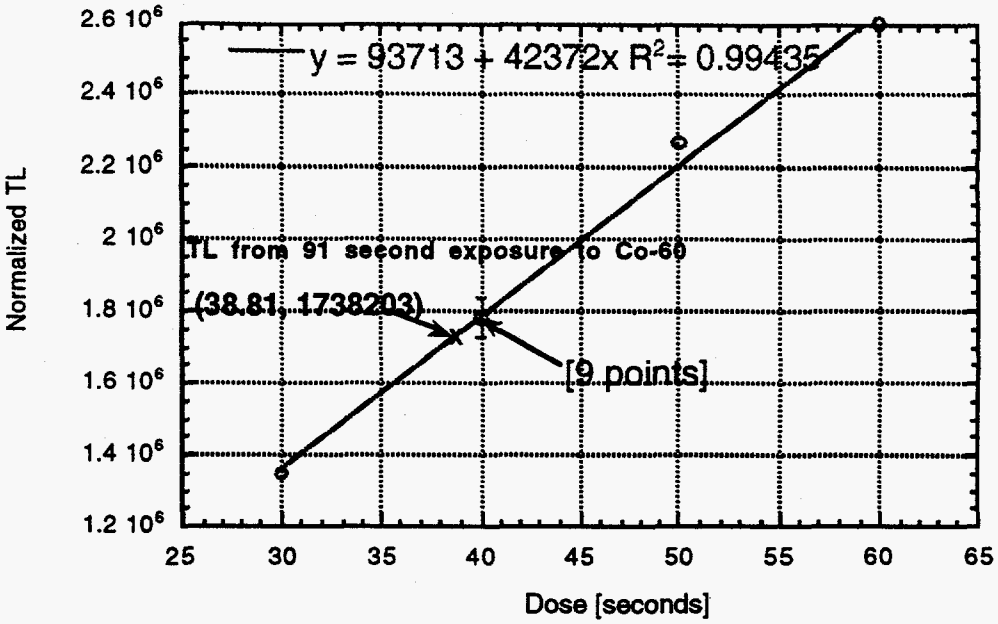

Figure 2.2: Normalized TL versus Beta Dose (Elevator Low) Plot of the normalized TL versus dose (in seconds), with the elevator low, using the beta source [Sr-90/Y-90]. This plot shows the linear relationship between the TL and the dose of irradiation. By doing a linear curve fitting and finding where the amount of TL from the 91 second gamma irradiation occurs [(TL from gamma)=(TL from beta)], the beta source was calibrated in Gy to porcelain for each second of irradiation.

***NOTE:** Doses for which the TL was measured for more than one sample (excluding the normalization peaks), the average thermoluminescence was plotted.

2.2.4 Measuring the alpha flux per second

Alpha particles, being heavy, do not get scattered by an amount that is significant in thermoluminescence measurements. They tend to travel in a straight line, slowing down and coming to rest at a specific range. This fact, along with the relatively large distance (≈27.9 mm) between the alpha source and the samples make it plausible to assume that the alphas hit the samples perpendicularly to the plane of sample deposition. Because of this, the alphas will most likely stop at the predetermined range when traveling through alpha thick samples. Alpha thick samples are much thicker than the range of an alpha particle for this material. If the alphas were hitting the alpha thick grain samples at large oblique angles, they may travel right out the side of the grains. If this happened, the amount of alphas being absorbed would be less than the number that hit the sample and the alpha flux would need to be measured in a different way than done here.

Using the setup shown in Figure 2.3, the alpha counts were measured for two different distances between the source and the zinc sulfide screen. By doing a linear curve fit to this data [see Figure 2.4], the average flux was found to be 0.055 ± 0.004 [counts/(μm^2*minute)], this is S in Eq. (2.1). The counter used is a 589 Alpha Counter from Daybreak Nuclear and Medical Instruments in Guilford, CT.

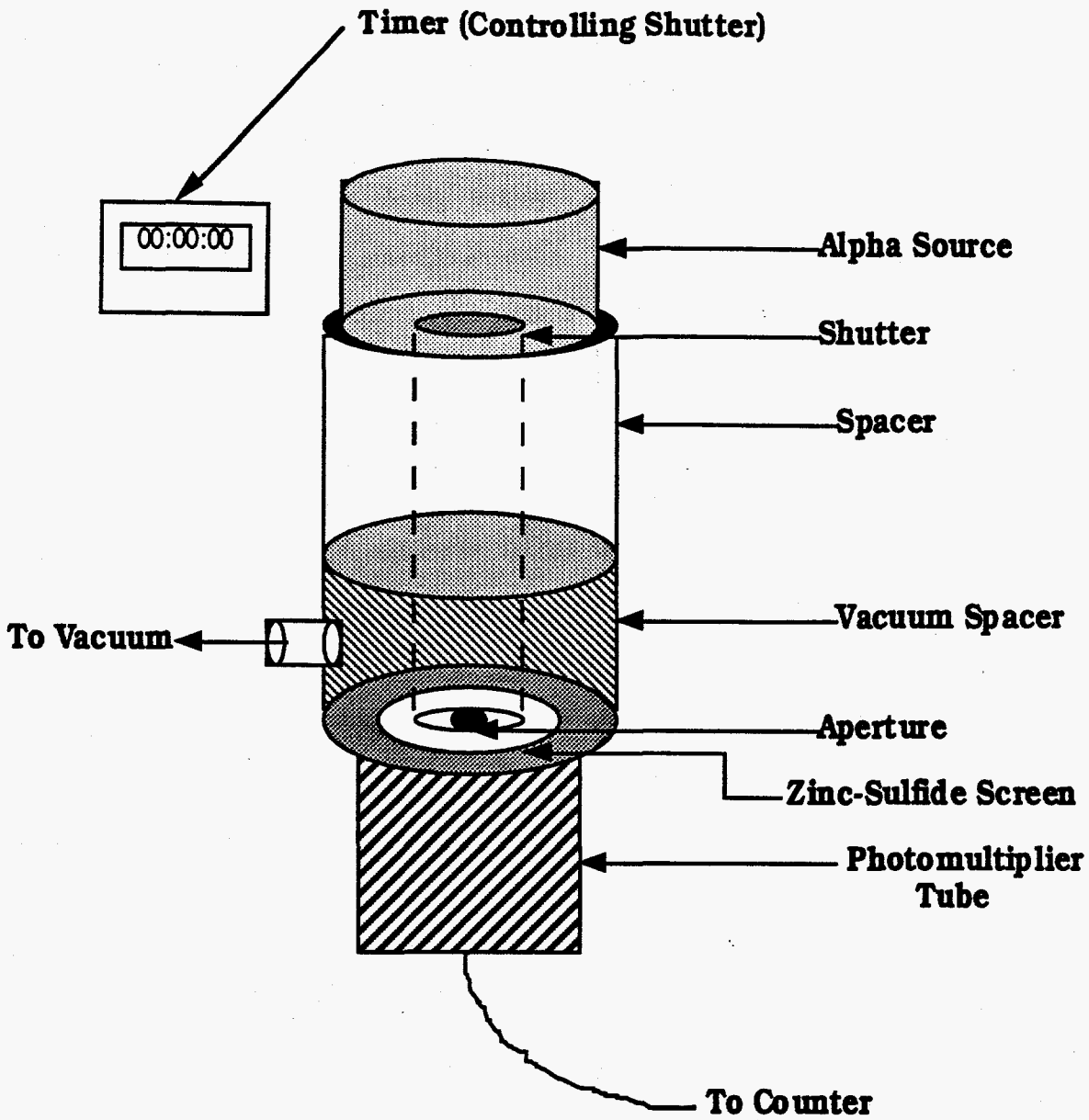

Figure 2.3: Alpha Flux Measurement Setup A timer controls the shutter on the bottom of the cylinder holding the alpha source. This shutter remains open for a set time, only allowing alphas to flow through for that time. The spacer and vacuum spacer help to make the sure that the alphas hit the zinc-sulfide screen in a parallel flux, and to minimize the flux. The vacuum allows the alphas to travel the full distance. The aperture [7.7 mm^2] minimizes the flux to a countable rate. There are vacuum O-rings in between each device in the setup.

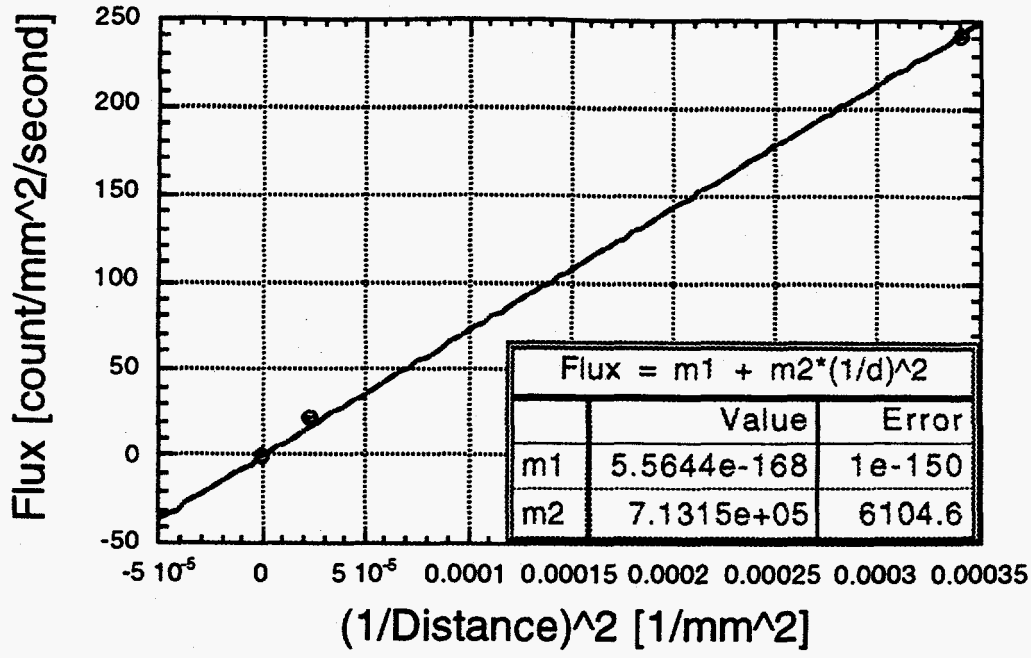

Figure 2.4: Alpha Flux versus (1/Distance)^2

2.2.5 Thermoluminescence per unit track length

The TL per unit track length for the alpha thick coarse grain samples is the TL produced divided by the total tracklength of all of the alphas entering the sample. All of the alpha doses applied in this project were applied under vacuum. The TL was found from the peak at 210°C. Here it was assumed that the alpha particles only travel as far as their range through the alpha thick grains.

The total number of alphas entering the sample each minute was found by multiplying the flux [counts/μm^2/minute] delivered to the sample by the area of the top of the sample, 78.5 mm^2, assuming that the surface of the coarse grain layer is flat and evenly distributed to the edges of the disks. The coarse grains

were held on the disks with Aerosil Silicone Instrument Lubricant (Aquatherm/H.M.T., 400 Rabro Drive, East, Hauppauge, NY 11788). Multiplying this value by the average range of an alpha particle [27.35 ± 5.3 μm, see Section 2.2.1], the tracklength delivered per minute was found. The total tracklength delivered to the sample by a dose of 1140 seconds was found by multiplying the tracklength delivered per minute by the dose, in minutes. Thus, the average TL per unit track length for the coarse grain samples is $(2.16 \pm 0.47)*10^{-6}$ [a.u./(mg*μm)] or $(2.01 \pm 0.44)*10^{-5}$ [a.u./μm] for an average mass of 9.29 milligrams. This represents ε_s' in the equation for the a-value of coarse grains [Eq. (2.1)]. Thus, the value of η' $[(\varepsilon_s)'/(\varepsilon_s)]$, in the equation for the a-value, was found to be 1.55 ± 0.35 by dividing by the value of the average TL per unit track length for alpha thin grains (ε_s) [$\varepsilon_s = (1.30 \pm 0.09)*10^{-5}$ [a.u./μm], see Section 2.3.2].

2.2.6 The equivalent beta dose

The beta dose equivalent to 1 minute of alpha irradiation (x' in Eq. (2.1)) was found by plotting the TL versus beta dose (in seconds). The TL per beta dose (in seconds) was found by doing a linear curve fitting to this plot [see Figure 2.5]. The TL was found using the 210°C peak. From the curve fitting, the beta dose equivalent to 1 minute of alpha irradiation is 26.62 ± 3.35 [seconds], or 129.76 ± 16.53 [mGy to porcelain], where it has been assumed that the attenuation in the coarse grains is similar to that for the slices.

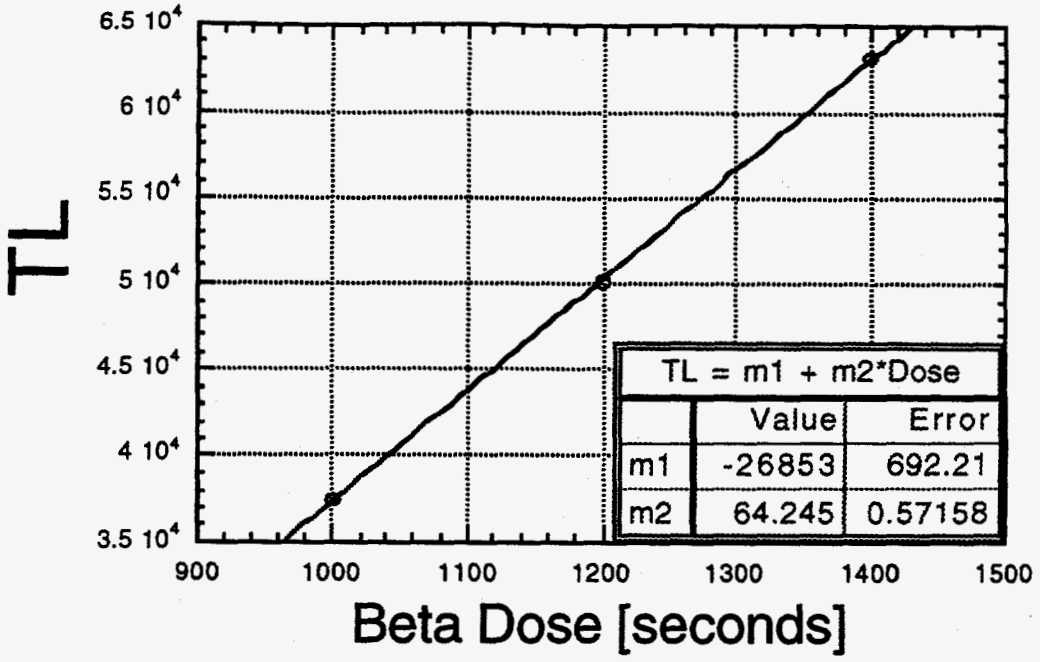

Figure 2.5: TL versus Beta Dose

2.2.7 Calculating the a-value for coarse grains

From the previous sections, the values for the parameters of Eq. (2.1), defining the a-value for coarse grains, are:

$x' = 129.76 \pm 16.53$ [mGy to porcelain]

$D = 270 \pm 0.028$ [μm]

$\eta' = 1.55 \pm 0.35$

$R = 27.4 \pm 1.4$ [μm]

$S = 0.05497 \pm 0.00369$ [counts/(μm^2*minute)]

Using these values with Eq. (2.1), the a-value for coarse grain porcelain was found to be:

$a = 0.77 \pm 0.21$.

This value does not account for optical attenuation. By finding the ratio of the average beta optical attenuation factors in the alpha region of a coarse grain to that in the alpha region of a slice, the approximate value of the beta optical attenuation factor for coarse grain porcelain was found from that for porcelain slices. The beta optical attenuation factor was found to be approximately 0.28. The alpha optical attenuation factor, since total absorption occurs for both cases, was assumed to be the same as for slices [0.85 ± 0.04]. By inserting the optical attenuation factors into the equation for the a-value for coarse grains in the same fashion that they appear in the a-value equation for slices [$\mathcal{E}_\beta/\mathcal{E}_\alpha$, in Eq. (2.3)], a more accurate a-value was found for coarse grain porcelain: $a = 0.25 \pm 0.07$.

2.3 The a-value for fine grain porcelain

The equation[9] representing the a-value for fine grain samples, in measurable quantities, is

$$a = (\varepsilon_S * v)/(13 * \chi_\beta) \qquad (2.2)$$

where ε_S is the thermoluminescence per track length for alpha thin grains, v is the volume of the thin layer of fine grains, and χ_β is the thermoluminescence per gray of the beta irradiation. Each of the parameters listed in Eq. (2.2) was determined experimentally. The procedures used for finding them are shown in the following subsections of Section 2.3.

2.3.1 Sample preparation

The alpha thin disks were prepared using grains that were less than 150 μm (see Section 2.2.2). These grains were crushed into smaller sizes using a motar and pestle. Next, the grains were washed in distilled water, followed by a methanol wash, and three times in an ultrasonic bath in spectral grade acetone for one minute each. None of the samples was subjected to magnetic separation or acid etching. The samples were then annealed at 1100°C for 3 hours in air.

To obtain only the grains that were alpha thin (diameters much smaller than 27 microns), Stoke's settling time was used.[13] This was done by placing the grains in a test tube of acetone approximately 6 centimeters deep. The test tube was placed in an ultrasonic bath for approximately 1 minute, then agitated by shaking. After 2 minutes, most of the grains larger than 9 μm in diameter had settled to the bottom. The grains still suspended were then placed in another test tube of acetone, approximately 6 centimeters deep. Once again, the test tube was placed in an ultrasonic bath for approximately 1 minute then agitated by

shaking. The grains were allowed to settle for 20 minutes. This separated the grains that have diameters greater than 2.5 microns from the smaller ones. The smaller ones, left suspended, were discarded since grains less than 1 μm in diameter tend to display spurious TL.

Approximately 4 centimeters of acetone was added to the tube containing the fine grains. After being placed in an ultrasonic bath for approximately 2 minutes and agitated by shaking, the acetone and grains were poured into a clean flat bottom test tube that contained a clean disk at the bottom. The acetone was then evaporated off by placing the sample in an oven at approximately 55°C for several hours. Each disk was examined under a microscope to confirm that the fine grains were distributed in alpha thin layers. There was some difficulty in obtaining an even distribution. After lowering the temperature of the oven to approximately 35°C, and using small beakers to keep the test tubes vertical, better results were obtained. The volume of these layers was then calculated, assuming that the layers were cylindrical. The disks were then distributed onto the platter for the TL reader.

In order to help prevent uneven distribution of the grains, the disks were washed in Alconox and then methanol before use. Also, any air bubbles that may be under the disks were removed by filling the tube with the disk to approximately 2 millimeters of acetone, and placing it in an ultrasonic vibrator before the grains were pipetted onto them. The thin grains were evenly distributed in alpha thin layers (« 27 μm), and the depth of the thin layer was used as the alpha track length through the layers.

2.3.2 Thermoluminescence per track length

The thermoluminescence per unit track length for the fine grain samples was found in the same way as the TL per unit track length for the coarse grains [see Section 2.2.5]. The fine grains on the disks were examined under a microscope and appeared to be evenly distributed to the edges. The average thickness was 25 ± 4 μm. Thus, the area of the top of the sample was assumed to be the same as the area of the face of the disk. As with the coarse grains, the TL was found from the peak at 210°C. The TL per unit track length for the fine grain samples was found to be (1.30 ± 0.09)* 10^{-5} [a.u./μm]. This represents ε_s in the equation for the a-value of fine grains [Eq. (2.2)]. The TL for a 1140 second alpha dose (20543 ± 3697 a.u.) was found by measuring and plotting the TL versus alpha dose and doing a linear curve fit [see Figure 2.6]. The layers of alpha thin grains are also alpha thin, making the track length of one alpha particle through the porcelain equal to the thickness of the layer. It was assumed that the spaces between the individual grains were much smaller than the diameter of the grains themselves, and did not need to be subtracted off from the thickness of the layer to find the path length that the alphas traveled through the porcelain.

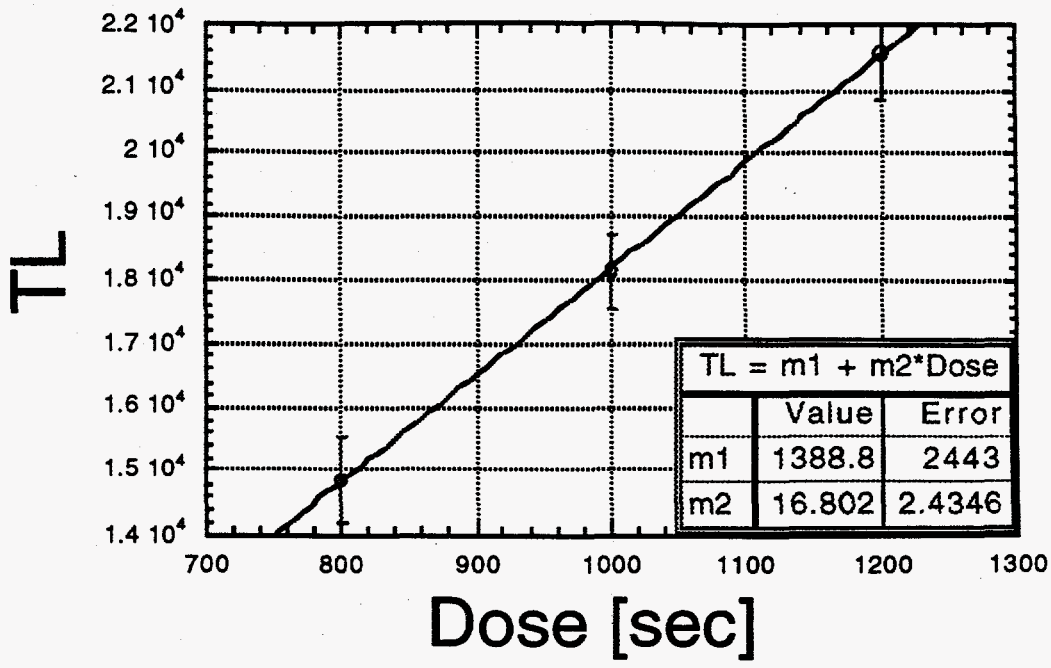

Figure 2.6: TL versus Alpha Dose (Fine Grains)

2.3.3 TL per gray of the beta irradiation

By plotting the TL produced by beta irradiation versus the dose applied (in seconds) [see Figure 2.7] and dividing the slope by the Gy to porcelain delivered per second by the beta source [see Section 2.2.3], the TL per gray of the beta irradiation was found to be 4.44 ± 0.15 [a.u./mGy to porcelain]. This value represents $\chi\beta$ in the equation for calculating the a-value of fine grain porcelain. (This was all done for the elevator in the low position.)

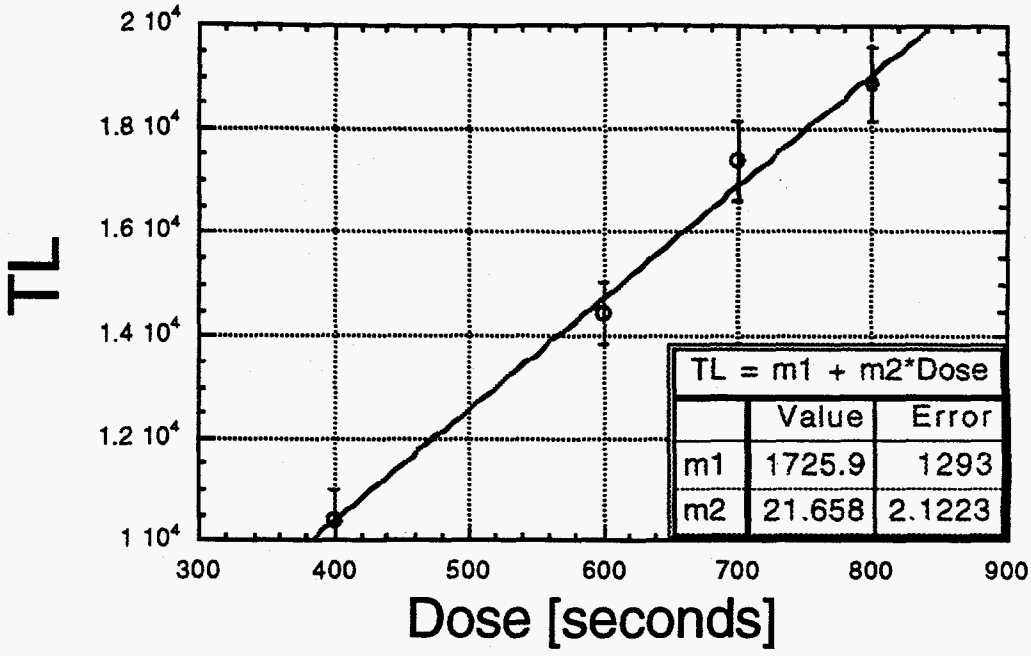

Figure 2.7: TL versus Beta Dose (Fine Grains)

2.3.4 Calculating the a-value for fine grains

From the previous sections, the values to be plugged into Eq. (2.2), defining the a-value, are:

$\varepsilon_S = (1.30 \pm 0.09)*10^{-5}$ [a.u./μm]

$v = (1.57 \pm 0.31)*10^{9}$ [μm^3]

$\chi_\beta = 4.443 \pm 0.147$ [a.u./mGy to porcelain].

Using these values with Eq. (2.2), the value of a is found to be:

$a = 0.35 \pm 0.07$.

2.4 The a-value for slices of porcelain

The equation[14] representing the a-value for slices of porcelain, in measurable quantities, is

$$a = (\varepsilon_\beta * x' * d)/(0.13 * \eta' * \varepsilon_\alpha * L) \qquad (2.3)$$

where ε_β is the optical attenuation factor for beta radiation, x' is the beta dose equivalent to 1 minute of alpha irradiation in cGy, d is the thickness of the slice in centimeters, η' is the ratio of the average TL per unit length of track for the case of total absorption of an alpha particle (alpha thick) to that for an alpha thin sample, ε_α is the optical attenuation factor for alpha radiation, and L is the track length delivered by the source to unit area of the surface of the slice [μm^{-1}/minute]. Each of the parameters listed in Eq. (2.3) was determined experimentally. The procedures for finding them are shown in the following subsections of Section 2.4.

2.4.1 Sample Preparation

Cores (≈ 5.6 or 5.7 mm in diameter) were cut out from the porcelain using a diamond coring bit. These porcelain cores were sliced into disks approximately 0.25 millimeters thick. The surfaces of the disks were sanded by hand, on a diamond plated disk, so that they were smooth, by observation. The disks were washed in distilled water then methanol, and three times in an ultrasonic bath in spectral grade acetone for one minute each. None of the samples were subjected to magnetic separation or acid etching. The samples were then annealed at 1100°C for three hours in air. The porcelain disks were placed on separate nickel plated copper disks that were then distributed onto the platter for the TL reader.

2.4.2 Optical attenuation factors

Optical attenuation occurs because the thicker samples do not have a very strong transparency, compared to the thinner samples. Because of this, the thermoluminescence reaching the photomultiplier will mainly be from the upper part of the sample. Also, the external dose deposited is not uniform throughout the sample. The variation of the dose throughout the sample is mostly due to increasing obliquity of the particle tracks as they get scattered while penetrating the slice.

The samples were sanded down into two different thicknesses (values of d in Eq. (2.4)). The optical attenuation coefficient was found by measuring the TL from the top of the samples, and then from the bottom, where the samples had been irradiated with the alpha source from the top for both readings. The optical attenuation coefficient (μ) is defined in Eq. (2.4).

$$I = I_0 * \exp(-\mu * d) \qquad (2.4)$$

In Eq. (2.4), I is the intensity of the luminescence at the depth d, I_0 is the intensity of the luminescence at the surface, μ is the optical attenuation coefficient, and d is the thickness of the slice. I and I_0 in Eq. (2.4) were used to represent the amount of TL reaching the photomultiplier tube from the bottom and top of the slices, respectively.

The slices were sanded into different thicknesses and irradiated with a 500 second alpha dose. First, the TL from the top of the slices was measured (I_0). The TL from the bottom of the slices was measured by irradiating the slices and then turning

them over prior to measurement (I). The TL from the bottom was normalized by mass and by the TL from the top of the respective slice. This normalized TL from the bottom was plotted as a function of thickness (see Figure 2.8). By doing an exponential curve fit to this plot, an estimation of the optical attenuation coefficient was found to be 14.1 ± 0.3 [1/mm].

The optical attenuation factor for betas is defined by:

$$\varepsilon_\beta = {}_0\int^d [\exp(-\mu * h) * f(h)]\,dh/d \qquad (2.5)^{11},$$

where μ is the optical attenuation coefficient, h is the depth in millimeters, f(h) = (dose delivered by source at depth h in slice)/(dose delivered to a fine grain disk placed on the same surface as the slice), and d is the thickness of the slice in millimeters. The first term in the integral, $\exp(-\mu * h)$, was found from the exponential curve fit for TL versus depth [see Figure 2.8]. The second term in the integral, f(h), was found using a plot of the fractional dose rate (f(h)) versus depth/mg/cm^2 from an article written by Wintle and Aitken.[15] The curve can be applied to porcelain because porcelain has similar beta absorption characteristics as SiO_2, one of the materials for which the curve applies. By knowing the mass density of the porcelain and dose deposited per second on the complete sample, the dose deposited at each depth divided by the dose delivered to a fine grain disk placed on the same surface as the slice, f(h), can be found from Wintle and Aitken's curve. The beta optical attenuation factor (ε_β) was found to be approximately 0.35.

The optical attenuation factor for alphas is defined by:

$$\varepsilon_\alpha = [1-\exp(-\mu h_\alpha)]/\mu h_\alpha \qquad (2.6)^{16},$$

where h_α is the depth of penetration of the alpha particles. It has been assumed that the irradiation is uniform to this depth and as long as μh_α is small this is valid. Using the value of μ obtained earlier, 14.1 ± 0.3 [1/mm], and setting h_α equal to the range of the alpha particle [27.4 ± 1.4 μm], the alpha optical attenuation factor was found to be 0.83 ± 0.04.

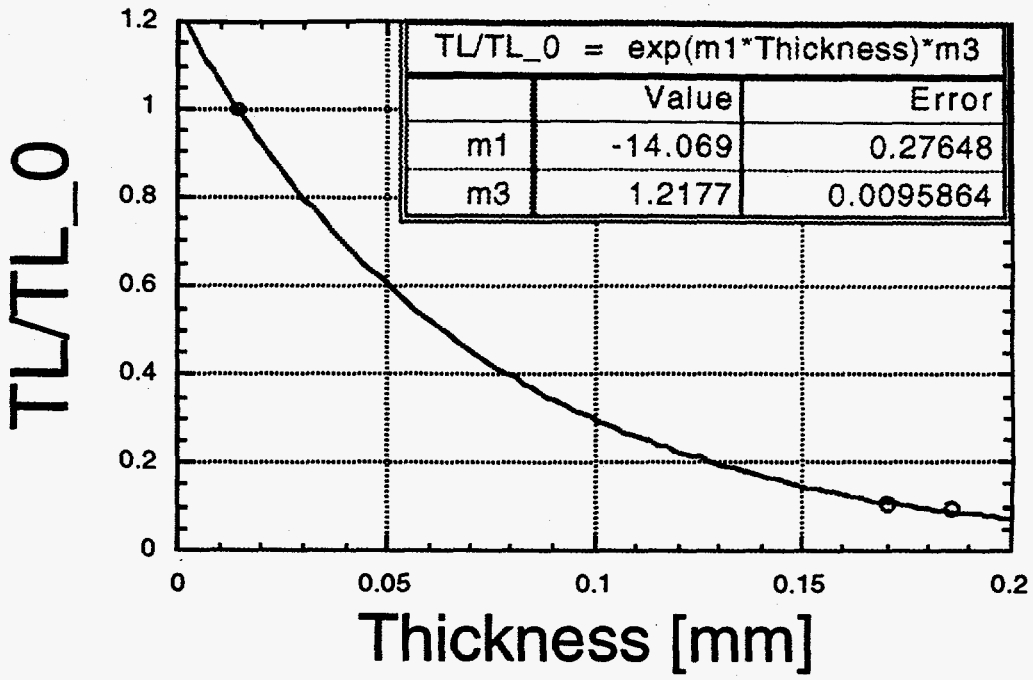

FIGURE 2.8: Fractional Alpha TL versus Thickness The ratio of the TL from a given thickness (TL) to the TL from the surface (TL_0) as a function of thickness.

2.4.3 The equivalent beta dose

The beta dose equivalent to 1 minute of alpha irradiation (x in the equation for the a-value) was found by plotting the TL versus beta dose (in seconds) [see Figure 2.9]. Since saturation effects were not observed, the TL produced was assumed to vary linearly with the applied beta dose. The TL per beta dose (in seconds) was found by doing a linear curve fit to this plot. This TL was found using the 210°C peak. From the curve fit, the beta dose (in seconds) equivalent to 1 minute of alpha irradiation was found. Multiplying the equivalent beta dose in seconds by the calibration

factor (in Gy to porcelain per second) the equivalent beta dose in Gy to porcelain was found. The beta dose equivalent to 1 minute of alpha irradiation is 19.8 ± 4.4 [seconds], or 9.6 ± 2.0 [cGy to porcelain]. The Gy to porcelain per second for the slices was calibrated as being equal to the value for coarse grains multiplied by 0.89 (E. Haskell, personal communication), or 4.34 ± 0.085 [mGy to porcelain/seconds].

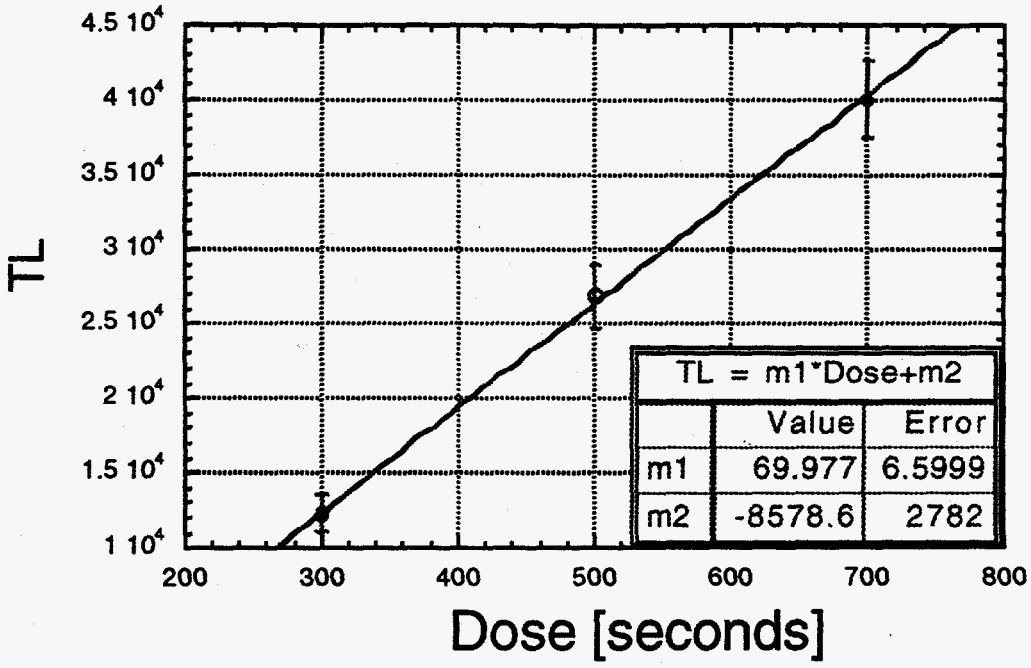

Figure 2.9: TL versus Beta Dose [Slices]

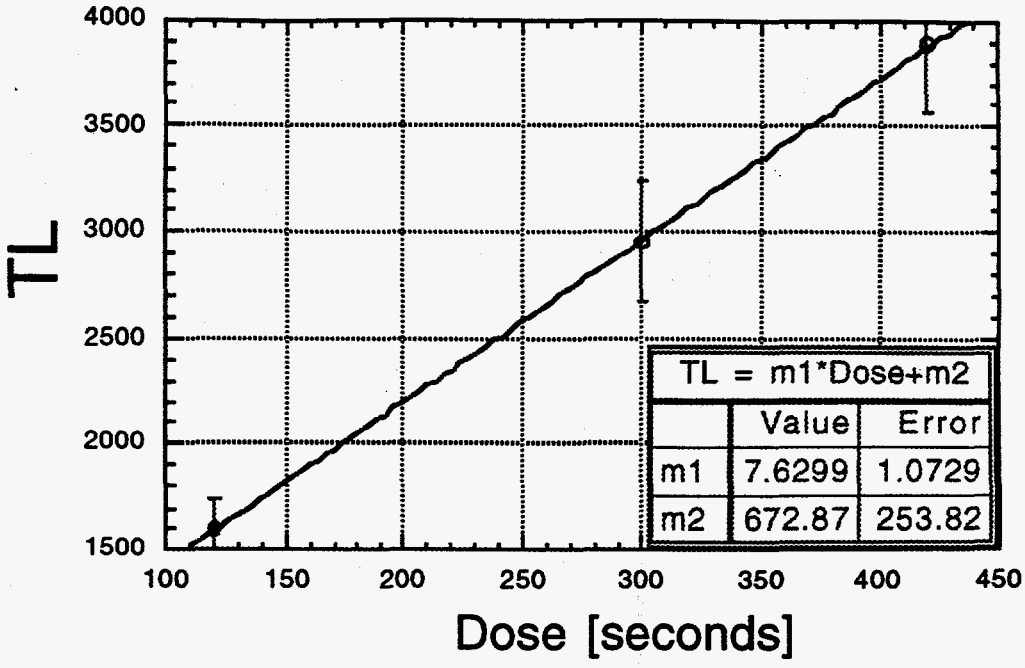

Figure 2.10: TL versus Alpha Dose [Slices]

2.4.4 Track length delivered by the source to unit area of the surface of the slice, per minute

The value of L, in Eq. (2.3), was found by multiplying the alpha flux delivered per minute [see Section 2.2.4] by the range of the alpha particles entering the slice. From these, the value of L was found to be 1.50 ± 0.31 [1/(μm*minute)].

2.4.5 Calculating the a-value for slices

From the previous sections, the parameters in Eq. (2.3), defining the a-value, are:

$\varepsilon_\beta = 0.35$

$x' = 9.63 \pm 0.02$ [cGy to porcelain]

$d = 0.025 \pm 0.001$ [cm]

$\eta' = 1.236 \pm 0.275$

$\varepsilon_\alpha = 0.83 \pm 0.04$

$L = 1.50 \pm 0.31$ [counts/(μm*minute)]

Using these values with Eq. (2.3), the value of a, for porcelain slices is found to be:

$a = 0.42 \pm 0.13$.

The a-value for porcelain slices was also found independently by calculation from the energy of the alphas being used. From the energy, flux and range of the alpha particles and the mass density of the porcelain slices, the Gy to porcelain per second delivered by the alpha source was found [see Section 3.2]. From a known alpha dose [in Gy to porcelain] and the beta dose [in Gy to porcelain] which produces the same amount of TL as the known alpha dose, the a-value for porcelain slices was found to be 0.46, in strong agreement with the value found using Aitken's equation.

2.4.6 The Alpha Sensitivity of Porcelain Slices

The average standard error in TL, for the TL versus alpha dose plot, was approximately 111 [a.u.]. Using this, the minimum detectable alpha dose was estimated to be 30 seconds or 130 mGy to porcelain.

CHAPTER 3

USING THE A-VALUE

3.1 Calibrating the Alpha Source from the a-value

From the basic definition of the a-value, the ratio of the beta equivalent dose to the amount of alpha radiation absorbed, its application is straight forward. Once the a-value is known for a given form of a material, the amount of alpha radiation absorbed is simply the equivalent beta dose divided by the a-value. The equivalent beta dose may be found by measuring the TL for different beta doses until one is found which matches the TL produced by the unknown amount of alpha radiation. A more precise value may be found by plotting the TL produced by the beta doses versus the doses (centered around the apparent equivalent dose) and doing a linear curve fit to the data. Then the beta equivalent dose can be found from the amount of TL produced by the unknown amount of alpha radiation and the equation for the linear curve fit. The porcelain samples used in this project were all from the same toilet tank lid. Thus, it was assumed that all of the coarse grain samples have the same a-value, all of the fine grain samples have the same a-value, and all of the slices have the same a-value.

3.1.1 Coarse grains

An arbitrary alpha dose was applied to annealed coarse grains of porcelain, with the elevator in the low position. Using the linear curve fit for the TL versus beta dose [see Figure 2.5], the beta dose (in seconds) which produces the same amount of TL as

the arbitrary alpha dose was found. This is the equivalent beta dose and was found to be 532= ± 67 [seconds], or 2.6 ± 0.3 [Gy to porcelain].

Dividing the equivalent beta dose (in Gy to porcelain) by the a-value for coarse grains (0.25 ± 0.07, see Section 2.2.7), the alpha dose absorbed by the porcelain was found to be 10.4 ± 3.1 [Gy to porcelain]. This should be equivalent to a 1200 second alpha dose. Thus, the alpha source was calibrated as delivering 8.7 ± 2.6 [mGy to porcelain/second].

3.1.2 Fine grains

The procedure used for the coarse grains (see section 3.1.1) was also applied to the fine grains, with the elevator in the low position for irradiations. The average TL produced by the arbitrary alpha dose was 21320 ± 344 [a.u.]. The TL per beta dose (in seconds) for fine grains was found in Section 2.3.3. Using the same method as in Section 3.1.1, the equivalent beta dose was found to be 874 ± 19 [seconds], or 4.26 ± 0.13 [Gy to porcelain].

Dividing the equivalent beta dose (in Gy to porcelain) by the a-value for fine grains (0.35 ± 0.07, see Section 2.3.4), the alpha dose absorbed by the porcelain was found to be 12.1 ± 0.4 [Gy to porcelain]). This should be equivalent to a 1140 second alpha dose. Thus, the alpha source was calibrated as delivering 10.58 ± 0.35 [mGy to porcelain/second].

3.1.3 Slices

The procedure used for the coarse grains (see Section 3.1.1) was also applied to the slices. The average TL produced by the arbitrary alpha dose was 9371 ± 1249 [a.u.]. Using the same

method as in Section 3.1.1, the equivalent beta dose was found to be 420.2 ± 76.2 [seconds], or 2.40 ± 0.33 [Gy to porcelain].

Dividing the equivalent beta dose (in Gy to porcelain) by the a-value for slices (0.42 ± 0.13, see Section 2.4.5), the alpha dose absorbed by the porcelain was found (5.7 ± 1.9 [Gy to porcelain]). The arbitrary alpha dose applied to the samples was 1140 [seconds]. Thus, the alpha source delivers 5.0 ± 1.7 mGy to porcelain per second.

3.2 Calibrating the Alpha Source from the Alpha Energy and Flux

The Gy to porcelain delivered per second by the alpha source may also be calculated using the flux, alpha energy and range of the alpha particle. By multiplying the average energy of the two alphas emitted from the source [5.79 MeV] by the alpha flux [$4.671*10^6$ alphas/cm^2/minute], the energy delivered per square centimeter per minute was found to be $2.702*10^7$ [MeV/cm^2/minute]. Dividing by the range of alphas in porcelain [28.2 ± 5.3 μm], the energy delivered per square centimeter per minute per tracklength was found. Converting electron volts to joules and dividing by the mass density, the dose delivered per second, in Gy to porcelain per second, was found by using the definition of one Gy to porcelain being the same as one joule per kilogram. The calibration was found to be 11.2 mGy to porcelain per second.

CHAPTER 4

AN ALTERNATIVE APPROACH

A more direct way of determining the amount of alpha radiation absorbed is by matching the TL from a sample that has absorbed an unknown amount of alpha radiation with the calibrated alpha dose that produces the same amount of TL. In order to distinguish the TL resulting from external alpha sources from that produced by other external and internal sources, a depth analysis must be done. The external alpha dose will only penetrate tens of microns of the sample. By plotting the TL versus depth, the TL from the internal sources is found where the curve reaches a plateau or constant slope. The plateau or constant slope indicates a uniformly irradiated portion of the sample. The internal sources irradiate uniformly throughout the sample. Theoretically, by subtracting the TL of the uniformly irradiated portion from the TL due to the whole slice, the TL due only to the externally alpha irradiated portion can be determined.

This process can be done by, after determining the TL from the unknown amount of external alpha radiation, testing different alpha doses until one is closely matched. By doing a linear curve fit to this calibration data, a more precise value can be obtained. This method does not require as many individual measurements and calculations as the a-value method.

4.1 Using Depth Analysis on Slices

This alternative method was applied to porcelain slices. This method involved measuring the TL from the top of some slices, and

then sanding off different amounts of the top of the other slices and measuring the TL from them. All of the slices had been previously irradiated by the alpha source with the elevator in the low position.

An idealized depth analysis was done on the porcelain slices. First, all of the slices were irradiated with a 900 second alpha dose. Then, before measuring the TL, different thicknesses were sanded off of the top side (irradiated side) of some of the disks. The TL was then measured for each of the disks, and the TL versus depth was plotted (see Figure 4.1), after subtracting the background. The background TL was found after the slices were sanded down in random amounts and cleaned, in the same fashion as the previous TL measurements. The reason the curve is exponential because the TL was measured from the whole sample and then from the remaining sample after different thicknesses were sanded off. A true depth profile would have measured the TL produced by at each precise depth, not that depth and the remaining sample.

The samples were cleaned after they were sanded, and before the TL was measured, in an ultrasonic bath of water for 30 minutes, then rinsed in acetone and allowed to dry. The plateau appears to start in the region between 0.02 and 0.04 millimeters. This is expected since the range of these alpha particles, in the porcelain samples used, is approximately 0.028 millimeters. The average TL value for the plateau region is 263.8 [a.u.]. Ideally, the plateau region would be along the depth axis, for no TL. The 263.8 [a.u.] may have come from small grains which were embedded in the slices during sanding and did not come off during cleaning.

CHAPTER 5

DISCUSSION

This project tested the feasibility of using porcelain to measure externally applied alpha doses. The sensitivity of porcelain to alpha irradiation was tested by comparing it with the sensitivity of porcelain to beta irradiation, using TL. Aitken's a-value was used to make this comparison. Aitken's a-value represents the inverse ratio of the alpha dose absorbed to the beta dose which produces the same amount of TL. The a-values for porcelain coarse grains, fine grains and slices were found using Aitken's equations.

The a-value results were evaluated by comparing the calibration of the alpha source obtained from the a-value [see Chapter 3] with the calibration calculated from the flux and energy of the alphas [11.2 mGy to porcelain per second]. The a-value for coarse grains gave a calibration of 8.7 ± 2.6 mGy to porcelain per second, differing by 23 percent from the calculated value, yet still within the uncertainty limits. The a-value for fine grains gave a calibration of 10.6 ± 0.4 mGy to porcelain per second, differing by only 5.6 percent from the calculated value, and just outside the uncertainty limits. The a-value for slices gave a calibration of 5.0 ± 1.7 mGy to porcelain per second, off by 55 percent from the calculated value. The expected a-value for slices, however, was calculated from the calibration of the alpha source using the alpha flux and energy and was found to be 0.46, only off by 9% from the a-value found using Aitken's equation. One possible source of

error may be the use of copper disks to hold the samples in the TL reader. The a-value was designed to be used with samples placed on aluminum disks in the TL reader to help control the backscatter. Copper has a larger electron concentration than aluminum and may cause a stronger backscatter. All of the results in this project can be improved by using more samples and taking more data, to get more precise curves.

The alpha flux which the porcelain samples were exposed to was not parallel, adding uncertainty to the a-values calculated. The alpha flux can be made more parallel by using a collimator, or a flat shield with holes. When testing the a-value, however, the alpha flux should mimic the alpha flux which the inside of a porcelain toilet tank would be exposed to from water containing alpha sources. The alpha flux from the water supply will not especially hit the porcelain toilet tanks in a parallel fashion. By creating an alpha flux which approaches in random directions, like that from the water supply, a more accurate test can be applied to the a-value.

Some difficulty was encountered when trying to account for the optical attenuation in the porcelain coarse grain samples. If the samples were in an evenly distributed single layer, the uncertainty would be somewhat reduced. With the setup used, however, the grains were only irradiated on the top alpha range, not all the way around. If the porcelain coarse grains were irradiated while in a vibrating pan, the complete outer shell, up to the alpha range, would be irradiated, making the smoothness of the grain distribution not as critical.

There was major difficulty in using the fine grain technique to prepare the fine grain disks. The mass of grains used to start the fine grain technique did not seem to guarantee that the final grains distributed on the copper disks were in alpha thin layers. By using a better crushing technique than the mortar and pestle, a larger majority of the starting grains can be made to have the desired diameters, making it easier to determine the mass of grains to start with.

One of the greatest uncertainties encountered in this project was in the depth profile. The depths were sanded off in increments of 10 μm, more than 1/3 the size of the alpha range in the porcelain. Also, the porcelain slices were sanded down by hand and the top and bottom edges may not have been parallel. By using more precise devices for sanding and measuring, a more detailed depth profile could have been obtained.

The smallest detectable alpha dose for porcelain, using the method tested in this project, was found to be approximately 130 mGy to porcelain for slices. Thus, the alpha sensitivity of porcelain based on current technology is not strong enough to be used for estimating any small alpha concentration in a water source. The alpha sensitivity could be improved by using more samples to get smaller standard error values, lowering the value of the smallest detectable alpha dose.

The methods applied in this project can potentially be used to approximate the dose from alpha sources or low energy betas in previously contaminated water supplies. This would be done by using porcelain samples from the inside of toilet tanks, which had contact with the water. The a-value for slices can be calculated

from the alpha energy and flux and the mass density of the porcelain. Separate porcelain slice samples are needed to get TL versus alpha and beta dose curves, and to get a detailed depth profile. A minimum of 9 samples each are needed to get the TL versus alpha and beta dose curves, 3 at each dose. The doses need to be in the linear, not supralinear, region of the curve. A minimum of 9 more samples should be used to get a depth profile, 3 sanded to each depth. In a real life situation however, some difficulties may arise. For example, the porcelain samples may not be pure, causing discrepancies in the TL properties.

By using the plateau method described in Chapter 4, the external alpha radiation can be distinguished from the other types of radiation. The first plateau region occurs at approximately the range of the alpha particle. Any plateaus occurring after the first one will be due to other types of external radiation, betas and gammas, which have larger range values. The plateau method makes the age of the samples unnecessary. Ideally, the TL versus depth curve would be a step function. However, the internal alpha irradiation will drop off towards the edges because the internal irradiation at the edges is coming from fewer directions than internal irradiation deeper in the sample. The depth profile used in this project was not a dose versus depth profile because the TL was measured after sanding different thicknesses off of the top of the slices and included TL from the remaining portion of the slice below the given depth. A dose versus depth profile would require measurement of the TL produced solely at each depth. Nevertheless the profile produced may be used to generate a dose versus depth profile by not only plotting the TL versus depth, but

also plotting the TL versus externally applied alpha dose for different samples. By using different samples for each applied alpha dose, including one with no new applied alpha dose, the doses which produced the TL in the alpha range of the porcelain slice and in the plateau region can be found. Also, by using different unannealed samples for each alpha dose, the sensitivities of the samples used to produce the plots of TL versus alpha dose and the TL versus depth curve should be the same.

REFERENCES

1. Heeb, C., Bates, D., Reconstruction of Hanford Production Reactor Releases to the Columbia River, 1944-71, *Health Physics Society 39th*, pp S113, (1994)
2. Widner, T., Oak Ridge Radioactive Barium/Lanthanum Production: History and a Screening Evaluation of Potential Off-Site Dose Significance, *Health Physics Society 39th*, pp S111, (1994).
3. O'Connell, P.V., Rongelap Resettlement Activities Pertaining to the U.S. Department of Energy's Marshall Islands Program, *Health Physics Society 39th*, pp S122, (1994).
4. Romanyukha, A., Wieser, A.; Regulla, D. Retrospective EPR Dosimetry with Different Tooth Tissues, 4th International Symposium on ESR Dosimetry and Applications, pp 210, (1995).
5. Maletskos, Constantine J., *Health Physics*, January 1991, Volume 60, Number 1, pp 1, (1991).
6. Stoneham, D., Porcelain Dating by Thermoluminescence Using the Predose Method.. 3rd TL Specialist Conference, 0, 0 (1982).
7. McKeever, S., Thermoluminescence of Solids, Cambridge Solid State Science Series, (1985).
8. Stoneham, D., Porcelain Dating by Thermoluminescence Using the Predose Method.. 3rd TL Specialist Conference, 0, 0 (1982).
9. Aitken, M.J., Thermoluminescence Dating, Academic Press, Inc., Florida, (1988).
10. Ziegler, James F. and Biersack, J. P., Stopping & Range of Ions in Matter, version 96.xx, (1996).
11. Stopping Powers and Ranges of Protons and Alpha Particles, International Commission on Radiation Units and Measurements Report 49, (May 1993).
12. Ziegler, J. F., Biersack, J. P., and Littmark, U., The Stopping and Range of Ions in Solids, Volume 1 of The Stopping and Range of Ions in Matter, (1985).
13. Fleming, Stuart, Thermoluminescence Techniques in Archaeology, Clarendon Press, Oxford (1979).
14. Aitken, M. J. and Wintle, A. G., Thermoluminescence Dating of Calcite and Burnt Flint: The Age Relation for Slices, *Archaeometry*, 19, 1, pp 100-105 (1977).
15. Wintle, A. G. and Aitken, M. J., Thermoluminescence Dating of Burnt Flint: Application to a Lower Palaeolithic Site, Terra Amata, *Archaeometry*, 19, 2, pp 11-130 (1977).

[16]. Aitken, M. J. and Wintle, A. G., Thermoluminescencee Dating of Calcite and Burnt Flint: The Age Relation for Slices, *Archaeometry*, 19 (1), pp 100-105 (1977).

APPENDIX 26.

The Development of a Computer Control System for Retrospective Luminescence Dosimetry. (Instruction manual written at the Center for Applied Dosimetry, University of Utah, 1996)

The Development of a Computer Control System for Retrospective Luminescence Dosimetry.

Center for Applied Dosimetry
University of Utah

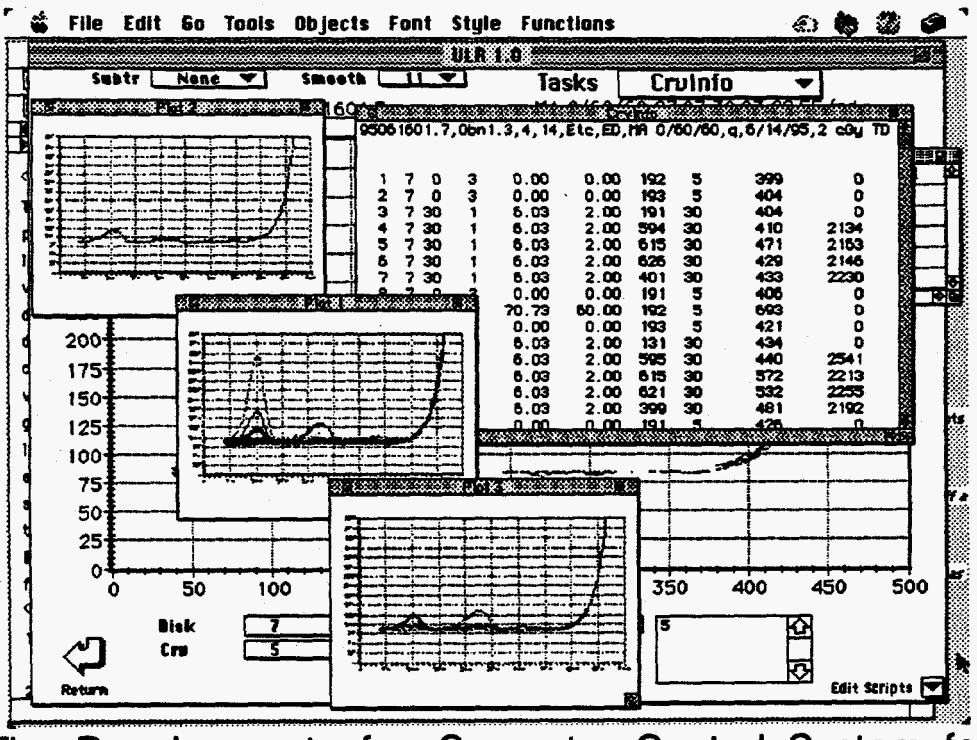

The Development of a Computer Control System for Retrospective Luminescence Dosimetry.

Introduction

Accident dosimetry using luminescence techniques on environmental materials differs from traditional luminescence dosimetry in a number of important ways. These differences, however, all stem from the fact that

the properties of virtually every sample analyzed differ from one another. As a result, much of what is thought of as routine, repetitive dosimetry is in fact a research project unto itself. For this reason a great deal of flexibility as well as automation is required of a good accident dosimetry system. Since its establishment in 1981, the TL Laboratory of the University of Utah has been developing a system of automated routines for use in accident situations. The system has flexibility in that most of the common diagnostic and corrective procedures could be performed and that results could be analyzed by built in procedures. The drawbacks were that the system only worked on the custom designed luminescence readers at the University of Utah, and that operation of the software required considerable training. In response to requests from laboratories involved in TL retrospective dosimetry, the Center for Applied Dosimetry has modified and expanded its software to allow it to control the Riso automated readers in use at many EC laboratories, to increase the flexibility of the system to allow more rapid specification of custom analyses and to simplify the operation of the software so that little training is required for its operation.

Specification of software control system.

A primary requirement of the project was that routines for predose analysis be included in the final package and that specification of parameters for analysis be intuitive and easily mastered by the non specialist. The predose routines required were the Thermal Activation Characteristic (TAC), the Additive Dose Technique (AD), the Modified Additive Dose Technique (MAD) and the Multiple Activation Technique (MA). An introductory discription of the predose technique is given in Appendix 1. In addition it was requested that routines be included for analysis of raw data accessed through a program database. Other routines specific to high temperature TL analysis as well as routines for optically stimulated luminescence (OSL) analysis were also specified. Greater flexibility in the creation of custom routines was a major requirement.

Description and function of the system.

The program runs on Macintosh computers or compatibles and requires System 7.0 or higher and Hypercard 2.2 or higher. RAM requirements for the program alone are 4Mb when virtual memory is active and 6Mb when it is not. Communication between the program and luminescence readers is via an RS-232 serial connection to an intermediate microcontroller board. This board, based on the Motorola 68-HC11 chip, contains A/D and D/A conversion capabilities as well as photon counting and serial interface. Communication with the board is with the aid of macro functions which

handle complex as well as simple tasks. The commands are listed in Appendix 2.

The program is written in Hypercard using the Hypertalk scripting language, together with code resources written in Pascal and C. The code resources were written to speed operation of the program where necessary and to provide access to low level serial interface and graphics routines. The code resource used for database manipulation is explained in detail in Appendix 3. The program is easy to operate and may be modified and expanded to perform custom, one off, functions, or to allow gradual additions and modifications to fit the requirements of a particular laboratory. Text handling capabilities are extensive and text/numerical conversions are transparent to the user/programmer. Data may be analyzed using the existing routines, and/or transferred to other graphing or analysis programs. These capabilities, together with the speed of independently compiled code resources make the program accessible to the computer novice as well as the experienced programmer.

To allow ease of use, the program provides three modes of operation, novice, advanced and manual. The first allows access only to predefined analytical routines which require minimum data input and parameter specification. This mode also provides access to step by step instructions. The built in routines include predose routines (MA, AD, MAD, and TAC), high temperature routines including additive dose as well as automated "curve matching" and the capability of plateau determination. The second mode allows the user to create custom control and analytical routines for research purposes or special applications. Once created the routines may be incorporated into the program for use at the novice level. At present OSL analyses are specified in this mode.
The third mode includes on screen, interactive commands for controlling all functions of the luminescence Reader. These may be operated in manual mode allowing the user to perform step by step procedures as though the reader were a manual unit. In additional to the basic controls, complex commands which control a sequence of operations such as irradiation, preheat and glowout are available. With these commands the user is prompted for such information as platter position, dose, and heating temperature. This mode is useful when a new sample is being examined and the method of analysis is not clear until initial properties of the sample are determined. The commands may also be recorded as they are input so that they may be used again at a later time as an unattended automated routine.

Operation

The program is network compatible, and with the use of the remote access program Timbuktu, available for the Macintosh and IBM compatible computers, a luminescence reader may be operated remotely, from another Macintosh or from an IBM compatible. With the use of Apple Talk Remote, the reader may be controlled over telephone lines via modem. Details of program operation are given in the user manual of Appendix 4.

Conclusion

The collaboration between the University of Durham and the University of Utah has resulted in a comprehensive data collection and analysis program designed for accident dosimetry using luminescence techniques. The program offers the flexibility needed of a research system and the simplicity required for routine analyses performed by the non expert. The program is suitable for laboratories new to the field of accident dosimetry since its built in routines are intuitive, straightforward and cover the range of procedures required for sample characterization. The program is also useful for the advanced laboratory since it allows for the creation and incorporation of custom routines, and the easy incorporation of complex routines for analysis of collected data. The included database engine insures that data will be kept in an ordered, standardized manner which will allow data exchange between all laboratories which use the system.

List of Appendices

Appendix 1

The Pre-dose Thermoluminescence Technique: An Introduction

E. H. Haskell

Thermoluminescence

If a material which has received a prior dose of radiation gives off light as it is heated it is said to be thermoluminescent. In many crystals such as quartz or feldspars, the light which is given off during heating is proportional to the amount of radiation the sample received before heating. This relationship of light output to radiation has lead to the development of thermoluminescence (TL) as a powerful tool for measuring doses of radiation applied in the past.

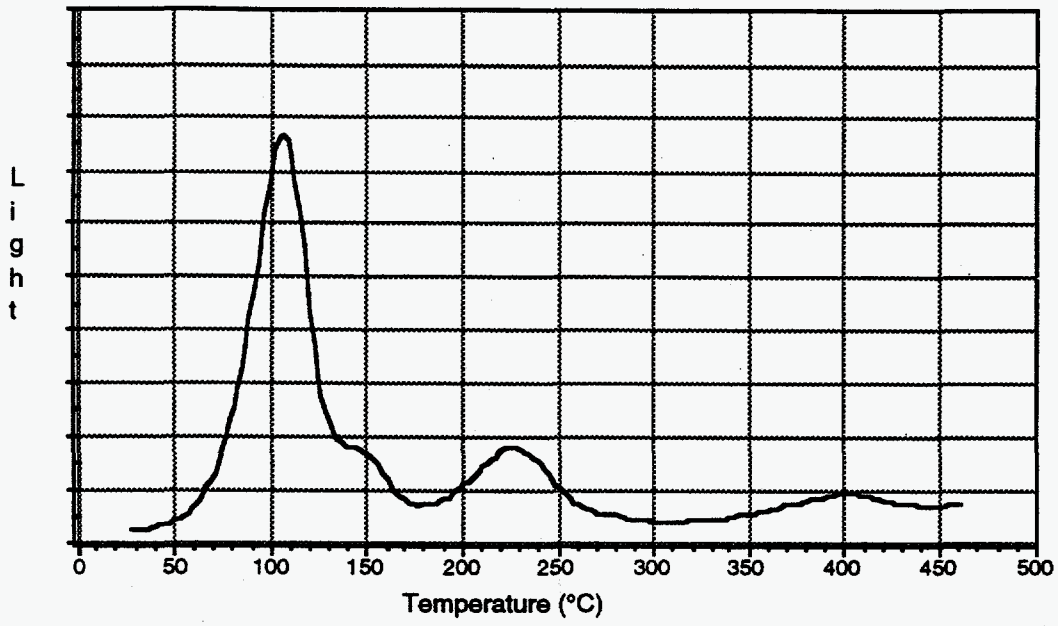

Figure 1. A TL Glow curve of quartz

Figure 1 shows light output (Y axis) as a function of heating temperature (X axis) for a sample of quartz given a dose of radiation shortly before heating. This plot is termed a glow curve. Notice that there are several temperature regions in the glow curve of quartz where the light output is particularly high. These regions are called TL glow peaks. The temperature of the glow peak is important for dosimetry because, in general, the higher the temperature at which the TL peak occurs, the longer the sample will be able to store the signal at normal temperatures before it fades away. High temperature TL peaks in materials such as quartz (such as the TL peak above 350°C in Figure 1) are stable enough to retain information about doses given thousands of years ago. Since natural sources of radiation constantly bombard all materials, these long lived TL peaks are useful for archaeological and geological dating techniques. Signals in the lower temperature peaks seen at 110°C and 160°C decay too rapidly to be of much use for dating or dosimetry under normal conditions. The 110°C TL peak, for instance, decays away in only hours. The TL peak between 200 and 250°C is stable enough to be

used for measuring radiation given in the past hundred years or so, but is not stable enough for archaeological or geological dating.

A useful, if overly simplified, way of picturing the process of thermoluminescence is to visualize an open air amusement park. Assume that all tickets for amusements are purchased when the park opens. The tickets don't have to be used right away. If it is cold and rainy people may stand under shelters without using their tickets. As the day warms up the hardier individuals (and the kids) will come out while others wait for an even warmer temperature. Assume that a popular booth in the park is the balloon pop. Tickets are traded for darts which are thrown at balloons. If a balloon pops, a prize is won. On any given day, the number of balloons popped (the TL light output) will be related to the number of tickets sold (the radiation applied) and the day's temperature (the thermoluminescence heating). One other factor which also affects how many balloons are popped is the number of balloons that are attached to the dart board. The more balloons on the dart board, the greater the chance that a single dart will pop one. This may be related to the sensitivity of the thermoluminescence material, or the amount of light which will be given off (the height of a TL peak) for a given dose of radiation.

A more accurate explanation for the thermoluminescence phenomenon involves the interplay of electrons in the crystal itself. Although the explanation lies in the realm of solid state physics, the more important points may be conceptualized using the example above. Electrons in crystals are normally very tightly bound to atoms (like money in the pocket of a frugal parent). Certain types of radiation, however, are strong enough to knock electrons away from their normal positions (whines of the kids wanting to go to the amusement park). This process of knocking an electron from its associated atom is called ionization and results in a free electron (in the form of a ticket in the hands of a child), and an electron vacancy, or hole, where the electron used to be (the parent's empty wallet). Once an electron is knocked away it may be trapped in a semi-stable position called an electron trap (the parent's pocket for save keeping), be returned to its original stable position (in the form of a ticket refund), be returned to a different stable position (the park owner's wallet) or be combined with a luminescence center with the output of light (pop the balloon /win a prize).

With traditional thermoluminescence the amount of radiation applied determines the number of electrons which will be released from stable positions (ionization) and thus the number which can be captured at electron traps. Some of the traps are very stable and the electrons which become trapped in them will only be released at high temperatures. Upon heating, a certain percentage of these thermally released electrons will combine with luminescence centers and give off light. This type of thermoluminescence forms the basis of "high temperature TL techniques". A requirement of these methods is that electrons remain firmly trapped until measurement.

The pre-dose method of thermoluminescence relies on a different phenomenon. Instead of assuming that the number of trapped electrons is proportional to applied dose, the pre-dose TL technique assumes that the number of luminescence centers (balloons on the dart board) will be increased in proportion to prior dose. Thus the chance that a given electron will find its way to a luminescence center (with light given off) is greater after irradiation than before. By measuring the sensitivity of a sample after irradiation and comparing it to the sensitivity before irradiation, information about the prior dose is obtained.

The pre-dose technique uses light given off from a TL glow peak at only 110°C (Fig. 1). The lifetime of electrons in these traps is so short that most escape within an hour or so following irradiation, even at room temperature. This means that no light will be given off in this temperature region when a sample is heated unless it has been irradiated shortly before heating. The short lifetime of the signal makes it unusable for normal TL dosimetry. It is useful for long term dosimetry, however, when used in a manner which is different from ordinary high temperature TL. This is because a dramatic, easily measurable, increase in sensitivity can be induced in the 110°C peak following irradiation. Fortunately, the increase does not occur

immediately after irradiation, but must be induced or "thermally activated" by heating the sample to very high temperatures (above 500°C) in the laboratory. This thermal activation increases the number of luminescence centers by transferring holes created during irradiation (in so called reservoir centers) to previously inactive luminescence centers (thereby increasing the number of balloons on the dart board). Once activated, the population of luminescence centers will then compete more effectively for electrons ejected from traps during glow out of any future dose of radiation (more balloons popped). The sensitivity may be measured before a dose of radiation is thermally activated as well as after the sensitivity has been increased by heating. The sensitivity increase is measured by applying uniform "test doses" (TDs) of radiation and then measuring the TL output during heating to 160°C (how many balloons are popped). A large prior dose of radiation results in a large increase in sensitivity following thermal activation, a small dose results in a small increase.

To estimate the size of an unknown dose of radiation, a measurement must be made of the increase in sensitivity produced by the unknown dose, and then measuring the increase in sensitivity produced by a known dose of radiation. By comparing the two increases and knowing the size of the calibrating dose, the unknown dose may be determined.

The laboratory procedure for doing this is as follows (see Figure 2).

1) Measure the light output of the sample prior to thermal activation by applying a TD and heating to 160°C. (The height of the 110°C peak at this point is termed S_0, or the initial sensitivity) *The population of luminescence centers has not yet been increased by thermal activation .*

2) Heat the sample to high temperature and let it cool. *This thermal activation increases the population of active luminescence centers in proportion to the unknown dose .*

3) Measure the light output again with another TD (the height of the 110°C peak is now termed S_n). *The measured signal (S_n) will be greater than the original sensitivity (S_o) due to the increased number of active luminescence centers.*

4) Apply a larger known dose of radiation to the sample (historically called a beta dose, β). *This is the "calibrating" dose. The sensitivity increase due to this dose (measured in step 8) will be compared with the sensitivity increase due to the unknown dose.*

5) Heat the sample to 160°C to drain the electrons in the 110°C TL region. *We must deplete electrons in the 110°C region due to the calibrating dose before we can accurately measure its sensitivity with a standard TD.*

6) Measure the light output again with a TD before thermally activating the sample (the height of the 110°C peak is now termed S_n', or S_n quenched). *This gives us the so called "radiation quenched" sensitivity. Which is lower than S_n for reasons described below.*

7) Thermally activate the calibrating dose by heating the sample to high temperature. *This increases the population of active luminescence centers by thermally transferring holes created during application of the calibrating dose to inactive luminescence centers thereby activating them (more balloons) .*

8) Let the sample cool and then measure the light output with another TD while heating past 110°C (110°C peak height now termed $S_{n+\beta}$). *Measure the new sensitivity of the 100°C TL region.*

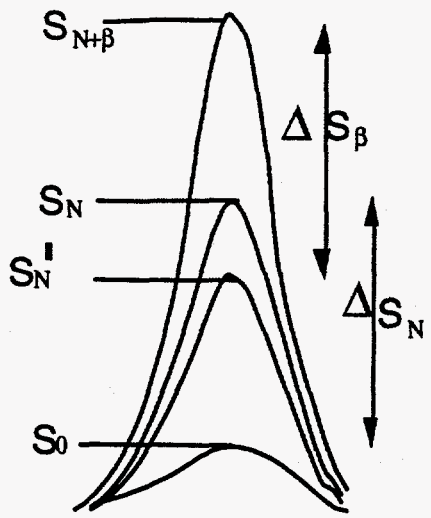

Figure 2.

We now determine the sensitivity increase due to the unknown dose and call that sensitivity increase ΔS_n (delta S_n), where $\Delta S_n = (S_n - S_0)$.

The sensitivity increase due to the calibrating dose of radiation is termed ΔS_β and is equal to $(S_{n+\beta} - S_n')$.

We know that the calibrating dose of radiation produced a sensitivity increase, ΔS_n. If the unknown dose produced this same amount of increase (if $\Delta S_n = \Delta S_\beta$) then we would know that the unknown dose was equal to the calibrating dose. If the unknown dose produced half the increase of the calibrating dose then we know the unknown dose was approximately half the calibrating dose, etc. This relationship of dose to sensitivity increase can be expressed in the following formula.

$$\text{unknown dose} = \beta * (\Delta S_n/\Delta S_\beta) \qquad \text{Equation 1}$$

When we consider that the test doses also contribute to the sensitivity increase, the formula becomes:

$$\text{unknown dose} = (\beta+TD_\beta) * (\Delta S_n/\Delta S_\beta) - TD_n \qquad \text{Equation 2}$$

Where TD_n is the sum of all test doses applied before activation of the unknown dose and TD_β is the sum of all test doses applied after activation of the unknown dose and before activation of the calibrating dose.

Because the predose technique is complex (as is the underlying mechanism of the phenomenon), a number of precautions must be taken when applying the pre-dose technique to radiation dosimetry.

Potential errors associated with predose measurements

The predose technique is very sensitive at low doses of radiation, but it has the drawback that the relationship of sensitivity increase to applied dose is often times not linear. As the dose applied increases, the nonlinearity gets more and more pronounced. This takes the form of smaller and smaller increases in sensitivity for radiation doses of the same size, until finally virtually no increase is seen. This effect of a leveling off of the sensitivity increase at higher doses is termed saturation. A saturation effect of some type is seen in all forms of thermoluminescence. What complicates predose analysis is that saturation effects can occur at relatively low doses and at several stages in the predose sensitization process. Saturation at

each stage behaves differently, has a different effect on the dose measurement, and must be tested in different ways. Because the predose phenomenon is a multistep process, saturation effects can best be understood by following the steps in sequence. The first step in the process involves ionization of atoms during irradiation. This ionization causes electrons to be trapped in electron traps and holes to be trapped in hole traps. Some of these hole traps are termed reservoir centers in the predose model. For dosimetry purposes the filling of reservoir centers should be proportional to the applied dose. As the reservoir centers approach saturation, however, there are fewer empty centers available to capture holes and the number captured slows dramatically. Nonlinear filling results and transfer of holes to reservoir centers during irradiation is no longer proportional to dose. This effect is termed **"R" center nonlinearity.**

The second step in the predose process at which saturation effects can occur concerns the transfer of holes from the reservoir centers to the inactive luminescence centers during thermal activation. For accurate dosimetry this process should involve transfer of holes to luminescence centers in proportion to holes released from reservoir centers during thermal activation. However as more and more luminescence centers become activated, the number of inactive centers available to receive holes from reservoir centers is reduced and filling is no longer proportional to holes released from the reservoir centers. Dose estimation is again compromised as a result. This effect is termed **"L" center nonlinearity.**

Another phenomenon which effects dose estimation is a reduction in the number of active luminescence centers which occurs during laboratory irradiation. This effect, termed **radiation quenching** does not result in a decrease of the original sensitivity of the sample (S_0) but it does reduce the sensitivity of samples which have already been thermally sensitized (such as S_n or $S_{n+\beta}$). The phenomenon is observed as a decrease in sensitivity of the 110°C TL region seen immediately after application of the calibrating dose of radiation, and is seen in Figure 2 as the difference between the S_n curve and the S_n' curve. This is the reason that measurement of the sensitivity of a sample must be made following application of the calibrating dose but before thermal activation (step 6 in the procedure described above). Failure to account for radiation quenching can result in an overestimate of the unknown dose.

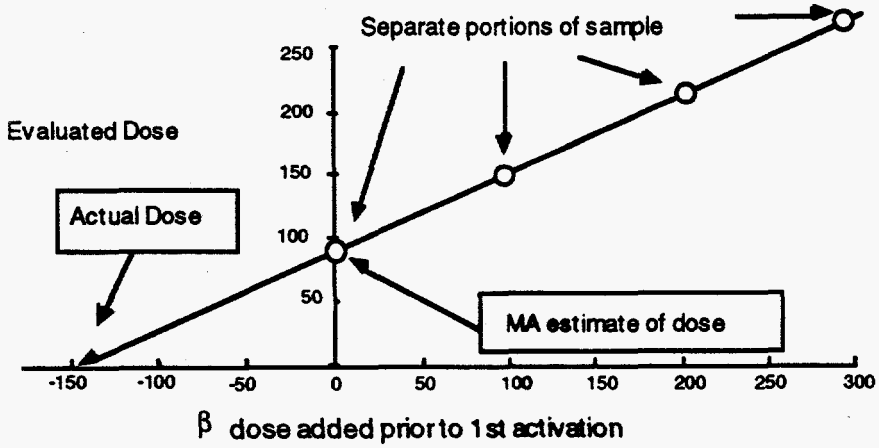

Figure 3.

A fourth effect which must be considered in all types of predose analysis, and which is impossible to detect without proper examination, is a **change in degree of sensitization** which occurs between the first thermal activation and all subsequent activations. This means

that the unknown dose of radiation might produce an increase in sensitivity which is considerably more or less than the sensitivity increase which will be induced by the same dose applied after the first thermal activation. The procedure for correcting for this change is shown in Figure 3.

The four effects described above, R center nonlinearity, L center nonlinearity, radiation quenching and change in degree of sensitization do not act in isolation, but effect subsequent stages of the predose phenomenon. For instance a change in degree of sensitization following first thermal activation will mean that the proportionality relationship assumed in equation 2 above is inaccurate. R center nonlinearity means that filling of the L centers will likewise not be proportional to dose, even if transfer from R centers to L centers is linear. Radiation quenching can have a large effect on L center filling as well. Assume that the L centers are nearly full so that only a small increase in L filling results during thermal transfer of holes from R to L centers. If a large calibrating dose of radiation is applied, radiation quenching will result in a partial emptying of L centers and may push the linearity of subsequent R to L center transfers back into the linear region. The interaction of these effects is complex and difficult to detect, however they may be seen at any dose level. Each sample analyzed must be checked for their occurrence since factors as diverse as impurity content of the clay and heating and cooling rates during manufacture can effect them.

One of the greatest hazards of predose analysis is that the effects described above are not easy to detect and are not easy to correct for. A sample may appear to behave in a consistent, linear fashion, but may still experience nonlinearity or change in degree of sensitization which will effect dose estimates. Because of the potential for substantial, yet unobvious, errors in predose measurement, procedures have been devised to detect, and in some cases correct for the errors. Unfortunately the procedures are time consuming, and are best performed on equipment capable of performing rapid, repeated irradiations and glow curve measurements. Because of this they are omitted in many laboratories, and the results obtained in their absence must be considered tentative until the effects have been demonstrated to be absent.

Appendix 2
MACRO COMMANDS

everything marked with *** are dummy parameters for compatibility only!

DELAY

params -> time
[0.01 sec]

returns -> <@
task done -> !@

description -> Causes a delay in hundredth's of seconds to occur before the system confirms command completion.

OSLOFF

params -> NONE

returns -> <A
task done -> !A

description -> Turns the OSL source OFF.

OSLON

params -> NONE

Returns -> <B
task done -> !B

description -> Turns the OSL source on.

ONPLT

params -> NONE

Returns -> <C
task done -> !C

description -> Raises the sample closer to the PM tube. Identical to the command PLTUP.

OFFPLT

params -> NONE

Returns -> <D
task done -> !D

description -> Lowers the sample, returning it to the sample platter. Identical to PLTDN.

PLTUP

params -> NONE

Returns -> <C
task done -> !C

description-> Raises the sample closer to the PM tube. Identical to the command ONPLT.

PLTDN

params -> NONE

Returns -> <D
task done -> !D

description -> Lowers the sample, returning it to the sample platter. Identical to OFFPLT.

MOVNXT

params -> NONE

Returns -> <E
task done -> !E

description -> Moves the sample platter to the next sample position.

MOVRD

Params ->
Position (1 thru 24)

Returns -> <G
task done -> !G

description -> Moves the corresponding sample into the irradiator position.

HOME

params -> NONE

Returns -> <H
task done -> !H

description -> Moves the sample platter so that sample number one is in the PM/oven position.

CALOFF

params -> NONE

returns -> <I
task done -> !I

description -> Turns the calibration source OFF.

CALON

params -> NONE

returns -> <J
task done -> !J

description -> Turns the calibration source ON.

MOVPOS

params ->
Position (1 thru 24)

returns -> <M
task done -> !M

description-> Moves the corresponding sample into the PM/oven position.

DOSE

params -> Irrad Time [0.01 sec]
Position (1 thru 24)
*** elevator (1 = high , 0 = low)

returns -> <N
task done -> !N

description -> Moves the corresponding sample into the irradiator position, and irradiates the sample for a given period of time. (hundredth's of seconds)\

NOTE: on the RISO multisample reader, their is not a high or low option.

POS

params -> NONE

Returns -> <P
task done -> !P

description -> Returns which sample is currently in the PM/oven position.

DNRT1

params -> Down RampRate [0.01 deg/sec]

returns -> <Q
task done -> !Q

description -> Defines the rate at which the temperature decreases (in hundredth's of degrees per second) until the lower cutoff temperature is achieved .

NOTE: This feature is currently unimplemented in the Risalyzer interface, but is available in other reader configurations.

DNTMP

params -> Temp (transition) [deg]

returns -> <S
task done -> !S

description -> Defines the lower temperature at which the down ramp rate drops at the Ramp Reset Rate to the setpoint.

NOTE: This feature is currently unimplemented in the Risalyzer interface, but is available in other reader configurations.

UPRT

params -> Up RampRate [0.01 deg/sec]

returns -> <T
task done -> !T

description -> Defines the rate at which the temperature increases (in hundredth's of degrees per second) from the setpoint until the endpoint temperature is achieved .

DATASP

params -> Data Space [deg/datum]

returns -> <U
task done -> !U

description -> Defines the sampling rate (in degrees per datum), during a ramp, that sample data will be collected .

SETPT

params ->
Setpoint [deg]

returns -> <V
task done -> !V

description -> Defines the initial temperature for the the ramp up , and the end temperature after the ramp down.

ENDPT

params ->
Endpoint [deg]

returns -> <W
task done -> !W

description -> Determines the target temperature for the heating plate for the duration of a Hold Time.

HDTIME

params ->
Holdtime [0.01sec]

returns -> <X
task done -> !X

description -> The time (in hundredth's of seconds) that the temperature remains at the endpoint.

ADTMP2

params -> NONE

returns -> {temp data }

description -> Returns the instantaneous temperature of the heating plate.

NOTE: Their is no verification that the command was successful, or that it has been completed. It returns the ascii equivelent of the temperature in celsius followed by a carriage return.

RMPRST

params -> NONE

returns -> <\
task done !\

description -> Ends and resets all ramp functions.

NOTE: This is an internal command, and is rarely implemented by itself.

RMPDN2

params -> NONE

returns -> <]
task done -> !]

description -> Defines ta seecond rate at which the temperature decreases (in hundredth's of degrees per second) until the lower cutoff temperature is achieved .

NOTE: This feature is currently unimplemented in the Risalyzer interface, but is available in other reader configurations.

RMPUP

params -> NONE

returns -> <^
task done -> !^
{counts},{temp}
{counts},{temp}
etc.

description -> Using the defined parameters, this command will preform an up ramp, a hold, and a ramp reset.

VACOFF

params -> NONE

returns -> <a
task done -> !a

description -> Turns the Vacuum OFF.

VACON

params -> NONE

returns -> <b
task done -> !b

description -> Turns the Vacuum ON.

PRGOFF

params -> NONE

returns -> <c
task done -> !c

description -> Turns the Nitrogen Purge valve OFF.

PRGON

params -> NONE

returns -> <d
task done -> !d

description -> Turns the Nitrogen Purge valve ON..

OVOFF

params -> NONE

returns -> <e
task done -> !e

description -> Turns the oven OFF.

NOTE: This command overides all oven commands.

OVON

params -> NONE

returns -> <f
task done -> !f

description -> Turns the oven ON.

NOTE: This command overides all oven commands.

IRDOFF

params -> NONE

returns -> <j
task done -> !j

description -> Turns the irradiator OFF.

IRDON

params -> NONE

returns -> <k
task done -> !k

description -> Turns the irradiator ON.

LAZOFF

params -> NONE

returns -> <s
task done -> !s

description -> Turns the Laser OFF.

LAZON

params NONE

returns -> <t
task done -> !t

description -> Turns the Laser ON.

INIT

params NONE

returns -> <g
task done -> !g

description -> Initializes the reader unit to boot conditions.

SETRMP

params ->
Setpoint [deg], DataSpace [deg/datum], UpRate [0.01 deg/sec], Dose Delay [sec]

returns -> <h
task done -> !h

description -> A macro command that sets all values to perform a user defined ramp, and then performs the ramp.

NOTE: Boot default values are:
- setpoint 30 degrees
- dataspace 2 degrees per datum
- up rate 10 degrees per second
- dose delay 0 seconds

SETPRE

params -> Endpoint [deg], Holdtime [0.01sec], RampUpRate [0.01 deg/sec]

returns -> <i
task done -> !i

description -> A macro command used in conjunction with BDMS, TDMS, and BKGMS. When the parameters are set, before one of these three macro commands is executed, the interface will preheat the sample with a ramp, to a given endpoint temperature, and then holds a given amount of time before returning instantaneously to the setpoint.

BDMS

params -> integer (0=no RmpDn, 1=RmpDn)
integer (0=RampUp, 1=FlatRamp),
*** Delta Holdtime [deg] [0.01sec],
Endpoint Position [deg], (1 thru 24),
Irrad Time [0.01 sec],
*** Position (1 thru 24),
*** elevator (1 = high , 0 = low)

returns -> <p
task done -> !p
{counts},{temp}
{counts},{temp}
etc.

description -> A macro command to perform a BD Multi-Sample. This will take a given sample, and irradiate it for a certain dose delay. It will then preform the appropriate heating analysis on the sample.

TDMS

params -> integer (0=no RmpDn, 1=RmpDn)
integer (0=RampUp, 1=FlatRamp),
*** Delta Holdtime [deg] [0.01sec],
Endpoint Position [deg], (1 thru 24),
Irrad Time [0.01 sec],
***Position (1 thru 24),
***elevator (1 = high , 0 = low)

returns -> <q
task done -> !q
{counts},{temp}
{counts},{temp}
etc.

description -> A macro command to perform a TD Multi-Sample. Similar in configuration, and setup to BDMS, and BKGMS.

BKGMS

params -> integer (0=no RmpDn, 1=RmpDn)
integer (0=RampUp, 1=FlatRamp),
*** Delta Holdtime [deg] [0.01sec],
Endpoint Position [deg], (1 thru 24),

returns -> <r
task done -> !r
{counts},{temp}
{counts},{temp}
etc.

description -> A macro command to perform a BacKGround Multi-Sample. Similar in configuration, and setup to TDMS, and BDMS.

LZTMP

params -> Temp [deg]

returns -> <v
task done !v

description -> Temperature at which the laser is to turn OFF.

LZTMP0

params -> Temp
[deg]

returns -> <w
task done -> !w

description -> Temperature at which the laser is to turn ON.

RRRATE

params ->
RampReset Rate [0.01 deg/sec]

Returns -> <x
task done -> !x

description -> Sets the ramp reset rate, the rate at which the ramp is reset to the setpoint.

PDLY

params -> time
[sec]

returns -> <y
time delay !y

description -> A timed delay in seconds

PARAM?

params -> NONE

returns -> <#
task done -> !#
Setpoint, Dataspace, Uprate, DoseDelay, PreEndpoint,
PreHoldtime, PreUpRate, DownRate1, DownRate2,
DownTemp, HVTemp

description -> Returns current value of the above listed variables.

******* ALL commands following this point are recognized, and dummy ******* values are returned, but they are not implemented!!!! **********

IRUP

params -> NONE

returns -> <A
task done !A

description -> Moves the irradiator plate UP.

IRDN

params -> NONE

returns -> <B
task done -> !B

description -> Moves the Irradiator plate DOWN.

MOVPRV

params -> NONE

returns -> <F
task done -> !F

description -> Moves the sample to the previous position.

DETEN

params -> NONE

returns -> <I
task done -> !I

description -> Enables the PM tube high voltage supply.

DETOFF

params -> NONE

returns -> <J
task done -> !J

description -> disables the PM tube high voltage supply.

RADHI

params -> NONE

returns -> <K
task done -> !A
in position ? [0 = yes, 1 = no]

description -> Selects the High radiation position. Returns a zero if the irradiator platter is in the high position. Returns a one if it is not.

RADLO

params -> NONE

returns -> <L
task done -> !L

description -> Selects the LOW radiation position.

DNRT2

params -> down ramp rate [0.01 deg/sec]

returns -> <R
task done -> !R

description -> Defines the rate at which the temperature decreases (in hundredth's of degrees per second) from the first cutoff temperature, until the lower second cutoff temperature is achieved .

HVTEMP

params ->
temperature [deg]

returns -> <k
task done -> !k

description -> Temperature at which the high voltage supply to the PM tube is turned off.

HVOFF

params -> NONE

returns -> <_
task done -> !_

description -> Turns the High Voltage supply to the PM tube OFF.

HVON

params -> NONE

returns -> <'
task done -> !'

description -> Turns the High Voltage supply to the PM tube ON.

PMPOFF

params -> NONE

returns -> <e
task done -> !e

description -> Turns the pump OFF.

PMPON

params -> NONE

returns -> <f
task done -> !f

description -> Turns the pump ON.

HVAC

params -> NONE

returns -> [vacuum]

description -> Returns the vacuum pressure in milli-pascals.

NOTE: System Returns -> !! when no more data to be sent.

FIV, Dose Reconstruction, EPR with teeth

Investigations on sample preparation techniques

FIV participants:	ISS, Rome
	GSF, Munich
Invited participants:	IMP, Ekaterinbourg
	MRRC, Obninsk
	URPI, Kiev
	UU, Utah

Objectives

Selection of the most suitable technique(s) for preparation of tooth enamel samples. It will be used to suggest a protocol for preparation of tooth enamel samples.

Each participant will chose one technique and suggest the most suitable set of EPR measurement parameters. Of special attention should be to determine an optimum level of microwave power. The quality criteria of a technique (including the set of measurement parameters) will be the reproducibility and the inter-sample variation of the quality parameters listed below. The best compromise needs to be found between reproducibility of background spectra and maximal intensity of the hydroxyapatite signal.

Milestones

November 96:	Comparison and discussion of results obtained by the participants for their own set of samples and technique.
	Pre-selection of techniques, exchange of samples and parameter sets.
February 97:	Comparison and discussion of results obtained by different participants for the same set of samples and measurement parameters.
	Final selection of techniques.

Quality parameters

The quality parameters are listed below and defined in the figures. They are chosen to allow for an objective comparison of EPR spectra measured by different spectrometers. The standard deviation of the parameters and the normalised signal amplitude will be a measure for the quality of the preparation technique. The quality parameters needs to be determined with the set of measurement parameters which are considered to be the best.

Background amplitude, Ab
Background position, H0b (g-value or field and frequency)
Background line width, dHb
Background symmetry factor, ratio dHb1/dHb2
Hydroxyapatite amplitude after 50 Gy irradiation, Ah50
Hydroxyapatite line width, dHh
Hydroxyapatite position, H0h (g-value or field and frequency)
Mean normalised background amplitude, ratio (mean Ab)/(mean Ah50)

For the chosen EPR measurement parameters the signal-to-noise ratio, (mean Ab)/N has to be determined. The noise amplitude, N, should be measured without sample.

For one representative unirradiated sample the background amplitude (Ab), the line width (dHb) and the symmetry factor (dH1/dH2) should be determined versus microwave power up to 200 mW.

For one representative 50 Gy irradiated sample the hydroxyapatite amplitude (Ah) should be determined versus microwave power up to 200 mW.

The 50 Gy irradiation has to be done with a 3 mm Plexiglas as build-up material by a ^{60}Co- or ^{137}Cs-source.

Samples

10 molars or wisdom teeth. Three of them has to be irradiated with 50 Gy for determination of the hydroxyapatite parameters. The remaining seven samples are used to determine the background parameters.

The conditions and time of storage of the samples after preparation should be given.

Measurements

Each sample has to be measured three times following refilling of the sample tube to determine the reproducibility. The orientation of the sample tube in the cavity has to be identical for all measurements.

Remarks

A quality assurance procedure including suitable reference samples to allow for comparison of accuracy of spectrometer parameter settings and signal intensities will be discussed at the meeting in November.

Figures for definition of quality parameters

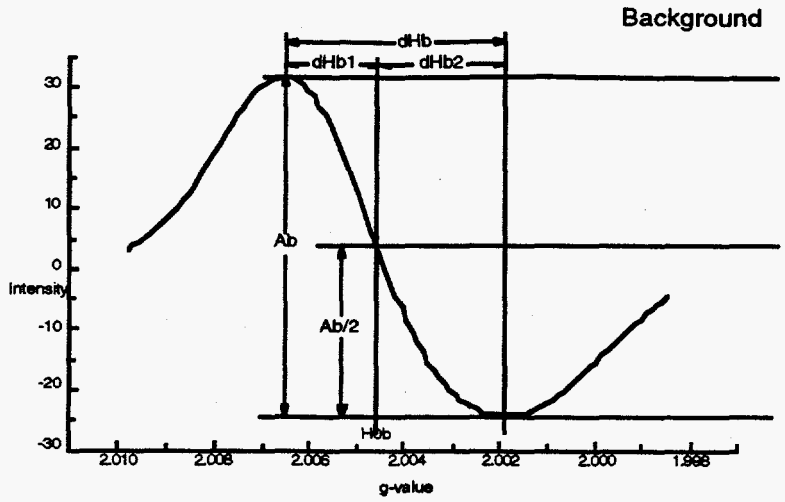

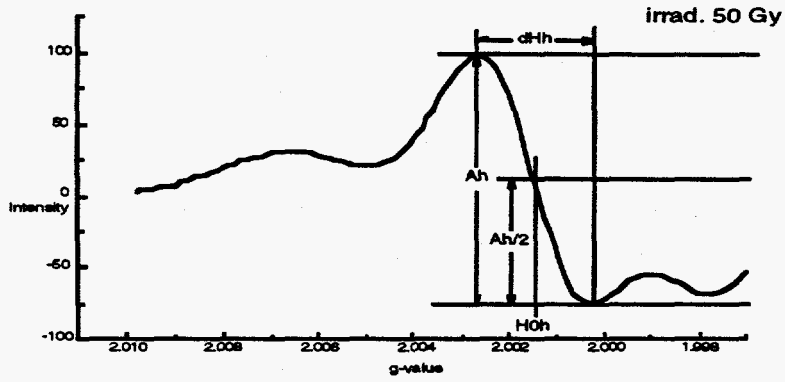

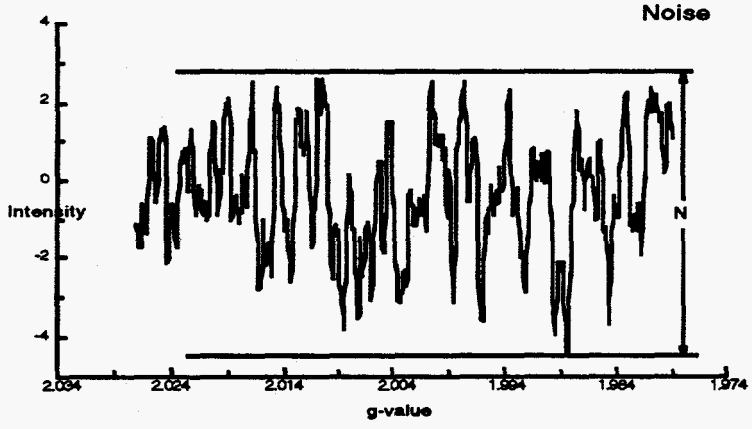

Appendix 3
The Universal Luminescence Reader Program Manual

ULR

The Universal Luminescence Reader Program

Reference Manual

v 0.9

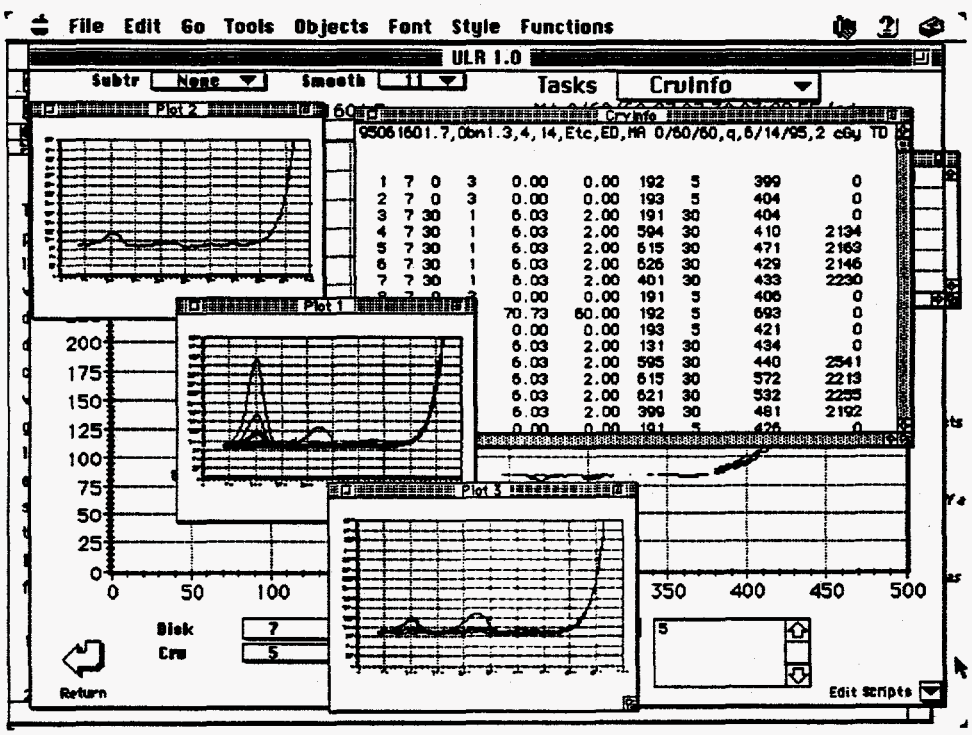

The Universal Luminescence Reader Program

ULR

Introduction

The Universal Luminescence Reader Program (ULR) was developed by the TL/EPR laboratory of the University of Utah in collaboration with the Luminescence Laboratory of Durham University for controlling automated TL/OSL readers and performing dosimetric analyses which are not included in any commercially available package. The program emphasizes low level TL accident dosimetry using environmental ceramics and incorporates routines for a variety of diagnostic and analytical procedures associated with the predose TL technique. The ULR program is network compatible, and with the use of the remote access program Timbuktu, available for the Macintosh and IBM compatible computers, the Riso reader may be controlled remotely, from another Macintosh or a PC. With the use of Apple Talk Remote, the reader may be controlled via modem. The program runs on the Macintosh platform and requires System 7.0 or higher and Hypercard 2.2 or higher. RAM requirements for the program alone are 4Mb when virtual memory is active and 6Mb when it is not. Communication between the ULR program and the Riso Reader is via an RS-232 serial connection to an intermediate microcontroller board. This board, based on the Motorola 68-HC11 chip, contains A/D and D/A conversion capabilities as well as photon counting and serial interface. Communication with the board is with the aid of Macro functions which handle complex as well as simple tasks. The commands are listed in Appendix 2 of the final report.

Principle of Operation

The ULR program is written in Hypercard using the Hypertalk scripting language, together with code resources written in Pascal and C. The code resources were written to speed operation of the program where necessary and to provide access to low level serial interface and graphics routines. The code resource used for database manipulation is explained in detail in Appendix 3. . The ULR program is easy to operate and may be modified and expanded to perform custom, one off, functions, or to allow gradual additions and modifications to fit the requirements of a particular laboratory. Text handling capabilities are extensive and text/numerical conversions are transparent to the user/programmer. Data may be analyzed using the existing routines, and/or transferred to other graphing or analysis programs. These capabilities, together with the power available through the high speed code resources make the ULR program equally suitable for the computer novice as well as the experienced programmer. To provide this ease of use the ULR program offers two modes of operation. The first allows access only to predefined analytical routines which require minimum data input and parameter specification. This mode also provides access to step by step instructions. The second mode allows the user to create custom control and analytical routines for research purposes or special applications. Once created the routines may be incorporated into the program for use at the novice level.

Control Capabilities

Manual Operation.

The program includes on screen, push button commands for controlling all functions of the Riso Reader. These may be operated in manual mode allowing the user to perform step by step procedures as though the reader were a manual unit. In additional to the basic controls, complex commands which control a sequence of operations such as irradiation, preheat and glowout are available. With these commands the user is prompted for such information as platter position, dose, and heating temperature. This

mode is useful when a new sample is being examined and the method of analysis is not clear until initial properties of the sample are determined. The commands may also be recorded as they are input so that they may be used again at a later time as an unattended automated routine.

Automated control using script generation capabilities
The script generation controls allow for easy determination and input of analytical parameters necessary for TL or OSL analyses or a combination of the two. The controls allow for specifications of complex analyses involving dozens or even hundreds of steps on multiple samples. The advantage of this mode of input is that non standard analytical routines can be generated very quickly and intuitively. Access to radiation source dose rates from a user library allows irradiation commands to be generated using decay-corrected irradiation times specified in units of dose. Comments may be inserted into the command list prior to analysis or at any time during the operation of the routines. Changes may also be made to the commands during run time. The automated sequence may be paused for manual operation and then restarted, or a new subset of automated commands may be inserted prior to completion of the running script.

Using the ULR Program

While the ULR program is starting up, it searches for the master index file and for the file containing the code resources. If it is unable to find them it prompts the user for their location. Once located, the user will not be prompted for locations on subsequent start ups of the program unless they have been moved or renamed. During startup, the screen below will be briefly displayed.

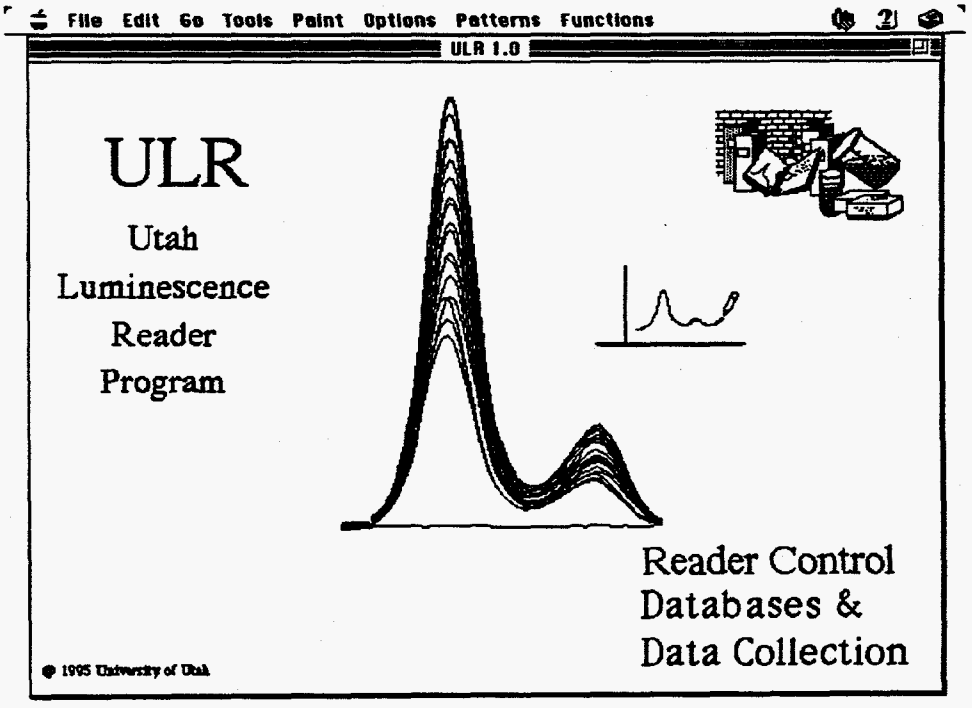

Startup Screen

The second screen seen by the user following startup is a general menu page for use by the novice operator (novice page 1). If the operator desires assisted use of the program,

the buttons on this page will guide him through program setup. If an advanced user wishes direct access to the programs capabilities, a menu option in the menu bar entitled "functions" provides direct access to all of the programs capabilities.

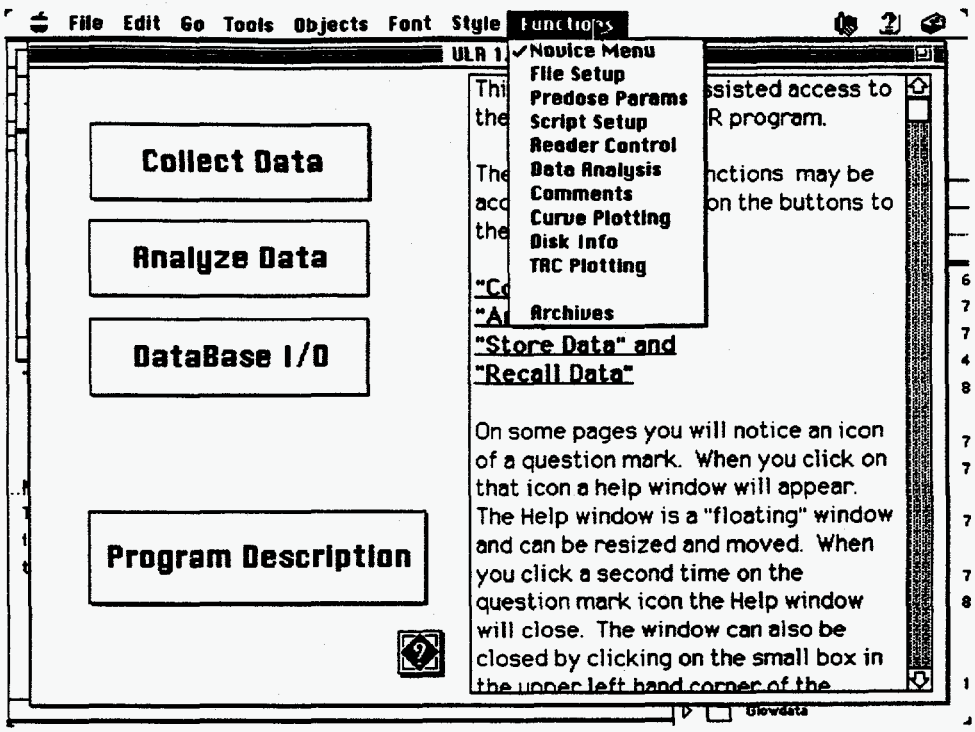

Function Menu Options

Novice operation

The menu page which is presented at startup has a help window which provides instruction to the novice user.

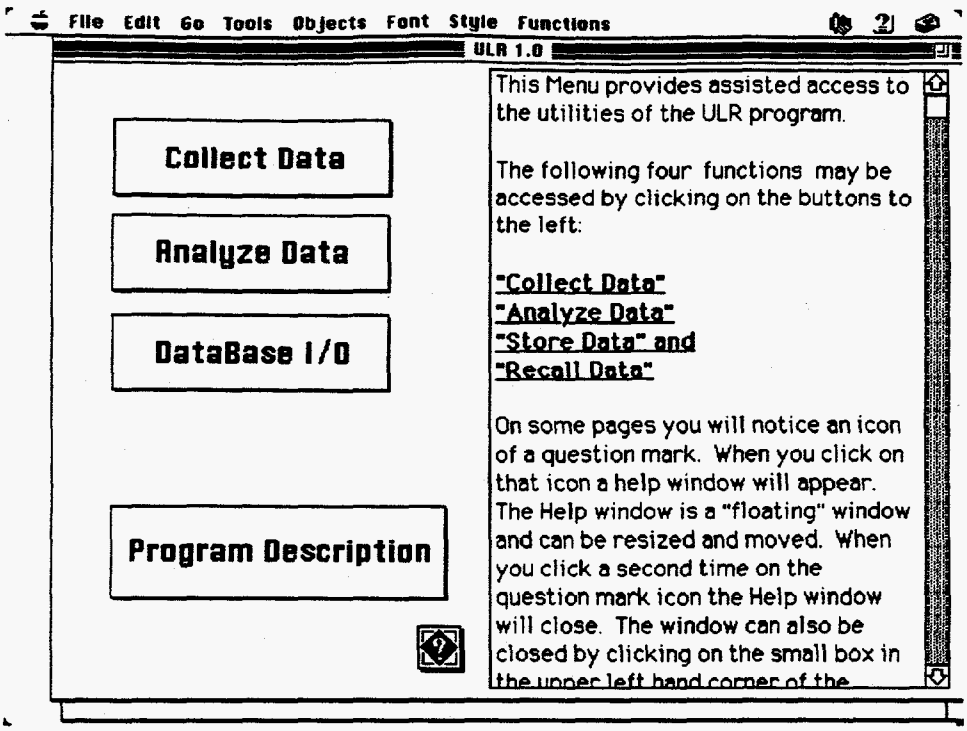

Novice Page 1

Each of the buttons guides you through a different operation which will be described below.

Collect Data

Clicking on the "Collect Data" button takes you to a window with several buttons additional help text in a scrollable window:

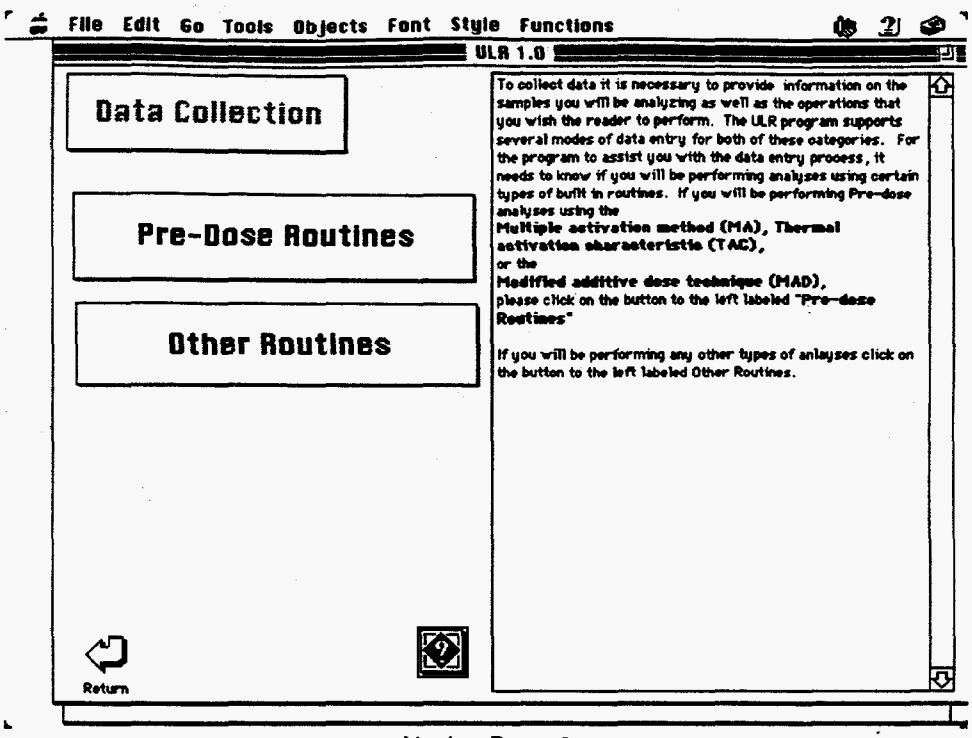

Novice Page 2

Clicking on the button "Pre-dose Routines" takes you to the new window below.

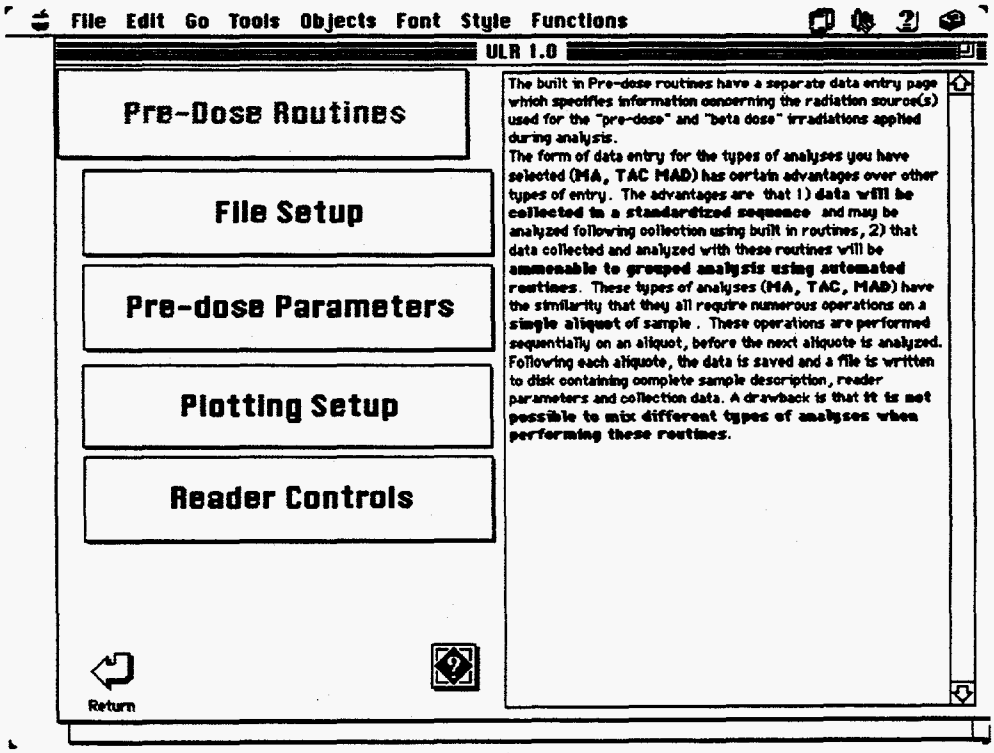

Novice Page 3

Clicking on the button "File Setup" takes you to a **File Setup** page where sample information and information on the type of analysis is input. Following entry of data into this page, the user will be taken to a **Pre-dose Parameters** page where parameters specific to predose analyses will be entered. Next the "Plotting Setup" button advances to the **Curve Plotting** for input of plottingparameters and integration limits, and finally the **Reader Control** page for initiation of analysis. The file setup page is shown in Fig. ___

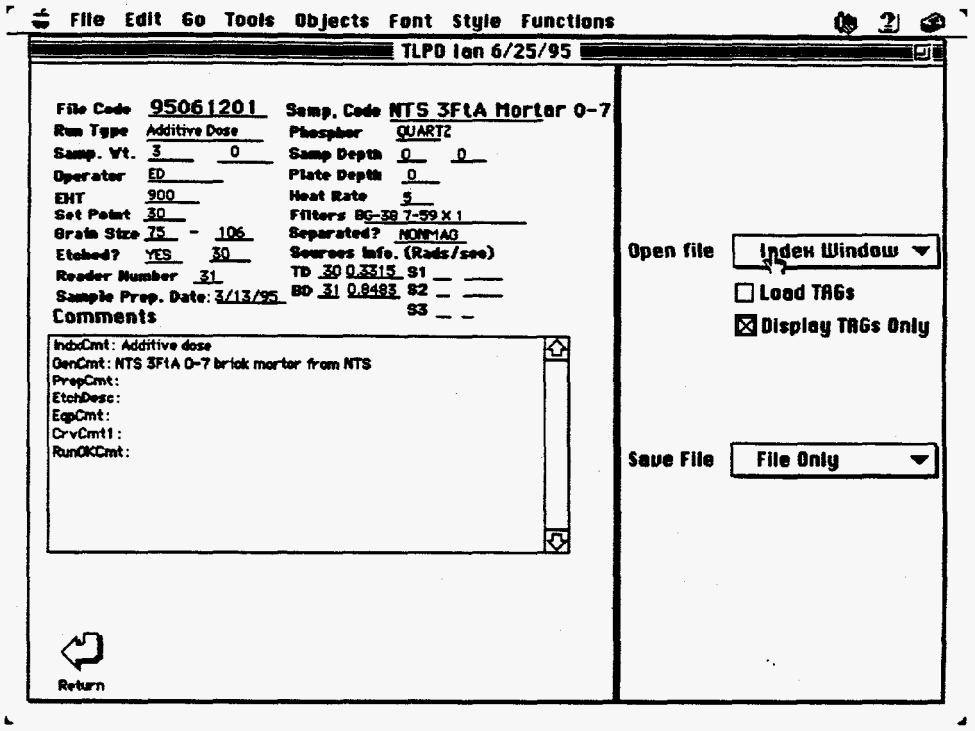

File Setup

Once in the file setup page, entry of data is usually easiest if a similar previous file is first accessed. This may be done by clicking and holding on the "Open File" button. A pop up window will be shown (fig) with several options for file access. The three options grouped together, via Filecode, via SmpCode and via IndxCmt each allow for key word searches through different fields of the indexfile. If the option "via SmpCode" is chosen a dialogue box will appear asking for entry of the code desired. Placing the character "]" before the entry will allow an embedded search for any occurrence of the word or words within the field. Once the OK button is clicked, the database will be searched and all entries conforming to the search criteria will be brought up in a window superimposed on the card (fig).

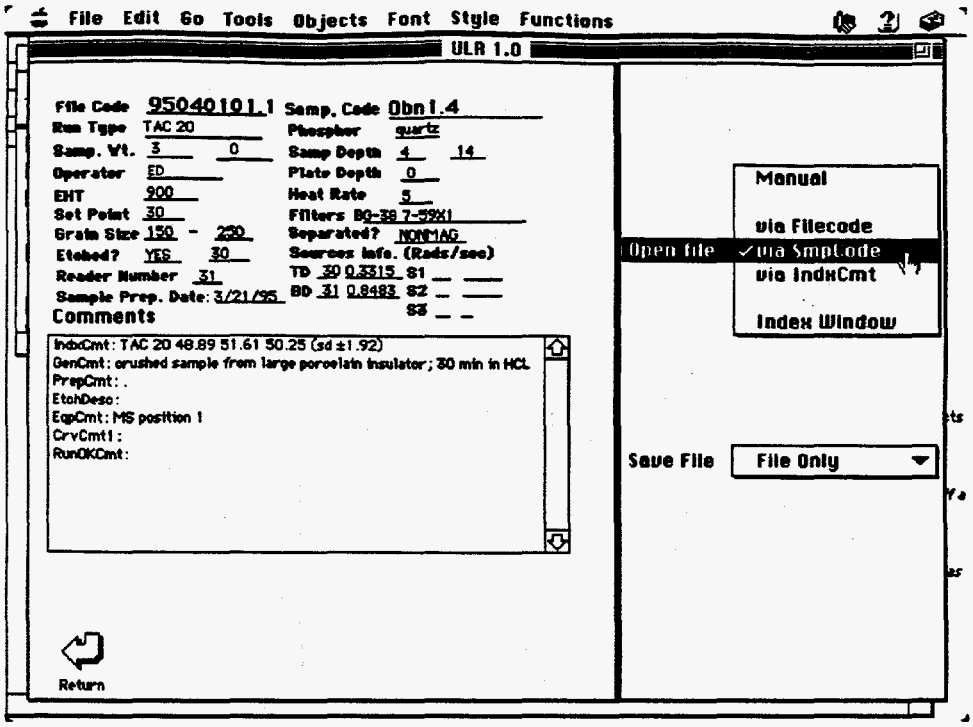

If the file desired is seen in the window, a single click on the line containing the file entry will access the individual file. If the button entitled "Load TAGs" is checked, the file will be loaded directly into the fields of the file setup page. If the button entitled Display TAGs Only is checked, three floating windows will appear as in fig .

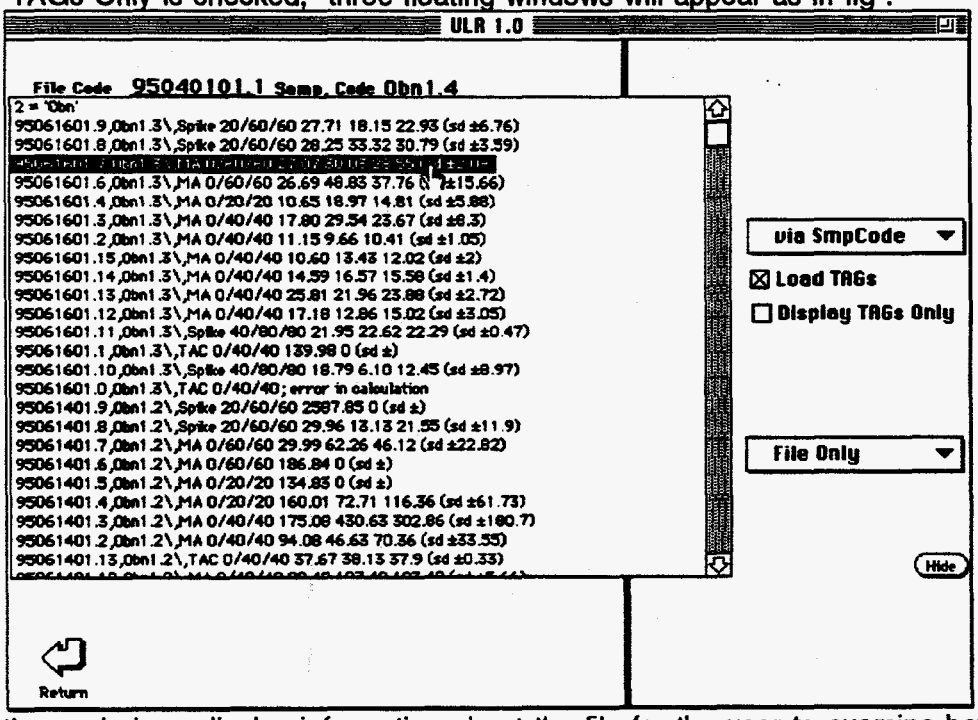

These three windows display information about the file for the user to examine before he recalls the data and erases the information from the previous file. A new pop up button also appears labeled "Load TAGs". The three windows contain descriptive information

about the file, the script or reader commands which were used for data entry for the file, and a summary window showing results of the analysis as well as a log of all the commands executed. If this file is the one sought, then the button Load TAGs can be used to select loading of either the entire file, or just the TAGs, or subinformation desired.

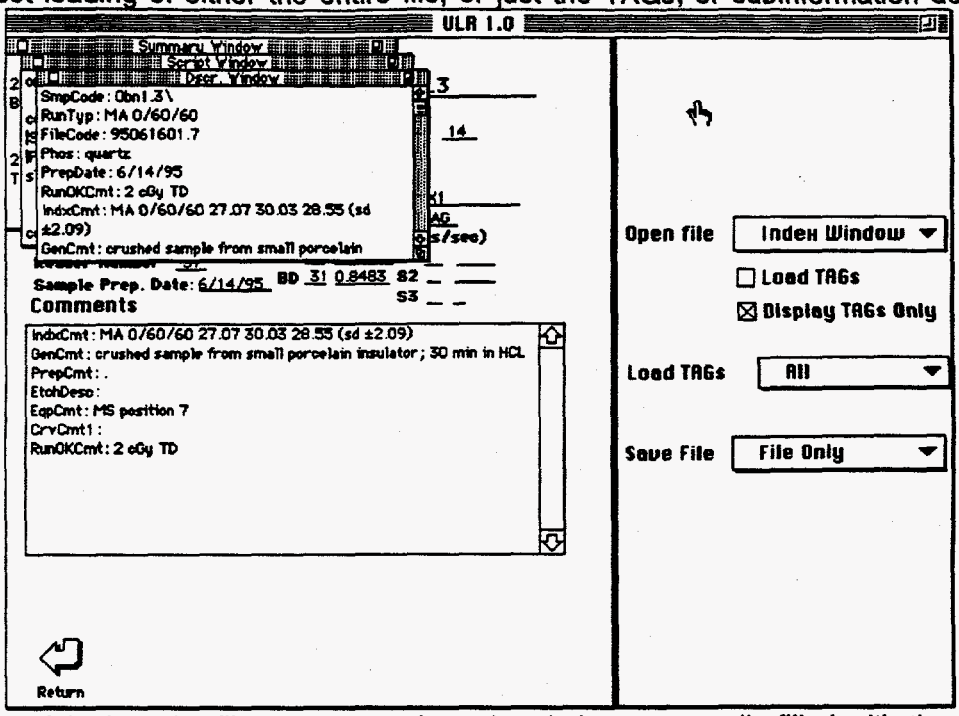

This is useful when the file setup page has already been manually filled with the correct data, however the script from a previous run is to be used. In this case the option "Script1" should be selected.

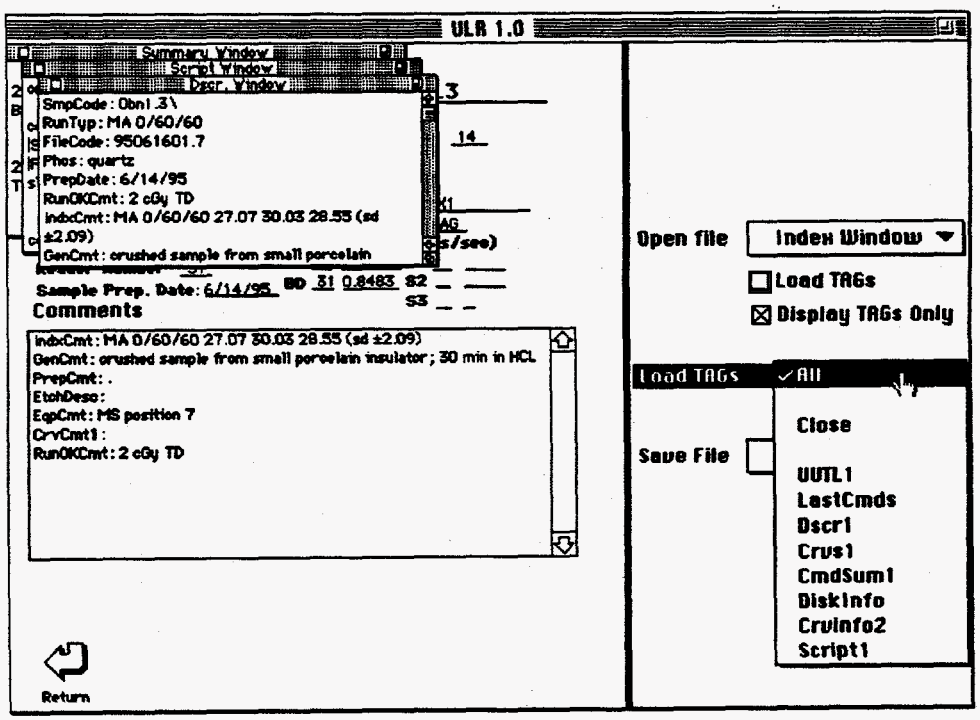

On both the File Setup page and the Pre-dose Parameters page, help is available concerning each of the fields to be entered. This form of help is via "Balloons" which appear when the mouse is dragged over a specific item. To activate balloons, system 7 or later must be operating. The "?" icon on the top right of the main menu bar should be accessed by clicking on it with the mouse button while holding and dragging down to the "show balloons" item where the mouse should be released. After a few seconds the cursor will turn into a question mark and will bring up help balloons specific to the item that the mouse is positioned over.

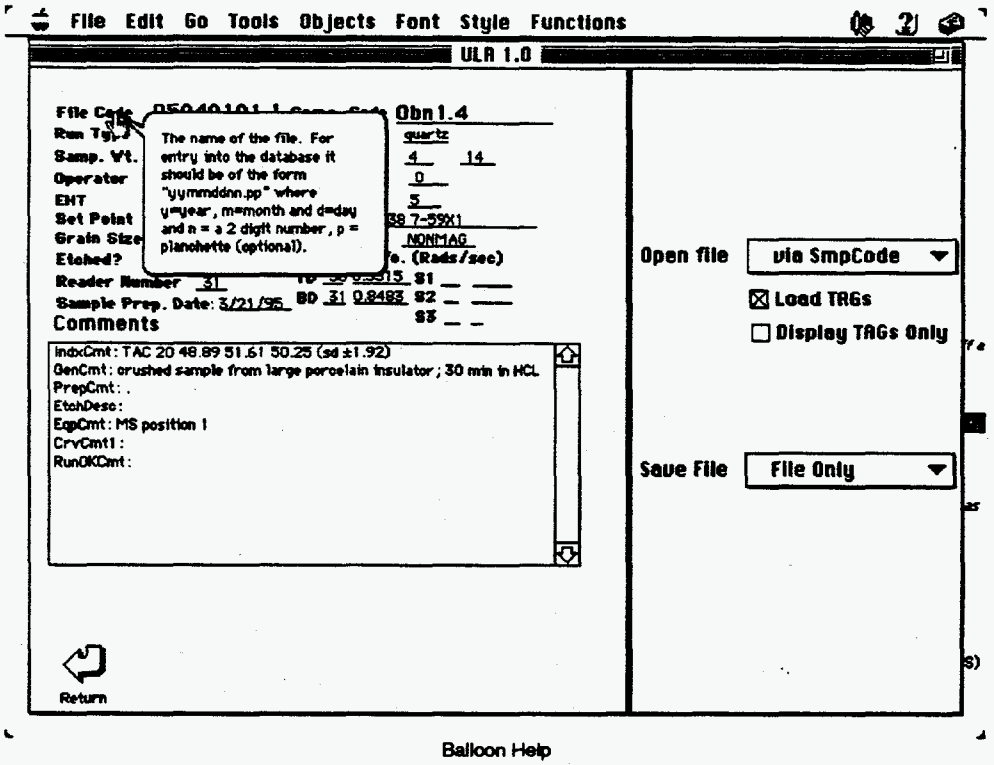

Balloon Help

The file setup page contains information on the sample, equipment, method of preparation and will later include results of the analyses performed. The data fields described below are accessed by pressing and holding down on the mouse while it is positioned over the desired date entry field. A **pop up menu** will appear with a number of previous data entries listed for this field and at the top of the list will be the option

"other" which will allow the user to enter unique information.

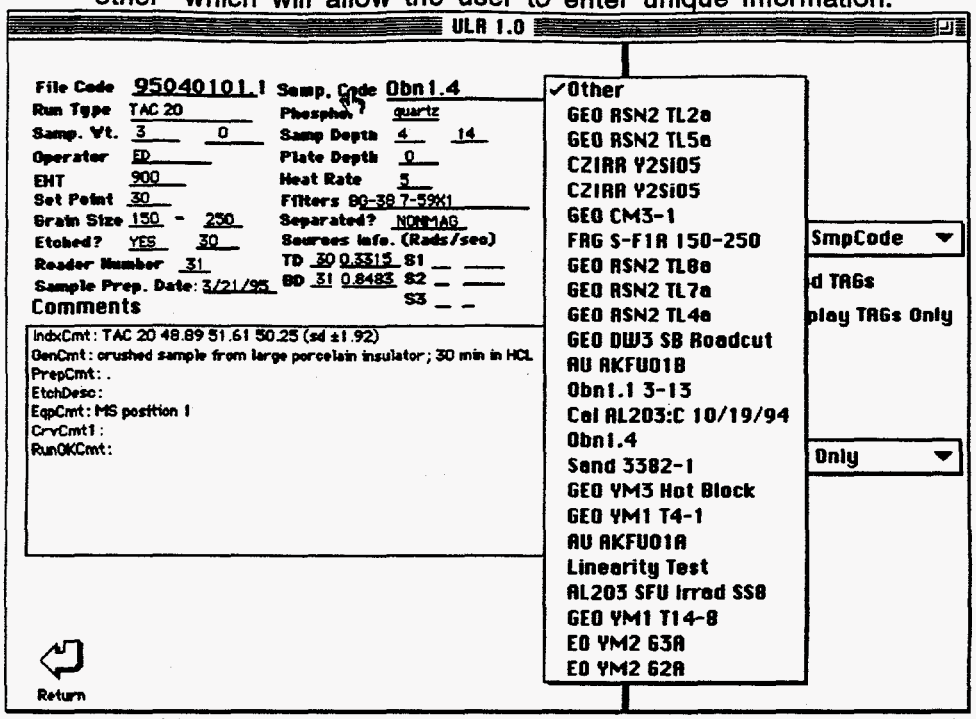

The exception to this entry method "comments" field, where the mouse should be positioned over the comment desired, clicked and released. A dialog box will appear allowing the user to enter a comment. This field is erased by holding down on the command key while clicking OK. In most of the fields, type checking is used to assure proper data entry.

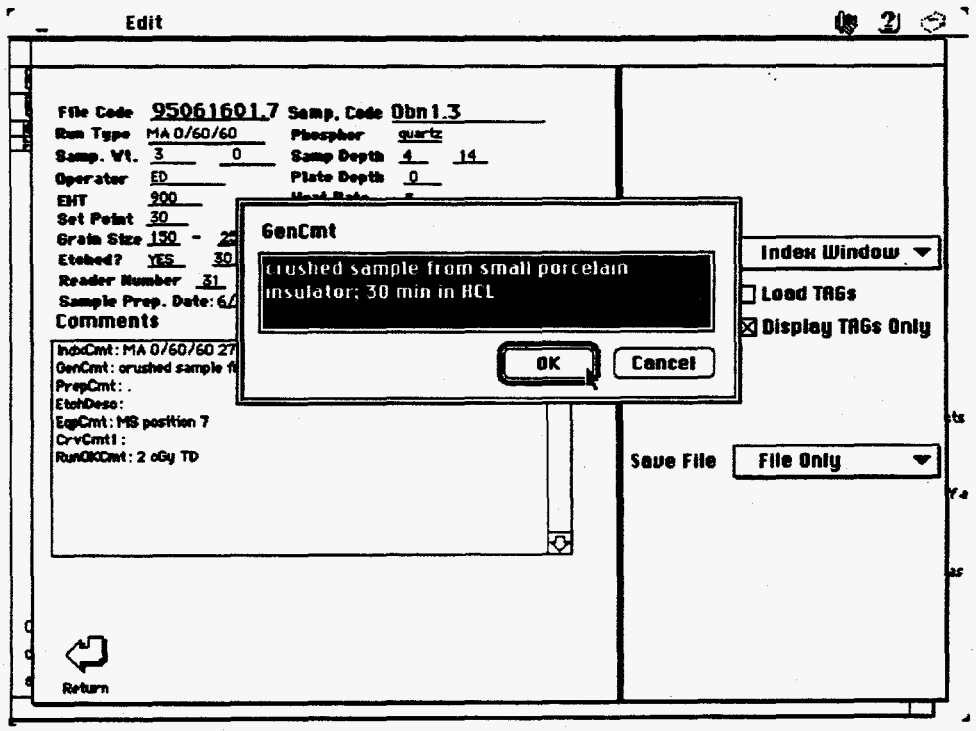

Pop Menu

The fields on the file setup page are used for inputting the following information.

1) the name of the file created (**File Code**, see above)
2) the sample code (**Samp.Code** which is used for identifying a particular sample or similar group of samples,
3) the type of analysis performed (**Run Type**, MA, TAC, OSL etc.),
4) the type of sample analyzed (**Phosphor**)
5) sample depth (**Samp Depth**) (how far into a brick, for instance, the current sample was taken,
6) the sample weight (**Samp. Wt.**), or mean weight if multiple samples are involved (a separate data entry sheet is available for entering specifics of the samples on each disk, if desired),
7) the name of the operator (**Operator**),
8) the distance from the radiation source to the disk the sample in resting on (**Plate Depth**),
9) The high voltage of the PMT (**EHT**),
10) The sample heating rate (**Heat Rate**),
11) the temperature at which the heating plate must be at or below before the next procedure is inititated (**Set Point**).
12) The optical filters employed (**Filters**),
13) the size of grains used for analysis (**Grain Size**),
14) whether or not the sample was magnetically separated (**Separated**),
15) whether or not the sample was **Etched** and
16) for how long it was etched
17) entries for the radiation sources used, specifically for pre-dose test dose (**TD**),
18) beta dose (**BD**) and for three additional sources which may be used
19) (**S1**) Additional source #1
20) (**S2**) Additional source #2
21) (**S3**). Additional source #3

Each of the source fields also has an unlabeled field following it for entering the source rate.

22) SR1 Dose rate for additional source #1
23) SR2 Dose rate for additional source #2
24) SR3 Dose rate for additional source #3
25) A field is provided for the number of the TL or OSL reader being used (**Reader Number**),
26) the date of sample preparation (**Sample Prep. Date**)

and separate entry for comments. The **comment fields** are for

28) index comment (**IndxCmt**), which will be automatically updated with results of predose analysis,
29) a general descriptive comment (**GenCmt**),
30) a comment concerning sample preparation (**PrepCmt**),
31) a comment concerning Etching (**EtchDesc**),
32) Equipment (**EqpCmt**),
33) specific curves or shine downs (**CrvCmt1**),
34) and a comment to be entered if the run, or routine analysis is in jeopardy (**RunOKCmt**).

Pre-Dose Parameters

Following data entry on the file setup page, the user presses the arrow button on the bottom of the page to return to the novice menu. The next choice on the novice menu is the **pre-dose parameters page.** Click on this button and the window shown in the figure below appears.

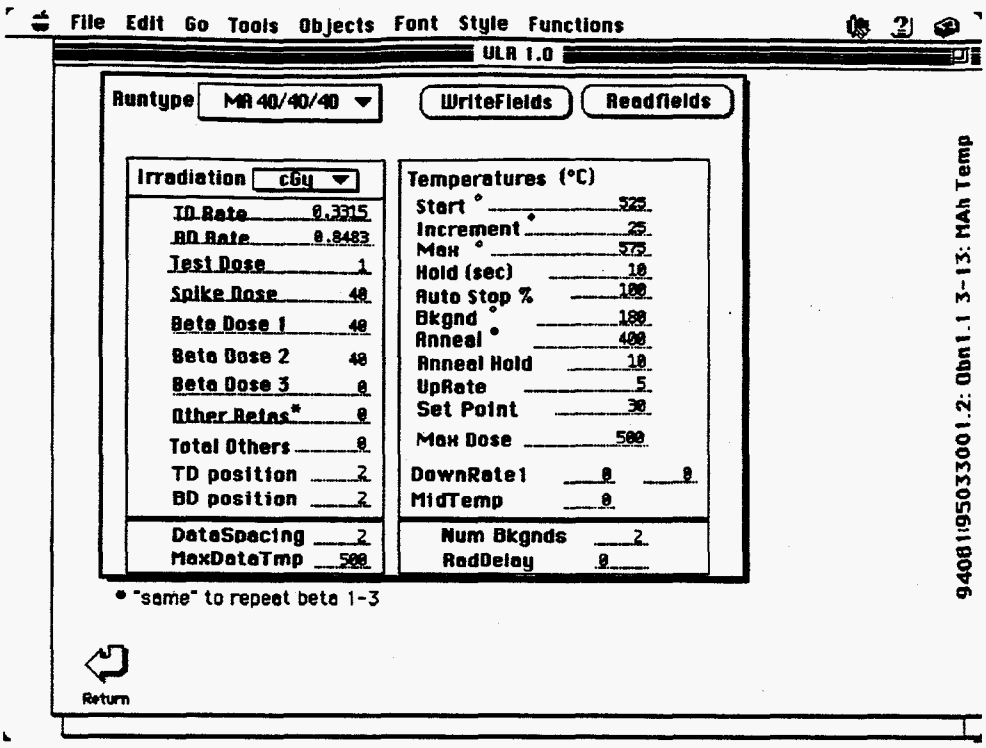

Pre-dose Parameters

The top left hand corner of the pre-dose parameters page has a popup button for the **RunType** this button should be set for pre-dose analysis using the following format. If a multiple activation analysis is to be performed, for example type MA followed by the so called spike dose, the additive dose given to a sample prior to activation, a slash "/", the first and subsequent beta doses all separated by slashes. So a multiple activation analysis given a 30 cGy spike followed by beta doses of 25, 35 and 45 Gy would be entered
MA 30/25/35/45.
The data entry fields in the left hand column are as follows.

1) The first one specifies whether display of dose values will be in terms of cGy or seconds.
2) the next fields list **TD Rate** and
3) **BD Rate**, the dose rates for test dose and beta dose respectively. These values will be automatically recalled from the previous data page when the button Read Fields at the top is pressed. The values cannot be set from the current page.
4) The next field lists values in cGy or seconds (depending on the setting in the irradiation field (seconds or cGy) for the test dose,
5) **Spike dose,**
6) **Beta Dose 1,**
7) **Beta Dose 2** and
8) **Beta Dose 3.**
9) If additional beta doses are desired, the dose for additional irradiations should be entered in the next field called "**Other Betas**".
10) The number of additional betas should be entered in the field called "**Total Others**".
11) The next two fields called **TD position** and
12) **BD position** are usedwith readers other than the Riso reader and are not used in this program.
13) The field called **Data Spacing** determines the interval in degrees C for which data will be collected. The usual value is 2.

14) The field called **MaxDataTmp** specifies the maximum temperature for which data will be retained. With pre-dose analyses temperatures often reach above 700°C, and glow data at this temperature is not used for analysis. Setting the field to a lower value saves on storage space.

The fields in the right hand column specify

1) the first activation temperature to heat to,
2) the number of degrees between successive activation,
3) the maximum temperature to heat to,
4) the number of seconds to hold at each activation temperature.
5) the percent drop below maximum at which to start a new dose/activation cycle (not usually used),
6) the temperature to perform background heating,
7) the temperature to perform the final heating of a cycle after the last activation (usually 400°C),
8) the number of seconds to hold at this temperature,
9) the heating rate,
10) the set point, or the temperature to perform irradiations on those readers which support this feature (or the temperature to allow the plate to cool to before proceeding with new reader operations).
11) the Maximum dose to apply to a sample in certain operations which automatically calculate dose based on data input (curve matching).
12) the Number of backgrounds to perform (to eliminate the low temperature effect of beta irradiations which is useful for getting an accurate determination of background value to subtract in cases where higher heating temperatures for background cycles might cause partial activation of the sample.
13) the number of seconds following irradiation to wait prior to performing a glow curve (normally zero).

Curve Plotting Setup

Once data on pre-dose parameters page has been entered clicking on the button listed plotting setup will return the user to the **Curve Plotting page** for plotting the glow curves. When this page is entered a small window appears which lists the plotting parameters. These are the **minimum** and **maximum** values for thetemperature or **x - axis** (in °C), the **min** and **max** for the TL, or **Y axis** (in arbitrary units), the **temperature range** for the **firstset** of **integration limits**, and the range for the **second set of integration limits**. If a previous file has already been opened, the parameters will be automatically entered from the data file. The x and y axis values are set by clicking the mouse while holding down on the option key as the mouse is positioned above the appropriate field. The cursor changes from a pointing finger to a "I". Clicking on the mouse button outlines the selected field with a heavy line. Double clicking in the field selects the entire field, pressing delete removes old data. Once entered, both the x and y ranges may be adjusted using the popup buttons called **X-scale and Y scale.**

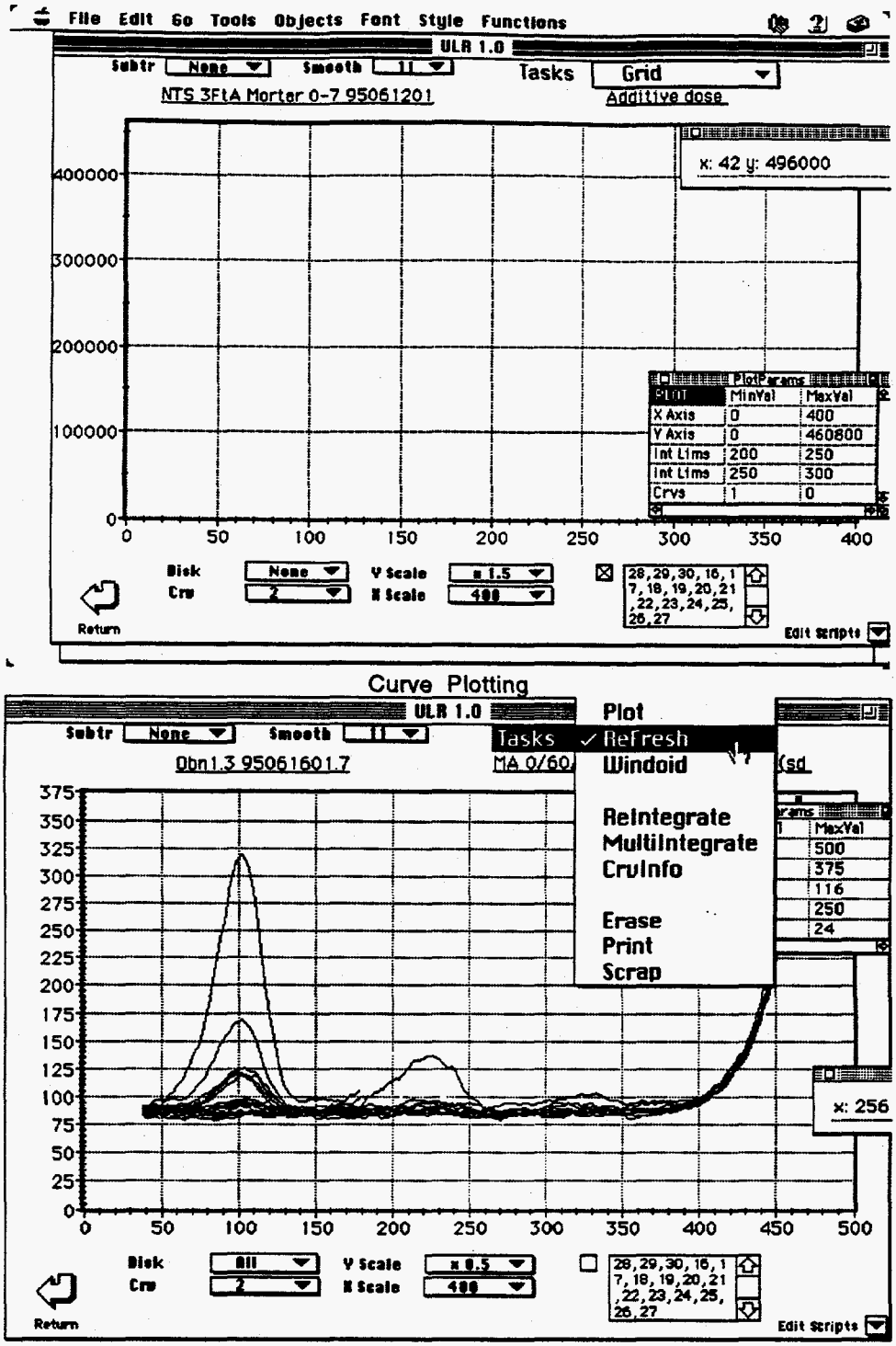

The **Integration ranges** may be entered directly from the graph. This is done by positioning the mouse at the desired starting point for the first or second integration limits. While the cursor is in the graph box, the message box contains the x and y values which change as the cursor is moved. If the mouse button is pressed as the option key is depressed, data entry will be initiated for the first set of limits (the ones used for pre-dose analysis). To set the second set of limits the mouse is clicked while depressing the command key. The temperature value in the message box at the time the mouse is pressed

will be the lower integration limit. By moving the mouse to the temperature on the graphs for the desired upper integration limit and then releasing the mouse, the upper limit will be entered. Both the values for lower and upper integration limits will be entered into the windoid. Once the limits and x and y axis ranges are set, the **Grid** option should be selected from the popup button labeled **tasks**. The full list of options in the tasks button include **Grid, Plot, Refresh, Windoid, Reintegrate, MultiIntegrate, Crvinfo, Erase, Print and Scrap**. These perform the following function.

1) **Grid** creates a new grid based on the parameter in the windoid. This command also erases the screen of any bit map images created with the Scrap command.
2) **Plot** will plot any data that has been collected in a current run or has been recalled from a file.
3) **Refresh** will redraw the curves if a dialog box has obscured them or if the plot page is returned to from a previous page.
4) **Windoid** will open a floating window on the screen containing a plot of the curves selected. Any number of windoids may be opened depending only on RAM. If system 7.5 is running, the windows may be compressed to the top bar by double clicking on the windoid bar.
5) The **Reintegrate** function reintegrates data if new limits have been set and updates these values in several locations in the program.
6) The **MultiIntegrate** button opens up a dialog and allows the user to set any number of successive integration limits, performs the integration operation and puts the results in tab delimited columnar format into the clipboard (if Hypercard 2.2 or newer is in operation).
7) **Crvinfo** opens a floating window containing information on the curves selected, including the two integration values selected in the plotparameters. At the same time, the crvinfo data becomes available in the clipboard in tab delimited form. This may be directly copied into a spreadsheet or plotting program.
8) The **Erase** options erases displayed glow curves,
9) The **Print** option prints the graphs and curves and the scrap option places a PICT copy of the graph into the clipboard.
10) **Scrap** replots the curves selected and places it into the clipboard for pasting into a word processing program. At the same time it forms a bit image of the curves and places it onto the Hypercard screen so that subsequent curves may be directly compared to it.

Data may be smoothed as it is collected (on screen only) and the degree of smoothing may be set with the **Smooth** box.

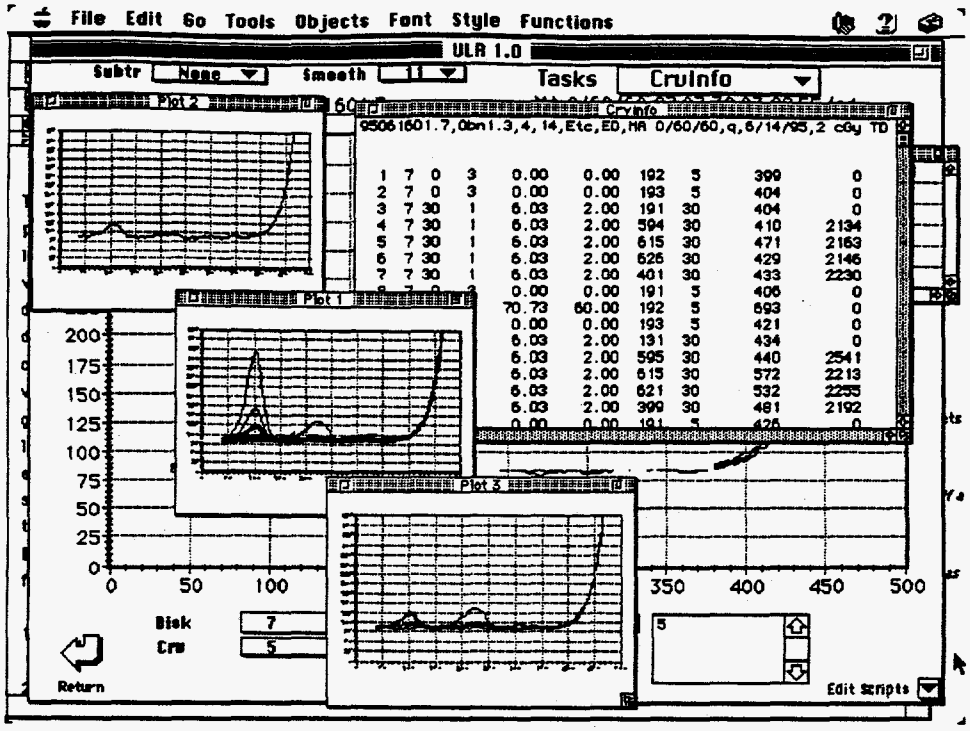

Reader Control

Once data on the pre-dose parameters page has been entered, the arrow button on the bottom of the page will return the user to the novice menu page. The button labeled **start run** on the novice menu page should be pressed which will advance theuser to the page which controls automated runs. On this page a number of options are available in expert mode which are not seen when entered via the novice menu page. Only the button **"pre-dose Run"** will be seen. Click on the button **Reset** to initiate analysis. During the reset procedure, several dialog boxes requesting additional information will appear. Once the procedure is started the appropriate analyses will be performed. During the course of analysis the program may be paused at certain times (not during an irradiation or glow out) by making a menu selection from the functions menu or by clicking on the Pause button. If the function menu is used to observe plotted curves, for instance, the program will resume automatically when the reader control page is again entered. The Pause button will save all of the data collected to this point and will pause collection until the button (no named resume) is again clicked. If a fast pause is desired, hold down on the option key while pressing the pause button. This avoids the process of saving a file before pausing.

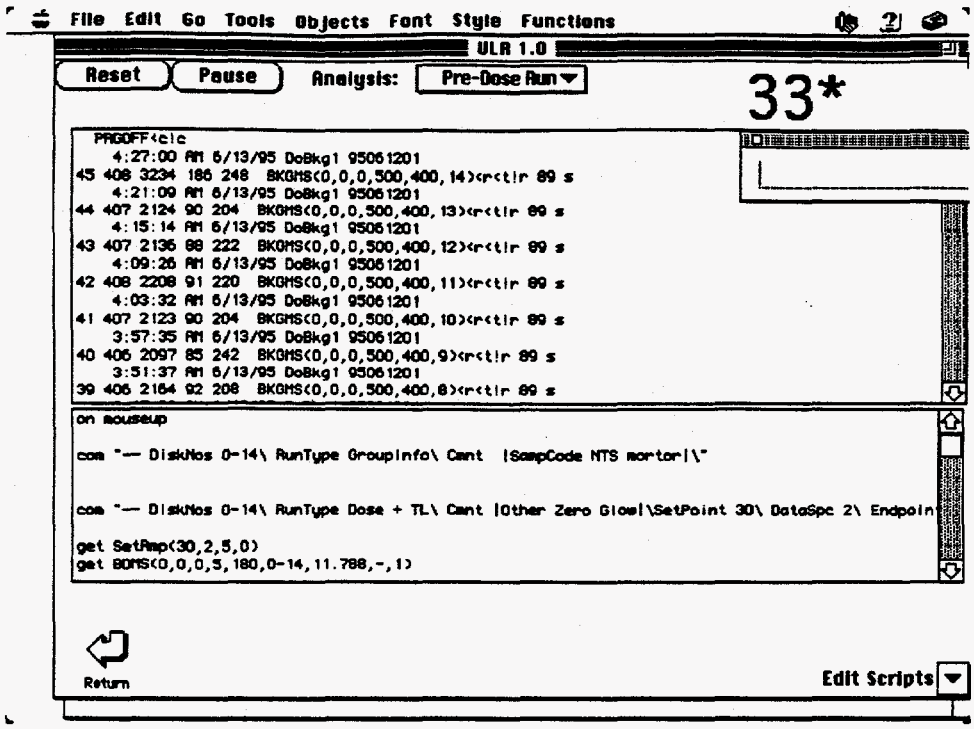

Reader Control

Following completion of data collection, data should be saved by returning to the file setup menu (by pressing the return button at the bottom of the page to return to the novice menu) or by selecting "File setup" from the functions menu.

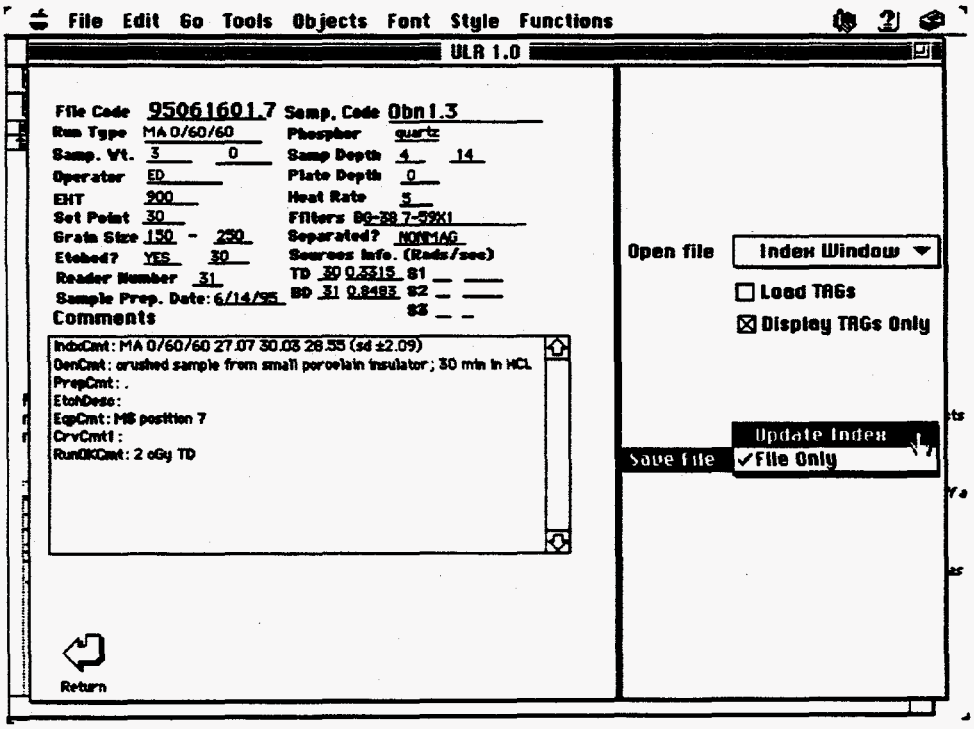

On the File setup page review the data entered and select "Update Index" from the Save File popup button. If a file with the same filecode already exists you will be asked if you would like to overwrite it.

Advanced Operation

ULR Scripting

The ULR program has a scripting option which allows the user to design use and store custom reader operations. The window below shows the scripting page.
The type of operation is specified in the popup button at the upper left of the page. This button has seven options as shown in fig. , OSL, TL, Dose + OSL, Dose + TL, Dose Only, Pause and GroupInfo. The button at the top right called DiskNos has the range of disks or platter positions which will be handled in a single command. Depending on the entry chosen, Dose + TL for instance, certain data entry buttons (beneath the pop up button in fig) will be enabled or disabled. The user is only faced with specifying those parameters which effect a particular type of operation. To specify "Dose + TL" operation on disks O to 2 (as shown) first select "Dose + TL" from the pop up menu.

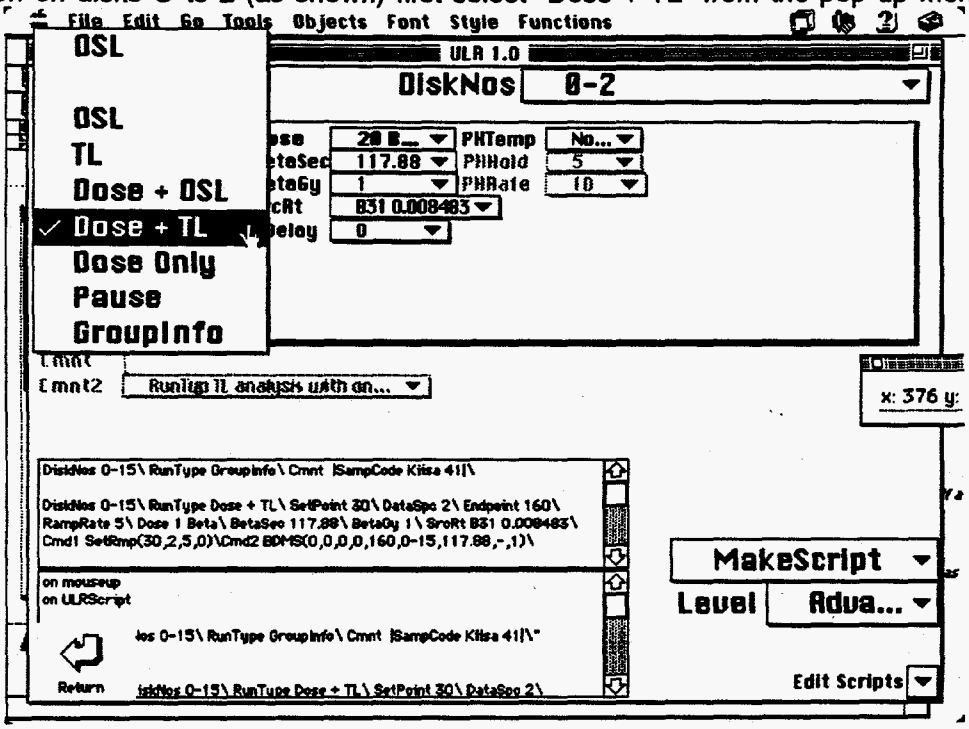

The data buttons related to OSL parameters will be dimmed (not seen well in the figure).

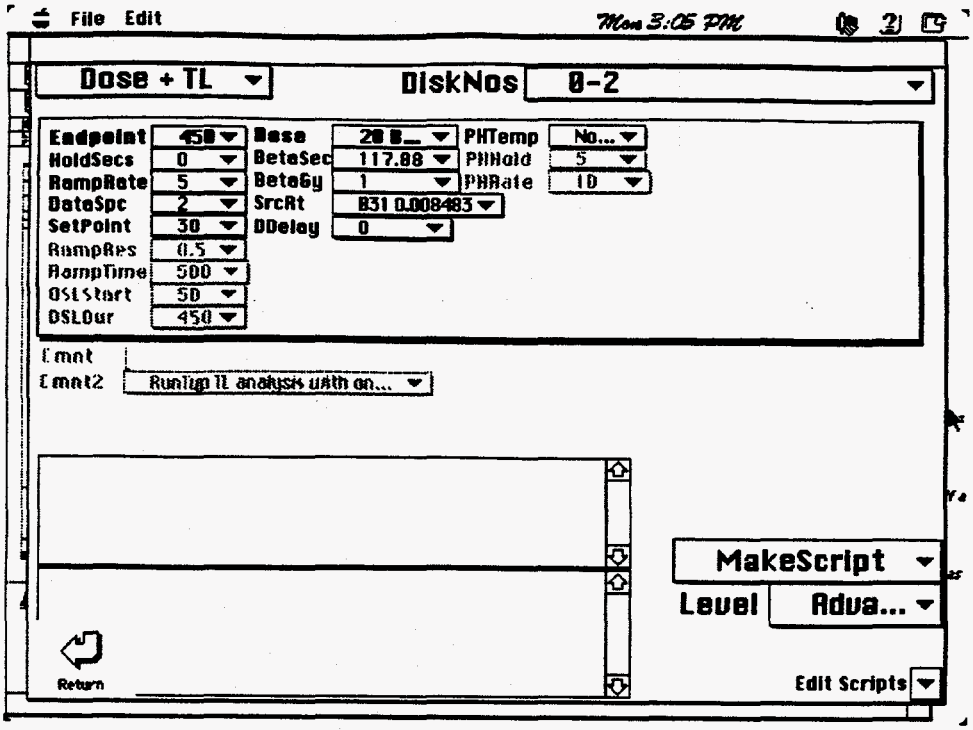

The data buttons on the left are self explanatory, however balloon help is available for all buttons as shown in fig.

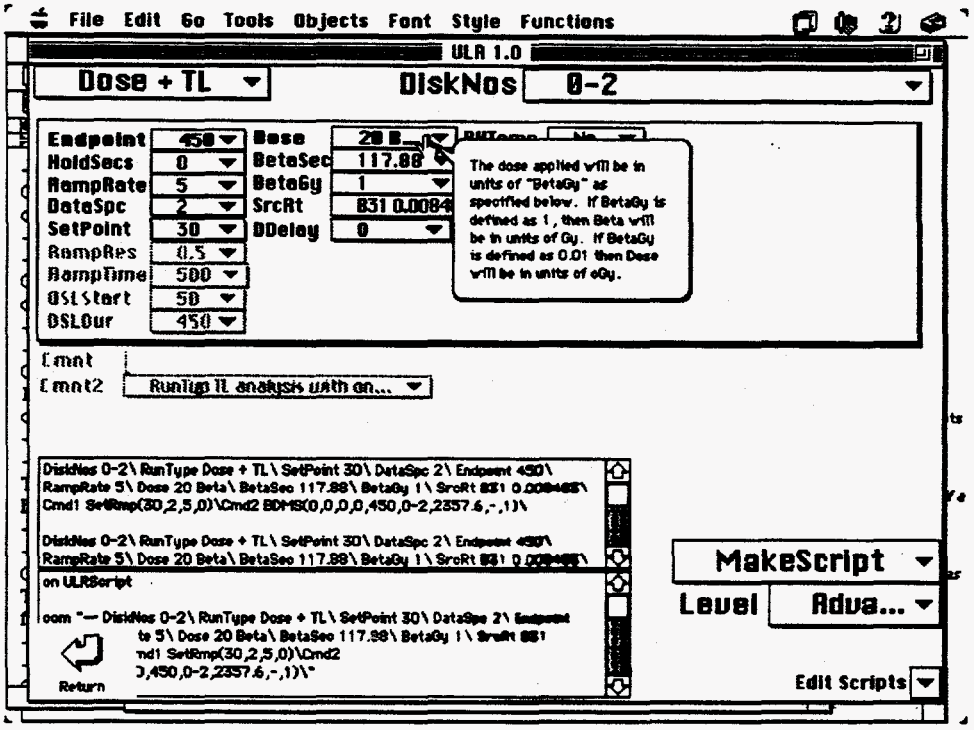

. Depending on the level option chosen, only minimal input will be required. This mode requires prior setup of certain parameters.

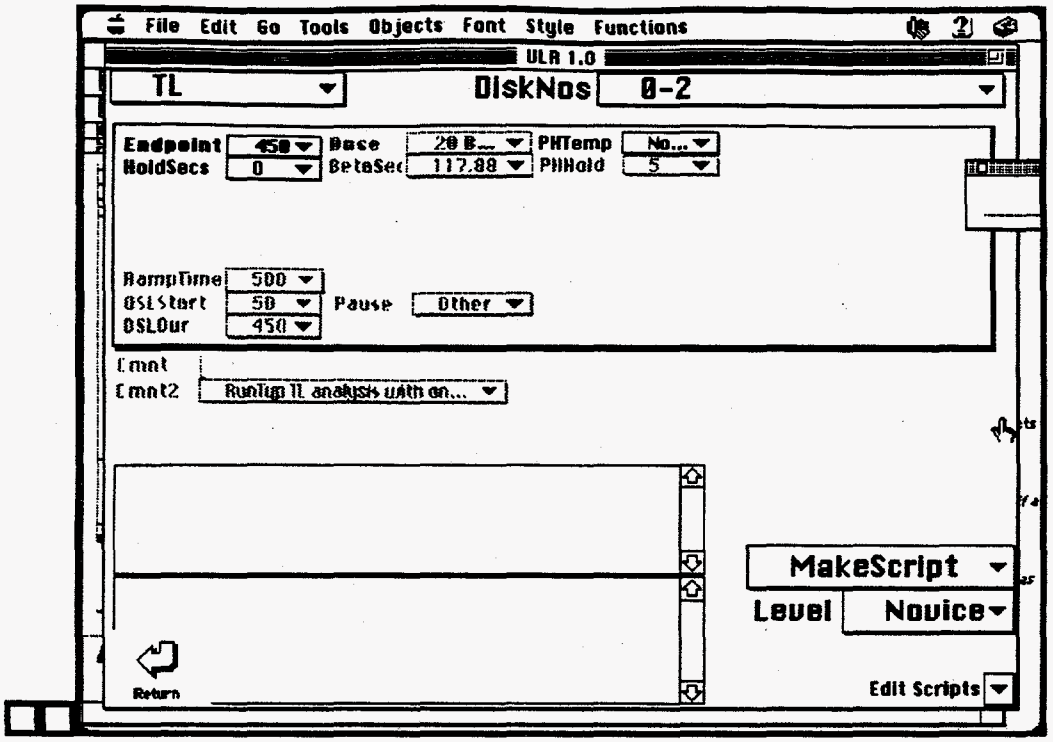

Novice Level

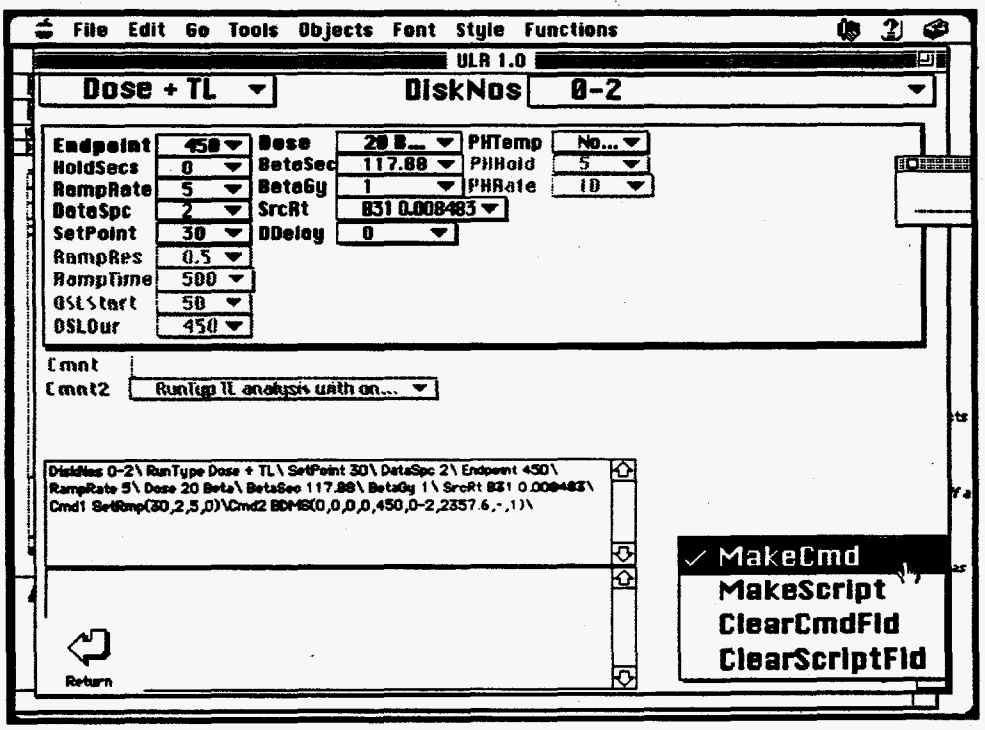

Once the data entry has been completed for a particular operation, press "MakeCmd" to create a command from the data. This command will be listed in the command window

shown above. To edit this window click on it and it will enlarge to a text editing window. To shrink it back click while pressing the command key.

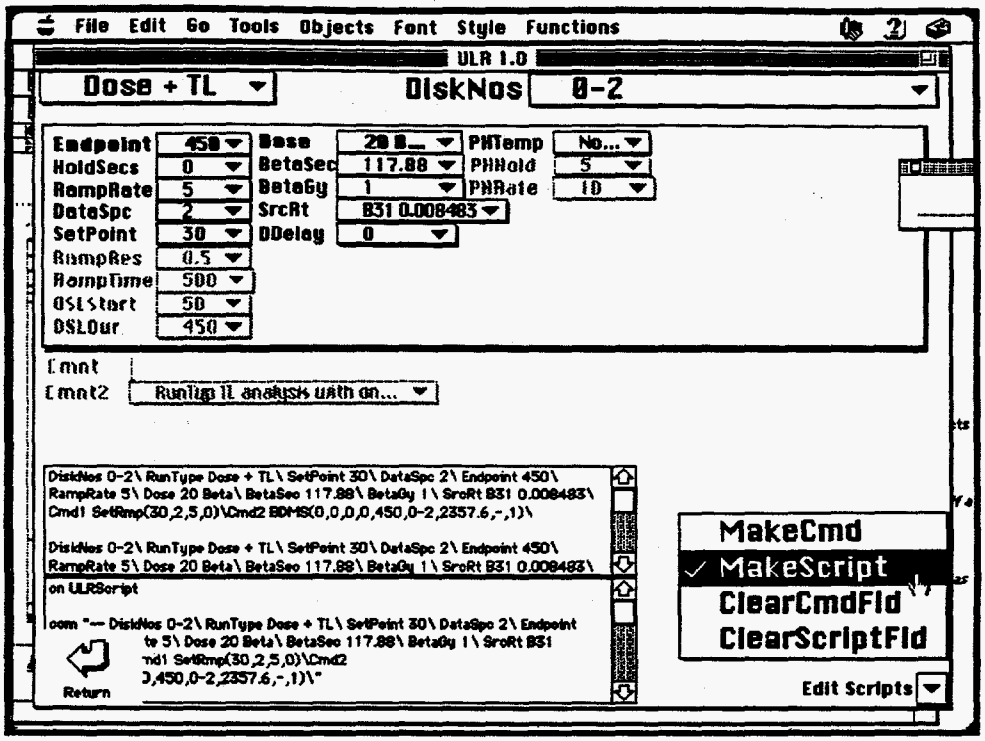

Once the commands have been reviewed they must be turned into script which will be interpreted by the program. To do this press on the MakeScritp button to the right. When the script has been created, a dialog box (below) will appear asking the user if he wishes to load the script onto the reader control page. Pressing yes replaces the existing script with the newly generated script.

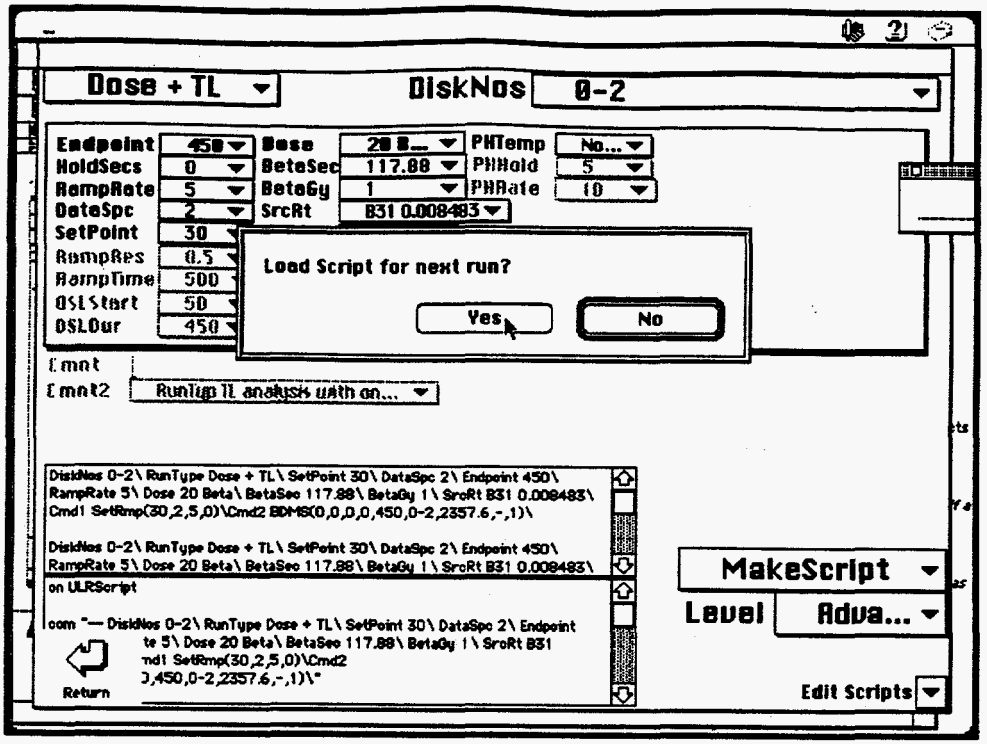

The new script is placed in the script window of the reader command page and the user is transferred out of the scripting page.

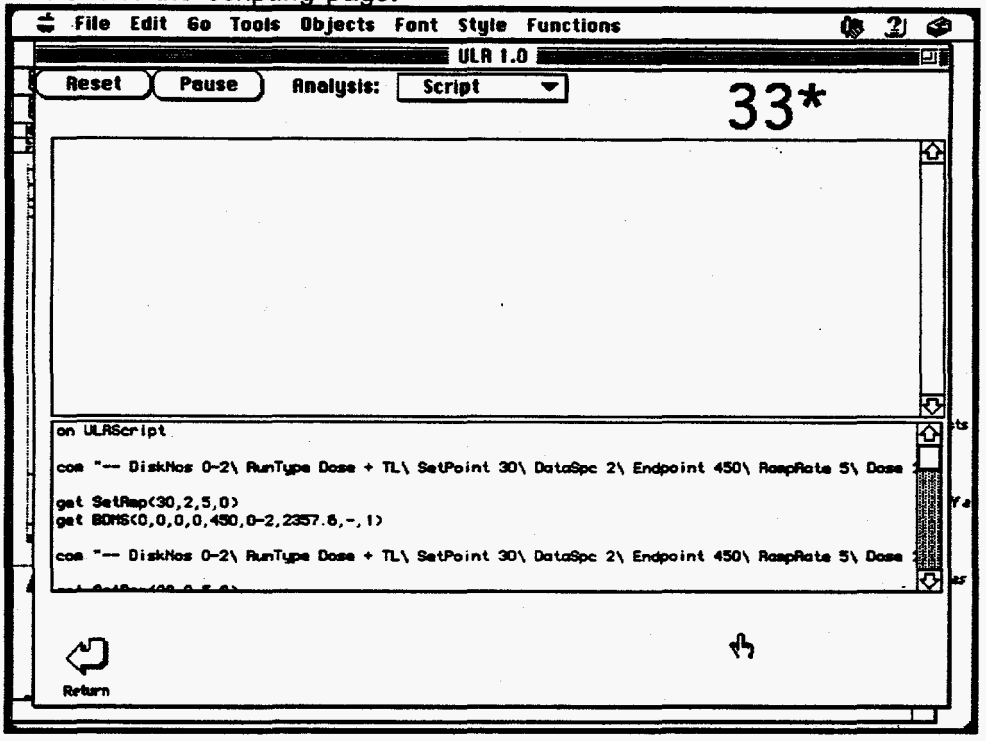

The script is then run by clicking on the Reset button shown above. As with the predose runs described above, the user may pause operation for examination of data or modification of script. Once data has been collected, the file is saved as specified above.

The ULR Data Base System

The ULR Program creates and maintains a file oriented data base system. An index file is maintained which contains summary information on samples analyzed, types of analyses performed and results of certain types of analyses. This indexfile is accessed and may be searched from the main acquisition window of the program. Searching may be performed by file code, sample code or file comment. As new files are created and stored, entry is automatically made to the indexfile. For the indexfile to work adequately, files must be created with a date format of the order YYMMDDNN.PP where Y is year, M is month, D is day, N is a sequential number from 1 to the number of files created in a particular day, and the extension .PP is optional and indicates the sample position on the platter. To keep the number of files in a folder at a manageable level, a certain folder/file structure is used.

For example, create a folder termed "ULR Data". Place the empty indexfile in this folder. Now create a folder called 95 and another called 96 (for the year), or 9501 and 9502 etc. for the year and month or 9501 and 9507 for semiannual storage. New files will automatically be created in the folder corresponding to the period of time in which they are created. The files are in text format and may be accessed individually with any text processing program. When the index file is searched and accessed, the files are automatically retrieved from their respective folders.

TAG Files

The data base files created with the ULR program are ASCII based for easy manipulation and transfer of data to and from text based word processing, spread sheet and plotting programs. The data is organized and accessed within the reader program using the ULR TAG format system. This system allows for rapid, organized storage and retrieval of data and for flexibility in creating new "TAGs", or data subgroupings which may be stored and retrieved as a unit within a new or existing TAG file.

The TAG structure format has a header and a footer string of the following format:

TAG header

The following four characters at the start of a line

-->|

Followed by the name of the TAG, all on the same line, such as

-->|Crvs1 (nothing else on line)

TAG Body

The TAG Body may be any number of lines of ASCII data

TAG Footer

The following three characters at the start of a line

--<|

Followed by a space and the name of the TAG, all on the same line, such as

--<|Crvs1 (nothing else on line)

Storing and Accessing TAGs

Two function are available for storing and accessing TAGs within a TAG file: GetTAG and PutTAG. The format of GetTAG is GetTAG(tagname, tagdata), where tagname is the header and footer name (without the "-->|" or "--<|"), tagdata is name of the field or variable that the existing tagfile is located in. The format of PutTAG is PutTAG(newtagname,newtagdata,tagdata), where newtagname is the header and footer name of the TAG to be added to the existing TAG file "tagdata", and newtagdata is the data to be added. if a TAG exists in tagdata with the same name as newtagname, then the old TAG with the same name is replaced by the new. Both GetTAG() and PutTAG() are Hypercard functions, and their parameters can be either literals or references to Hypercard variables or containers (see Hypercard Reference Guide).

TAG Rules

1. Any number of tags may be entered into a TAG file limited only by RAM.
2. TAGs may be nested.
3. TAG names within a given hierarchical level must be unique.
4. If a TAG name is requested, only the first occurrence of that tag will be accessed. Other occurrences may be accessed as follows. (This example is given for those who desire to add new TAGS to the system.)
   In the example below, both TAGA and TAGC contain a subTAG TAGB. . To access the second TAGB, you must first access TAGC and then access TAGB from TAGC.

```
head TAG1
        head TAGA
                head TAGB
                foot TAGB
        foot TAGA
        head TAGC
                head TAGB
                foot TAGB
        head TAGC
foot TAG1
```